technische universität
dortmund

INAUGURAL – DISSERTATION

Zur Erlangung der Doktorwürde
der Fakultät Raumplanung
der Technischen Universität Dortmund

Vorgelegt von
Ahmed Yasser Abdelmejeed, M.Sc.
aus **Kairo, Ägypten**

Fakultät Raumplanung

Lehrstuhl Landschaftsökologie
und Landschaftsplanung

Developing a comprehensive strategy to optimize tree use for mitigating heat stress.

Considering urban morphology and limited resources through dynamic and static thermal comfort analysis.

A case study of Cairo city.

Examination committee:

Prof. Dr. Lars-Peter Lauven, TU Dortmund University, Germany (Chair of the examination committee)

Prof. Dr. Dietwald Gruehn, TU Dortmund University, Germany (Supervisor and First reviewer)

Prof. Dr. Laila El-Masry, Cairo University, Egypt (Second reviewer)

Acknowledgements

I would like to express my profound gratitude to ***Allah*** for granting me the strength and perseverance essential to completing this research study.

I extend my sincere appreciation to my supervisor, ***Prof. Dr. Dietwald Gruehn***, from TU Dortmund University in Germany. His guidance and unwavering support have been pivotal in advancing my work. His dedication, encouragement, and consistent recognition of my efforts throughout my PhD journey have been exceptional. I am grateful for his belief in my abilities and the autonomy he provided to explore my ideas and interests. His support during various challenges has been invaluable, and I consider myself fortunate to have completed my PhD under his supervision.

Additionally, I am thankful to ***Prof. Dr. Laila ElMasry*** from Cairo University in Egypt for her role as the external reviewer. Her unwavering support and constructive critiques have greatly contributed to the refinement of my dissertation.

I also wish to acknowledge ***Prof. Dr. Lars-Peter Lauven***, from TU Dortmund University in Germany who served as the chair of the examination committee. His essential feedback on my dissertation significantly enhanced the quality of my work.

My heartfelt gratitude extends to the entire Department of Spatial Planning in TU Dortmund University and the LLP team for their steadfast support and assistance throughout my academic journey. I would specifically like to recognize ***Anne-Marie Geudens, Janine Bayer, Mohammad Bashirizadeh, Carmen Van Meegen, Florian Klopfer, Jacqueline Osthues, and Kirsten Wildoer*** for their contributions.

I would also like to express my appreciation to ***Greg McBride*** for his extensive support, as well as to ***Amir Abolata*** for his ongoing guidance, during different stages of the PhD study. Furthermore, I wish to thank ***Tane Raffa*** for his assistance in English proofreading my dissertation.

Lastly, I would like to extend my deepest gratitude to my family, whose unwavering support has been crucial. To my beloved ***parents***, my wife ***Nahla***, my cherished children ***Yahya, Yousef, and Talia***, and my sister ***Aya*** who always inspired and supported me, thank you for your encouragement and support during this journey.

Also to my dear friends ***Eslam Abeed, Abdallah Galal, Eslam El-Nazer, Essam Gamal, Omar Essam, and Anas Aladdin.***

This dissertation is dedicated to everyone worldwide who advocate for fairness, justice, freedom, equality, and peace. Also, for people who are doing efforts against climate change and supporting sustainability.

“This dissertation is gifted to Hind Rajb's soul”.

Ahmed Yasser Dortmund, 15. July 2025

Abstract

This cumulative dissertation aims to develop a comprehensive and efficient strategy to enhance urban microclimate conditions in cities experiencing heat stress and intense solar radiation, with a focus on the metropolitan area of Greater Cairo. This study is conducted in three main stages, each addressing different aspects of urban microclimate management and optimization through the strategic use of trees. Stage 1 involves developing an efficient urban tree strategy (UTS) aimed at balancing an enhancement of microclimate conditions with the city's water scarcity. This stage implements three strategic components: (1) selecting suitable tree species, (2) utilizing innovative irrigation technologies, and (3) determining the optimal number and arrangement of trees. When applying the strategy's recommendations to a study area within Cairo's downtown center and when testing different tree coverage percentages within urban canyons of various aspect ratios and orientations using ENVI-met, the microclimate conditions are significantly enhanced in certain streets during summertime compared to wintertime. For example, there are average physiological equivalent temperature (PET) reductions of -5.18˚ and -6.36˚ at 16:00 and 17:00, respectively. Additionally, applying the UTS to the study area significantly enhances microclimate conditions. Furthermore, through the implementation of irrigation technologies that are part of the UTS, water demand is reduced to only 15% when trees with larger canopies are used. Stage 2 focuses on optimizing the use of trees to enhance microclimate conditions by considering elements of urban morphology, such as the aspect ratio and orientation of canyons, both of which significantly influence microclimate conditions. In this stage, both sides of each canyon are considered, as urban shading depends on orientation and aspect ratios. This shading arrangement may provide sufficient shade on one side of the canyon while the other remains exposed to direct and indirect radiation. Thus, a comprehensive assessment in necessary to determine the optimal use of trees. Due to the vast size and diverse urban morphology of Cairo, a total of 144 theoretical cases are simulated using ENVI-met to represent the majority of urban conditions within the city (Step 1). Following this, the same tree scenarios used in the theoretical study are applied to an existing urban area in downtown Cairo, characterized by diverse urban morphologies, to validate the results of the theoretical study (Step 2). After testing all scenarios in both stages, it becomes evident that the addition of trees must account for different aspect ratios, orientations, and the specific sides of urban canyons. For example, eastern-oriented roads require more trees than other orientations across all aspect ratios. However, the required number of trees is greater for the northern side of these streets. This is because, in moderate and deep canyons, the southern side is partially shaded by buildings for several hours during the day. The results from applying trees to an existing urban area closely align with the theoretical study's results, with very slight differences resulting from irregularities in the study area. These findings demonstrate that for optimal pedestrian microclimate conditions and tree use, it is important to consider not only the aspect ratio and orientation of canyons but also which side of the canyon trees are planted. Stage 3 analyzes and assesses the impact of different urban forms and tree densities on the dynamic physiological equivalent temperature (DPET) experienced by pedestrians walking further than the average walking distance (750 m), using ENVI-met. This stage includes five different areas within Greater Cairo, which is suffering from extreme heat stress. These areas are chosen for their diversity in canyon aspect ratios, orientations, urban forms, green areas, mixed land uses, and tree densities. Two tree density scenarios are analyzed: the current density and an increased density scenario, where each area is increased to full

capacity. The results prove that the DPET exhibits different values from the steady physiological equivalent temperature (SPET) at each point along the walking routes. However, the DPET is closely related to changes in the SPET. On the one hand, prolonged periods of lower or higher SPET result in reductions or increases in the DPET. On the other hand, frequent fluctuations in the SPET stabilize the DPET. Changes in the DPET values are driven more significantly by the microclimate conditions of individual spaces or canyons than the broader area, and controlling these conditions within a whole urban canyon is found to control the DPET. Changes in the DPET can reach as high as 10 °C across different walking routes, and in some cases, increasing the tree density may help lower the DPET by as much as 6 °C. Overall, this research provides a scientifically validated framework for optimizing urban greenery to mitigate extreme heat while conserving water. The findings are pivotal for developing sustainable, climate-resilient urban environments.

Kurzzusammenfassung

Ziel dieser kumulativen Dissertation ist die Entwicklung einer umfassenden und effizienten Strategie zur Verbesserung der mikroklimatischen Bedingungen in Städten, die unter Hitzestress und starker Sonneneinstrahlung leiden. Die Studie wurde in drei Hauptphasen durchgeführt, die jeweils verschiedene Aspekte des städtischen Mikroklimamanagements und der Optimierung durch den strategischen Einsatz von Bäumen behandeln. Stufe 1, die Entwicklung einer effizienten Stadtbaumstrategie (UTS), zielt darauf ab, ein Gleichgewicht zwischen der Verbesserung der mikroklimatischen Bedingungen und der Berücksichtigung der Wasserknappheit in der Stadt herzustellen. Dabei sollen alle strategischen Faktoren berücksichtigt werden, die für die lokalen Bedingungen geeignet sind, einschließlich der Auswahl der Baumarten (Schritt 1), der Nutzung innovativer Bewässerungstechnologien (Schritt 2) und der Bestimmung der optimalen Anzahl und Anordnung von Bäumen (Schritt 3). Durch die Anwendung der Strategieempfehlungen auf ein Untersuchungsgebiet im Stadtzentrum von Kairo werden die mikroklimatischen Bedingungen in bestimmten Straßen während der Sommerzeit im Vergleich zur Winterzeit erheblich verbessert. Diese Verbesserungen wurden bewertet, indem verschiedene Prozentsätze der Baumbedeckung in städtischen Straßenschluchten mit unterschiedlichen Seitenverhältnissen und Ausrichtungen mit ENVI-met getestet wurden. So ergibt sich z. B. eine durchschnittliche Verringerung der physiologischen Äquivalenttemperatur (PET) von -5,18˚ und -6,36˚ um 16:00 bzw. 17:00 Uhr. Die Anwendung der UTS im Untersuchungsgebiet führt zu einer deutlichen Verbesserung des Mikroklimas. Außerdem wird durch die Anwendung von Bewässerungstechnologien, die Teil der UTS sind, der Wasserbedarf auf nur 15 % gesenkt, wenn Bäume mit größeren Baumkronen verwendet werden.

Phase 2 zielt darauf ab, die Verwendung von Bäumen zur Verbesserung des Mikroklimas zu optimieren, indem Elemente der städtischen Morphologie berücksichtigt werden, wie das Seitenverhältnis und die Ausrichtung von Straßenschluchten, die beide erheblichen Einfluss auf die Veränderung des Mikroklimas haben. In dieser Phase werden beide Seiten jeder Schlucht berücksichtigt, da die städtische Beschattung von der Ausrichtung und den Seitenverhältnissen abhängt. Dadurch kann diese Beschattungsanordnung auf einer Seite der Schlucht ausreichend Schatten spenden, während die andere Seite der direkten und indirekten Strahlung ausgesetzt bleibt. Daher ist eine ausführliche Bewertung der Möglichkeiten erforderlich, um den optimalen Einsatz an Bäumen zu bestimmen. Aufgrund der beträchtlichen Größe und der vielfältigen urbanen Morphologie von Kairo werden insgesamt 144 theoretische Fälle mit ENVI-met simuliert, um die Mehrheit der urbanen Bedingungen innerhalb der Stadt darzustellen (Schritt 1). Anschließend werden dieselben Baumszenarien, die in der theoretischen Studie verwendet wurden, auf ein bestehendes Stadtgebiet im Stadtzentrum von Kairo, das durch unterschiedliche städtische Morphologien geprägt ist, angewandt, um die Ergebnisse der theoretischen Studie zu validieren (Schritt 2). Nach dem Testen all dieser Szenarien in beiden Phasen wird deutlich, dass bei der Anpflanzung von Bäumen unterschiedliche Seitenverhältnisse, Ausrichtungen und spezielle Seiten von Straßenschluchten berücksichtigt werden müssen. Östlich ausgerichtete Straßen benötigen beispielsweise bei allen Seitenverhältnissen mehr Bäume als andere Ausrichtungen. Die

erforderliche Anzahl von Bäumen ist allerdings auf der Nordseite dieser Straßen höher. Dies liegt in der Tatsache begründet, dass in mittelschweren und tiefen Straßenschluchten die Südseite mehrere Stunden am Tag teilweise von Gebäuden beschattet wird. Die Ergebnisse der Anpflanzung von Bäumen in einem bestehenden städtischen Gebiet entsprechen weitgehend den Ergebnissen der theoretischen Studie, wobei aufgrund von Unregelmäßigkeiten im bestehenden Untersuchungsgebiet nur sehr geringe Unterschiede zu verzeichnen sind. Diese Ergebnisse zeigen, dass es für ein optimales Mikroklima für Fußgänger und die Nutzung von Bäumen wichtig ist, nicht nur das Seitenverhältnis und die Ausrichtung von Straßenschluchten zu berücksichtigen, sondern auf welcher Seite der Schlucht Bäume gepflanzt werden.

In Phase 3 werden die Effekte verschiedener Stadtformen und Baumdichten auf die dynamische, physiologische Äquivalenttemperatur (DPET) von Fußgängern, die weiter als die durchschnittliche Wegstrecke (750m) gehen, mit ENVI-met analysiert und bewertet. Diese Studie umfasst fünf verschiedene Gebiete im Großraum Kairo, der unter extremem Hitzestress leidet. Die Untersuchungsgebiete wurden aufgrund ihrer hohen urbanen Vielfalt in Bezug auf das Seitenverhältnis der Schluchten, die Ausrichtung, die städtischen Formen, die Grünflächen, die gemischte Landnutzung und die Baumdichte ausgewählt. Zwei Baumdichteszenarien werden analysiert: die derzeitige Baumdichte und ein Szenario mit erhöhter Dichte, bei dem jedes Gebiet bis zur vollen Kapazität erweitert wird. Die Ergebnisse zeigen, dass die DPET an jedem Punkt entlang der Gehstrecken andere Werte aufweist als die konstante physiologische Äquivalenttemperatur (SPET). Die DPET steht jedoch in engem Zusammenhang mit den Veränderungen der SPET. Einerseits führen längere Perioden mit niedrigeren oder höheren SPET-Werten zu einer Reduzierung oder Erhöhung der DPET-Werte. Andererseits stabilisieren häufige Schwankungen der SPET den DPET-Wert. Änderungen der DPET-Werte werden stärker durch die mikroklimatischen Bedingungen einzelner Räume oder Straßenschluchten beeinflusst als durch die Bedingungen des Gesamtgebiets und es hat sich gezeigt, dass die Kontrolle dieser mikroklimatischen Bedingungen innerhalb einer ganzen Straßenschlucht die DPET steuert. Die Veränderungen der DPET-Werte können auf verschiedenen Wegstrecken bis zu 10 °C erreichen, und in einigen Fällen kann eine Erhöhung der Baumdichte zu einer Senkung der DPET um bis zu 6 °C beitragen. Zusammenfassend bietet diese Forschungsarbeit einen wissenschaftlich abgesicherten Rahmen für die Optimierung der städtischen Begrünung, um extreme Hitze abzumildern und gleichzeitig Wasser zu sparen. Die Ergebnisse sind für die Entwicklung und Gestaltung nachhaltiger, klimaverträglicher städtischer Umgebungen von entscheidender Bedeutung.

Eidesstattliche Versicherung

Gemäß § 11 der Promotionsordnung der Fakultät Raumplanung der Technischen Universität Dortmund erkläre ich folgende Punkte:

1. Bei der eingereichten Dissertation zu dem Thema ” Developing a comprehensive strategy to optimize tree use for mitigating heat stress. Considering urban morphology and limited resources through dynamic and static thermal comfort analysis. A case study of Cairo city.“ handelt es sich um meine eigenständig erbrachte Leistung.

2. Ich habe nur die angegebenen Quellen und Hilfsmittel benutzt und mich keiner unzulässigen Hilfe Dritter bedient. Insbesondere habe ich wörtlich oder sinngemäß aus anderen Werken übernommene Inhalte als solche kenntlich gemacht.

3. Die Arbeit oder Teile davon habe ich bislang nicht an einer Hochschule des In- oder Auslands als Bestandteil einer Prüfungs-oder Qualifikationsleistung vorgelegt.

4. Die Richtigkeit der vorstehenden Erklärungen bestätige ich.

5. Die Bedeutung der eidesstattlichen Versicherung und die strafrechtlichen Folgen einer unrichtigen oder unvollständigen eidesstattlichen Versicherung sind mir bekannt.

Ich versichere an Eides statt, dass ich nach bestem Wissen die reine Wahrheit erklärt und nichts verschwiegen habe.

Dortmund, 15. July 2025

Ort und Datum

Ahmed Yasser Abdelmejeed

This Page Intentionally Left Blank.

Contents

List of Figures

List of Tables

List of Abbreviations

AR	Aspect ratio
DPET	(Dynamic) Physiological Equivalent Temperature
DI	Deficit irrigation
d	Index of Agreement
EPW	Energy plus weather format
ET	Evapotranspiration-based controller
FAR	Floor area ratio
H	Specific humidity
LAD	Leaf area density
LAI	Leaf area index
LCZ	Local Climate Zone
PET	Physiological equivalent temperature
UTS	Urban tree strategy
RH%	Relative humidity
SDG	Sustainable Development Goals
SMS	Soil moisture sensor-based controller
SPET	(Steady/Static) Physiological Equivalent Temperature
RMSE	Root Mean Square Error
RS	Rain sensor controller
SVF	Sky view factor
TA	Air temperature
T Skin	Skin temperature
T Core	Core Temperature
TMRT	The mean radiant temperature
UHI	Urban heat island
WS	Wind speed
WP	Water productivity

This Page Intentionally Left Blank.

Part I

Synopsis

This Page Intentionally Left Blank.

Chapter 1

1. Introduction

"We do have a choice: Creating tipping points for climate progress – or careening to tipping points for climate disaster. This is an all-in moment" said António Guterres the current secretary-general of the United Nations (Guterres. A, 2024). Furthermore, Ban Ki-Moon, the eighth secretary-general of the United Nations, once said, "Climate change is destroying our path to sustainability. Ours is a world of looming challenges and increasingly limited resources. Sustainable development offers the best chance to adjust our course"(Ki-Moon, 2012). In a similar vein, the Egyptian pioneer architect Hassan Fathy (1900-1989) shared "Build your architecture from what is beneath your feet" (Fathy. H, 1973). First and second quotes convey an important message about how much climate change is affecting us, and the third encourages the use of natural resources in development to mitigate this impact.

Climate change will substantially affect human and biological systems and likely alter the boundaries of climate variability beyond historical observations. Frequent heat waves and escalating temperatures and humidity have exacerbated heat stress. Heat waves and heat stress have caused widespread economic losses, reductions in crop yields, tree mortality, and water and energy shortages. Most concerning of all is the impact on human health and mortality (Ahmadalipour, 2019).

As a global action, the World Bank Group Partnership Fund for the Sustainable Development Goals (SDG Fund) was established to promote best practices and knowledge sharing for the implementation of the Sustainable Development Goals (SDGs) under the 2030 Agenda for Sustainable Development (Group, 2019). The 2030 Agenda for Sustainable Development was initiated by the United Nations in 2015, providing 17 SDGs to address the world's most pressing issues in terms of social, environmental, and economic development (Affairs, n.d.).

SDG 13: Action urges action against climate change by strengthening resilience and adaptive capacity to climate-related disasters, integrating climate change measures into policies and planning, and implementing the UN framework convention on climate change (Mortimer A, 2023).

This cumulative dissertation aims to present detailed research and recommendations under the umbrella of climate change and heat stress mitigation, thus promoting human wellbeing by creating better microclimate conditions, contributing to completely sustainable development, and raising awareness about the importance of heat stress mitigation and its various benefits.

This dissertation is structured as follows: Chapter 2 introduces the state of the art relevant to the three publications that form the framework of this dissertation. In Subchapter 2.4, the research questions are derived based on the identified knowledge gaps and desiderata. Chapter 3 summarizes the included studies. Chapter 4 discusses the obtained results and draws major conclusions through a synoptic integration of the contributions; the research questions are answered in the framework of this chapter. Chapter 5 explores the limitations of the included studies and outlines future research that builds on the insights gained from this work. The original published studies are attached in Part II (Publications).

Chapter 2

2. The State of the Art, Research Questions, and Methodology

It is crucial to develop healthy cities and communities, particularly in the context of climate change. Walking, considered the most widely used transport mode (Sauter, 2008), is a link between other transport modes, and engaging in pedestrian activities contributes to fulfilling recreational needs (Vasilikou, 2013). Individuals navigating interconnected spaces engage in active physical behavior, thus promoting sustainability and well-being. However, adverse weather conditions can lead to uncomfortable thermal sensations, potentially altering or diminishing the experiences of people walking outdoors (Vasilikou, 2020). Thus, it is crucial to enhance pedestrian thermal comfort and microclimate conditions.

2.1. Thermal Comfort

ASHRAE 55 defines thermal comfort (De Dear, 2022) as a mental condition in which individuals express satisfaction with their thermal environment. To regulate the body's metabolic rate and organ function, the body temperature should be maintained at approximately 36–37 °C (Fang, 2021).

The physiological equivalent temperature (PET) was designed to measure environmental and personal parameters, including air temperature, air humidity, air velocity, the mean radiant temperature (Tmrt), clothing insulation, and the level of activity, thus allowing for predicting thermal comfort (Taleghani, 2015). The assessment and analysis of thermal comfort can be carried out using two primary approaches. The first, which is assumed to be close to steady, is based on individuals' instantaneous subjective thermal sensation or comfort while sitting or standing (Hwang, 2022). In this research, this is named the steady PET (SPET). The second approach focuses on pedestrians' thermal comfort while walking. Thus, both the outdoor thermal environment and human physiological response play crucial roles as determinants of thermal comfort during the dynamic process of walking (Hwang, 2022). This is hereafter referred to as dynamic PET (DPET).

2.1.1. Difference between DPET and SPET

Pedestrians are subject to ever-fluctuating variations in microclimate conditions while walking outdoors. Their sensations may change along the course of a route, often exhibiting notable shifts in thermal perception. Physiological responses and the experience of thermal experiences are key factors influencing pedestrian thermal sensation. The steady thermal comfort model is only applicable to people who stay in outdoor environments for 10 to 30 min (Hwang, 2022) (Li, 2022) (Huang, 2020).

Thermal comfort indices and insights from earlier studies, derived from thermally homogenous and stable environments, are inadequate for effectively explaining the transient thermal perceptions of pedestrians exposed to constantly changing environmental conditions caused by urban geometry (Lau, 2019) (Katavoutas, 2015). Traditional environments with stable thermal conditions may sometimes fail to meet

people's needs, making dynamic thermal comfort a preferable alternative. An outdoor summer study examined participants who walked along a specific route, passing through diverse urban morphologies and experiencing a range of thermal environments that routine fixed-point observations could not capture (Nakayoshi, 2015). An analysis of changes in subjective perception and physiological parameters concluded that achieving thermal equilibrium requires 17–21 min to return to steady-state sedentary levels after walking (Jia, 2022). For an individual transitioning from a shaded sidewalk to a 200-meter-long sunny segment, their actual skin temperature approached the value simulated by a steady-state thermal comfort model after 180 seconds, while their core temperature was lower than the simulated value. Further suggestions estimated that around 30 min was required for a person to reach a steady state after leaving a room with thermal comfort to enter hot conditions (Höppe, 2002).

2.1.2. Thermal Comfort Parameters

Step changes in microclimatic conditions occur during alternating exposures to cool-biased and warm-biased environments, primarily characterized by combined variations in radiation, wind speed, humidity, and air temperature. Furthermore, these step changes occur at varying frequencies depending on the movement speed, activity demands, and environmental design. As such, people are subjected to highly dynamic and complex environments during outdoor activities, which are thought to elicit thermal responses distinct from those observed in relatively steady environments (Li, 2022). A prior study identified wind and solar radiation as the primary factors influencing variations in outdoor thermal comfort over a given period (Vasilikou, 2020). At a university campus in Hong Kong, a study was conducted from May to July with subtropical weather conditions. The study's results indicated that subjective thermal perceptions fluctuated with alternating exposure to sunlight and shade at different frequencies. Higher alternating frequencies resulted in reduced thermal dissatisfaction on hot summer days and a reduced need for shade (Li, 2022). In addition, the metabolic rate was a significant variable that impacted the DPET. Variations in this component should be given full consideration. Typically, walking indoors takes 3–5 min to reach new metabolic levels, whereas it takes 9–11 min in a transition space. Moreover, metabolic levels return to normal sedentary levels within 3–5 min following the cessation of walking, both in indoor and transition spaces (Zhang Y. L., 2020).

2.2. Urban Cooling Strategies

To achieve efficient urban cooling, two approaches can be utilized. The first includes the modification of urban morphology and geometry in new communities. This can be achieved by adjusting the orientation and aspect ratio of urban streets. The second approach integrates environmental elements into existing urban areas, including features like vegetation and cooling materials such as trees, greenery, cool-colored surfaces, roof and vertical gardens, and water bodies (Doick, 2013) (Stewart, 2011) (Ramadan, 2010).
This research specifically focuses on enhancing the microclimate conditions of existing areas, with a particular focus on vegetation. Shady trees, along with other vegetation elements such as small trees, bushes, lawns, ground coverage, and climbing plants, help enhance urban climate conditions by providing shade and facilitating evapotranspiration in urban areas and streets (Stewart, 2011) (Ramadan, 2010) (Pearlmutter, 2000). The findings of previous studies have demonstrated that mature trees with sufficient foliage density could absorb at least 60% of solar radiation (Rowntree, 1991). Additionally, it has been shown that the temperature beneath trees is 5°C lower than the surrounding

environment, and the temperature above agricultural land surfaces is 3°C lower than the surrounding area (Doick, 2013). Furthermore, urban trees can reduce the 2 m air temperature by 2 °C to 9 °C (Déoux, 2004).

2.2.1. Urban Morphology

Urban morphology, sky view factor (SVF), and shading play significant roles in enhancing microclimate conditions and mitigating UHI effects (Rodríguez-Algeciras, 2018) (N. E. Theeuwes, 2014). The shadow-casting effect of buildings reduces the radiant load on pedestrians, thereby improving thermal comfort, particularly in high-density cities, despite a reduction in ventilation (Morakinyo T. E, 2017) (Ketterer, 2014). Notably, shallow canyons are more prone to adverse thermal conditions compared to deeper canyons (Morakinyo T. E, 2017). Increasing the SVF through urban configuration choices can reduce the intensity of UHIs (Yola, 2020). Deep urban canyons are effective in reducing solar radiation during the daytime. Consequently, thermal comfort levels in open spaces (i.e., high SVF) are generally lower than those in shaded spaces (i.e., low SVF) (Wang Y. B., 2016). The analysis results thus confirm that thermal comfort is primarily influenced by solar radiation exposure (Andreou E., 2013). Against this background, it can be concluded that shading from direct radiation plays a more significant role in enhancing thermal comfort than the effects of increased radiation absorbance due to urban reflectance.

The meteorological parameters influencing physiological equivalent temperature (PET) can be managed and improved through urban morphology (Matzarakis, 2008). In particular, mean radiant temperature (Tmrt) is a critical factor in regulating the human energy balance and serves as a metric for assessing thermal comfort (Morakinyo T. E., 2016). Maintaining Tmrt below 45 ˚C is an essential target (Rodríguez-Algeciras, 2018). Conversely, air temperature and specific humidity have proven to be the least modifiable by urban configurations, indicating limited influence on their values (Abdollahzadeh, 2021) (Ketterer, 2014). Outdoor thermal comfort levels are significantly reliant on the speed and direction of urban wind flow (De, 2018). Wind speed has been widely reported to affect urban heating, with a strong negative correlation between wind speed and air temperature (Memon, 2010). These PET-related meteorological parameters—alongside urban shading and the SVF—can be optimized using urban morphology and geometry strategies, such as adjusting street canyon aspect ratios and orientations (Kolokotsa, 2022) (Jamei, 2020) (Morakinyo T. E., 2016) (Ketterer, 2014).

2.2.1.1. Aspect Ratio Effect

The aspect ratio (AR), or the height-to-width ratio (H/W) of an urban canyon, is a critical metric commonly used to assess the impact of urban geometry on outdoor environments (Abdollahzadeh, 2021) (Balany, 2020). The aspect ratio significantly influences daily net solar radiation gains on road and wall surfaces. Additionally, shadowing effects on surrounding buildings play a vital role in shaping the radiation environment within urban street canyons (Takebayashi, 2012). Moreover, enhanced shading due to increased H/W ratios can substantially reduce PET values (Lan, 2021) (Morakinyo T. E., 2016) (Emmanuel, 2007). A strong association exists between the UHI effect and aspect ratio during nighttime. For example, a study in Basel, Switzerland, found a linear relationship between the intensity of the maximum nighttime UHI and the SVF, which is directly influenced by the aspect ratio (Hamdi, 2008). Moreover, there are variations in air temperature between higher and lower aspect ratios (Memon, 2010). Air temperatures slightly decrease as

aspect ratios increase, although radiation fluxes, as expressed by the mean radiant temperature, are far more influential (de Lieto Vollaro, 2014).
In Osaka, roads with aspect ratios greater than approximately 1.5 (W/H) experience large daily net solar radiation gains. Roads with aspect ratios between 1.0 and 1.5 (W/H) are also within the target range for effective urban heat island mitigation measures, with particular attention needed for the north sides of east–west roads and the centers of north–south roads (Takebayashi, 2012). In Malaysia, an aspect ratio of 2–0.8 is recommended for the six asymmetrical aspect ratios of Putrajaya Boulevard. This configuration reduces surface temperatures by 10 to 14 ˚C and air temperatures by 4.7 ˚C, enhancing the boulevard's microclimates and mitigating tropical heat islands. For roads oriented northeast to southwest, aspect ratios of 0.8–2 effectively reduce morning microclimates and nighttime heat islands; the negative daytime effects, however, outweigh the positive nighttime effects (Qaid, 2015). On Wall Street, New York City, winter and summer analyses reveal high daytime air temperatures along the widest street canyon, where the aspect ratio is 0.33 (Pioppi, 2020). Increasing the aspect ratio by 0.5 can decrease the maximum mean radiant temperature by an overage of 2.90 ˚C in the early morning and late afternoon, thereby lowering the PET (Abdollahzadeh, 2021). In Tokyo, surface temperature comparisons of east–west- and north–south-oriented streets revealed that the shading effects of tall buildings in north–south street canyons are less impactful on solar gains than those in east–west streets. Tall buildings and narrow canyons reduce the SVF and increase shaded areas on surfaces, thus resulting in lower daytime temperatures but higher nighttime temperatures within the canyons (Lan, 2021).

2.2.1.2. Street Orientation Effect

Street orientation significantly alters the urban microclimate by affecting the exposure of canyon surfaces to direct solar radiation. North–south (N–S)-oriented streets are fully exposed to solar radiation at midday but are mostly shaded in the early morning and late afternoon. Conversely, east–west (E–W)-oriented streets are fully exposed in the early morning and late afternoon, resulting in greater overall sunlight exposure (Abdollahzadeh, 2021) (Aboelata A., 2020) (Balany, 2020) (Andreou E. &., 2012) (Emmanuel, 2007). North–south-oriented streets are cooler than those with east–west orientations, with thermal comfort levels increasing with higher H/W ratios (Jamei, 2020). This is because east–west-oriented canyons remain exposed to sunlight throughout the day, regardless of their H/W ratio, while north–south-oriented canyons experience sunlight only during specific times (Jamei, 2020). A study on urban heat island mitigation measures identified the north side of east–west roads and the center of north–south roads as key areas requiring intervention (Takebayashi, 2012). An orientation angle between 30° and 60° with the wind direction, along with a canyon aspect ratio of 2.5, can reduce PET values by 5 to 9 ˚C across most of the study area during midafternoon on summer days (De, 2018). In Sydney (Abdollahzadeh, 2021), north–south-oriented streets were found to offer superior levels of thermal comfort compared to east–west-oriented streets, with PET values showing 12.33% of daytime conditions within a comfortable range. Streets oriented NE–SW provided the highest thermal comfort level, averaging 24.95%, while streets with a NW–SE orientation were assessed as least favorable.

2.2.1.3. Combined Effect of Aspect Ratio and Street Orientation

Street orientation and canyon aspect ratio profoundly impact the urban microclimate, directly affecting street-level thermal comfort. In particular, PET values at the street level are strongly dependent on the aspect ratio and street orientation (Aboelata A., 2020)

(Lobaccaro G. A., 2019) (De, 2018) (Andreou E., 2013) (Andreou E. &., 2012) (Emmanuel, 2007). Street geometry and orientation determine solar radiation absorbance by street surfaces, as well as urban canyon airflow (Nastaran Shishegar, 2013). For E–W-oriented streets, those with W/H ratios greater than two should be fully shaded only during the hottest and coolest months of the year (Jamei, 2020). Streets with E–W orientations exhibit the most unfavorable conditions across all H/W ratios (up to 3.0). Increasing H/W ratios on E–W streets does not significantly enhance PET values (Andreou E., 2013). Mitigating heat stress along E–W-oriented streets is challenging, as walls provides only limited shading, even with proportions as high as H/W 4:1. Conversely, N–S-oriented streets with high aspect ratios—equal to or greater than H/W 2:1—provide a more favorable thermal environment, characterized by lower PET maxima and shorter periods of intense heat stress (Jamei, 2020) (Andreou E., 2013). Additionally, thermal stress can be mitigated in street canyons with a northwest–southeast orientation and an AR of at least 1.5. Such configurations can help reduce heat stress, increase the frequency of comfortable thermal conditions, and ensure year-round solar access in midlatitude regions (Ketterer, 2014).

2.2.2. Trees and Vegetation

Among the various vegetation strategies used to enhance microclimate conditions, planting trees is the most effective for lowering urban surface temperatures. A study in Port Fillip demonstrated that combining green rooftops with urban trees resulted in the greatest reductions in air temperature. The reduction reached 2.4˚C at the pedestrian level of the street (Bruse, 1999). Similarly, research carried out in Ho Chi Minh City showed that the PET value was reduced by 6°C in shaded areas compared to only 1°C in unshaded areas. Among the scenarios analyzed, urban tree planting exhibited the greatest impact on improving thermal comfort (Huynh, 2012). A study conducted in Dubai suggested prioritizing only the application of trees, as the outcomes of the urban tree scenario were almost identical to those involving a combination of all other vegetation elements (Rajabi, 2011). In Balbo, researchers evaluated five greenery planning scenarios across three typical street canyons in Balbo, concluding that green surfaces yielded the most significant impact, with PET reductions of 2 °C (Lobaccaro G. &., 2015). In arid regions, trees also excel in mitigating heat. A study in the Phoenix Metropolitan area revealed their capacity to lower urban surface and air temperatures by approximately 2°C to 9°C and 1°C to 5°C, respectively (Upreti, 2017). Further analysis of small residential neighborhoods in the same area identified an ideal shading scenario: achieving 25% shading coverage in urban canyons was most effective in enhancing thermal comfort (Middel, 2015).
Case studies from various parts of the world highlight the significant role of vegetation in urban climate adaptation, with trees emerging as the most effective solution. Notably, scenarios utilizing only trees scenario have demonstrated outcomes comparable to those involving a combination of all vegetation elements.

2.2.2.1. Efficient Morphological Characteristics of Trees

Trees contribute significantly to cooling through two primary mechanisms: providing shade and facilitating evapotranspiration (Stewart, 2011) (Ramadan, 2010) (Pearlmutter, 2000). Among these, shade is particularly crucial, as it distinguishes trees from other vegetation types that do not offer similar benefits (Lobaccaro G. &., 2015) (Sodoudi, 2014) (Huynh, 2012) (Rajabi, 2011) (Bruse, 1999). The shading and cooling effects of trees are influenced by their physical characteristics, including shape, size, density, and leaf features (Zhang J. G., 2023) (Zhang J. K., 2022) (Rahman M. A., 2018) (Shahidan, 2010). Each tree species possesses unique attributes that determine its growth, structure,

physiology, and capacity to cool its surroundings (Monteiro, 2019). Key factors such as canopy size, density, and leaf properties play a critical role in enhancing the cooling effects of trees. In particular, tree canopies are integral to creating favorable microclimatic environments, caused by their cooling effect (Rahman M. A., 2018) (Kong F. Y., 2016). Vegetation canopy characteristics are crucial for predicting thermal mitigation in urban areas and selecting the most effective species for urban greening efforts (Kong F. Y., 2016). Canopy shapes, as well as the arrangement and density of leaves and branches, impact the level of shading provided. Trees with broad canopies and dense foliage offer more efficient shading (Monteiro, 2019). Among the various tree parameters, the leaf area index (LAI) is a key parameter affecting light penetration and the below-canopy microclimate (Kong L. L., 2017) (Lin, 2010). The leaf area, determined by the crown diameter and LAI, plays a critical role across all three cooling mechanisms: transpiration, solar radiation reflection, and shading (Liu Y. L., 2023) (Zhang J. G., 2022) (Monteiro, 2019) (Kong L. L., 2017) (Kong F. Y., 2016) (Lin, 2010). Thus, it can be concluded that urban trees exert species-specific effects, primarily dependent on canopy characteristics. However, leaf traits, the LAI, and the surrounding microclimate also contribute significantly to mitigating urban heat (Kong F. Y., 2016).

2.2.2.2. Urban Tree Performance Within Different Aspect Ratios and Orientations

Urban trees play a role in mitigating surrounding building mass effects and creating lower SVF environments, which are cooler both during daytime and nighttime (Wang Y. B., 2016). Urban morphology and vegetation shading influence the storage of solar radiation storage during summer days, significantly contributing to UHI mitigation (Wang Y. B., 2016). Shade provision is particularly important during the summertime, as outdoor activities between 10:00 and 15:00 in unshaded areas are generally not recommended. Incorporating canopies and vegetation is necessary to facilitate outdoor activities during these heat peaks (Rodríguez-Algeciras, 2018). In open-set high-rise urban areas, the presence of trees could substantially reduce pedestrian-level thermal stress (Lobaccaro G. A., 2019). Moreover, trees are an effective solution for improving thermal conditions on streets, particularly those with nonoptimal orientations or low-rise buildings (Abdollahzadeh, 2021). For example, in a study of streets angled at 30° from the north with an aspect ratio of 1.0, continuous shaded zones were created by buildings along both parallel and perpendicular streets, thus eliminating the need for additional vegetation. However, when the aspect ratio decreased, the increased distance between buildings created a need for shade-providing trees on the streets, particularly for those in the perpendicular direction (De, 2018). Trees are especially impactful on E–W streets. Research has shown that they significantly reduce PET values, particularly for the south-facing side of the street (Andreou E., 2013). Furthermore, increasing vegetation density in shallow urban canyons (H/W = 0.5) can realize PET increases of more than 4% compared to low-density vegetation in similar urban canyons (Abdollahzadeh, 2021).

2.2.3. Urban tree selection and planting considerations

When selecting urban tree types, it is crucial to consider not only their climatic adaptability but also other factors, such as whether the species are native or adaptive to the region and the most efficient methods for irrigation.

2.2.3.1. Tree Adaptation to Local Conditions (Water Demand and Tolerance)

Trees should be selected based on their ability to thrive in a city's local climate and effectively counteract the UHI effect. Key factors also include the average and maximum

temperatures of the warmest month, propagation efficiency, and tolerance to drought, high pH, and saline soil (Zalesny Jr, 2011).
It is important to also consider tree type—evergreen or deciduous—as cooling effects could be effectively doubled on clear, hot days in comparison to cloudy, cold days. Furthermore, evergreen trees can produce slight decreases in temperatures in the wintertime, with weather conditions exerting little influence on their microclimate impact. However, their ability to block wind and sunlight may have undesirable effects, such as reducing warming in colder months (Wang Y. B., 2015). Moreover, water demand varies significantly across species (Elmasry, 2014). Trees requiring low to moderate water supplies are generally the most suitable for urban environments. As such, water demand should be a critical factor in selecting the most appropriate species.

2.2.3.2. Efficient Irrigation Technology

Globally, irrigation accounts for the largest level of water consumption (Fereres, 2007). Environmental experts and policy makers promote the enhancement of water irrigation efficiency, as this would conserve precious water resources for environmental and urban use (Ward, 2008). Emerging irrigation techniques and technologies offer promising solutions to enhance water use efficiency and reduce overall consumption. One such technique is deficit irrigation (DI), which involves applying water at levels below full crop-water requirements. Deficit irrigation is a valuable strategy for minimizing water use during irrigation while maintaining productivity, particularly when full irrigation is not feasible (Fereres, 2007). A well-designed deficit irrigation regime can optimize water productivity (WP) across a given area. Another effective method, widely believed to conserve water, is the drip irrigation system (DP), which can complement deficit irrigation practices. The drip irrigation allows for precise water delivery to the root zones of plants, thus minimizing losses to run-off or deep percolation. Compared to traditional flood irrigation, drip irrigation not only conserves water but also enhances evapotranspiration and crop yields (Zalesny Jr, 2011) (Ward, 2008).
The use of software in irrigation systems allows for precise calculations of water requirements based on soil parameters and weather conditions. However, many irrigation operators lack access to real-time weather data systems and often rely on historical data to estimate irrigation requirements. Integrating irrigation systems with live weather forecast websites ensures frequent updates about current weather data, thereby enhancing daily irrigation efficiency (Nada, 2014). To further enhance water efficiency and conservation, software can be supplemented with other sources of real-time weather data and data on site conditions. Automating landscape irrigation scheduling offers convenience while reducing water use and maintaining high landscape quality (Dukes, 2012). Various types of irrigation controllers can be used to reduce irrigation levels, including evapotranspiration-based controllers (ETs), soil moisture sensor-based controllers (SMSs), and rain sensor controllers (RSs).

2.3. Greater Cairo—The Study Area

2.3.1. The Climate of Greater Cairo

Greater Cairo's metropolitan area lies in a hot, arid desert within a subtropical climatic zone, classified as having a warm summer climate under the Köppen–Geiger climate system (Kottek, M., 2006). This environment is defined by high air temperatures, there is intense solar radiation, and the prevalence of the urban heat island (UHI) effect. Despite its limited rainfall, humidity levels often remain high due to the influence of the Nile River

Valley. Seasonal temperature variations in Cairo are pronounced. During wintertime, temperatures range from 9°C to 24.8°C, while summertime brings higher averages between 20.1°C and 34.7°C, with peaks occasionally exceeding 40°C during extreme heat events (Abou El-Magd, 2016). The summer months, particularly between June and August, are marked by hot, dry conditions, with an average temperature of 28°C (Abutaleb K. N., 2015). The high levels of solar radiation not only contribute to thermal discomfort but also provide opportunities for energy generation via solar power stations (Panagiotis Kosmopoulos, 2018). These adverse conditions, however, impact the well-being and thermal comfort of local residents, with occupational heat stress affecting workers' health, safety, productivity, and social well-being (Nunfam, 2018). Cairo's population was approximately 20.5 million in 2012 and is projected to increase by 11.2 million people by 2050. Consequently, this population increase will intensify the demand for residential housing, resulting in greater city density. Consequently, the UHI effect and air temperatures are likely to worsen as the city expands, leading to heightened anthropogenic heat emissions (Fahmy, 2009) (Rizwan, 2008) (Pearlmutter, 2000).

2.3.2. UHI Effects on Greater Cairo

An urban study conducted in 2015 revealed that air temperatures were significantly higher in downtown Cairo compared to cooler suburban areas (Abutaleb K. N., 2015). This highlights the UHI phenomenon, which causes above-average increases in surface temperatures in urban areas of Cairo. These temperature increases range from 0.5 to 3.5°C. The maximum difference observed was 10°C compared to the surrounding surfaces (Taheri Shahraiyni H. S.-Z., 2016) (Abutaleb K. N., 2015). Land surface temperature analyses further indicate these increases reached 7.8˚C during summer and 2.1˚C during winter (Abou El-Magd, 2016) (Abou El-Magd, 2016) (Taheri Shahraiyni H. S.-Z., 2016) (Abutaleb K. N., 2015). These findings confirm the presence of the UHI effect in Cairo, contributing to significant discomfort, particularly during nighttime hours.

2.3.3. Scarcity of Greenery and Water in Cairo

Cairo experiences high levels of heat stress, thus affecting both quality of life and human health. Thus, increasing the number of trees and vegetation levels should, thus, be prioritized; however, Cairo faces challenges such as limited greenery and severe water scarcity. Currently, more than half of the city's population has access to less than 0.5 m2 of green space per person—a strikingly low ratio compared to the city's average of 1.7 m2 (Hamdy, 2022). In recent years, Greater Cairo has seen a notable decline in green spaces, with many trees removed to widen road lanes in an effort to ease traffic congestion. This has further diminished the already limited greenery levels throughout the city. Figure 1 illustrates neighborhoods such as Heliopolis, ElNozha, Nacr City, and Masaken Cheraton, that witnessed the removal of trees and green spaces to facilitate road expansion and alleviate traffic.

Water scarcity exacerbates the challenge of restoring greenery in the city. Egypt relies heavily on external water sources, with 98% of its freshwater originating outside its borders. The Nile River alone supplies over 95% of the country's water needs, presenting a significant challenge for decision makers tasked with addressing water policy (El-Nashar, 2018) (Abdin, 2009).

Egypt's per capita freshwater availability has drastically declined, dropping from 1893 m3 in 1959 to 875-950 m3 in 2000 and further to 670 m3 in 2017. Projections estimate this figure will further decrease to 536 m3 by 2025 (El-Sadek, 2010) (Abdin, 2009). This decline is driven by rapidly increasing water demands resulting from rapid population growth,

urbanization, rising living standards, and an agricultural policy aimed at expanding production to sustain the growing population. Domestic water use also reflects this trend, increasing from 3.1 BCM in 1990 to 5.23 BCM in 2000 (Abdelhaleem, 2015). Compounding these challenges, in 2011, the Ethiopian government announced the construction of a dam on the primary water source of the Nile River (El-Nashar, 2018).

2.3.4. City Urban Morphology

The Greater Cairo Metropolitan Area boasts the largest urban area in Africa and ranks as the eleventh largest city in the world (Taheri Shahraiyni H. S.-Z., 2016). A study found that Cairo's land cover was 233.78 km2 in 1973, growing to 557.87 km2 in 2006, more than doubling in size over this period. The urbanization rate over this period was 9.8 km2 per year (Mohamed, 2012). This rapid urban expansion occurred on both agricultural and desert lands (Hassan A. A., 2011), driven by formal and informal rapid growth patterns. As a result, Cairo's density and size have experienced massive increases, leading to the development of diverse urban morphologies and fabrics.

2.4. Research questions and methodology

This cumulative dissertation aims to develop a comprehensive strategy to improve climate conditions in metropolitan areas experiencing extreme heat stress. The strategy focuses on optimizing urban morphologies and tree use while tailoring solutions to the unique local conditions of cities, thus ensuring applicability. The outcomes of the strategy will be analyzed at various levels of detail to provide a thorough understanding of how to optimize the use of limited city resources and achieve the best possible results.

This study applies the strategy to Greater Cairo, a city facing extreme heat stress, significant urban diversity, a severe lack of greenery, and limited water resources. These challenges make it an ideal case study for testing the strategy and achieving the research objectives.

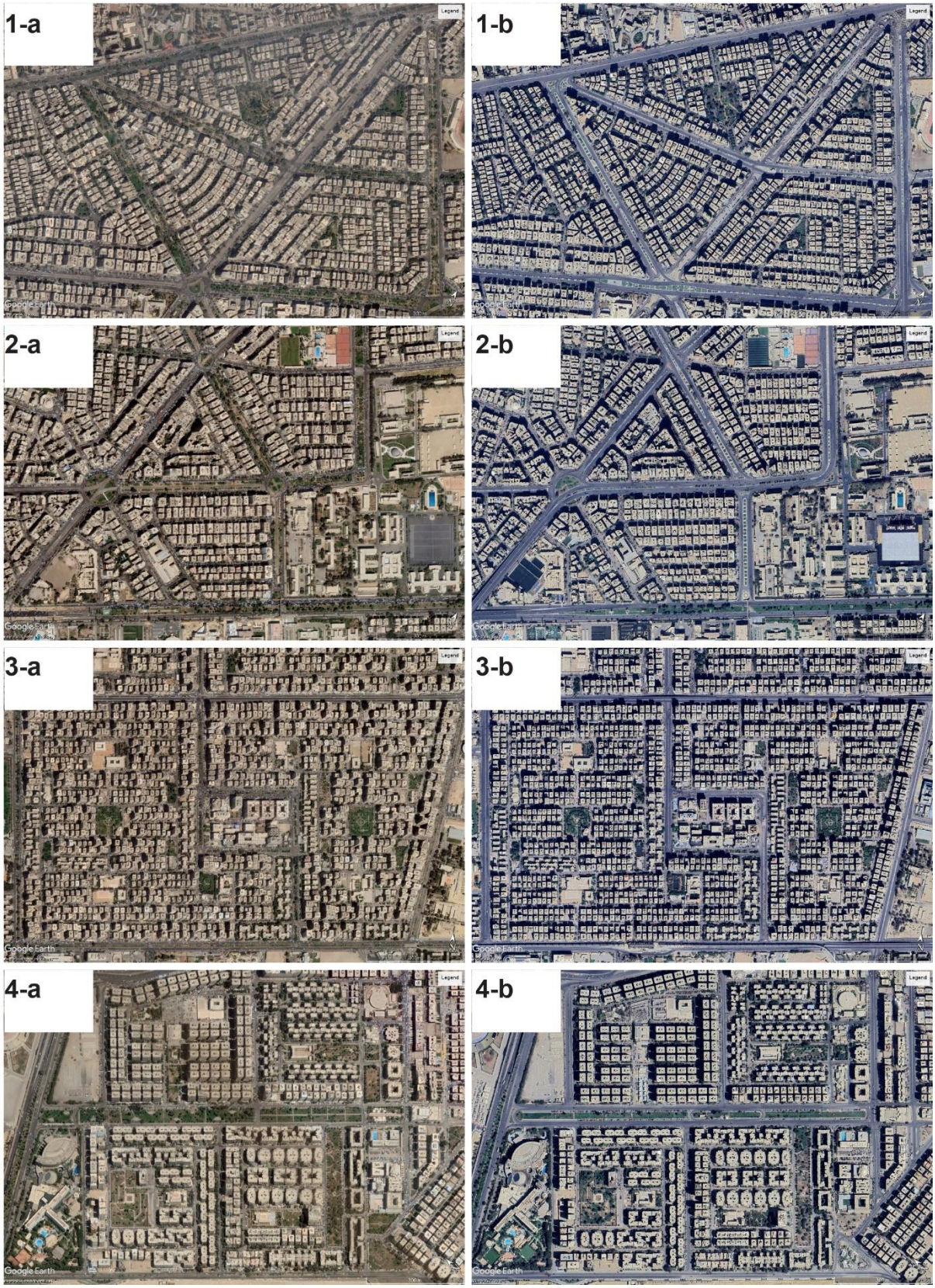

Figure 1. 1—Heliopolis, 2—ElNozha, 3—Nacr City, 4—Masaken Cheraton before (a) and after (b) renovation. All maps were exported from ''Google Earth Pro''. The image on the left was exported in September 2013 and the one on the right in September 2023.

2.4.1. Research questions:

Based on the scientific discussions present, the contributions of this cumulative dissertation are dedicated to developing a scientific study and addressing the main research questions (RQs), which represent the scientific gaps this research seeks to fill.
The epistemological focus of this work is articulated through the following research questions, which are addressed through the publications produced as part of this dissertation:

RQ1. What is the impact of implementing a comprehensive urban tree strategy that considers climate conditions and water scarcity on the city of Cairo?
RQ2. How could a detailed analysis and understanding of the different steady PET cases optimize the use of trees?
RQ3. What is the relationship between dynamic PET and steady PET, and how does analyzing both optimize the use of trees?
RQ4. How could implementing a comprehensive, complete, and detailed strategy that considers city conditions enhance climate conditions and optimize the use of resources?

2.4.2. Research Methodology

To answer the research questions and achieve the research objectives, three stages of research (corresponding to three publications) were conducted in Greater Cairo. While RQs 1, 2, and 3 are addressed in publications (1), (2), and (3), respectively, and discussed in Chapters (3.1), (3.2), and (3.3), RQ 4 requires a synthesis of the findings from all three papers and is addressed in Chapter (4), as shown in Figure 2.
This study is divided into three stages: The first stage involves developing an efficient urban tree strategy UTS tailored to the local conditions of Greater Cairo, addressing challenges such as water scarcity and limited greenery. Stage 2 investigates the various microclimate conditions in greater detail, analyzing how urban tree use can be optimized within different urban canyons. Stage 3 introduces a temporal dimension to the study by considering dynamic thermal comfort for pedestrians. This stage compares and evaluates pedestrian experiences as they move through different urban canyons with varying different tree densities and shading conditions.

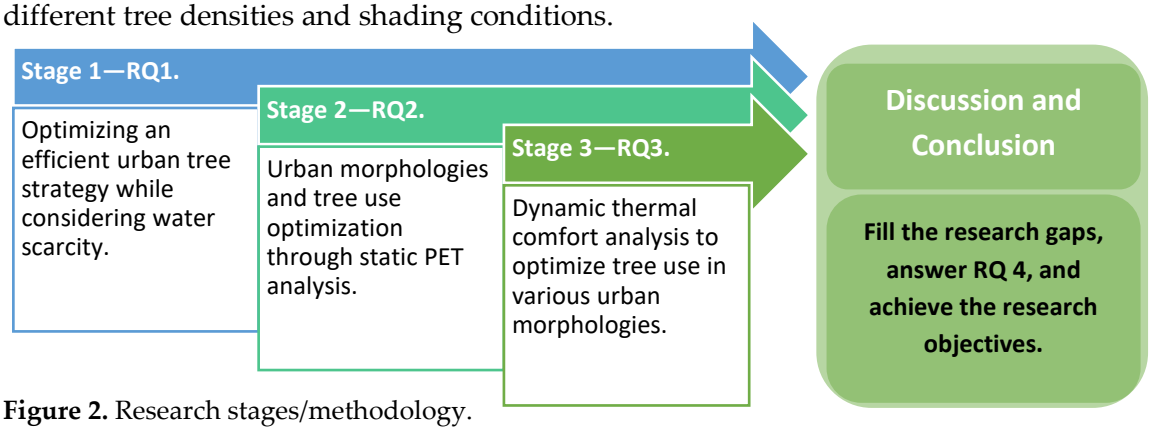

Figure 2. Research stages/methodology.

2.5. Scientific Contributions

The following chapter offers brief summaries of the publications produced as the framework of this dissertation. In Part II, which includes the article PDFs, each paper is preceded by an information box summarizing key details. It highlights information on character counts, review modalities, and the author's contributions to each publication. The three articles presented were published between 2023 and 2024, and all are available as open-access publications.

This Page Intentionally Left Blank.

Chapter 3

Scientific Contributions

3.1. Optimizing an efficient urban tree strategy to improve microclimate conditions while considering water scarcity: a case study of Cairo

The first publication proposes a comprehensive green strategy to improve thermal comfort and mitigate UHI effects within Cairo. This strategy focuses on utilizing the most effective urban greenery elements, with urban trees identified as the most suitable element based on findings from previous studies. This study seeks to develop an urban tree strategy for the entire metropolitan area of Cairo, accounting for Egypt's limited water resources. In particular, given that trees consume one of the largest quantities of water among greenery elements (Elmasry, 2014), significant amounts will be required to irrigate the large number of trees proposed for planting across the city. This strategy aims to exert positive impacts that not only support its implementation but also raise public awareness about the value and application of urban trees. This, in turn, could help curb the ongoing removal of trees in urban areas.

3.1.1. Urban Tree Strategy Stages

Figure 3 illustrates the three steps involved in the strategy: (1) choosing appropriate tree species, (2) implementing effective irrigation methods, and (3) determining the optimal number of trees.

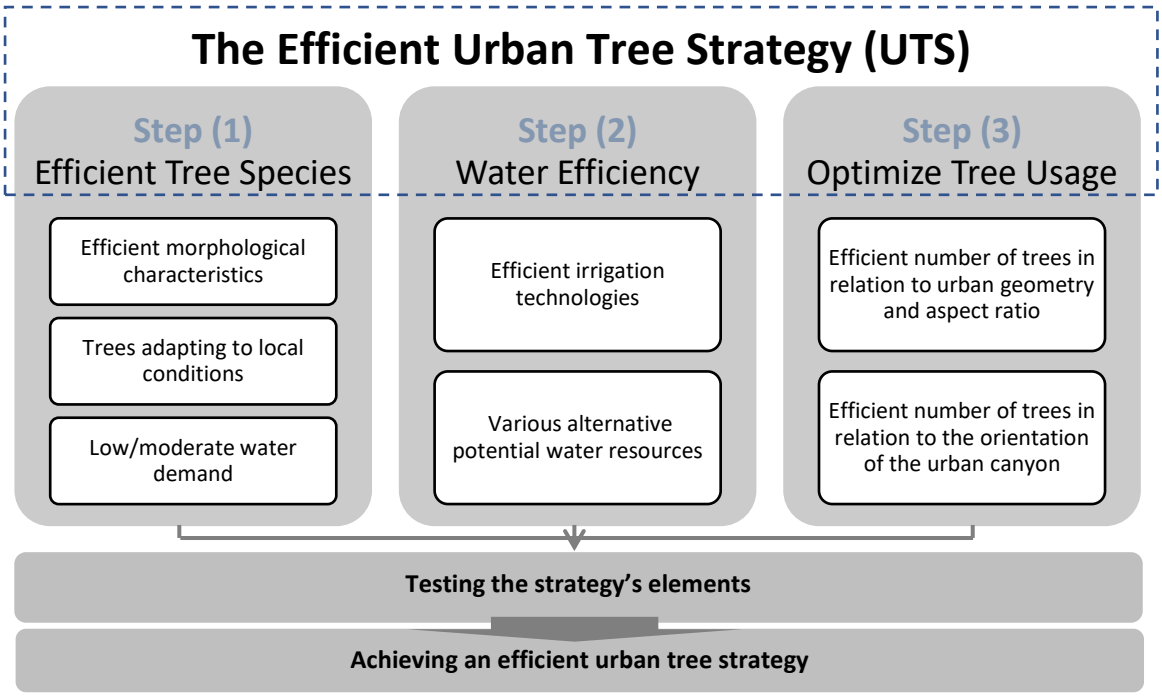

Figure 3. First publication's methodology.

3.1.1.1. UTS Step 1: Efficient Tree Species

The tree species(s) selected for the UTS should consume minimal water to align with the study's objective, as Cairo faces severe water scarcity and lacks sufficient greenery. Implementing this strategy across the metropolitan area will require the planting of millions of trees, thus highlighting the importance of carefully considering tree species. While the water consumption and cooling effects of a single tree may seem negligible, their cumulative impact can be substantial when applied across the city. To ensure the most appropriate species are chosen, all relevant parameters must be considered. Microclimatic shading and air-cooling efficiency can vary significantly among tree species (Konarska, 2016) (Rahman M. A., 2015) (Armson, 2013) and are influenced by morphological characteristics, such as the shape, canopy size and density, and foliage features (Rahman M. A., 2018) (Georgi, 2010) (Shahidan, 2010). A comparative study of these characteristics is, thus, essential to determine which tree species will provide optimal benefits while remaining within the city's environmental and resource constraints.

Based on insights from previous studies, the selection of tree species for urban planting should be guided by the following criteria:

- Canopy size: Trees with larger canopies are essential and should be categorized as trees that provide shade.
- Tree density: Species with a higher LAI are preferable.
- Tree type: Deciduous trees are generally favored over evergreen species.
- Adaptability to local conditions: Trees that require excessive water or are intolerant to salinity and drought should be avoided.

These selection criteria were applied to a database of 114 trees listed in the *Plant Guidebook for Al-Azhar Park and the City of Cairo* (Elmasry, 2014). As detailed in the corresponding publication, minor differences in the crown size, water demand, LAI, and tolerance to drought and salinity were observed among the tree species evaluated. Ultimately, 21 tree species were shortlisted (in part II, page 85), conferring the following advantages:

- The diversity in tree sizes allows for planting in various urban morphologies, such as differing street widths, streetscapes, and urban canyon configurations.
- As 21 species were shortlisted, visual esthetics are enhanced, contributing to the city's image while improving biodiversity and creating more naturally vibrant streetscapes.

3.1.1.2. UTS Step 2: Irrigation Technologies

This study aims to evaluate water usage during irrigation, comparing traditional time-based systems with advanced technologies such as SMSs and RSs. SMSs, in particular, have been proven to be highly effective, reducing water irrigation use by up to 65% compared to traditional systems (Haley, 2012).

Minimizing water consumption is crucial, but identifying alternative water sources is equally essential for irrigation. Given that Egypt cannot solely rely on the Nile River to meet rising water demands, the country has turned to non-conventional methods, such as wastewater reuse, to meet future requirements (Zalesny Jr, 2011). Data from the Holding Company for Water and Wastewater in 2013 indicate that Egypt produces approximately 9.6 mcm of treated wastewater daily, totaling around 3.5 bcm annually (Wahaab, 2011). This volume represents 6.5% of the Nile's total water supply. These alternative water sources are vital to supporting the greening strategy proposed in this study, making its implementation feasible and sustainable.

Calculating water demand is a crucial step in evaluating the UTS. Water demand is influenced by three key factors—the plant factor, evapotranspiration, and tree crown sizes—all of which vary across tree species. Cooling effectiveness for trees highlights the

importance of large canopies to maximize tree coverage. However, increasing canopy coverage also markedly increases water demand. This demand can be managed by sufficiently decreasing total tree coverage and number. Achieving a balance between desirable tree coverage for thermal comfort and water demand is necessary to avoid compromising either cooling efficiency or optimal water usage.

3.1.1.3. UTS Step 3: Tree Amounts and Shading Percentage

The impact of tree coverage percentage can vary based on the aspect ratio and orientation of street canyons (Lin, 2010). In Athens, a study analyzing air temperature patterns under different tree coverage scenarios found that the outcome variations were primarily caused by tree coverage percentages and aspect ratios within urban canyons (Shashua-Bar, 2010). In Phoenix, a study demonstrated that an increase in tree coverage from 0% to 25% could reduce air temperature by 4.4°C (Middel, 2015). However, a Hong Kong study recommended a tree coverage of 56% to enhance microclimate conditions most effectively (Ng, 2012). Notably, a study conducted in Cairo proposed 50% tree coverage as ideal for enhancing thermal comfort in dense urban areas (Aboelata A., 2019). Against this background, the tree coverage percentage should vary depending on the type of urban canyon, aspect ratio, and street orientation. A detailed study is necessary to determine each urban canyon's optimal tree coverage percentage. This ensures the implementation of an efficient tree strategy, avoiding issues caused by insufficient or excessive tree coverage.

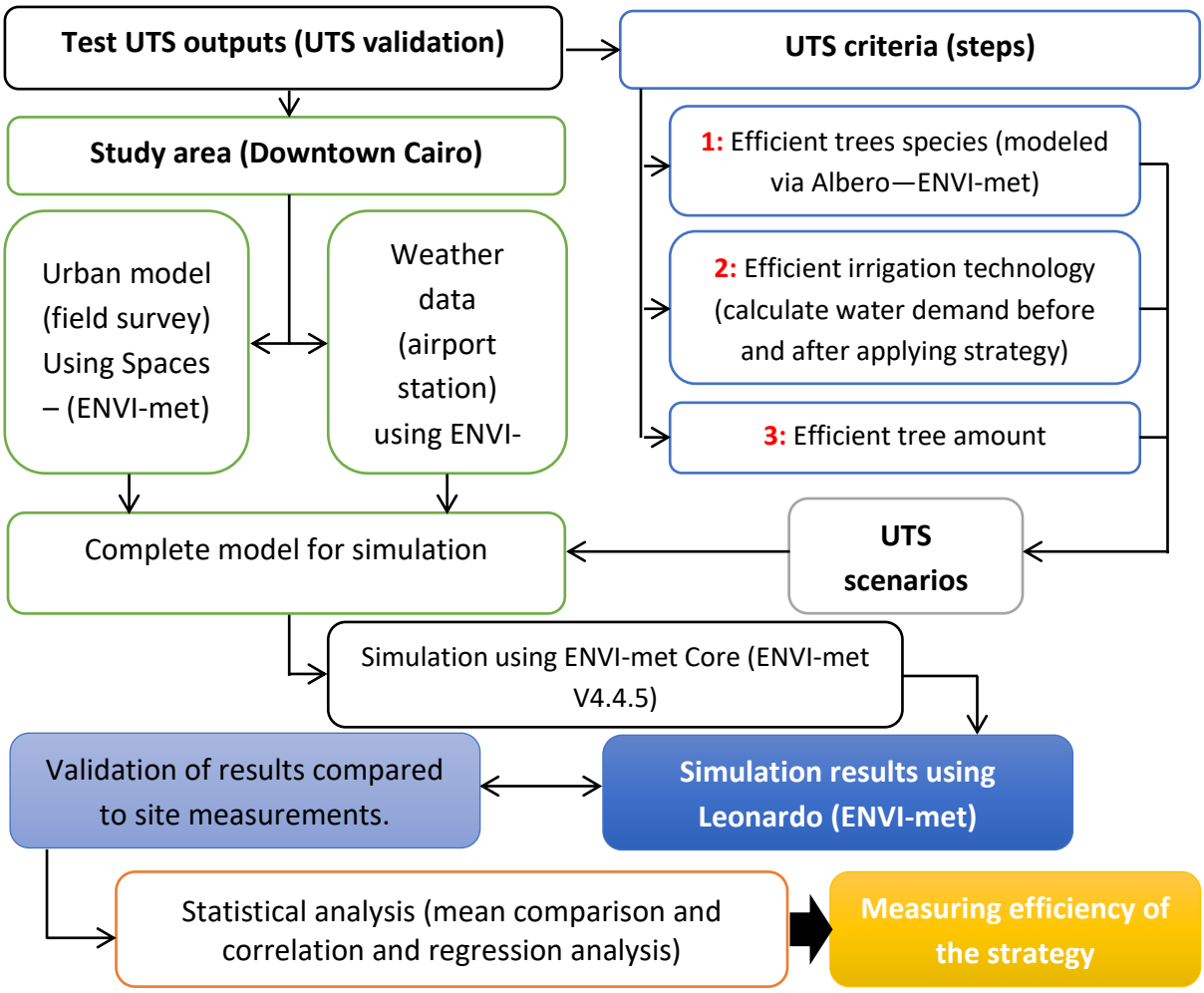

Figure 4. Method of testing and validating the UTS criteria.

3.1.2. Methodology for Testing the Strategy

Figure 4 illustrates the method for testing the efficiency of the UTS. ENVI-met simulations are conducted to evaluate its impact on the microclimate conditions and assess its applicability and effectiveness in Cairo. Moreover, a comparison between the ENVI-met simulation results for the current state of the study area and the outcomes after applying the UTS criteria was carried out.

3.1.2.1. The study area

The study area was situated in Cairo's downtown area, where the UHI effect is most pronounced (Taheri Shahraiyni H. S.-Z., 2016) (Abutaleb K. N., 2015). Figure 5 depicts the study area location and elements.

Figure 5. Study area location. A. Location within the downtown area. B. Streets selected for the study. C. Old and new images of the study area. D. Field survey photos of the existing trees.

3.1.2.2. Different Scenarios

As illustrated in Figure 6, the UTS outcomes (Step 3) will guide the application of four different scenarios to selected inner streets within the study area. Each scenario is designed to evaluate different tree coverage percentages: scenario A—0%, scenario B—20%, scenario C—35%, and scenario D—50%. Each scenario will be evaluated during both summertime and wintertime, thus additional winter scenarios labeled e, f, g, and h. Due to the presence of deciduous trees, which lose their leaves in winter, the tree coverage percentages in winter scenarios will differ from those in the summer scenarios. The

outcomes of these scenarios will be compared with the baseline for both summer and winter conditions.

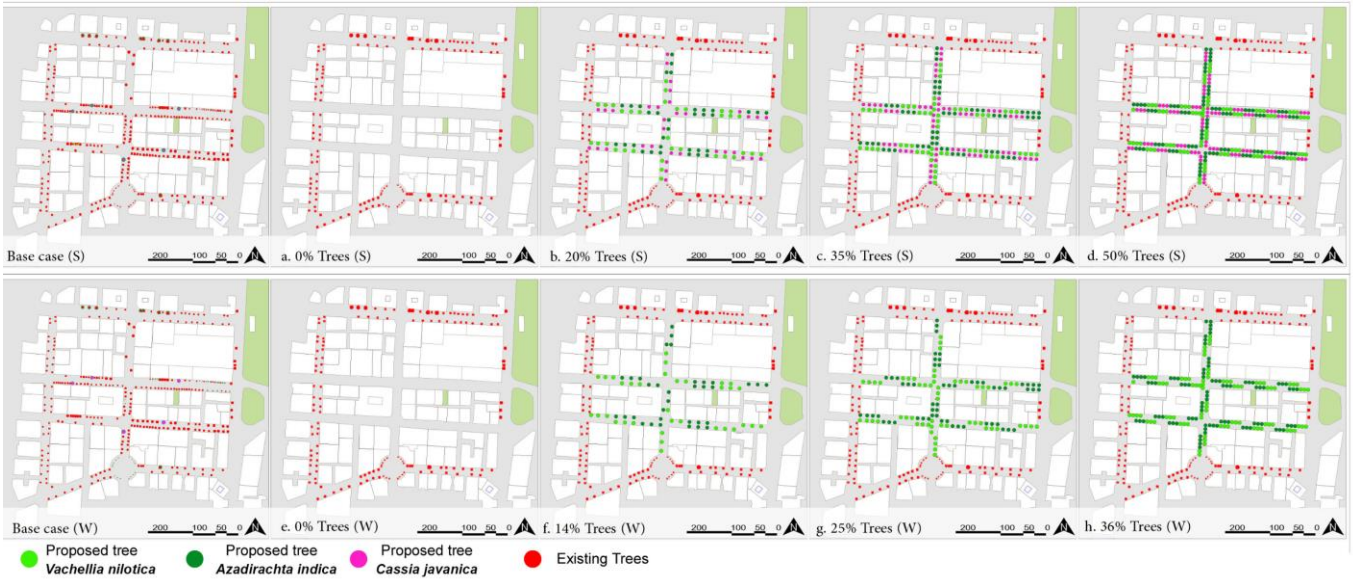

Figure 6. All tree scenarios proposed for both summer and winter.

3.1.3. Comparison of PET Results During Summer

A comparison of the summer PET values across all streets reveals that adding trees to urban canyons generally improves PET values. To gain a more comprehensive understanding of this effect impact, a more detailed hourly analysis is carried out. This approach assesses the impact more precisely and provides recommendations for incorporating trees into various urban canyon configurations.

3.1.3.1. Comparison of Mean PET Values for S1 Scenarios During Summer

The application of varying urban tree coverage percentages to S1 only slightly improved its mean PET values. As Figure 7 illustrates, the PET values for the baseline scenario remain within the hot range during peak hours and throughout the day. In addition, the PET values for this scenario are almost identical to those using 0% tree coverage, with a maximum difference of -0.37˚C, an average difference of -0.04˚C, and most differences being less than -0.1˚C. These findings indicate that planting numerous trees with small crowns would not significantly improve thermal comfort in this urban canyon, thus aligning with theoretical recommendations for an efficient UTS (Rahman M. A., 2018) (Smithers, 2018).

Applying 20% tree coverage to S1 slightly increases the PET values, with maximum and average reductions of -0.83°C and -0.10°C, respectively, during the daytime. Although this scenario performs better than one without trees, the PET enhancement remains minimal. Moreover, applying 35% tree coverage to S1 results in more pronounced improvements in the PET values, reaching maximum and average reductions of -0.69˚C and -0.41˚C, respectively, during the daytime. Although this scenario shows greater effectiveness than a no-tree scenario, the enhancement in the PET values during the daytime also remains minimal. During nighttime, PET values increase slightly but remain within a comparable range.

Applying 50% tree coverage to S1 results in a greater enhancement in PET values, with a maximum reduction of -1.52˚C and an average reduction of -0.79˚C during the daytime. While this leads to slight improvements in thermal comfort, the improvement is not significant enough to shift the thermal range. Across all scenarios (20%, 35%, and 50%), the PET values were higher during nighttime compared to the daytime; however, these increases were considered minor and did not significantly affect the thermal range.

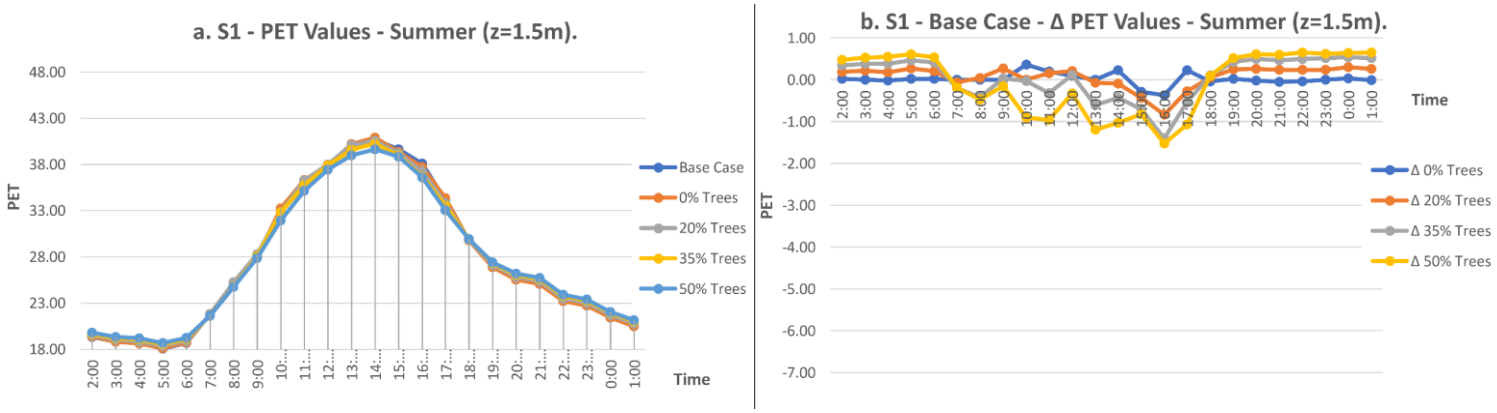

Figure 7. a. S1—mean PET values for S1 scenarios, b. S1—base case ΔPET for summer (01-07-20).

3.1.3.2. Comparison of Mean PET Values for S2 and S3 Scenarios During Summer

The application of varying levels of urban tree coverage to S2 and S3 significantly improves their mean PET values. As illustrated in Figure 8, the PET values for the baseline scenario during peak hours and daytime fall within the extreme heat stress zone. Additionally, the PET values for this case are nearly identical to those for the scenario with 0% tree coverage, with a maximum difference of 0.04˚C, an average difference of 0.02˚C, and most differences being less than 0.01˚C. These results indicate that planting numerous trees with very small crowns in both urban street scenarios (S2 and S3) does not lead to any meaningful improvement in thermal comfort, which also aligns with theoretical recommendations for an efficient UTS (Rahman M. A., 2018) (Smithers, 2018).

Applying 20% tree coverage results in noticeable improvements in PET values, with daytime reductions reaching maximums of -3˚C and -3.16˚C in S2 and S3, respectively. The average daytime reductions are -1.55˚C in S2 and -1.89˚C in S3, representing a considerable improvement compared to the 0% tree coverage scenario. During nighttime, PET values remain within a smaller range, with a maximum reduction of -0.35˚C in both streets. Increasing the tree coverage percentage to 35% further enhances PET values, achieving maximum reductions of -4.71˚C in S2 and -4.51˚C in S3 during the daytime. The average reductions during the daytime are -2.69˚C in S2 and -3.18˚C in S3, representing notable enhancements. During the nighttime, PET values show slight additional reductions, reaching a maximum of -0.55˚C in both streets.

The application of 50% tree coverage resulted in substantial improvements in the PET values, achieving maximum reductions of -6.36˚C in S2 and 6.49˚C in S3 during the daytime. The average reductions during the daytime are -3.95˚C in S2 and -4.66˚C in S3. These are marked enhancements, particularly during peak hours, where average reductions are -3.56˚C in S2 and -4.41˚C in S3. The PET values are higher during the nighttime and reach a maximum of -0.7˚C in both streets.

The overall impact of applying different tree coverage percentages is substantial, markedly improving thermal comfort and shifting the thermal comfort zone in S2 at 11:00, 12:00, 16:00, and 17:00 and in S3 at 11:00, 12:00, and 17:00. These PET reductions effectively

transition the thermal comfort zone from extreme heat stress to strong heat stress. Figure 9 illustrates the effects of tree coverage at 13:00 and 15:00.

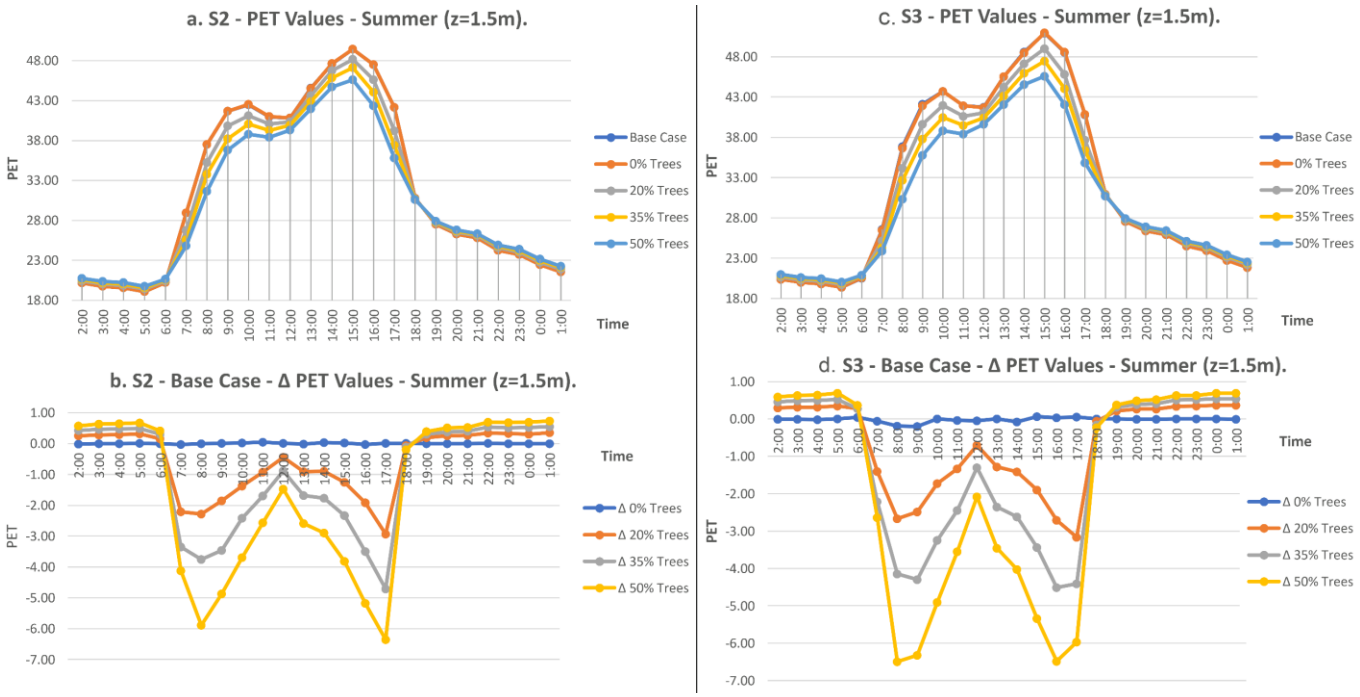

Figure 8. a. S2—mean PET values for S2 scenarios, b. S2—base case ΔPET, c. S3—mean PET values for S3 scenarios, d. S3—base case ΔPET for summer (01-07-20).

3.1.3.3. Comparison of PET Values During Winter

A comparison of the PET values across all streets in the wintertime demonstrates that adding trees to the urban canyons does not significantly reduce PET values. This impact usually goes unnoticed due to the cooler microclimate conditions during winter, as simulations were conducted on January 1st, which is considered the middle of winter. Generally, the absence of trees in urban canyons during the winter does not negatively affect human thermal comfort. Similarly, the inclusion of different tree species—whether evergreen or deciduous—does not significantly alter the microclimate conditions during this season.

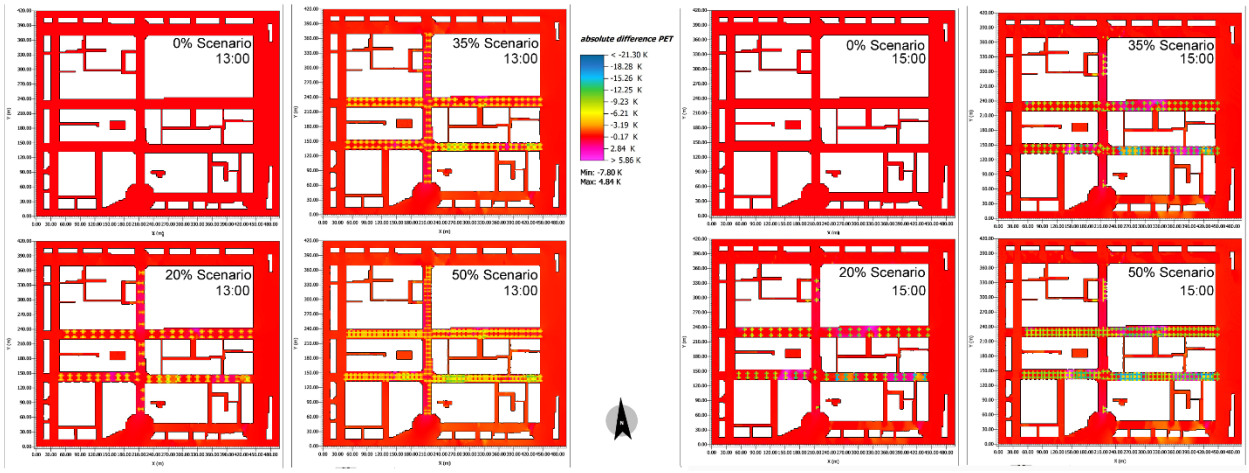

Figure 9. PET reduction values for each scenario compared to the base case (on the left at 13:00, and on the right at 15:00 on 01-07-20) Z = 1.5m.

3.1.4. Comparing Summer PET Parameter Results for S2 and S3

To identify the key factors contributing to the enhancement in the microclimate conditions in S2 and S3, a detailed analysis should be conducted by examining all thermal comfort parameters for both streets. Measurements should be taken at a central point in each street (R2, and R3), allowing for consistent comparison. Parameters such as air temperature

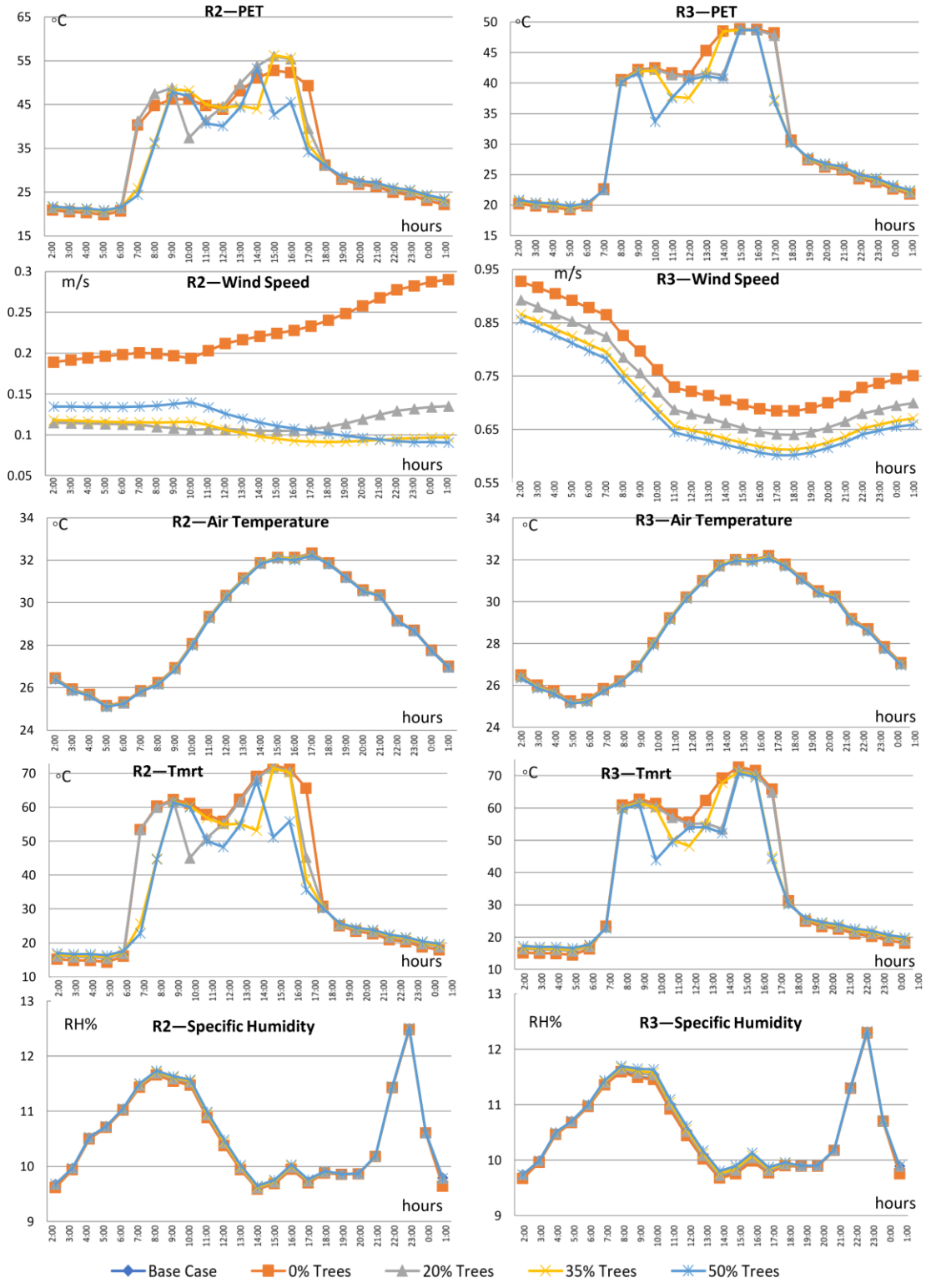

Figure 10. Comparison between PET, WS, TA, TMRT, and H for R2 and R3.

(TA), wind speed (WS), TMRT, and specific humidity (H) should be analyzed to determine which factors are most influenced by the presence of trees and how these changes contribute to meaningful improvements in PET values. As shown in Figure 10, a comparison of results for both R2 and R3 reveals that adding trees significantly impacts WS and TMRT. These changes can be attributed to the shading provided by trees, which reduces the TMRT, and their physical obstruction of the wind, which decreases wind speed. However, no substantial changes are observed in the air temperature and humidity of either street before or after the addition of trees.

3.1.4.1. The Impact of Adding Trees on Air Temperature and Humidity

The addition of trees results in minimal improvements in air temperature, with a maximum reduction of -0.124˚C at 17:00 in R3 and -0.113˚C at 16:00 in R2. However, this slight change is not considered a significant factor contributing to the observed enhancements in
PET values. Similarly, the impact on specific humidity was negligible, with maximum reductions of 0.09% at 10:00, 11:00, and 12:00 in R2 and 0.17% during the same hours in R3.

3.1.4.2. The Impact of Adding Trees on Wind Speed

As shown in Figure 11, the addition of trees to all streets causes significant reductions in wind speed. This effect is due to the vertical obstruction created by trees planted along both sides of the street. The extent of this impact varies between streets, as wind speed is influenced by the various street orientations. While S1 is oriented toward the north, S2 and S3 are oriented toward the east. Figure 11a compares wind speed values for the baseline scenario at the receptor points within each street (R1, R2, and R3). As shown in the figure, S1 experiences significantly higher wind speeds due to its northern orientation, which aligns with Cairo's prevailing wind direction. In S1, wind speeds range from 3.25 m/s to 2.86 m/s, remaining within the comfort range of 1 m/s to 5 m/s (Guo, 2015). Conversely, S2 and S3, with their eastern orientation opposing Cairo's prevailing wind direction, exhibit significantly lower wind speeds. These values range from 0.29 m/s to 0.19 m/s in R2 and 0.74 m/s to 0.92 m/s in R3, which are minimal compared to those of S1. While planting trees reduces wind speed across all streets, the extent of this reduction varies. In S1, trees reduce wind speeds by -1.7 m/s to -1.8 m/s in R1

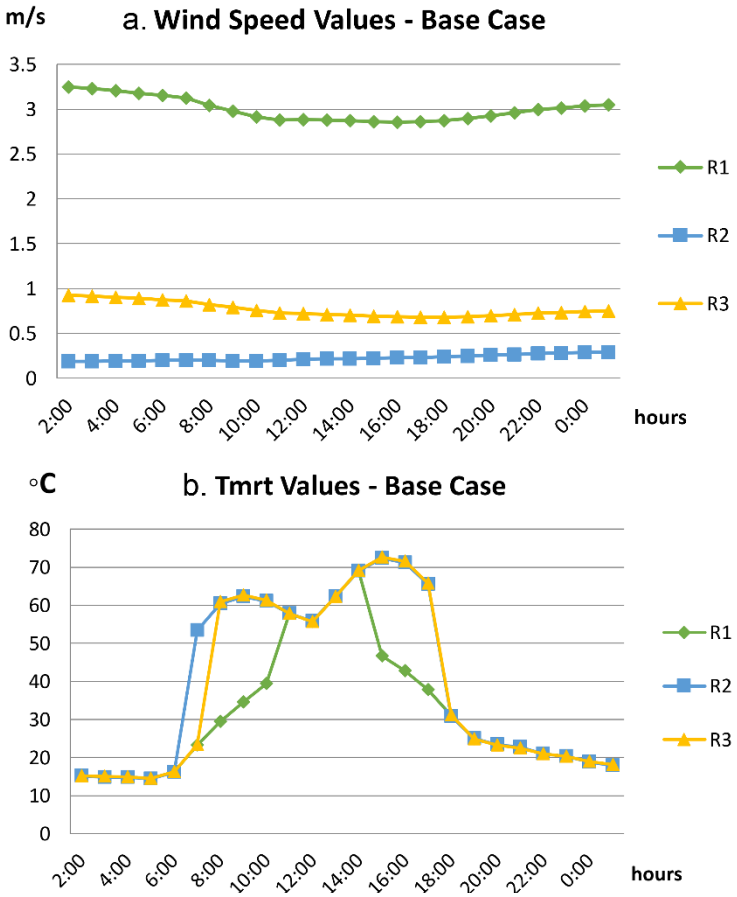

Figure 11. a. Wind speed values. b. Tmrt values for the base case for R1, R2, and R3.

during the day—more than double the maximum wind speeds recorded in S2 and S3. By comparison, the reductions in wind speeds are much smaller in S2 and S3, reaching -0.05 m/s to -0.2 m/s in R2 and -0.07 m/s to -0.09 m/s in R3.
The addition of trees to both S2 and S3 has a negligible impact on their PET due to the already extremely low wind speeds in both streets. As a result, further reductions in wind speed do not significantly influence their PET values. Instead, other factors may play a more critical role in enhancing the PET values in S1 and S2, as shown in Figure 10. Conversely, the wind speed reduction in S1 is quite significant, with wind speed reduced to nearly half its original value. However, the improvements in the PET values in S1 remain quite limited. This indicates that while planting trees in S1 significantly reduces wind speed, it does not result in marked improvements in PET values.

3.1.4.3. The Impact of Adding Trees on TMRT

Figure 11.b demonstrates the obvious influence on the TMRT values for R2 and R3. The changes observed in the TMRT stand out as the most significant compared to the other measured parameters shown in Figure 10. This highlights the critical role of tree shading in urban areas, which effectively reduces total radiant temperature, including solar radiation, at the pedestrian level within urban canyons. In S2, the addition of trees led to notable reductions in TMRT at R2, with maximum decreases of -21.3°C at 15:00, -15.4°C at 16:00, and -29.9°C at 17:00. Similarly, in S3, the maximum TMRT reductions at R3 were recorded as -17.0°C at 17:00 and -21.6°C at 14:00. As illustrated in Figure 10, the PET and TMRT charts closely mirror each other, with nearly identical reduction values for both streets. This correlation indicates that the substantial improvement in PET is directly driven by the significant reductions in TMRT. In contrast, the minor TMRT reductions in S1 correspond to a negligible enhancement in PET, further emphasizing the strong relationship between these two parameters. Figure 11b illustrates the TMRT values for all streets under the base case scenario. During the daytime, when solar radiation is present, TMRT values in S1 are considerably lower than in S2 and S3 due to differences in street orientation. The addition of trees plays a critical role in shielding the street canyon at the pedestrian level from intense solar radiation. In S2 and S3, where TMRT values are much higher, the introduction of trees significantly reduces TMRT, resulting in substantial improvements in PET for both streets. In contrast, S1's northern orientation naturally limits solar exposure, and its TMRT values are already lower. As a result, the addition of trees does not further reduce TMRT, leading to only minor enhancements in PET.

3.1.5. Correlation Between PET and TMRT

A strong relationship exists between TMRT reduction and PET enhancement within urban canyons, particularly at the pedestrian level. To analyze this relationship, a statistical analysis was conducted using SPSS. The correlation study examines the results of the 50% tree coverage scenario in R3. Before calculating the correlation between the two variables, the Kolmogorov–Smirnov (K-S) test is conducted on all input data to ensure data follow a normal distribution. The test results

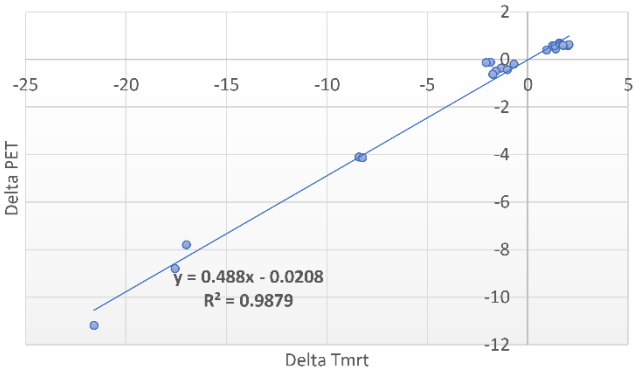

Figure 12. Correlation between ΔPET and ΔTMRT.

informed the choice of the appropriate correlation method. As data were not normally distributed, Spearman correlation was applied. Figure 12 reveals a strong positive correlation in the study, with a correlation coefficient of r=0.898, indicating a significant relationship between ΔTMRT and ΔPET. Regression analysis yields an R^2 value of 0.9879 and a significant F-value of <0.001, confirming that the study results are reliable and statistically significant. The co-efficiency value can be calculated as Y=0.488x-0.0208. These findings statistically validate the strong relationship between ΔTMRT and ΔPET, further emphasizing the direct association between shading and PET enhancement.

3.1.6. Comparison of Water Demand

Different scenarios necessitate varying numbers of trees and tree coverage percentages. While the 20% and 35% tree coverage scenarios require fewer trees compared to the existing baseline scenario, both scenarios demand increased water for irrigation due to their higher coverage percentages. The primary advantage of these scenarios is the reduced maintenance requirements, as fewer trees are needed overall. Table 1 presents the irrigation required for each scenario relative to the baseline. The percentage changes are calculated based on variations in canopy coverage, which is the primary determinant of water demand. To avoid increased water demand while maintaining thermal comfort improvements, the recommended urban tree strategy should prioritize the lowest feasible tree coverage percentage. Additionally, the irrigation and planting technologies proposed in Step (2) should be implemented to further reduce water demand.

Table 1. Water demand increases/decreases relative to the baseline scenario.

Scenario	Tree coverage %	Number of trees	Water demand increase (+)/decrease (-)	Water demand decrease based on irrigation and planting technology criteria -65%
Base Case	9%	195	0	0
0%	0%	0	-9%	-9%
20%	20%	102	+11%	+3.85%
35%	35%	174	+26%	+9.1%
50%	50%	256	+41%	+14.35%

3.2. Optimization of Microclimate Conditions Considering Urban Morphologies and Urban Trees Using ENVI-met: A Case Study of Cairo City

The second publication aimed to optimize the integration of various urban morphologies, characterized by differing aspect ratios and orientations, and urban tree densities—low and high—to identify any significant correlations and optimize the microclimate conditions for the case study area. The research objectives extended beyond addressing knowledge gaps about how different urban canyons respond to extreme microclimate conditions. It also explored methods for integrating urban canyons with varying tree densities and assessing the performance of these trees within various configurations. Unlike previous studies, which predominantly focused on enhancing the entire canyon, this study specifically emphasized the sides of canyons. These areas are particularly important as they accommodate pedestrian activities, such as walking, sitting, and standing, while central portions are reserved for vehicles. The research findings aim to assist urban designers and landscape architects in making informed decisions about the most appropriate decisions in terms of aspect ratios, street orientations, and tree densities from an urban climate perspective in the context of project development in Greater Cairo.

3.2.1. Materials and methods

To achieve the research objectives, a study was conducted to analyze and test the characteristics of urban morphology with and without varying tree densities. This analysis was conducted over two stages (Figure 13): Stage (1) involved creating a theoretical model representing common urban canyons in Cairo city along different orientations. This model was initially tested without trees and then with different tree densities. Stage (2) applied the outcomes of the theoretical model to an existing case study in downtown Cairo, focusing on areas with similar aspect ratios and orientations. To gain an in-depth understanding of the relationship between urban canyons and tree densities, both stages analyzed both sides of the urban canyon. This approach is critical for understanding how each side (where pedestrians walk) responds to climate conditions. It also explored how changes in aspect ratio, orientation, and tree density affect thermal comfort and UHI effects at the pedestrian level. By studying both sides of the street, the research yielded more accurate and detailed results. For instance, one side may be shaded by buildings, while the other is fully exposed to direct solar radiation (Elbardisy, 2021). This disparity influences the optimization of tree placement, aligning with water efficiency strategies. Such considerations are particularly important for water scarcity in Egypt (Osman, 2016).

3.2.1.1. Stage (1): Theoretical Model

In Stage (1), a theoretical model representing varying aspect ratios and orientations was developed. These urban characteristics are highly common in Cairo (Step (a)). Tree scenarios were then applied to the base case (Step (b)) to evaluate their effects. This analysis was conducted by comparing the results from both steps.

3.2.1.2. Stage (1): Step (a) Theoretical Model (Base Case)

The evaluated range of aspect ratios varied between very shallow and very deep, with six aspect ratios developed (H/W: 3:1, 2:1, 1:1.5, 1:1, 0.5:1, and 0.25:1), covering the majority of urban canyon configurations within the city. Six aspect ratios were developed and oriented in four directions, spaced 45 degrees apart. These orientations represented the primary directions: north–south, east–west, northeast–southwest, and northwest–southeast. Consequently, the theoretical model's base case included 24 scenarios.

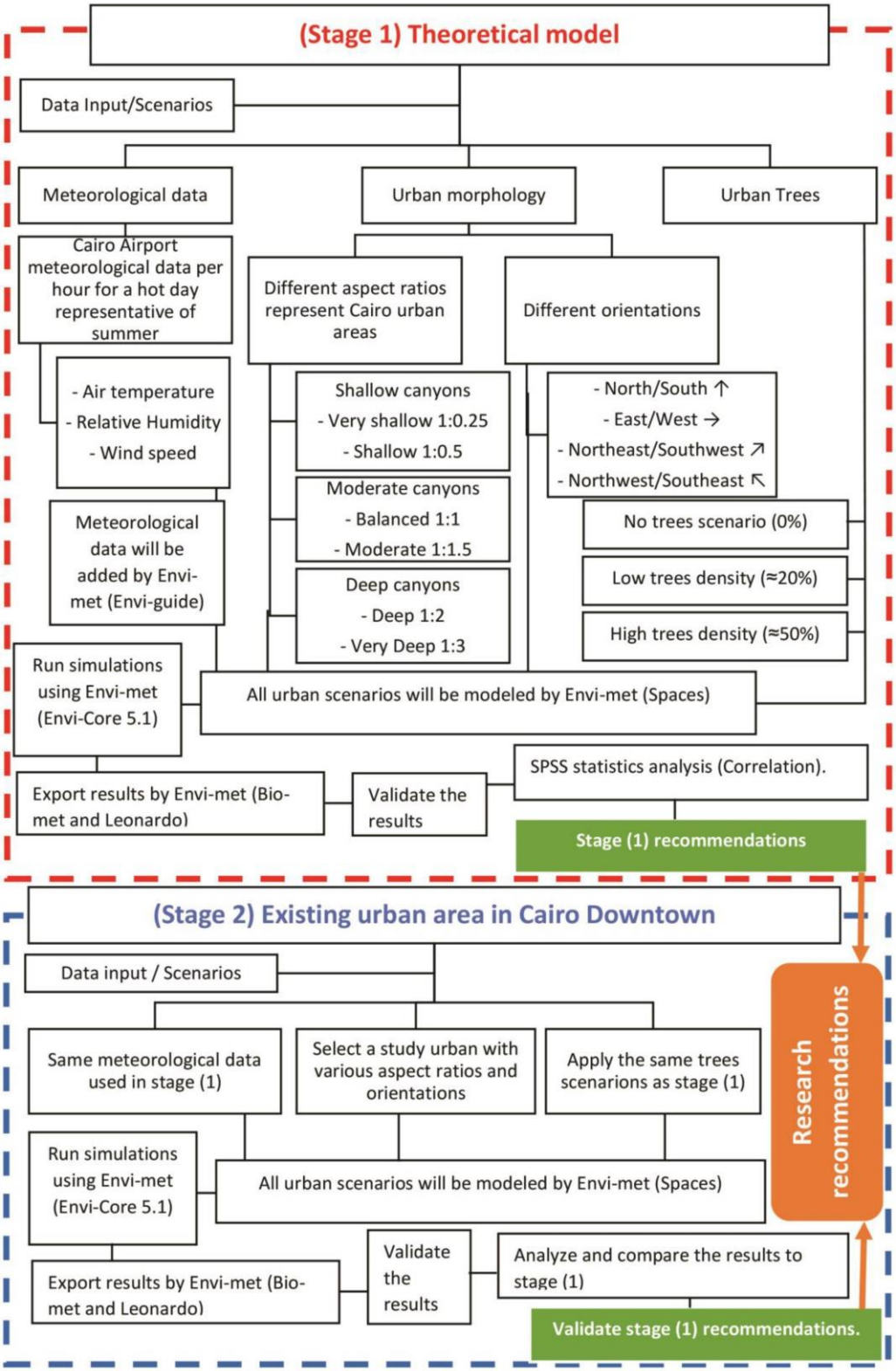

Figure 13. Second publication methodology.

Figure 14 shows the theoretical model's baseline scenario, including a shading analysis for the various aspect ratios and different orientations. To comprehensively understand how each urban canyon responds and performs, both sides of each canyon were analyzed and compared using receptors (i.e., measuring points), as shown in Figure 14A; hence, the total number of base cases increased to 48.

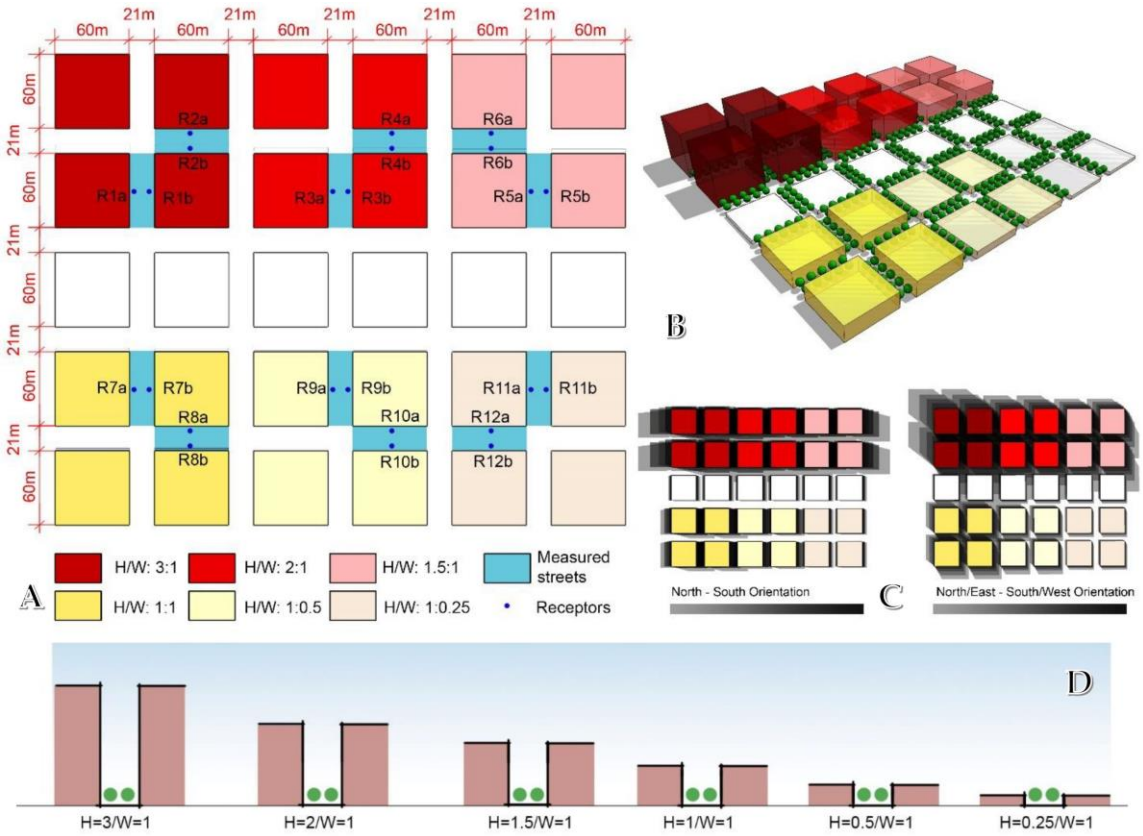

Figure 14. The theoretical model's urban geometry. (A) Plan showing the measured canyons and receptors' locations. (B) A 3D view. (C) Shading analysis. (D) AR cross-sections.

3.2.1.3. Stage (1): Step (b) Tree Scenarios

Tree scenarios were developed and incorporated into baseline scenarios to compare the results of scenarios with trees to those without, enabling an understanding of the trees' effects on each street and side. Two tree scenarios were created to represent two tree densities: low density (≈20%) and high density (≈50%). After adding the tree scenarios to the base case, the total number of cases increased to 144 (48 base cases; 96 tree scenario cases). This number was sufficient for comparing diverse urban configurations with different aspect ratios and orientations, as well as for integrating different tree scenarios. The tree scenarios were applied to all urban canyons, accounting for different aspect ratios and orientations. Measurements were conducted on both sides for all tree scenarios to ensure a comprehensive analysis. The performances of both canyon sides in each scenario were compared to gain deeper insights into the interaction between urban canyons and urban trees. These findings provide critical guidance for urban designers and landscape architects, thus enabling informed decision making when developing areas in Cairo.

3.2.1.4. Stage (2): Existing Case Study Area

This part aims to evaluate an existing urban area and compare its findings with those derived from the theoretical model. This comparison corroborates the theoretical model's results, which are based on highly symmetrical and uniform conditions. In contrast, however, real-world urban areas, particularly in historic city zones, often exhibit irregularities. By comparing the outcomes of both theoretical and existing case studies, the research can assess the tolerance and accuracy of the findings. These insights will then serve as the foundation for the research recommendations.

3.2.1.5. Study Area's Location and Urban Characteristics

The selected study area is located in Khedival Cairo, within the city's downtown area. This area features streets with varying widths due to its hierarchical road network, resulting in a range of aspect ratios and orientations. These urban variations make it an ideal case study for representing the majority of scenarios represented in the theoretical study. Additionally, the area experiences the impact of the UHI effect due to its central location. Figure 15 illustrates the selected study area's location and its urban characteristics.

As depicted in Figure 15B, the study area encompasses diverse urban morphologies, offering a variety of scenarios for comparison with the theoretical model. The streets within the area ranged from 10 m for local pedestrian streets to 40 m for major roads (Rameses St., S1). Building heights also vary, resulting in aspect ratios ranging from 0.5:1 to 2:1. Furthermore, the streets exhibit four primary orientations—N–S, E–W, NE-SW, and NW-SE)—as shown in Figure 15C. These orientations align with those in the theoretical model. This variety within the study area allowed for comprehensive representation and validation of the theoretical cases, making it highly relevant to this research and integral to achieving the study's objectives. Figure 15D showing the selected streets for the study.

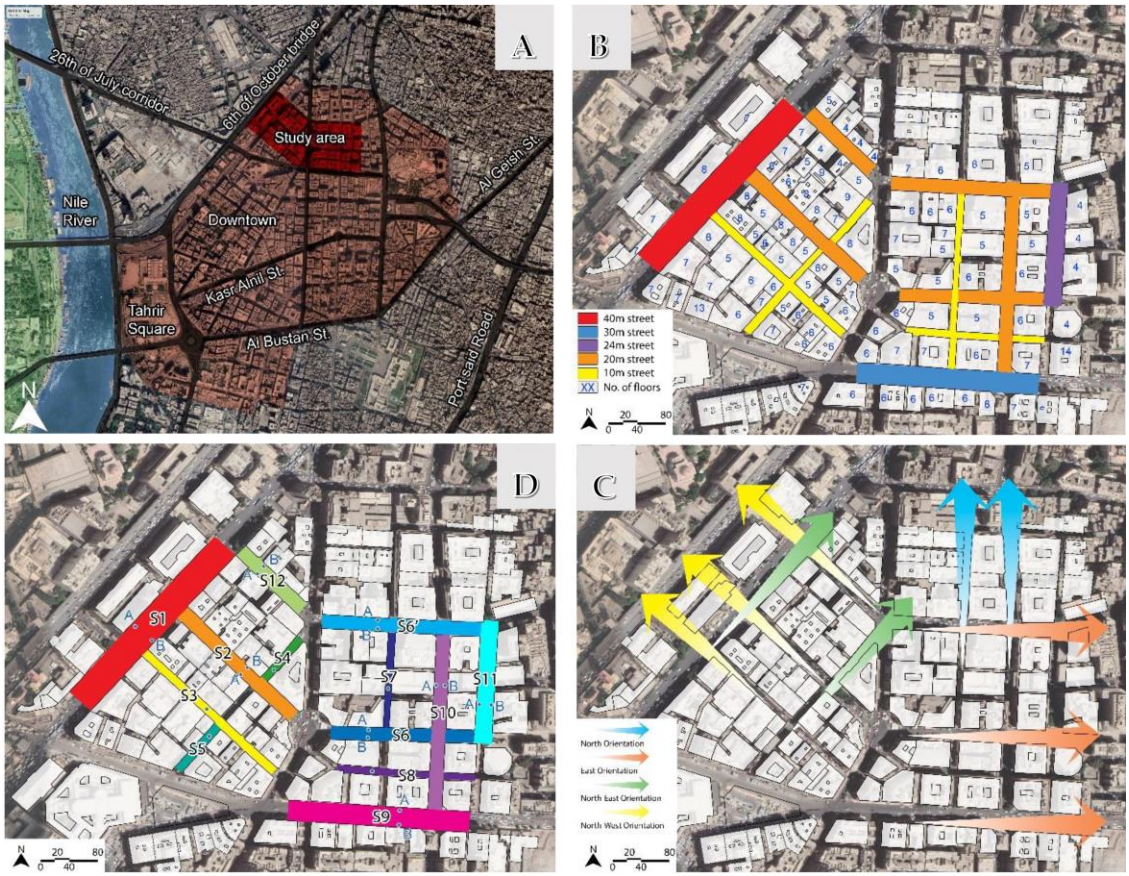

Figure 15. Existing study area. (A) study area location; (B) different street widths and building heights; (C) different street orientations; (D) selected streets and location of the receptors.

3.2.1.6. Study Area Tree Scenarios

The same tree scenarios used in the theoretical model were applied to the study area. These included three scenarios: no trees (0%), low tree density (20%), and high tree density (50%). Consistently applying these scenarios enabled a direct comparison of the impact of trees across different canyons in both the theoretical model and the case study.

3.2.2. Theoretical Model's Results

The results are presented in two stages: The first stage examines the performance of different canyons by comparing the PET values for each side, considering the varying aspect ratios and orientations. The second stage evaluates the impact of trees on each side of the street canyons. The purpose of the first stage is to analyze how changes in aspect ratios, orientations, and canyon side influence thermal comfort and PET values before the addition of trees. This analysis also helps to identify which canyons require trees to enhance thermal comfort and which ones perform adequately without them.

3.2.2.1. Stage (1): Results for the 0% Tree Scenario

By comparing the PET values for each side of all urban canyons, as shown in Figure 16,variations in the PET values were observed across different aspect ratios, orientations, and canyon sides. The worst PET values were recorded on the (a) sides of the eastern streets, where PET values exceeded 50 ˚C for all aspect ratios over many daytime hours. The highest PET value of 58 ˚C (R2a) occurred at 15:00. On the (b) sides of the eastern canyons, the PET values were slightly lower than on the (a) sides; however, both sides remained under extreme heat stress. The reduction in PET values due to aspect ratio changes was minimal (approximately 2-3 ˚C) and limited to only moderate to deep urban canyons on the (b) side (e.g., R4b, R6b, and R8b). The aspect ratio had a more pronounced effect in reducing PET values for other orientations. This was achieved via sufficient urban shading, particularly in moderate and deep canyons. In northern-oriented canyons (Figure 16, left side a,b), on the (a) sides, increasing the aspect ratio reduced the PET by approximately 5 ˚C. This reduction persisted for varying durations—4 hours in R1a, 7 hours in R3a and R5a, 6 hours in R7a, and 3 hours in R9a for 3 hours—compared to R11a, the shallowest urban canyon. On the (b) sides, the impact of the aspect ratio was less pronounced, with smaller PET reductions and shorter durations. For northwester-oriented canyons (Figure 16, right side), the impact of aspect ratios was substantial on both sides. Urban shading was especially effective, maintaining PET values below 50 ˚C in all cases. Increasing the aspect ratio reduced the PET by 5 ˚C or more, with a longer duration of PET reduction—4 hours in R9a,b, 6 hours in R7a,b, 7 hours in R5a,b, 8 hours in R3a,b, and 3 hours in R1a,b—compared to R11a,b, the shallowest canyon. Notable PET improvements were also observed along northeast-oriented canyons, with both sides benefiting from increased aspect ratios. This effect was particularly pronounced during afternoon hours, where average PET reductions of 5 ˚C were observed. Specifically, PET values decreased in R2a,b for 8 hours, R4a,b for 9 hours, R6a,b for 7 hours, R8a,b for 7 hours, and R10a,b for 4 hours and 2 hours compared to the shallowest canyon (R12a,b). In summary, the influence of urban aspect ratios is particularly significant for northern, northeast, and northwest orientations. This is most apparent on side (a) of northern streets and side (b) of northeast and northwest street canyons.

Figure 17 illustrates the Δ PET between the two sides of each street canyon across varying aspect ratios and orientations, highlighting the significant difference for eastern roads, where the maximum PET variations between side (a) and side (b) reached 14 ˚C in deep and moderate canyons. This significant difference within the same canyon is attributed to the combined influence of aspect ratio and orientation, which reduces the PET on side (b) more effectively than that of side (a) for most of the day. For northern-, northeast-, and northwest-oriented canyons, the differences in PET varied between morning and afternoon hours due to the Sun's changing angle throughout the day.

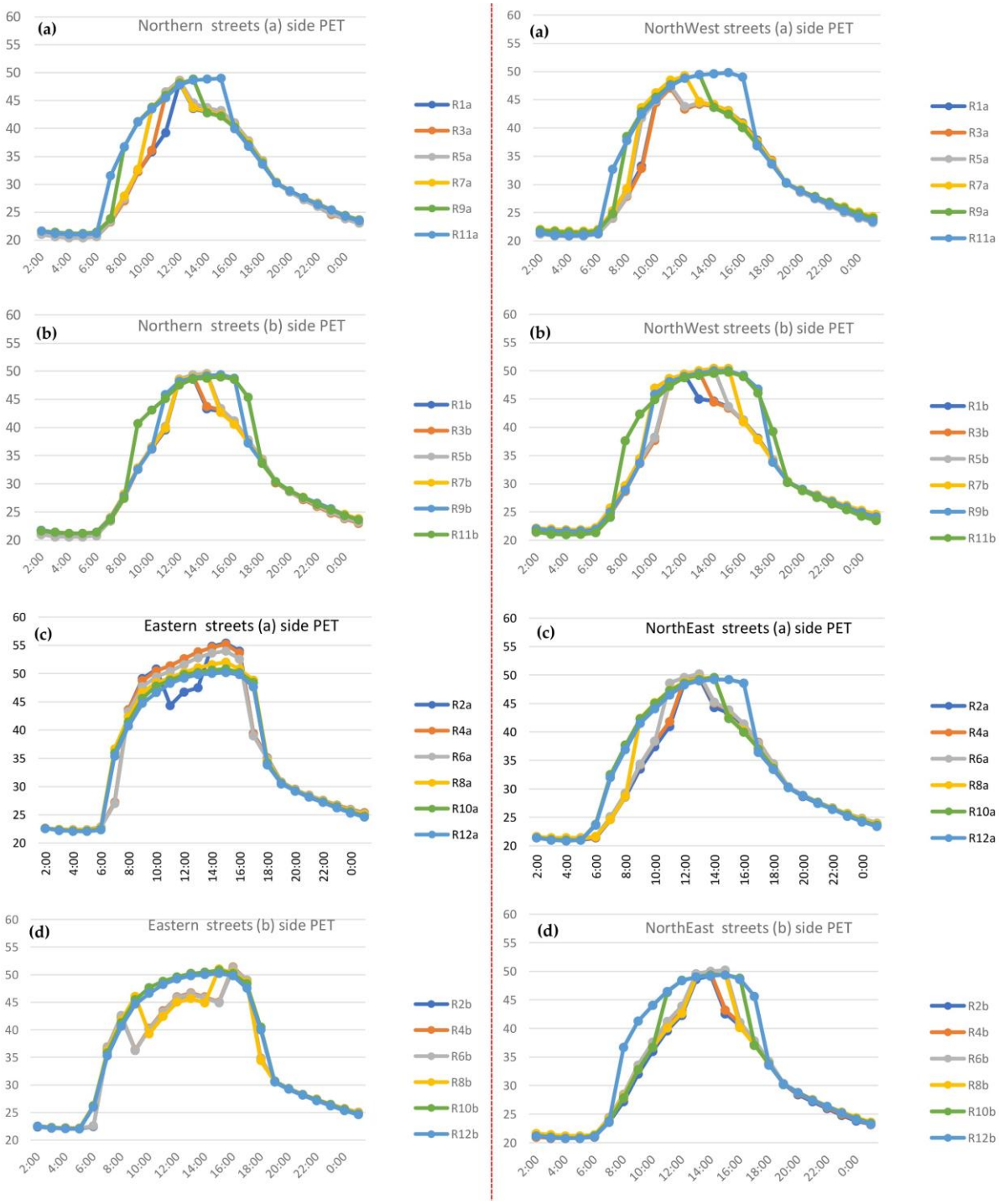

Figure 16. PET values for all aspect ratios of the northern and eastern canyons (Left column), and the northwest and northeast canyons (Right column) on both sides at Z=1.5m.

Northeast-oriented streets experience their most significant improvements in the morning, while northern-oriented canyons experience significant enhancements in the afternoon. Northwest-oriented canyons showed a consistent enhancement across both morning and afternoon. Shallow canyons, such as R11 and R12, exhibited minimal differences between sides across all orientations, indicating that aspect ratio had little effect. Conversely, in moderate and deep canyons, the impact of aspect ratio was substantial, with significant variations between canyons with N, NE, and NW orientations, depending on the time of day.

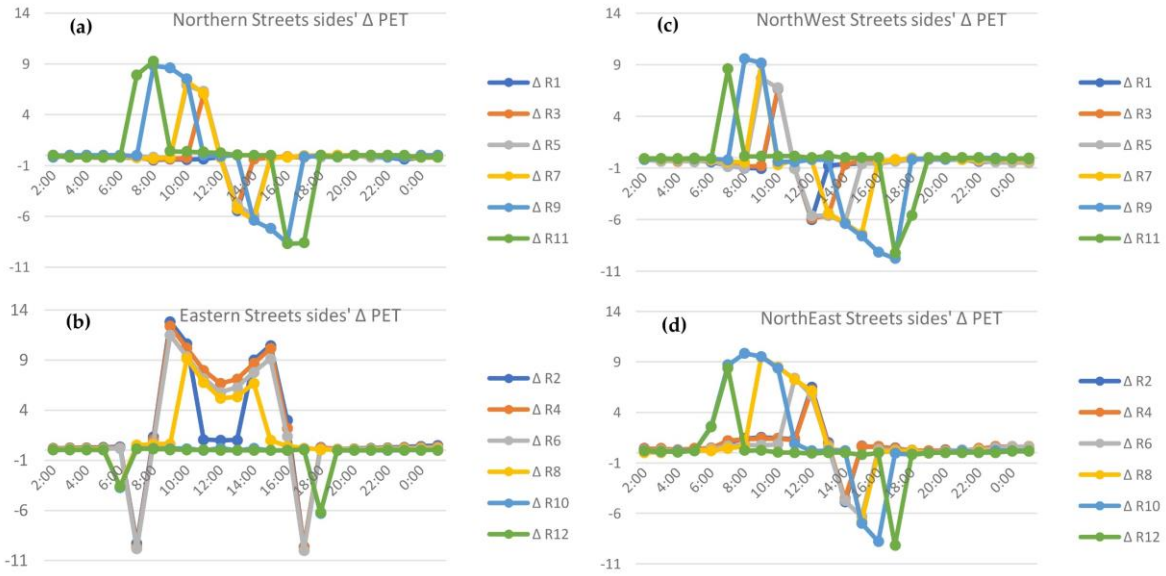

Figure 17. ΔPET for both sides of each canyon (a–b sides) for different aspect ratios and orientations at Z=1.5m.

This concludes the analysis of how the different sides of urban canyons with varying aspect ratios and orientations perform without the addition of trees. These findings offer valuable insights into the expected performance of trees when incorporated into each side, considering the varying aspect ratios and orientations.

3.2.2.2. Stage (2): Results of the Tree Scenarios

In Stage (2), the impact of adding different tree percentages was evaluated by comparing PET values for each tree scenario across different road sides, aspect ratios, and orientations. The two tree densities (20% and 50%) were applied to analyze the relationship between tree coverage and the thermal performance of various street canyon sides. As shown in Figure 18, tree performance varied significantly based on aspect ratio, orientation, and street side. Trees had the greatest impact in two cases: (1) across all aspect ratios in eastern canyons and (2) across all orientations in shallow urban canyons. Figure 18 displays two distinct charts: M-shaped and A-shaped. M- shaped charts (b, d, f, h, I, j, k, and l) indicate significant tree performance. These charts depict PET reductions reaching the maximum for most of the day, except during noon hours. This consistent reduction resulted in an M-shaped pattern, with maximum ΔPET reductions reaching up to 17 ˚C and average reductions reaching 12–15 ˚C. These reductions lasted, on average, for 8–10 hours, covering nearly the entire daytime period, signifying a significant improvement in thermal comfort. However, the A-shaped charts observed in moderate and deep northern canyons reflect limited PET enhancements. Here, maximum ΔPET values reached 13 ˚C but only for about 3 hours in a few cases, while average ΔPET reductions ranged between 4 and 7 ˚C for most of the daytime. The results in Figure 18 also show that increasing the tree percentage from 20% to 50% was particularly effect on both sides of shallow canyons and on side (a) in moderate and deep eastern canyons. However, higher tree densities in deep and moderate northern-oriented canyons did not lead to any significant improvements. In Figure 19, northwest- and northeast-oriented canyons showed comparable tree performances, with significant improvements in shallow canyons for both orientations on both sides, as seen in canyons R9, R10, R11, and R12. For moderate and deep aspect ratios, tree performance for both orientations was nearly identical and closely aligned with the performance observed in the northern

canyons. In addition, the maximum ΔPET reduction reached an average of 12-14 ˚C, and the average reduction reached 4-7 ˚C. Tree performance on both sides of the canyons was nearly identical, with side (b) showing a slight advantage. Increasing tree density from 20% to 50% had a significant impact on PET reductions in shallow canyons for both orientations, with ΔPET differences reaching up to 10°C during certain hours. In contrast, for moderate and deep canyons, increasing tree density resulted in only minor reductions in PET, averaging just 2-3 ˚C between the 20% and 50% tree scenarios.

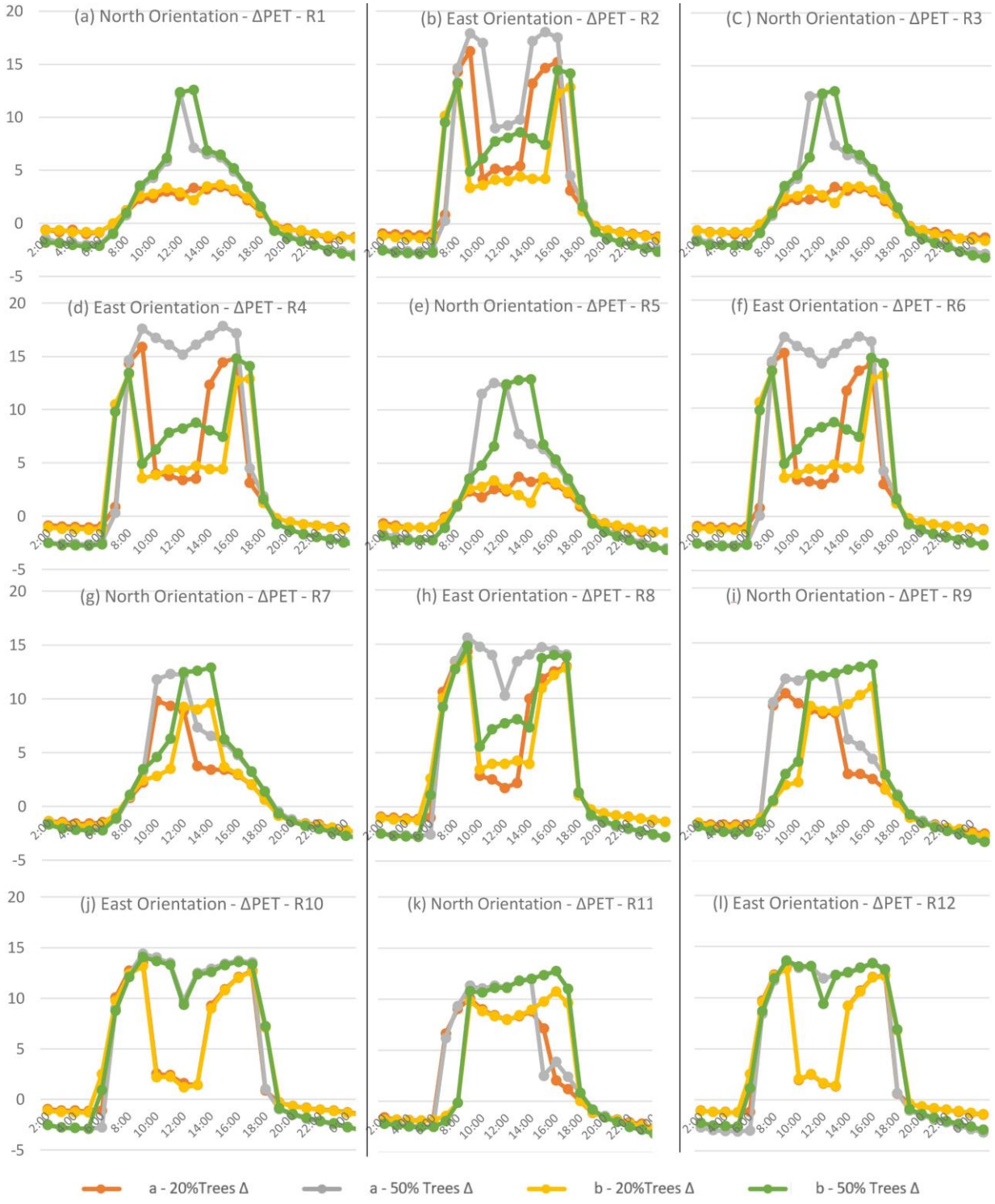

Figure 18. ΔPET with the 20% and 50% tree scenarios in comparison with the 0% tree scenario for northern and eastern canyons on both sides (a and b) at Z=1.5m.

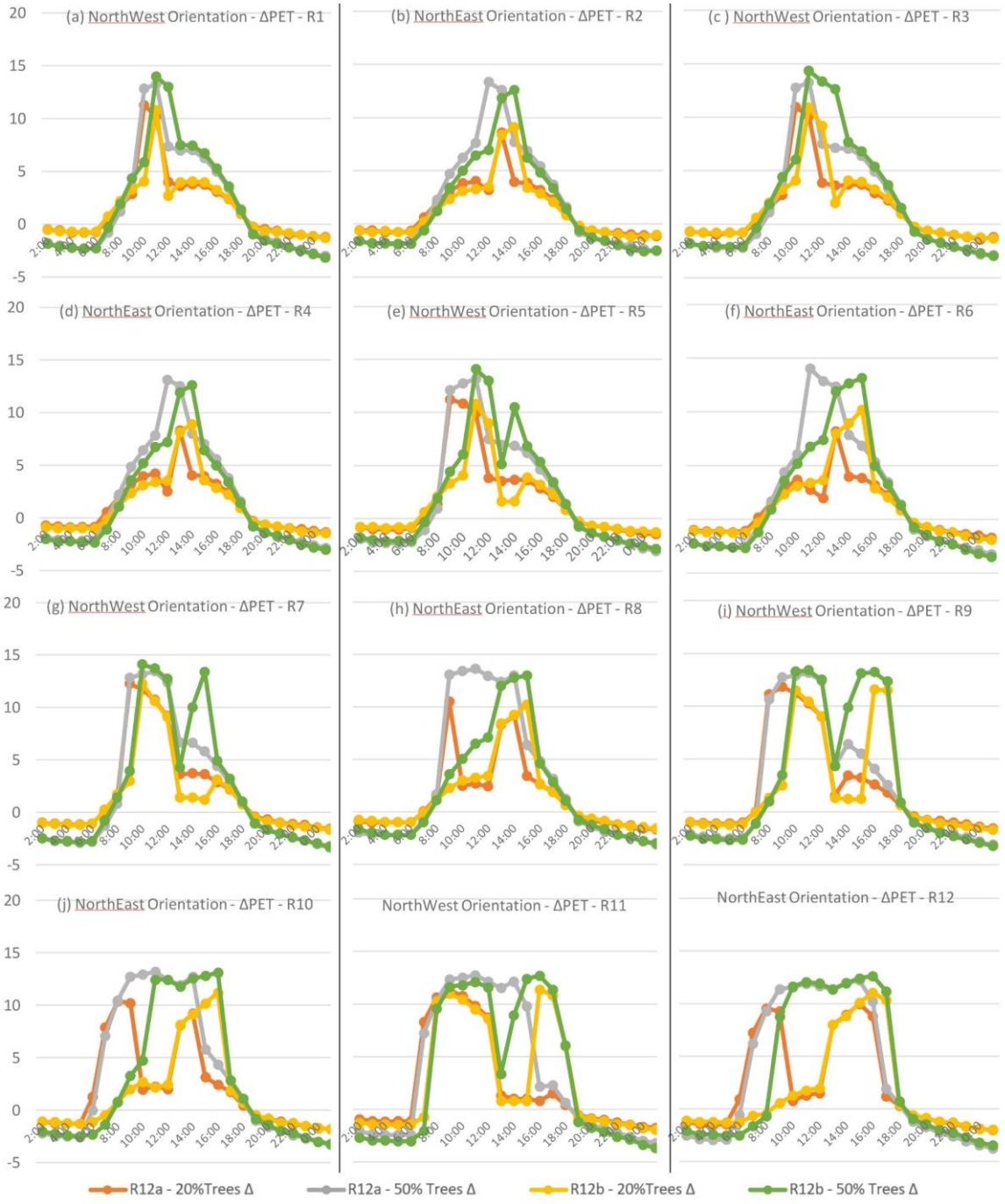

Figure 19. ΔPET with the 20% and 50% tree scenarios in comparison with the 0% tree scenario for the northeast and northwest canyons on both sides (a and b) at Z=1.5m.

Figures 20 and 21 provide a detailed comparison of both sides of various street canyons with different orientations and aspect ratios, analyzed using two distinct approaches. The first approach compared the average ΔPET during the peak daytime hours (from 11:00 to 16:00), as shown in Figure 20.

The second approach analyzed the number of hours during which PET was reduced by 8°C or more Figure 21. Such a reduction is significant, as it can improve thermal comfort by almost two thermal zones (Lobaccaro G. A., 2019). Both comparisons (Figures 20 and 21) illustrate the substantial impact of high tree densities in shallow streets and eastern

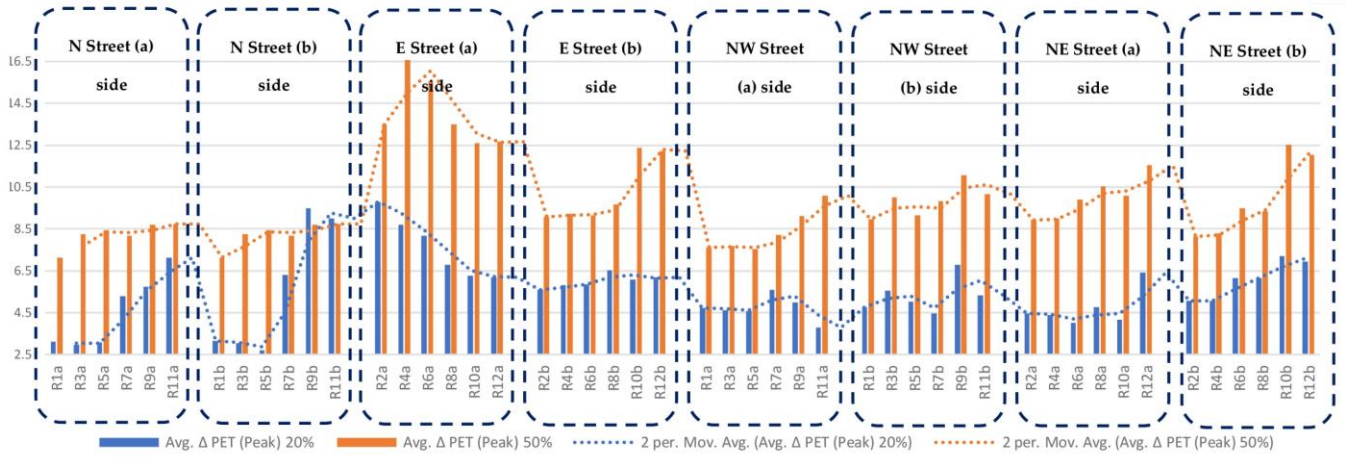

Figure 20. Comparing the average ΔPET during the peak daytime period (from 11:00 to 16:00) on both sides for all aspect ratios and orientations at Z=1.5m.

canyons on both sides. The comparisons also highlight the gradual improvement in tree performance across moderate to deep canyons with varying aspect ratios and orientations. However, the effectiveness of trees decreased as the aspect ratio (H/W) increased. For deep and moderate canyons with northern, northeast, and northwest orientations, increasing tree density from 20% to 50% resulted in minimal PET reductions, with some cases showing no notable difference.

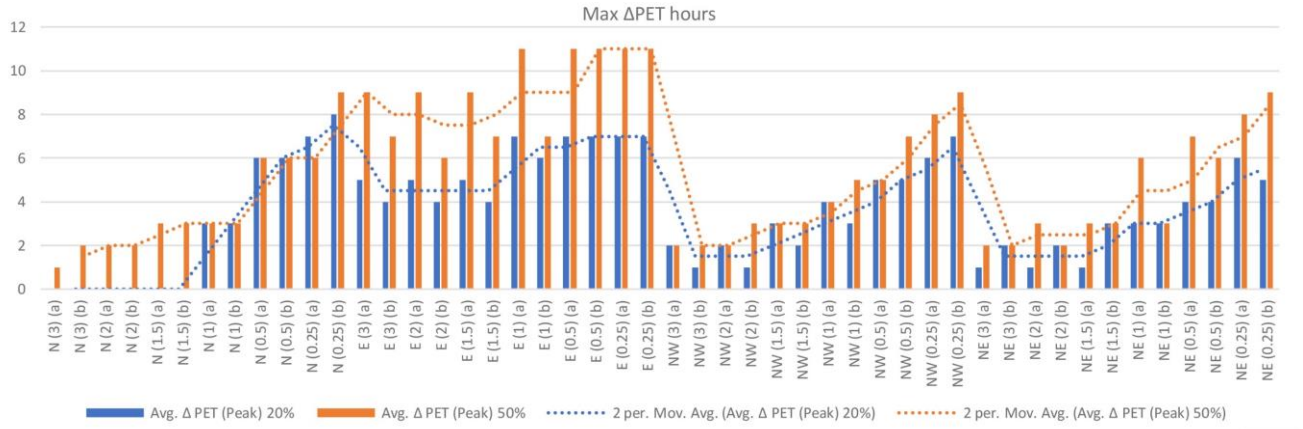

Figure 21. Comparing the number of hours the PET was reduced by 8 ˚C or more on both sides for all aspect ratios and orientations at Z=1.5m

The relationship between the aspect ratio and the tree scenario performance for different orientations on both canyon sides was statically analyzed. Before calculating the correlation between variables, the Kolmogorov–Smirnov (KS) test confirmed that all input data for aspect ratios and average Δ PET (during peak hours) across all orientations and both sides were normally distributed, with the exception of the Δ PET values for the 50% tree scenario for the north orientation on side (b) and the 50% tree scenario for the east orientation on side (b). For these exceptions, Spearman correlation was applied, while Pearson's correlation was used for all other cases. The results revealed a very strong negative correlation between an increase in the aspect ratio and the Δ PET during peak for all tree coverage percentages, orientations, and sides. However, the strength of the correlation varied across orientations and sides. For example, the correlation for eastern roads was weaker (-0.849, -0.849, -0.878, and -0.802) compared to most other orientations, which typically ranged from -0.971 to -0.900. Similarly, side (b) on NE-oriented canyons

and side (a) on NW-oriented canyons showed less significant correlations, resembling the results for the eastern orientation. These findings align with the measured PET reductions, indicating that tree performance in these orientations is less dependent on urban canyon shading due to the limited natural shading. Additionally, other factors, such as wind speed, do not provide any benefit. Thus, the presence of trees is crucial to mitigate heat and enhance thermal comfort in these canyons. The mean values further underscore the differences between eastern-oriented canyons and other orientations, thus supporting the PET reduction and correlation results. The correlation outcomes could potentially show more significant trends if shallow aspect ratios (0.5 and 0.25) were excluded, as their results were identical for the eastern orientation, whereby aspect ratio impact diminishes. Linear scatter plots and regression analyses of the aspect ratio and ΔPET for reductions of 8 °C or more for how many hours for both tree scenarios (20% and 50%) demonstrated a clear negative linear relationship. However, this relationship varied depending on the street's aspect ratio, orientation, canyon side, and tree density. The 50% tree scenario consistently showed a stronger relationship than the 20% tree scenario across all orientations. Northern, northwest, and northwest orientations exhibited higher R2 values (≥ 0.8) for the 50% tree scenario, indicating a strong correlation between ΔPET and aspect ratio. In contrast, eastern canyons exhibited lower R2 values, with R2 ≤ 0.72 for side (a) and R2 ≤ 0.77 for side (b).

3.2.3. Case Study Results

To validate the findings of the theoretical study, the same tree scenarios were applied to the case study area in downtown Cairo. As shown in Figure 22, the results closely align with those of the theoretical model. The impact of trees was particularly significant in shallow canyons and eastern canyons. In charts (f) and (i) of Figure 22, the eastern canyons exhibited substantial PET reductions on both sides, with maximum reductions of approximately 18°C and average reductions of 13–14°C sustained during most daytime hours. The 50% tree scenario consistently outperformed the 20% scenario, with average reductions of 4 to 5 °C greater. In contrast, reductions in northern, northeast, and northwest orientations were more limited, rarely exceeding 10 °C PET reductions for brief periods in some canyons. Average PET reductions in these orientations ranged between 4 and 7 °C, closely mirroring the theoretical model's results. A slight improvement was noted in specific streets, such as S1 (northeast) and S12 (northwest), where PET reductions slightly exceeded those of the theoretical model, though they remained well below the significant improvements observed in eastern-oriented canyons. Figure 23 compares the average ΔPET during peak hours (11:00–16:00) on both sides across various aspect ratios and orientations, while Figure 24 offers a detailed comparison of the total hours with PET reductions of 7 hours or more. Both analyses prove that tree impact varied significantly, with the most pronounced effect observed in shallow and eastern-oriented canyons on both sides.

The overall linear patterns of each chart (Figures 23 and 24) closely resemble those of the theoretical model analysis, as shown in Figures 20 and 21, validating the theoretical model's results. However, slight differences were observed in the case study results. These variations are expected due to the irregularities of the study area, including variations in aspect ratios and building heights within each urban canyon. Unlike the theoretical model, the real-world study area lacks uniformity. Despite these differences, the overall results align well between the theoretical model and the existing study area, thus reinforcing the validity of the findings.

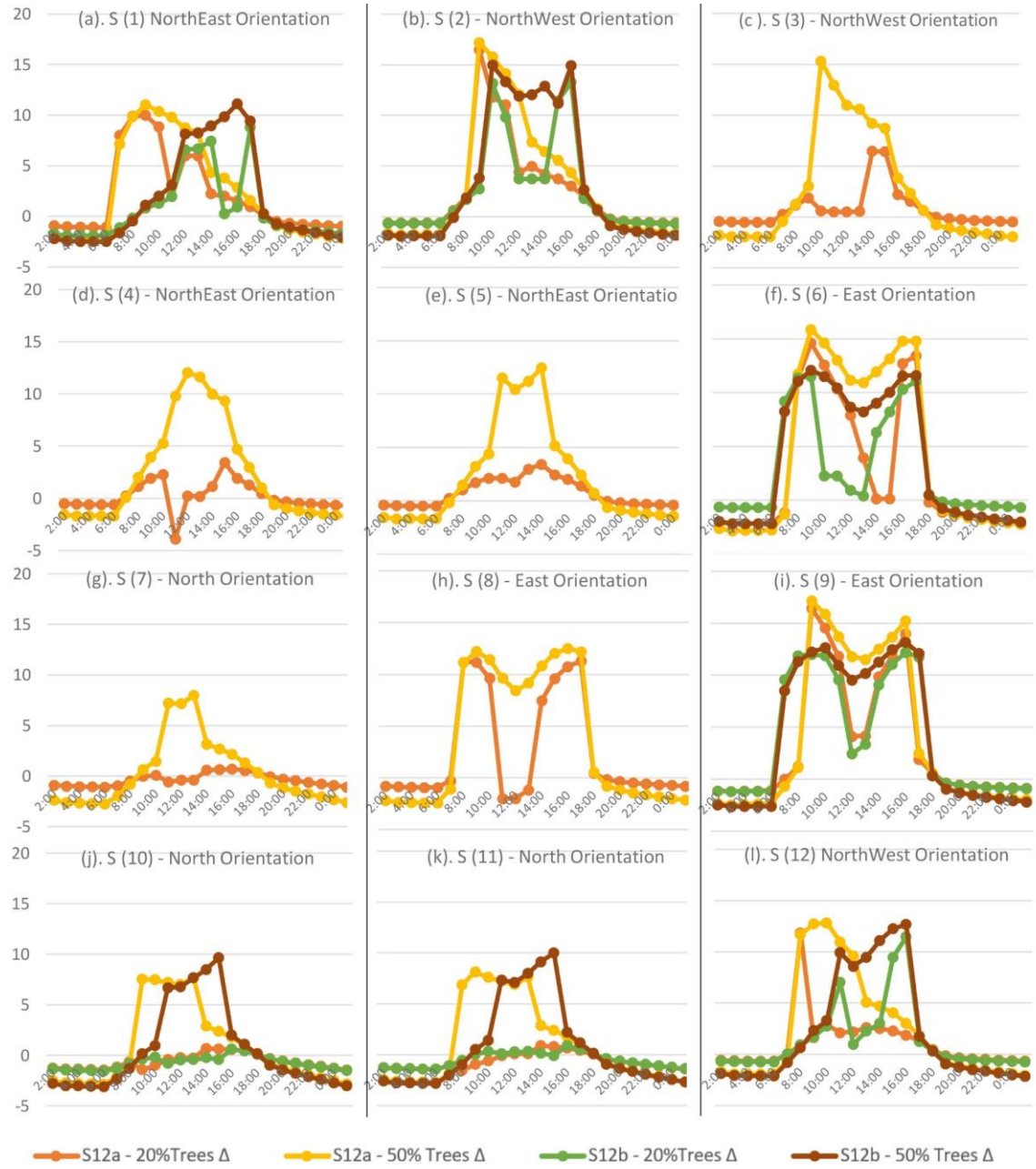

Figure 22. ΔPET with the 20% and 50% tree scenarios in comparison with the 0% tree scenario for all canyons on both sides (a and b) at Z=1.5m.

A review of the theoretical and case study results clearly demonstrates the significant value trees have as well as their importance in different urban canyons. The extent of their impact, however, varies based on the orientation, aspect ratio, and specific canyon side.

Eastern-oriented canyons require a high density of trees on both sides, with the northern side benefiting the most. This finding aligns with previous studies (Jamei, 2020) (Rodríguez-Algeciras, 2018) (Andreou E., 2013). Northern, northeast, and northwest canyons generally performed better than eastern canyons. While adding trees to western canyons provided slight improvements, the impact was less significant compared to eastern canyons, which is consistent with findings from other research (Jamei, 2020) (Lobaccaro G. A., 2019). For some moderate to deep canyons in northern, northeast, and

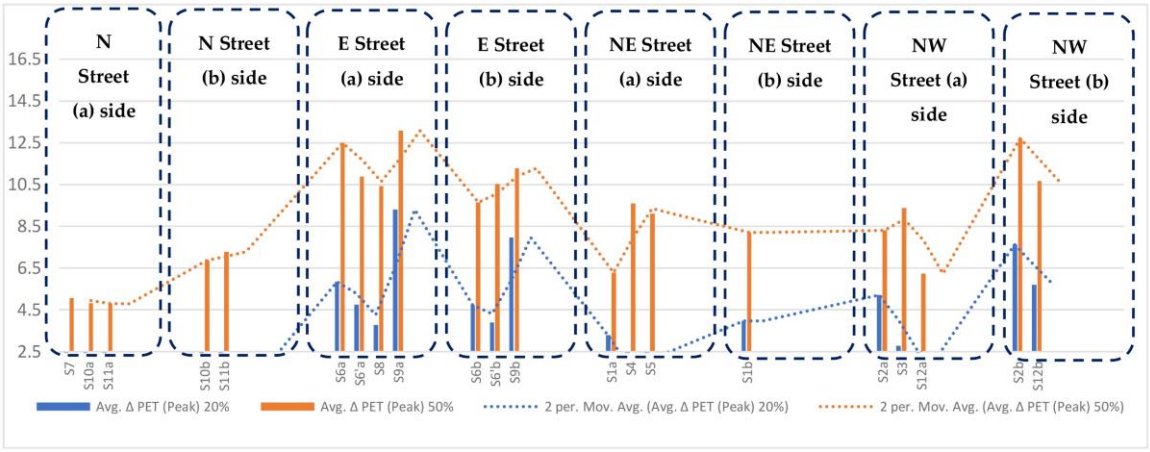

Figure 23. Comparing the average ΔPET for the peak daytime hours (from 11:00 to 16:00) on both sides for all aspect ratios and orientations at Z=1.5m.

northwest areas, the presence of tall buildings helps maintain cooler conditions by blocking direct sunlight from reaching the streets, thus contributing to thermal comfort. These canyons also experience the benefit of cooling from the presence of strong winds. Adding trees to moderate and deep canyons in these orientations may have a limited on thermal comfort and could potentially obstruct wind and airflow. However, strategically planting trees on side (b) could have an overall beneficial impact. Trees on side (b) provide afternoon shade, thereby enhancing natural cooling without significantly disrupting wind. In contrast, shallow canyons across all orientations and aspect ratios fail to provide sufficient shading on either side, thus highlighting the importance of high tree densities in these canyons to enhance thermal comfort. This is due to the fact that the canyon effect is entirely absent in these areas—particularly on the northern side of the eastern canyon (side a). In deep canyons with northern, northwest, and northeast orientations, applying low tree densities on side (b) could still provide effective shading and cooling. However, a high density is necessary on both sides of eastern and shallow canyons to achieve significant thermal comfort improvements. A comparison of the theoretical study with the real-world case study highlights the influence of urban forms. The uniformity and regularity of the theoretical model produce slightly different results compared to the irregular urban canyons of existing areas. While the key findings remain mostly consistent, discrepancies arise due to differences in urban conditions at specific measurement points.

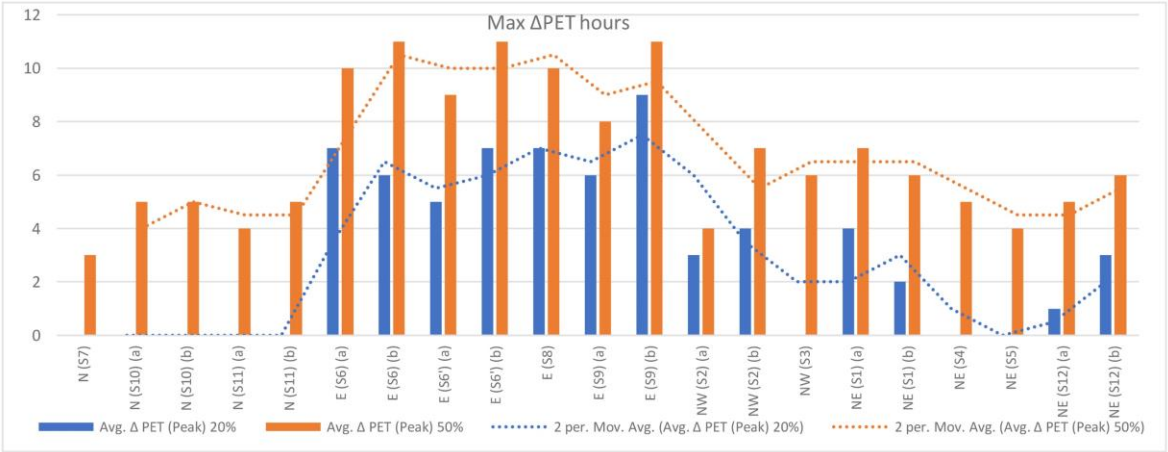

Figure 24. Comparing the number of hours the PET reduced by 7 ˚C or more on both sides for all aspect ratios and orientations at Z=1.5m.

3.3. Pedestrian Dynamic Thermal Comfort Analysis for Optimizing Tree Use in Various Urban Morphologies: Case Study of Cairo City

Publication (3) focused on assessing dynamic thermal comfort (DPET) across various urban forms and tree densities. The study examined walking routes in diverse urban areas with varying tree densities, aiming to evaluate different urban configurations (characterized by aspect ratios and orientations) and tree canopy coverage levels. Using the microclimate simulations software ENVI-met V5.6.1, the study measured DPET in each route and conducted dynamic thermal comfort analysis under different tree scenarios. This study was conducted in two steps, as presented in Figure 25.

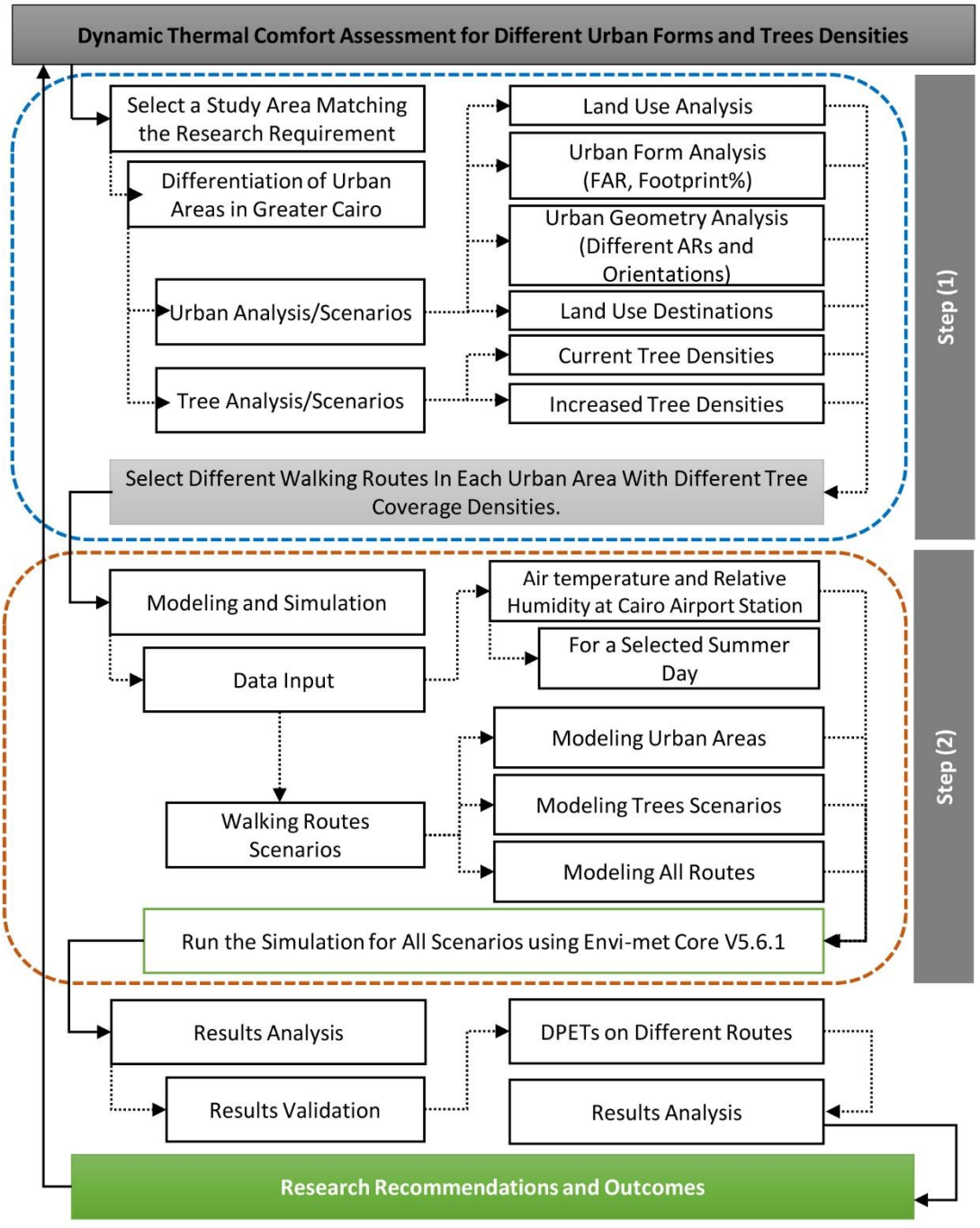

Figure 25. Dynamic thermal comfort analysis methodology.

3.3.1. Step (1): Study Area Selection and Analysis

Cairo was chosen due to its diverse urban morphologies, and its significant heat stress, making it well suited to the study's objectives. Thus, this diversity allowed for a clear understanding of the impacts on pedestrians while walking, particularly the effects of tree density under different scenarios and the changes observed as tree densities increased.

3.3.1.1. Urban Analysis of Study Areas

As shown in Figure 26, five study areas were selected: Bulaq Ad Daqrur (commonly known as Bulaq), Khedival Cairo (Downtown), Mohandisen, New Cairo, and Mivida. These specific areas were chosen for their distinct urban morphologies and varying tree densities. The selected study areas also differed in terms of location. Three of them—Bulaq, Downtown, and Mohandisen—are situated very near the center of Cairo, within a 4– 5 km range, while the remaining two areas—New Cairo and Mivida—are suburban areas located approximately 17–29 km away from the city center. Table 2 shows the local climate zones and the main urban characteristics of each study area. The selected study areas had similar sizes, as they varied between 18 and 22.9 hectares, and changes in the solid-to-void ratio were obvious. These ratios varied significantly across the study areas, ranging from 75% solid in Bulaq to 61% and 59% in Mohandisen and Downtown, respectively, down to a low of 29% in New Cairo and a very low 13% in Mivida. In addition, green spaces also showed significant variation. Bulaq and Khedival Cairo had 0%, while Mohandisen featured a very limited green area of 3%. In contrast, New Cairo had moderate greenery levels at 12%, while Mivida boasted the highest greenery at 23%. The floor area ratio (FAR) also varied across the study areas, reflecting differences in footprint percentage and building heights. FAR values ranged from a high of 5.2 in Bulaq to moderate values of 4.58 in Downtown and 4.31 in Mohandisen, dropping to a low of 1.15 in New Cairo and a very low 0.39 in Mivida. Building heights varied significantly in each area. Mohandisen featured the tallest buildings, ranging from 28 m to 40 m. Medium building heights, ranging from 22 m to 27 m, were observed in Bulaq and Downtown. The shortest buildings, ranging between 9 m and 12 m, were located in New Cairo and Mivida. Access to public transportation differed widely across the study areas. Downtown had the most facilities, including a metro station and a bus stop. Bulaq and Mohandisen each had

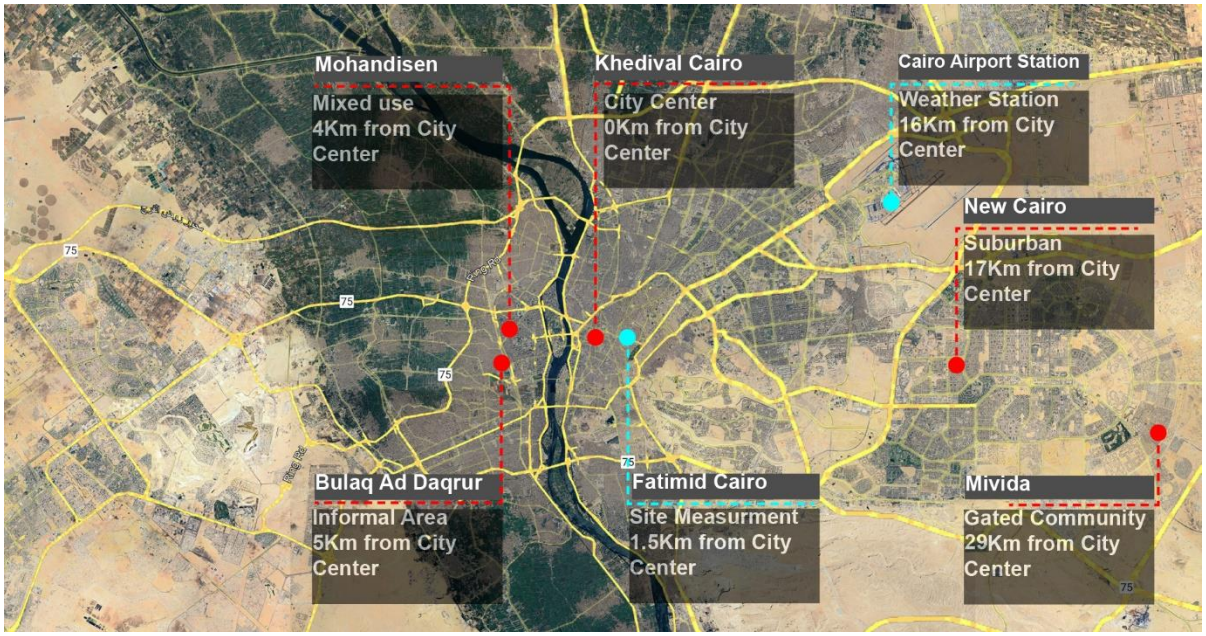

Figure 26. Selected study areas, Cairo weather station, and site measurement location.

two bus stops, while New Cairo had one. Mivida, in contrast, had no public transportation facilities due to its car-centric, gated-community design, where walking was primarily limited to internal circulation between community amenities. These urban analyses revealed significant differences among the study areas, underscoring the variety and diversity of the selected locations.

Table 2. Selected urban areas characteristics.

Study Area	Bulaq Ad Daqrur	Khedival Cairo	Mohandisen	New Cairo	Mivida
Local Climate Zone (LCZ)*	LCZ2 Compacted midrise	LCZ2 Compacted midrise	LCZ1 Compacted high rise.	LCZ5 Open midrise	LCZ6 Open low rise
Urban Classification	Informal area	City center	Business center	Suburban community	Gated community
Aspect ratio	Deep	Moderate	Moderate	Open canyons	Shallow canyons
Mixed uses and car/transit	Low mixed uses, transit-oriented	High mixed uses, transit-oriented	High mixed uses, transit- and car-oriented	Low mixed uses, car-oriented	No mixed uses, car-oriented
Density	Very high	Moderate	Moderate	Low	Very low

*Local climate zones (LCZs) were classified as explained in (Abougendia, 2023), (Elmarakby, E., 2020).

3.3.1.2. Tree Scenarios

The study areas demonstrated not only diverse urban morphologies but also significant variation in terms of tree density. As shown in Figure 27, existing tree coverage percentages varied widely among the study areas. Tree coverage was very low in Bulaq (2.1%), Downtown (6.2%), and Mohandisen (7.8%), reflecting the scarcity of open spaces. In contrast, tree coverage was moderate in New Cairo (9.4%) and high in Mivida (13%).

To assess the impacts of trees in each area, this study evaluated both the current tree coverage and scenarios with increased tree densities. The proposed increases, illustrated on the right side of Figure 27, were tested to analyze how higher tree densities influence DPET for pedestrians in different urban morphologies. Tree density was strategically increased to ensure a balanced distribution and adequate spacing of trees along roads and in parks. This resulted in varying tree coverage percentages across the study areas, as shown in Figure 27. These adjustments aimed to optimize the use of trees, consistent with findings from previous research (Abdelmejeed A. Y., 2023) (Elbardisy, 2021).

3.3.1.3. Walking Routes

This study focused on the dynamic thermal comfort of pedestrians, making the selection of walking routes in each scenario a critical aspect. Since the study results emphasized the DPET values of the routes and locations, the design of each route—considering aspect ratios, orientations, and tree densities—was central to the research. In each study area, two routes were carefully selected to ensure comprehensive coverage of the study area. These were non-overlapping and connected key urban features, such as transportation stations, retail areas, amenities, parks, etc. (Hwang, 2022).

Figure 27. Current and proposed tree densities for each study area.

Figure 28 shows the proposed routes in each study area, which were designed to traverse diverse urban elements. In Bulaq, the routes incorporated various aspect ratios and orientations. Route (A) started at the bus stop, passed through a wide eastern canyon (H: W 1:0.75), and then moved through a narrow northern canyon (H: W 3:1) before reaching a residential destination. Route (B) began at the second bus stop, traversed a narrow eastern canyon (H: W 3:1), and continued to another residential destination via a narrow northern canyon (H: W 1:2.5).
Similarly, in Downtown, two routes were designed to traverse diverse urban canyons and destinations. Route (A) started at the metro station and then passed through a wide eastern canyon (H: W 1:1.25), a moderate northern canyon (H: W 1:1), and a moderate eastern canyon (H: W 1:1.25) before reaching a retail destination. Route (B) began at an urban park next to a bus stop and then passed through a moderate eastern canyon (H: W 1:1), a moderate northern canyon (H: W 1:1.3), and a moderate eastern canyon (H: W 1:1.5) before reaching a coffee shop area.
In Mohandisen, the routes included urban parks and varied canyon configurations. Route (A) started at a bus stop, moved through a moderate eastern canyon (H: W 1:1) and a northern canyon, passing by an urban park with dense vegetation, and then moved through an eastern canyon (H: W 1:1) before reaching a residential destination. Route (B) began at the same bus station, moved through a shallow northeastern canyon (H: W 1:3.5) for most of its length, and ended in a moderate northwestern canyon (H: W 1:1). In New Cairo and Mivida, the routes passed different urban contexts, including very shallow roads (H: W 1:3) and urban parks, as shown in Figure 28.
The routes were intentionally designed to be longer than the typical walking distance of 500 m (Vasilikou, 2020), as the study aimed to address the primary research gap concerning long-distance pedestrian routes (Hwang, 2022). The route lengths in Bulaq, Downtown, Mohandisen, New Cairo, and Mivida were A=697 m and B=704 m, A=712 m and B=651 m, A=727 m and B=722 m, A=839 m and B=771 m, and A=747 m and B=758 m, respectively. In total, this study examined 20 unique routes with varied morphologies and urban tree densities. This variation provided more detailed results, enriching the research findings and offering comprehensive insights into pedestrian thermal comfort.

3.3.2. Step (2): Data Input, Model Set-Up, and Measuring Points

The simulations for each study area and tree scenario were conducted using ENVI-met V5.6.1 (Winter 2023). The model incorporated all necessary data, including the existing urban configurations (materials and soil) commonly found in Cairo and meteorological input. The simulation's geographical location was 30.02 latitude and 31.22 longitude, selected from the ENVI-met application “Spaces” database for Greater Cairo.

3.3.2.1. Simulation Outputs

Output data were processed using the ENVI-met ‘’Bio-met’’ tool to calculate the DPET and SPET values of each route in each study area under the different tree scenarios. The results were extracted for five key daytime hours: 9:00, 11:00, 13:00, 15:00, and 17:00. These hours were chosen to represent times when pedestrians are most likely to engage in activities or travel between destinations. The parameters for analysis comprised dynamic thermal comfort (DPET), steady thermal comfort (SPET), dynamic skin temperature (T Skin), and average core temperature (T Core). Data were exported for all selected routes in each study area for both tree scenarios for the five selected hours. This approach ensured coverage of pedestrian thermal comfort throughout the daytime while capturing key variations during common travel times.

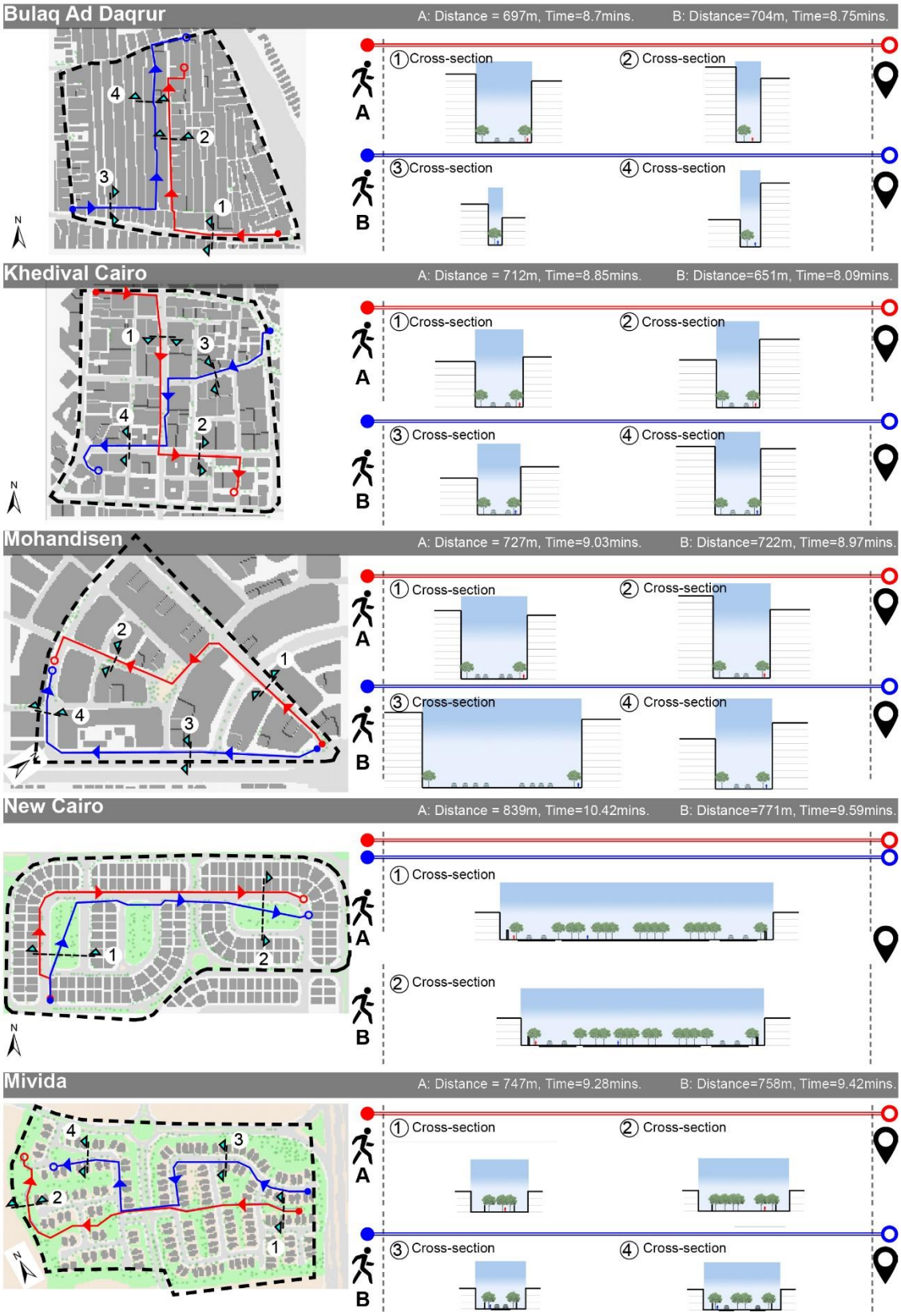

Figure 28. Alignment of pedestrian routes and cross-sections of different segments in each study area.

3.3.3. DPET Results

After validating the results, the results analysis was divided into two stages. In the first stage, the DPET, SPET, T Skin, and avg. TCore values were evaluated for each route in all study areas before and after increasing tree density. This analysis examined the effects of urban morphology, urban trees, and contributing factors, such as the SPET and T Skin, on the DPET values. In the second stage, three levels of comparisons were conducted. Each route's DPET values were compared before and after adding trees to assess the effects of increased tree density. Thermal classification percentages were also analyzed under both tree scenarios to evaluate the shifts in comfort levels. In the second case, the routes within each study area were compared to understand localized variations in dynamic thermal comfort. In the third case, selected routes from different study areas were compared to assess how urban morphology, tree density, and other variables influenced dynamic thermal comfort across varying contexts. These comprehensive comparisons provided an in-depth understanding of how multiple factors—urban form, tree density, and thermal conditions—affect dynamic thermal comfort for pedestrians.

In Bulaq (Bulaq Ad Daqrur), as shown in Figure 29, at 11:00, the tight canyons on route B contributed to a total reduction of 5 °C. In contrast, route A showed an initial increase of 4.5 °C along the eastern road over a very short distance, followed by a decrease on the

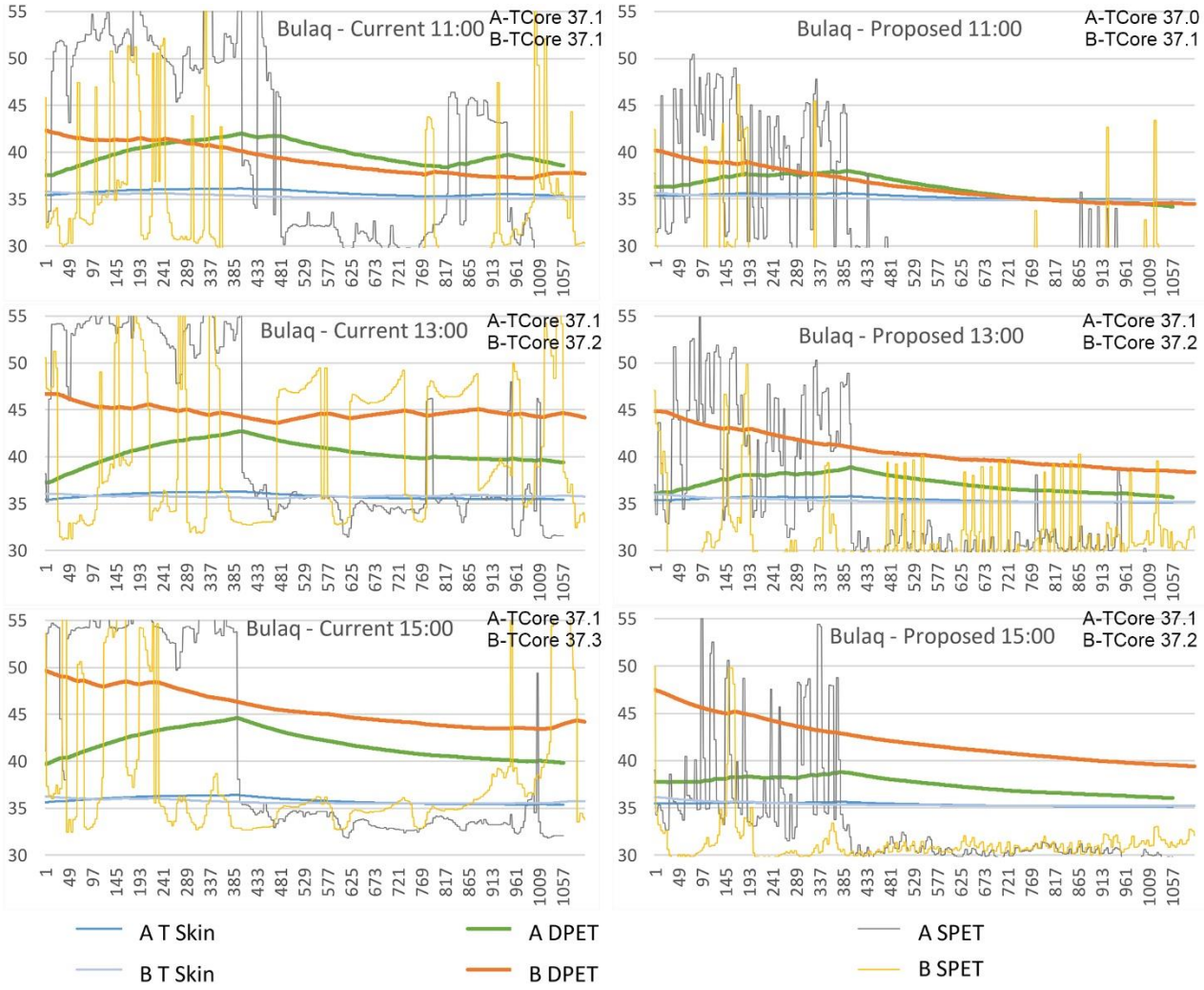

Figure 29. DPET, SPET, skin temperature (T Skin), and average core temperature (TCore) results for Bulaq routes (A and B) in both tree scenarios (current and proposed) at Z=1.5 m. Y axis = °C and X axis = seconds while walking each route.

northern road, where the DPET nearly returned to its starting value. This clearly showed the impact of the wide eastern canyon. Adding more trees did not change the performance of route B but mitigated the wide eastern canyon's effect on route A, reducing the temperature increase to 1.5 °C instead of 5 °C.

At 13:00, when the shade from the buildings was minimal, the DPET on route A increased by 5 °C along the eastern route and then dropped slightly by 3 °C by the end of the northern road. Route B showed minor and irregular reduction within 1 °C from start to finish. Increasing tree density significantly lowered DPET values. On routes A and B, trees reduced DPET by 3.5 °C and 7 °C, respectively.

At 15:00, the tight canyons on route B resulted in a significant DPET reduction of 6 °C by the end of the walk. Route A experienced an increase of 5°C due to the wide eastern canyon, followed by a reduction in the tight northern canyon, bringing this value back to its starting value (40 °C). Adding trees to both routes mitigated these effects. On route A, the increase in the eastern canyon was limited to just 1 °C, while route B maintained its consistent reduction pattern, achieving an overall decrease in DPET of 8 °C. At both hours (13:00 and 15:00), small fluctuations in skin temperature were observed on route A. These fluctuations were attributed to the strong heat stress in the wide eastern road, which caused an initial rise in skin temperature. However, as the route transitioned to the tight

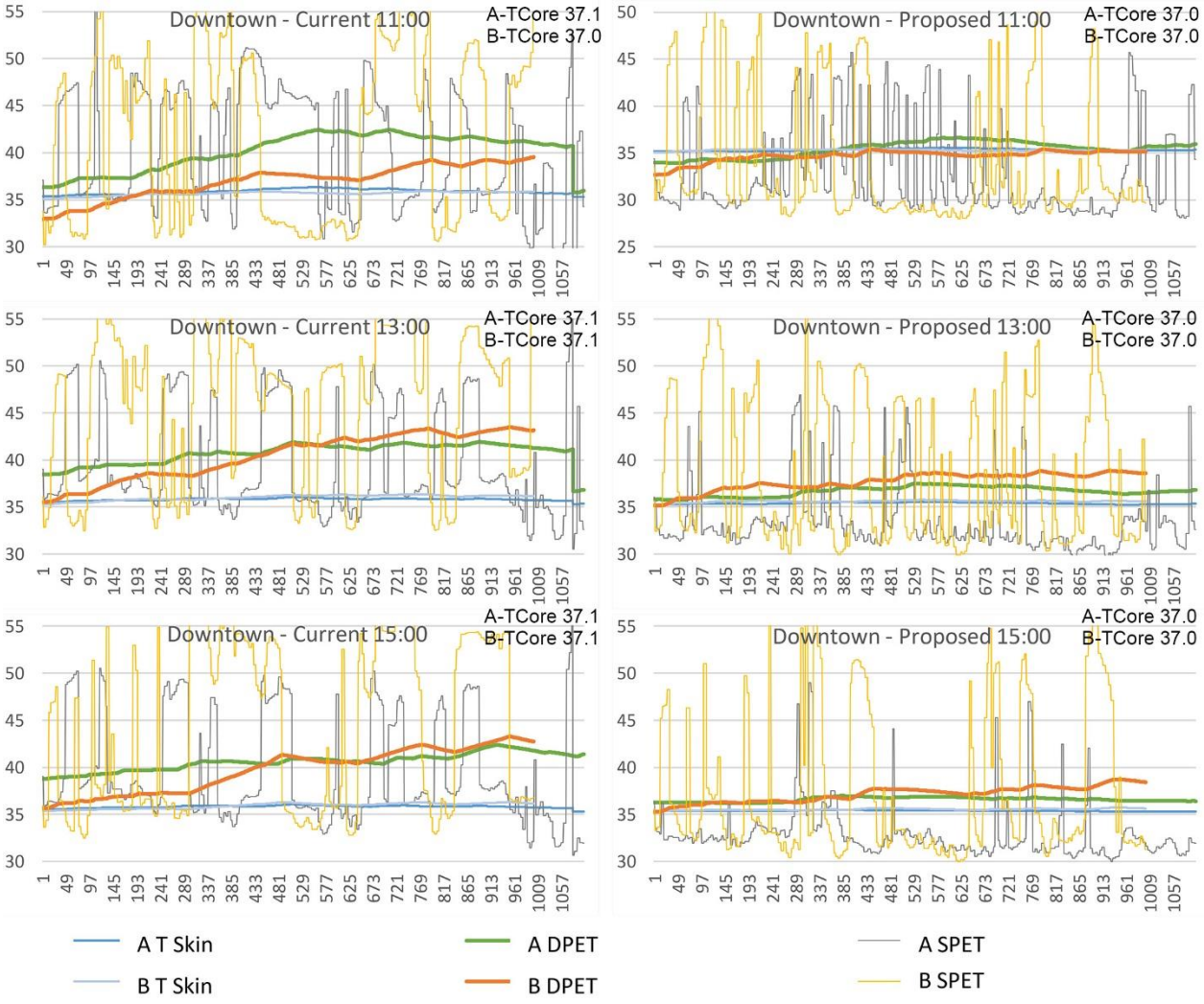

Figure 30. DPET, SPET, skin temperature (T Skin), and average core temperature (TCore) results for Downtown routes (A and B) under both tree scenarios (current and proposed) at Z=1.5 m. Y axis = °C and X axis = seconds while walking each route.

northern canyon with improved urban shading, skin temperature gradually decreased until the end of the walk.

The results for Downtown (Khedival Cairo) are shown in Figure 30. At 11:00, regular DPET increase occurred. Route A started at DPET = 36 °C, peaked at 42.5 °C, and ended at DPET = 41 °C, reflecting a total increase of 5 °C. Route B exhibited a more pronounced increase, particularly along the eastern roads, with a total rise of 6.5 °C. Increasing tree density helped stabilize DPET values for the duration of the walk, maintaining them within the range of 34 °C to 36 °C, which corresponded closely to the range of skin temperature

At 13:00, the results showed contrasting performance. Route A performed well, with only a 2.5 °C increase throughout the walk. However, route B, despite starting at a lower DPET value, experienced a significant rise of 7.5°C due to the eastern canyons, ending at 43 °C. Increasing tree density effectively reduced these values for both routes. On route A, the values remained consistent until the end of the walk; on route B, the increase was dramatically reduced to just 3°C—a 60% improvement.

At 15:00, a similar trend was observed. Route A showed a slight DPET increase of 3 °C, reflecting the effective cooling performance of the northern road. Route B experienced an increase of 7 °C by the end of the walk, with regular increases along eastern roads and steady values along the northern road. Notably, route B began with a DPET value 3.5 °C lower than that of route A's starting point but ended 1 °C higher, highlighting the influence of canyon orientation on thermal conditions. Increasing tree density resulted in similar performances, and both routes maintained good DPET values. Route A maintained values within 36 °C to 37.5 °C, while route B showed a slight increase of just 1.5 °C, representing a significant improvement in thermal comfort.

The results for Mohandisen, as shown in Figure 31, highlight the thermal performance of both routes under different conditions. At 11:00, both routes started with very high DPET values. Route A decreased by 2.5 °C initially but then increased again, ending with the same value. Route B increased sharply, reaching 52.5 °C at the end of the shallow northeastern canyon, before decreasing to 48.5°C in the moderate northwestern canyon by the end of the walk. Increasing tree density helped mitigate the massive increase and extreme heat stress values along both routes. On route A, trees reduced the high starting value by 3.0 °C, resulting in an ending value of 42.5 °C. On route B, trees helped limit the maximum DPET value to 49.0 °C at the end of the shallow northeastern canyon, a 3.5 °C improvement compared to the lower tree density scenario. The route started at DPET = 46.0 °C and ended with a slightly reduced value of 45.0 °C. T Skin fluctuations were observed on both routes at 11:00, caused by extreme heat stress and a lack of shading, leading to an increase of 1.5 °C in skin temperature.

At 13:00, a similar DPET pattern was observed, but with higher values overall. Route A fluctuated slightly (within 2 °C) due to the moderate canyons and urban park in the middle of the route. The walk ended with the same value as the starting point. Route B started with a very high DPET value of 50.5 °C. This value peaked at 54.0 °C at the end of the shallow northeastern canyon before decreasing to match the starting value by the route's end. Increasing tree density was particularly important at this hour, as building shade was nearly completely absent. On route A, trees reduced the DPET values by 3 °C at the end of the route. On route B, trees maintained DPET values below 50.0 °C throughout the route, with a 1.5 °C reduction at the end.

At 15:00, urban shading significantly reduced DPET values on both routes. Routes A and B exhibited slight, regular DPET increases of 7 °C by the end. Adding trees enhanced the thermal performance further, as the combination of tree shading and building shading

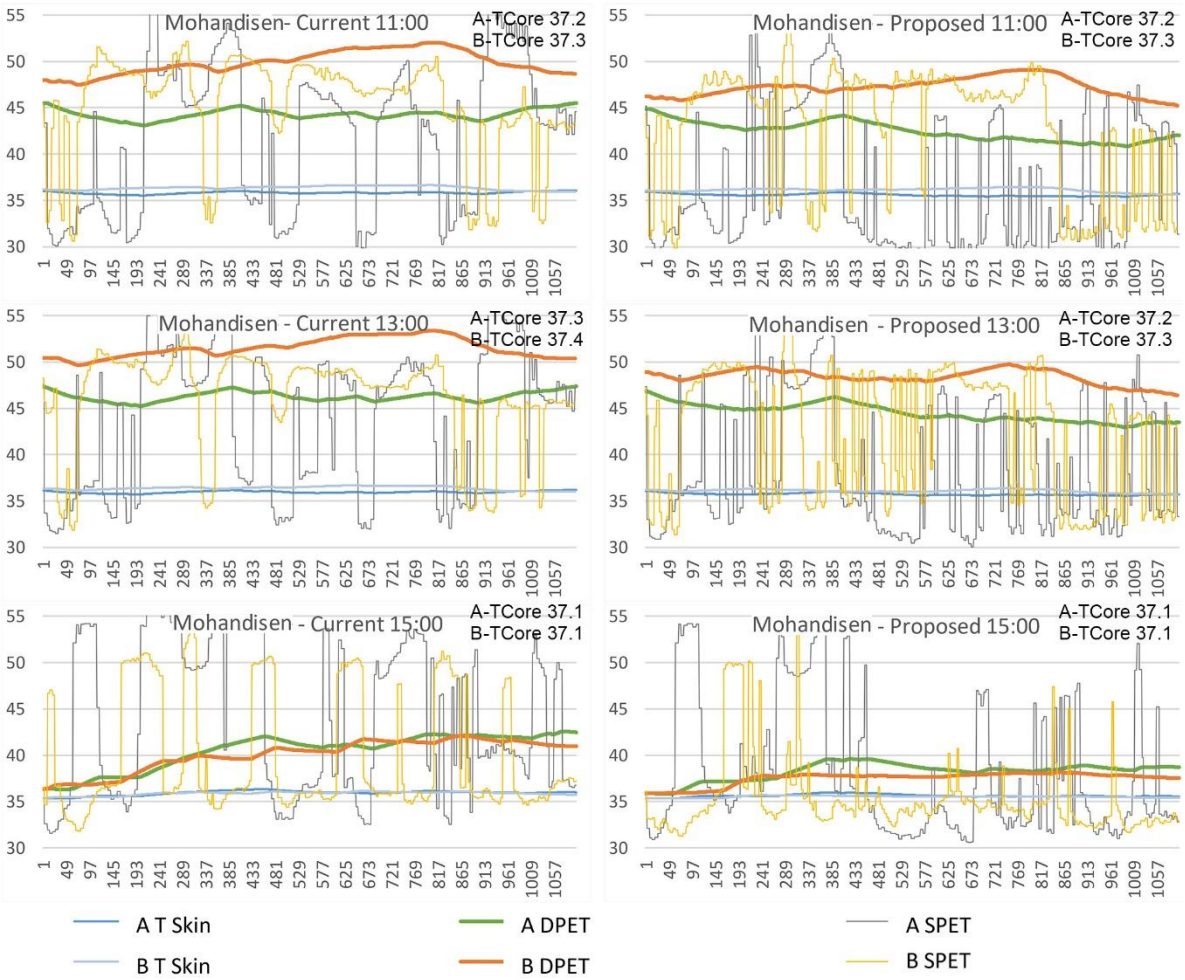

Figure 31. DPET, SPET, skin temperature (T Skin), and average core temperature (TCore) results for Mohandisen routes (A and B) in both tree scenarios (current and proposed) at Z=1.5 m. Y axis = °C and X axis = seconds while walking each route.

limited DPET increases to 3.0–4.0 °C on both routes. This result highlights the critical role of combining urban and tree shading for moderate canyons during peak hours (15:00).

In New Cairo, as shown in Figure 32, the existing green open spaces (12%) and tree coverage (9.4%) in the current configuration helped keep DPET values relatively low. However, due to the limited urban shading caused by lower building heights and plot setbacks, trees played a crucial role in enhancing pedestrian thermal comfort.

At 11:00, both routes exhibited regular DPET increases, reaching 9.0 °C by the end of the walk. Increasing tree density reduced these increases to only 4.5 °C, which remained below skin temperature levels. At 13:00, similar thermal conditions were observed, with starting DPET values of 35.0 °C on both routes. Regular increases followed, peaking at 43.0 °C by the end of the walks, an increase of 8.0 °C. With increased tree density, the increase in value was significantly reduced to only 3.5 °C by the end of both routes.

At 15:00, the same trend persisted, with regular gradual increases of 9.0 °C on routes A and B. Increasing tree density further mitigated these increases, limiting the DPET rise to only 2.5 °C at the end of both routes.

The results for New Cairo emphasized the importance of trees in both scenarios (low and high tree density). In open urban forms where urban shading is nearly absent, tree shading proved to be an effective solution for enhancing microclimate conditions. This case also

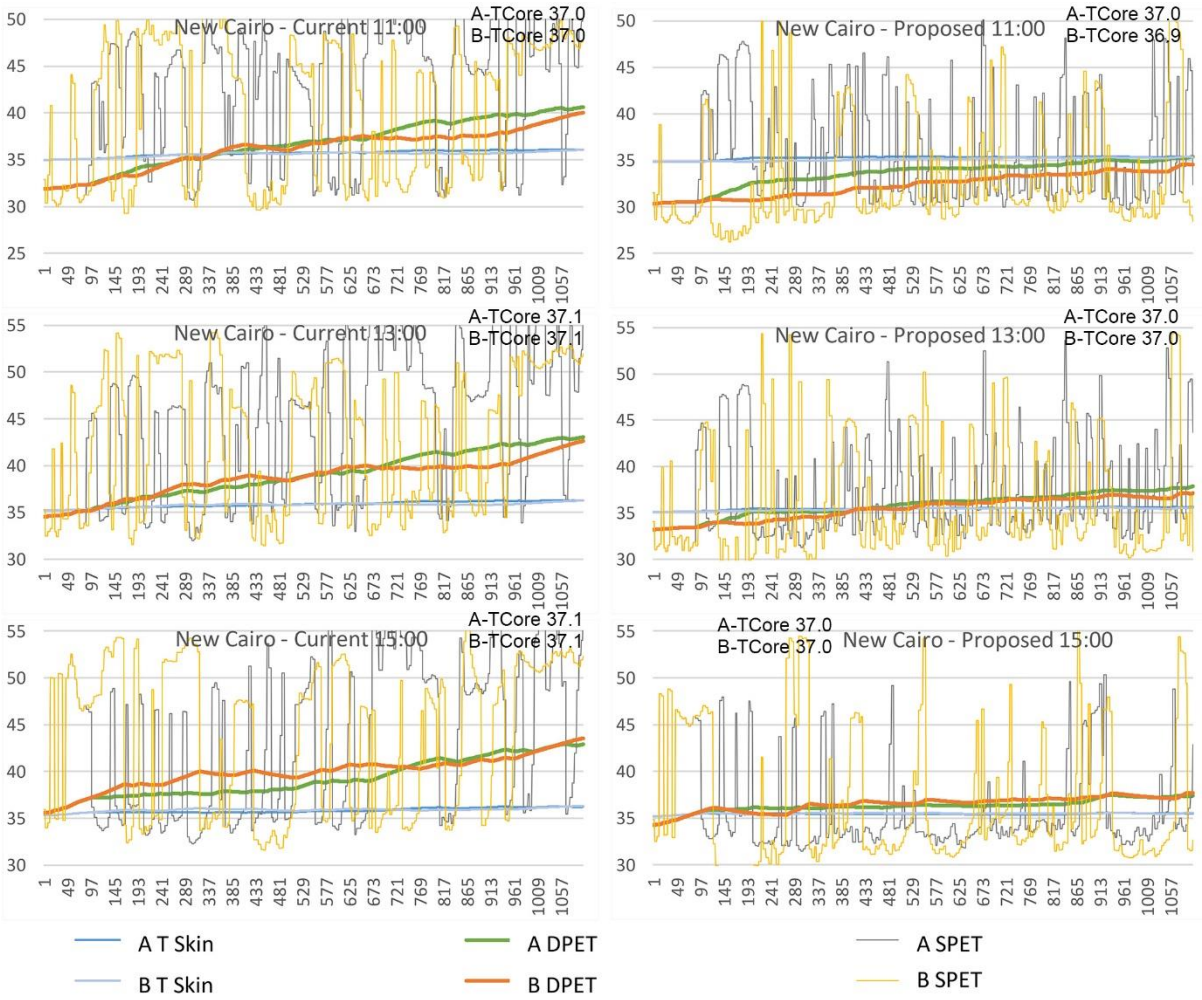

Figure 32. DPET, SPET, skin temperature (T Skin), and average core temperature (TCore) results for New Cairo routes (A and B) in both tree scenarios (current and proposed) at Z=1.5 m. Y axis = °C and X axis = seconds while walking each route.

demonstrated that surface materials had a limited impact; walking inside a park or on a sidewalk produced similar thermal performance under the same tree coverage.

In Mivida, as shown in Figure 33, similar DPET patterns were observed. Given the absence of shading from the short buildings, tree cover percentage played a critical role in determining DPET values. The low-rise buildings (villas with G+2) and large plot setbacks inside positioned all structures away from sidewalks and walking trails, leaving trees as the primary shading element.

At 11:00, route A started with a lower DPET value (32.5 °C) compared to route B (37.5 °C). However, route A exhibited a larger DPET increase, and both routes ended at the same value (39.5 °C). The smaller DPET increase on route B was attributed to a higher density of trees along this section of the route in the current scenario.

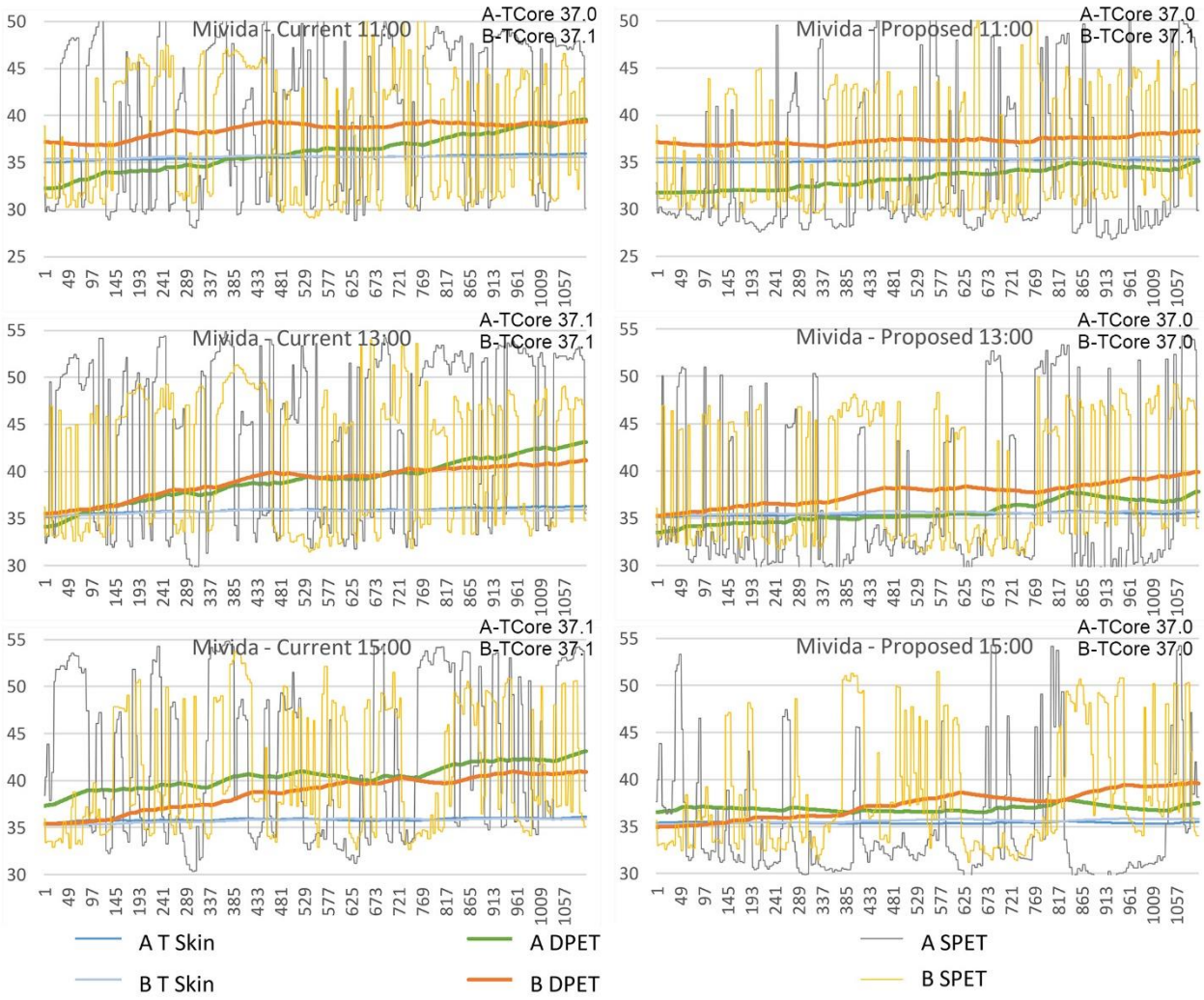

Figure 33. DPET, SPET, skin temperature (T Skin), and average core temperature (TCore) results for Mivida routes (A and B) in both tree scenarios (current and proposed) at Z=1.5 m. Y axis = °C and X axis = seconds while walking each route.

Increasing tree density on both routes (particularly in parks) helped them maintain lower DPET values, especially route A, with starting and ending values remaining within the range of skin temperature. On route B, the added tree density maintained more consistent DPET values, ranging from 37.0 °C to 38.0 °C.

At 13:00, DPET increased by 8.5 °C by the end of route A and by 6.5 °C by the end of route B. Increasing the tree density, particularly in parks, cooled route A by 2.0 °C to 3.0 °C more compared to route B, maintaining their values below 40.0 °C throughout the entire walk on both routes.

At 15:00, route B was cooler than route A due to the combined shading effects of trees and buildings. Route A started with DPET = 37.0 °C and increased to 39.0 °C by the end of the route. Route B started with DPET = 34.0 °C but increased to 41.0 °C by the end of the route. Increasing tree density reversed this trend. Route A became 2.0 °C cooler than route B by the end of the route, despite starting with a value 1 °C higher than route B.

Table 3. Main DPET value classifications (every 50 seconds) on all routes in all scenarios at critical hours (13:00 and 15:00).

Time	13:00										15:00									
	A					B					A					B				
	Downtown	Bulaq	Mohandisen	New Cairo	Mivida	Downtown	Bulaq	Mohandisen	New Cairo	Mivida	Downtown	Bulaq	Mohandisen	New Cairo	Mivida	Downtown	Bulaq	Mohandisen	New Cairo	Mivida
Current tree density																				
0	38	37	47	35	34	36	47	50	35	36	39	40	36	36	37	36	50	36	36	35
50	39	39	46	35	36	37	45	50	35	36	39	41	37	37	39	36	48	37	37	36
100	40	41	45	37	37	38	45	51	37	37	40	43	38	38	39	37	48	38	39	37
150	41	42	46	37	38	38	45	52	38	38	40	44	40	38	39	37	47	40	40	37
200	41	43	47	38	39	40	44	51	39	39	41	45	41	38	41	39	46	40	40	38
250	42	41	46	38	39	42	44	52	38	40	41	43	42	38	41	41	45	41	39	39
300	41	41	46	39	39	42	44	53	40	39	41	42	41	39	40	41	45	40	40	40
350	42	40	46	40	40	43	45	53	40	40	41	41	41	40	40	41	44	42	41	40
400	41	40	47	41	40	43	45	53	40	40	41	41	42	41	41	42	44	41	41	40
450	42	40	46	42	41	43	45	52	40	40	42	40	42	42	42	43	44	42	41	41
500	41	40	47	42	42	43	44	51	41	41	42	40	42	42	42	43	43	41	42	41
Proposed tree density																				
0	36	36	47	33	34	35	45	49	33	35	36	38	36	34	37	35	47	36	34	35
50	36	37	45	34	34	36	43	48	34	36	36	38	37	36	37	36	46	36	36	35
100	36	38	45	35	35	37	43	49	34	36	36	38	37	36	37	36	45	37	36	36
150	37	38	45	35	35	37	42	49	35	37	37	38	38	36	37	36	44	38	36	36
200	37	39	46	35	35	37	41	48	35	37	37	39	39	36	36	37	43	38	36	37
250	37	38	45	36	35	38	40	48	35	38	37	38	39	36	37	38	42	38	37	37
300	37	37	44	36	36	39	40	48	36	38	37	37	39	36	37	37	41	38	37	38
350	37	37	44	37	36	38	40	49	36	38	37	37	38	36	37	38	41	38	37	38
400	37	36	44	37	37	39	39	49	37	38	37	37	38	36	37	38	40	38	37	38
450	37	36	43	37	37	39	39	48	37	39	37	36	39	37	37	38	40	38	37	39
500	37	36	43	37	37	39	39	47	37	39	36	36	38	37	37	38	40	38	37	39
Scale	Better conditions																		Worse conditions	

In the Mohandisen study, the maximum core and skin temperatures were recorded under the current scenario. The average core temperature on route B reached 37.4 °C, reflecting the severe climate conditions on this route at 13:00. Similarly, the second-highest average core temperature was recorded on route A under the same conditions and at same time.

The DPET value varied significantly across routes and tree scenarios. Table 3 presents the DPET classifications at critical hours (13:00 and 15:00), recorded every 50 seconds from the start to the end of each route. Routes A and B in Mohandisen and route B in Bulaq were identified as critical routes, frequently falling under the worst condition category (red range) throughout the walk under the current scenarios. Tree scenarios significantly altered DPET classifications, particularly in Bulaq cases, where notable improvements were observed. Other routes were more often classified in better condition (blue range) under increased tree density scenarios.

3.3.3.1. Impact of Trees

The impact of trees varied across different areas, with significant effects in some areas and minor effects in others. Increasing tree density proved particularly important in wide canyons, especially those oriented to the east. These findings align with those from other studies (Abdelmejeed A. G., 2024) (Abdelmejeed A. Y., 2023) (Abdollahzadeh, 2021) (De, 2018). Comprehensive comparisons were conducted across all routes before and after increasing tree density to evaluate how the impact of the trees varied among the various routes in different areas. A second-by-second classification analysis was applied to each route to assess how trees influenced thermal comfort zones for pedestrians while walking. The analysis quantified the duration of each walk within each thermal comfort category. The thermal comfort zones were based on the following grades of physiological stress (PET) and categorized as follows: 23–29 °C, slight heat stress (slightly warm); 29–35 °C, moderate heat stress (warm); 35–41 °C, strong heat stress (hot); and above 41 °C, extreme heat stress (very hot) (Ballinas, 2022). The value used for internal heat production was 80 W, and heat transfer from clothing was set at 0.9 clo (Heaviside, 2017). As shown in Figure 34, routes in specific study areas experienced extreme heat stress, particularly during the peak hours (11:00, 13:00, and 15:00). In Mohandisen, over 90% of both routes were under extreme heat stress, reflecting the harsh thermal conditions in this area. In contrast, Downtown and Bulaq showed better performance, with routes having a balance between strong and moderate heat stress zones during peak hours. In New Cairo and Mivida, the thermal conditions were significantly better. Most routes fell within the moderate heat stress zone, with a very small percentage experiencing extreme heat stress. Across all tree scenarios, notable changes in thermal classifications were observed, including the emergence of new zones, such as slightly warm. Most classifications fell within the warm zone, with a very limited presence of extreme heat stress, appearing only on route B in Mohandisen due to the presence of a large shallow canyon. The impact of increasing tree density was particularly substantial in New Cairo and Mivida, as most routes fell within warm-to-hot categories. Similar improvements were observed in Downtown and Bulaq, with minor variations in Bulaq attributed to the wide canyon at the start of the walk.

The performance of trees was influenced by urban form. In Bulaq, DPET values were enhanced even without the presence of trees when pedestrians walked through deep northern canyons (Abdelmejeed A. Y., 2023) (Sanusi, 2016). However, the significance of trees became evident in shallow canyons with limited shading (Hassan A. T., 2018) (Wei, 2018) (Liu B. Y., 2016). Notably, in areas like New Cairo and Mivida, which already had adequate tree coverage percentages, increasing tree density further enhanced dynamic thermal comfort (Ochiai, 2015). Thus, these findings highlight that while adding trees can confer substantial improvements, optimizing their use requires careful consideration of urban forms and characteristics (Abdelmejeed A. G., 2024) (Abdelmejeed A. Y., 2023).

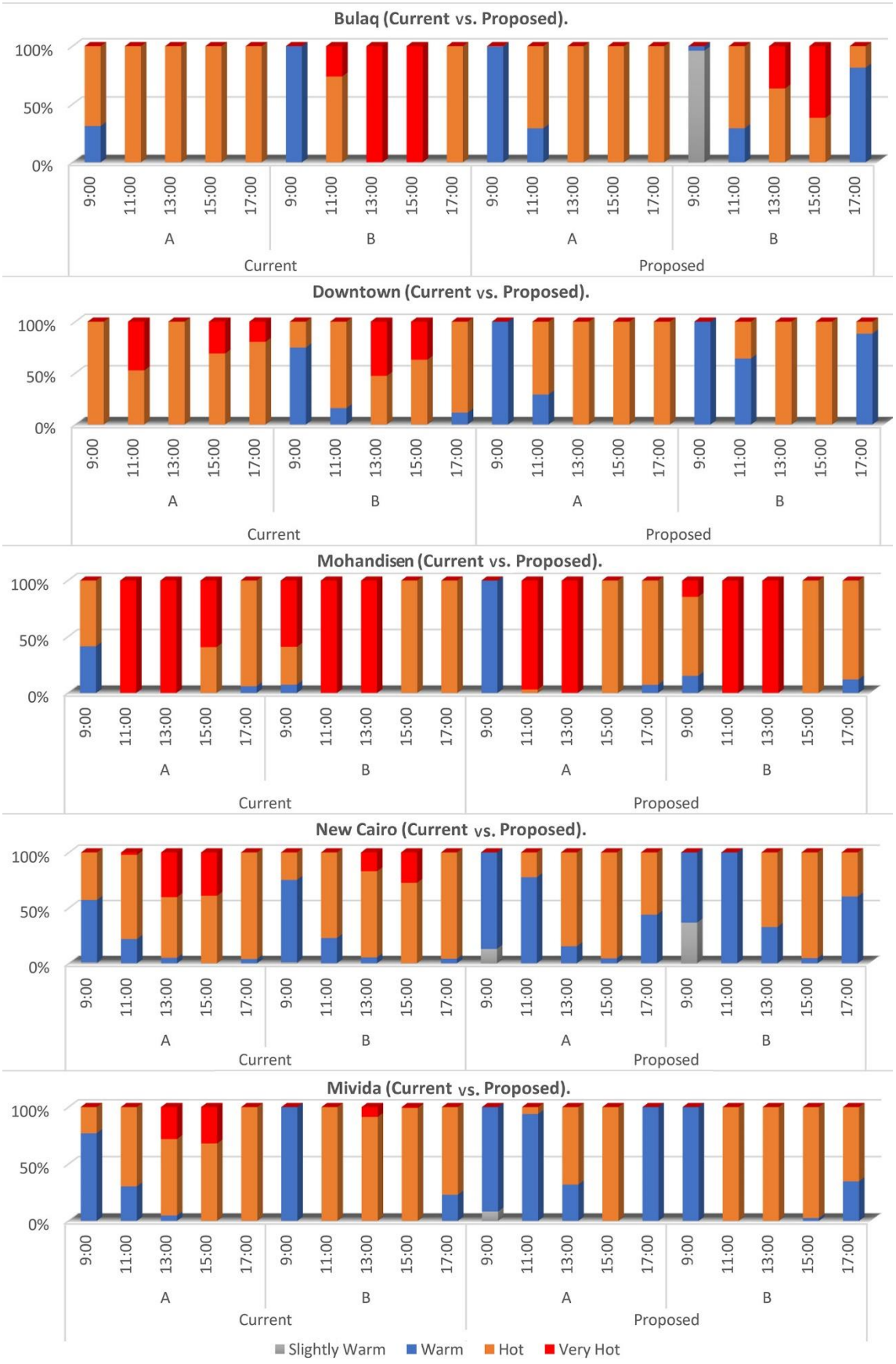

Figure 34. The dynamic thermal comfort classifications for each route (A and B) in both tree scenarios (current and proposed). The DPET values were exported at Z=1.5. The X axis represents the hours, and the Y axis represents the percentages.

3.3.3.2. DPET Changes between Routes

The DPET results for routes A and B under both tree scenarios were compared to analyze the influence of urban forms and trees on thermal comfort. In figure 35, Bulaq's current scenario, route B exhibited significantly higher values at 13:00 and 15:00. Due to the better canyon aspect ratio, this difference decreased significantly to only 1.5 °C. Then, Both routes performed similarly on the northern road. On average, route B demonstrated superior performance with DPET values 3 °C lower than route A. In Bulaq's tree scenario, a similar pattern emerged, with slightly improved DPET values across the same time intervals. In Downtown, route A initially had higher DPET values, averaging 3.5 °C for all hours. However, the improved canyon orientation helped mitigate this discrepancy during peak hours (13:00 and 15:00), ultimately rendering route A superior to route B by an average of 1 °C in the latter part of the walk. In the tree scenario, tree cover influenced DPET increases, narrowing the temperature range. At the starting point, route A was only 1 °C, while at the end of the route, DPET values were consistently lower than 1 °C across most hours. In Mohandisen, the harsher climate conditions along route B led to massively increased DPET values, reaching an average of 8 to 9 °C at three time points (9:00, 11:00, and 13:00). A modest increase in tree cover offered minimal improvement, with only a 2 °C reduction in DPET. These results indicate the need for a more substantial increase in tree cover to achieve meaningful thermal comfort. In New Cairo, routes A and B exhibited minor DPET differences, ranging between 1 °C and -1 °C. Route A initially recorded higher values, while route B became consistently higher during most hours. In the proposed tree scenario, route B remained cooler throughout the walk, whereas route A exhibited a DPET increase of up to 2.5 °C during the first half of the walk before decreasing to a 1 °C difference by the end. In Mivida, similar patterns were observed. Route A, which passed through green parks, initially had higher values due to the limited tree cover in the current scenario. On average, it exceeded route B by 2 °C, although this disparity dropped to zero at the end of the walk at 11:00. In the tree scenario, the trend reversed, indicating that thermal comfort is heavily influenced by local microclimatic conditions within a canyon or specific space. The findings underscore that pedestrian thermal comfort is not dictated solely by the broader study area but is shaped by localized canyon factors.

3.3.3.3. DPET Changes between Different Study Areas

The analysis of changes between the hotter routes in each study area focused on comparing the DPET values of routes A in Bulaq, B in Mohandisen, A in New Cairo, and B in Mivida with route B in Downtown, as illustrated in Figure 36. At 9:00, all study areas, except Mohandisen, exhibited a similar DPET range of 33 °C to 37 °C for the majority of walks. Bulaq exhibited higher values, but route B in Mohandisen showed a marked increase in DPET values, reaching up to 10 °C. The addition of trees mitigated these effects, keeping the DPET range between 29 °C and 32 °C by the end of each walk across all routes, with the exception of route B in Mohandisen. At 11:00, similar performances were observed, with all routes maintaining DPET values around 39.5 °C. However, initial DPET values varied across routes, with route B in Mohandisen continuing to show significantly higher DPET values, recording a much higher average of 50 °C under the current scenario—10 °C higher than route B in Downtown. The addition of trees improved DPET values for most routes, with a good reduction by the end of each walk for all routes. Route B in Mohandisen only showed a slight improvement, with the DPET decreasing to around 47 °C. At 13:00, similar patterns were observed. Route B in Mohandisen continued to exhibit a significant DEPT difference of 10 °C, while route A in Bulaq showed minor fluctuations, with changes of approximately 3.0 °C. Increasing tree density effectively

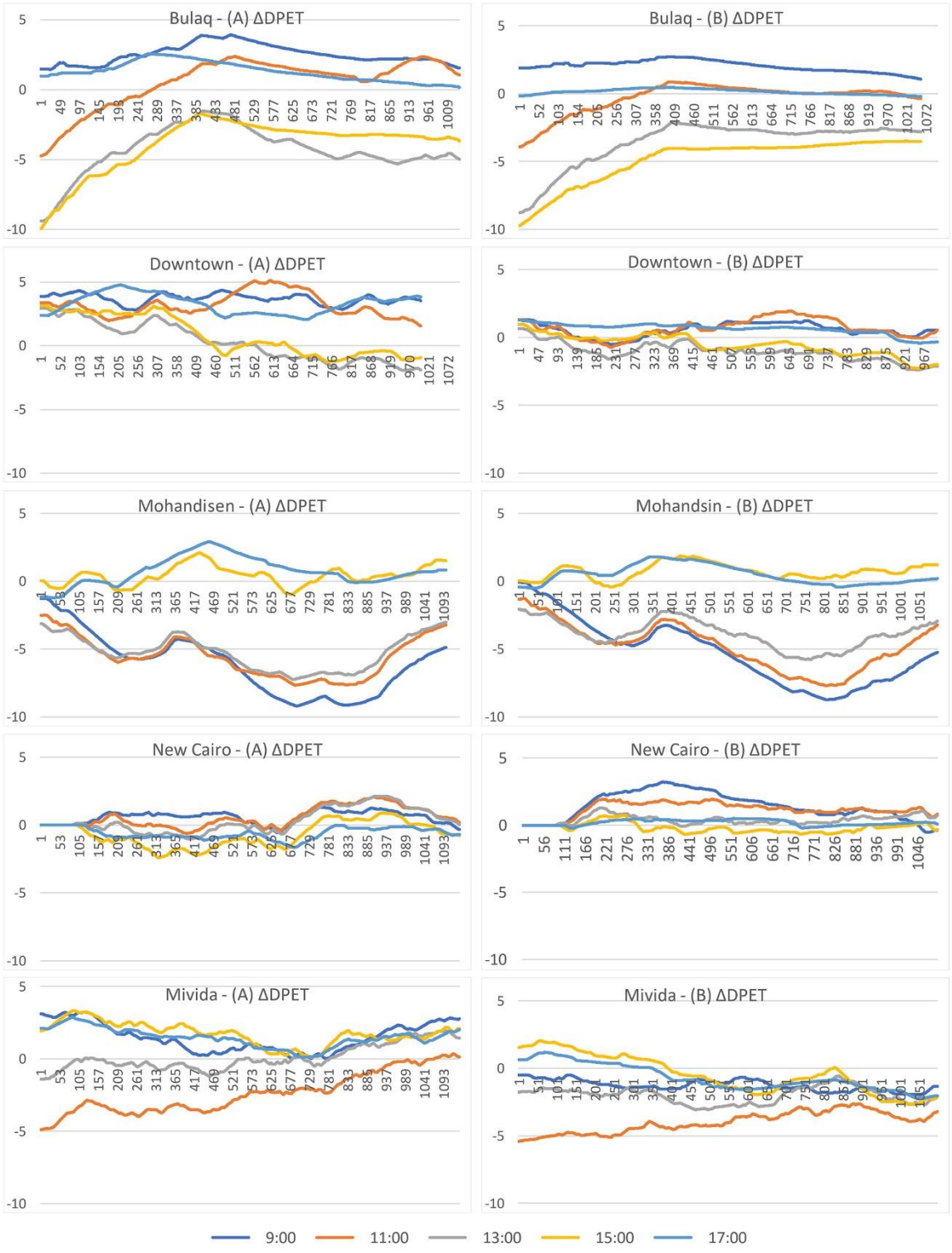

Figure 35. Δ DPET in each study area. A represents (A-B) in the current situation, and B represents (A -B) in the proposed situation at Z=1.5m. X axis represents ΔDPET (°C), and Y axis represents the duration of the walk (seconds).

reduced this range to 1 °C, thus slightly improving conditions by 1 °C on route B in Mohandisen. At 15:00 and 17:00, better shading provided by surrounding buildings led to a substantial decrease in DPET differences along route B in Mohandisen. During these hours, the DPET values across all routes fell within a similar range. These findings underscore the significant influence of local microclimatic conditions within urban

canyons on DPET, highlighting that thermal comfort differences between different urban canyons can reach as high as 10 °C, even when situated within the same overall urban context.

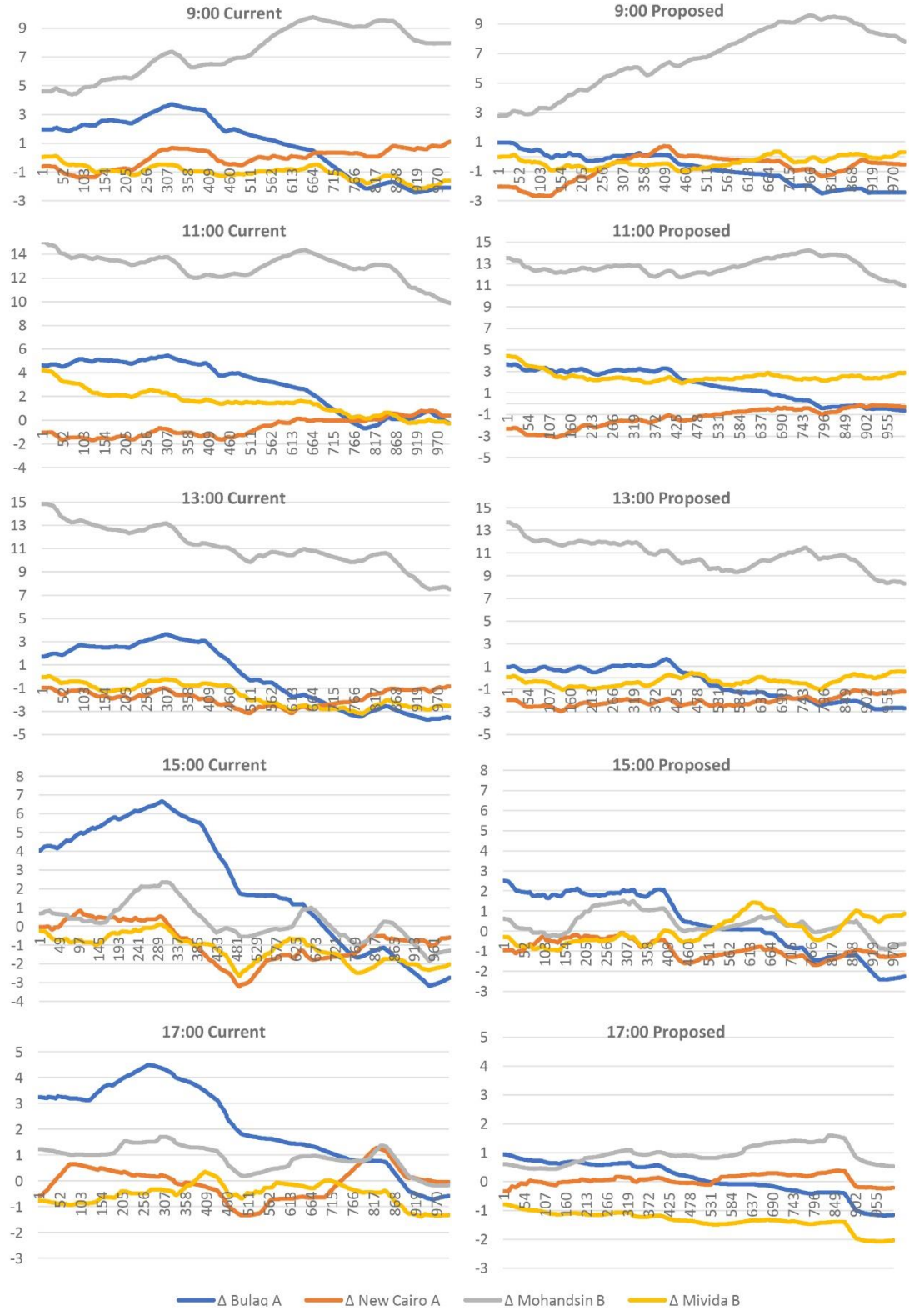

Figure 36. DPET values along hot routes in each study area for current and proposed scenarios per hour at Z=1.5m. X axis represents DPET (°C), and Y axis represents the duration of the walk.

Chapter 4

4. Discussion of the results and conclusion

In the following chapter, the results included in the publications are discussed and connected to the state of the art, research goals, and research questions through synoptic integration. The four research questions are addressed, highlighting the contributions to the relevant research areas. The main conclusions and insights gained are connected, with cross-links elaborated upon.

RQ1. What is the impact of implementing a comprehensive urban tree strategy that considers climate conditions and water scarcity on the city of Cairo?

According to the results of publication 1, the recommended tree coverage percentage to be applied should not be the same for all streets; instead, it should vary. Additionally, the tree model should be independently designed for each street such that it matches its geometry, orientation, and other conditions, which aligns with the findings of previous studies (Aboelata A., 2019) (Morakinyo T. E., 2017). The recommended tree model should consider tree seasonality and tree variety for biodiversity, as well as contribute to a visually appealing image for the city. Nothing, however, would be required to enhance the microclimate condition, as all winter results show that applying different tree coverage percentages to different street canyons would not significantly impact thermal comfort. To decrease water demand while maintaining enhanced microclimate conditions, it is recommended to limit tree usage and apply irrigation technologies. The tree coverage percentages that enhance microclimate conditions for all three streets, while also considering water demand, are 0% for S1, 35% for S2, and 50% for S3. As trees did not provide any significant enhancements in S1, the improvements in S2 with 35% tree coverage were very similar to those achieved with 50% coverage. However, in S3, 50% tree coverage produced greater enhancements compared to 35% tree coverage, attributed to the wider aspect ratio in S3. The recommended ratio of deciduous trees depends on the intended design purpose and not on the requirements of thermal comfort and UHI mitigation. This recommendation is based on the abovementioned tree coverage percentages.
According to the recommended model, although the total number of trees is reduced (with 146 large trees added to replace the 195 smaller existing trees), the total water demand increases by 58.18% compared to the current situation. This is because water demand is influenced by the crown size of the trees rather than their quantity. Based on the recommendations of the efficient UTS, irrigation methods and technologies should help absorb this increase in water demand. Applying such methods and technologies to the current situation should reduce at least 65% of the total water consumption (Haley, 2012). Specifically, their application would reduce the increase in water demand from

+65.48% to +22.92% in both S2 and S3 while saving 7.3% in S1 and increasing the tree coverage percentage. This approach would achieve significant PET enhancements while limiting water demand. Urban shading is a critical factor that should be prioritized, as it consistently influences the effects of urban trees and impacts the application of the strategy. Therefore, the UTS should be carefully considered in relation to urban shading when implementing the strategy in various locations throughout the city.

RQ2. How a detailed analysis and understanding of the different steady PET cases could optimize the use of trees?

According to the findings presented in publication 2, the theoretical study and case study results indicate that trees play a significant role in enhancing urban canyons. The extent of their impact varies based on the orientation, aspect ratio, and side of the canyon. Eastern canyons require a high density of trees on both sides but particularly on the northern side, which is consistent with previous studies (Jamei, 2020), (Rodríguez-Algeciras, 2018), (Andreou E. , 2013). Northern, northeast, and northwest canyons showed better performance in microclimate enhancement than eastern canyons. Although adding trees to northern canyons led to slight improvements, these effects were not as significant as those observed when adding trees to eastern canyons, which aligns with the findings of other studies(Jamei, 2020), (Lobaccaro G. A., 2019). In various northern, northeast, and northwest canyons, the presence of tall buildings (moderate to deep canyons) helps maintain cooler conditions by blocking sunlight from shining directly on the streets. Additionally, these canyons experience strong winds, which further contribute to a cooling effect. Adding trees to moderate and deep canyons in these orientations may not significantly affect thermal comfort and could potentially block some of the wind. However, it can be beneficial to add trees to one side of the canyons, specifically side (b). Trees on side (b) may provide afternoon shade, thus cooling the canyons without blocking the wind. Shallow canyons across all orientations and aspect ratios do not provide enough shading on either side. Consequently, a high density of trees is necessary to enhance thermal comfort in these canyons, as the canyon effect completely disappears, particularly on the northern side of eastern canyons (side a). In deep canyons with northern, northwest, and northeast orientations, applying a low density of trees on one side (side b) may also be advantageous. However, a high tree density is necessary on both sides of eastern and shallow canyons. Comparing the results of the theoretical study with those of the existing case study reveals that uniform and regular urban canyons yield slightly different outcomes compared to the irregular canyons found in existing urban areas. While the main results are generally consistent, slight differences arise due to varying urban conditions at the measurement points. Any alteration to the aspect ratios, orientations, or other urban elements can influence the outcomes, albeit not significantly. It is not feasible to obtain the exact values from a uniform and regular theoretical model. The slight variations in the results were observed when altering the street widths and building heights while maintaining the same aspect ratios and orientation.

The results demonstrate the significant impact of tree placement on microclimate performance, with variations depending on the aspect ratio, orientation, and the side of the canyon on which trees were planted. In shallow canyons, a high tree density reduced the PET by 12 ˚C, while the PET reduction reached 14 ˚C in deep canyons with an eastern orientation when compared to those with a northern orientation. Additionally, PET

reductions were 6 to 7 ˚C greater when a high density of trees was added to the northern side of eastern-oriented canyons compared to the southern side. Based on these results, the addition of trees to urban canyons should account for urban morphology characteristics, such as aspect ratio, orientation, and specific placement (canyon sides). Alterations to any of these factors necessitate a wholly different approach. This guidance is of paramount importance for cities grappling with heat stress and water scarcity, as is the case in Cairo. The findings of this study are applicable to a broad range of urban scenarios within Cairo and should be considered by stakeholders, city planners, and municipal authorities. By playing a part in design guidelines and city management, these results provide a detailed approach for optimizing tree placement to enhance microclimate conditions for pedestrians, whether in developing new communities or upgrading existing areas.

RQ3. What is the relation between the Dynamic PET and the Steady PET and how analyzing both optimizing the use of trees?

According to the results presented in publication 3, the parameters currently used to measure thermal comfort, such as steady/static thermal comfort (SPET), are insufficient for representing actual pedestrian thermal comfort while walking, as they do not consider changes and dynamic variations in the thermal environment (Hwang, 2022). This study aimed to enhance the dynamic thermal comfort (DPET) of pedestrians walking through different urban forms with different aspect ratios, orientations, and building and tree densities, using consistent climate data across all cases. After assessing five different study areas in Cairo City under two tree scenarios (the current tree density and a proposed increase), the results indicated that the DPET values differed from the SPET values at each point along the routes. However, the DPET was closely related to changes in the SPET. The main findings of this study are summarized as follows:

- Since the DPET was impacted by the SPET, maintaining a consistently lower or higher SPET reduced or increased the DPET.
- Frequent equivalent fluctuations in the SPET stabilized the DPET.
- Variations in DPET values were more strongly driven by the microclimate conditions of a space or canyon than the conditions of the overall area, and controlling the microclimate conditions of an entire urban canyon controlled the DPET.
- Differences in the DPET between canyons could reach up to 10 °C, and in some cases, increasing the tree density could lower the DPET by as much as 6 °C.
- The DPET was more affected by urban shading (from buildings or trees) and wind than by changing paving materials or adding grass surfaces.

RQ4. How implementing a comprehensive complete and detailed strategy that considers the city conditions could enhance the climate conditions and optimize the use of resources?

According to the combined results of publications 1 to 3, the research begins by developing a comprehensive framework (strategy) for urban trees to enhance thermal comfort while considering limited water resources and the city's lack of greenery. This framework optimizes the number of trees, the selection of species, and irrigation techniques. The research focuses on a detailed static thermal comfort analysis of 144

theoretical cases, each representing different aspect ratios, orientations, and sides of each canyon. These scenarios are then applied to an existing urban area with similar urban morphologies, thus providing a second layer of tree use optimization. In the final stage, a detailed dynamic thermal comfort analysis is conducted to gain a comprehensive understanding of how trees can be optimized under varying urban conditions, that is, different aspect ratios and orientations, for both steady and dynamic thermal comfort. The overall results and recommendations from these three publications address the final research question and provide a complete framework for optimizing tree use from multiple perspectives and considerations.

Chapter 5

5. Research Limitations and Future Research

In this chapter, the limitations and shortcomings of the three publications are discussed, along with potential future research directions that could add significant important value. This chapter also explores further details that may provide valuable outcomes.

5.1. Research Limitations

Publication 1 highlighted an urban tree strategy (UTS). Although the strategy recommendations can be applied and generalized to the city of Cairo, the recommended canyon tree coverage percentage cannot be generalized, as urban canyons with varying aspect ratios and/or orientations produce completely different results. The methodology used to determine tree coverage percentages in this research can be generalized and applied consistently across Cairo, using the same inputs, scenarios, and analyses.
Another limitation of this study is that it was only applied to one existing area in downtown Cairo, which was adequate to measure the efficiency of the study; however, application across diverse situations would provide more comprehensive results and a stronger assessment of the strategy's effectiveness. Additionally, the lack of current information regarding the required level of irrigation for trees prevented a full comparison and assessment of irrigation consumption, as the trees were irrigated manually. In addition, the field survey was somewhat challenging due to security restrictions.

Publication 2 addressed the various shortcomings of publication number 1 by including many case studies—up to 144—but it still did not cover all scenarios. However, the research methodology could be applied to different urban contexts in Cairo, particularly in cases where urban canyons are not fully defined, which is not covered in this research. This approach would help to achieve the same target of optimizing tree usage. Linking the study's results with field measurements could further improve its applicability.

Publication 3 examined various urban forms and tree varieties, testing them using the simulation software ENVI-met. The findings could also be enhanced by linking them to real-world experiments, such as investigating the experiences of people walking along these routes. In addition, a greater number of diverse urban routes could be studied, including waterfront promenades, large-scale park walkways, or walkways inside large parking areas.

In conclusion, conducting a detailed simulation study enables the exploration of numerous scenarios with limited research resources, thus providing a trusted tool to study various cases under different situations. It is crucial, however, to link the simulation study findings with real-world field studies and gather feedback on people's experiences. Both studies could then be compared to validate the findings at scale.

5.2. Future research

In general, the field of Urban Climate is highly dynamic and evolving. This cumulative research could be extended through various future studies, starting with further developing the Urban Tree Strategy (UTS) by incorporating more variables, such as economic aspects that could influence the strategy. Additionally, including social dimensions—such as how community organizations could implement this strategy and raise awareness—might also help decision-makers and relevant authorities in taking action to prevent tree cutting. This would promote an urban tree strategy aimed at enhancing thermal comfort, mitigating the UHI effect, and expanding greenery across the city to an acceptable level. Future studies could enhance the strategy by conducting in-depth research on tree species, supported by field measurements across different tree species and considering tree ages. This approach would help estimate the time required for trees to achieve optimal performance.

Publication 2, as mentioned in the study's limitations, could explore areas without defined urban canyons, such as promenades, parks, open spaces, and nature trails. These additional cases could be analyzed using both simulation software and field measurements or questionnaires to add depth to the study and allow for comparing outcomes.

Publication 3 covers a range of variables. The study's outcomes could support design decisions, such as positioning bus stops in relation to surrounding land use and walking conditions, as well as the distribution of retail and commercial spaces along routes. Additionally, the distribution and frequency of urban parks could be defined not only by the urban scenario but also by considering thermal comfort.

Bibliography

Abdelhaleem, F. S., & Helal, E. Y. (2015). Impacts of Grand Ethiopian Renaissance Dam on different water usages in upper Egypt. Br. J. Appl. Sci. Technol, 8(5), 461-483. http://doi.org/10.9734/BJAST/2015/17252

Abdelmejeed, A. Y., & Gruehn, D. (2024). Pedestrian Dynamic Thermal Comfort Analysis to Optimize Using Trees in Various Urban Morphologies: A Case Study of Cairo City. Land, 13(9), 1489. https://doi.org/10.3390/land13091489

Abdelmejeed, A.Y., Gruehn, D. Optimizing an efficient urban tree strategy to improve microclimate conditions while considering water scarcity: a case study of Cairo. Discov Sustain 5, 66 (2024). https://doi.org/10.1007/s43621-024-00247-w

Abdelmejeed AY, Gruehn D. Optimization of Microclimate Conditions Considering Urban Morphology and Trees Using ENVI-Met: A Case Study of Cairo City. *Land*. 2023; 12(12):2145. https://doi.org/10.3390/land12122145

Abdel Wahaab, R., & Omar, M. (2011). Wastewater reuse in Egypt: opportunities and challenges. Arab World. Arab Water Council Report. Cross Ref.

Abdin, A. E., & Gaafar, I. (2009). Rational water use in Egypt. *Technological perspectives for rational use of water resources in the Mediterranean region*, *88*, 11-27. http://om.ciheam.org/om/pdf/a88/00801177.pdf

Abdollahzadeh, N., & Biloria, N. (2021). Outdoor thermal comfort: Analyzing the impact of urban configurations on the thermal performance of street canyons in the humid subtropical climate of Sydney. Frontiers of Architectural Research, 10(2), 394-409. https://doi.org/10.1016/j.foar.2020.11.006

Aboelata, A. (2020). Vegetation in different street orientations of aspect ratio (H/W 1: 1) to mitigate UHI and reduce buildings' energy in arid climate. Building and Environment, 172, 106712. https://doi.org/10.1016/j.buildenv.2020.106712

Aboelata, A., & Sodoudi, S. (2019). Evaluating urban vegetation scenarios to mitigate urban heat island and reduce buildings' energy in dense built-up areas in Cairo. Building and environment, 166, 106407. https://doi.org/10.1016/j.buildenv.2019.106407

Abou El-Magd, I., Ismail, A., & Zanaty, N. (2016). Spatial variability of urban heat islands in Cairo City, Egypt using time series of Landsat Satellite images. International Journal of Advanced Remote Sensing and GIS, 5(3), 1618-1638. https://doi.org/10.23953/cloud.ijarsg.48

Abougendia, S. M. (2023). Investigating surface UHI using local climate zones (LCZs), the case study of Cairo's River Islands. Alexandria Engineering Journal, 77, 293-307. https://doi.org/10.1016/j.aej.2023.06.071

Abutaleb, K., Ngie, A., Darwish, A., Ahmed, M., Arafat, S., & Ahmed, F. (2015). Assessment of urban heat island using remotely sensed imagery over Greater Cairo, Egypt. Advances in Remote Sensing, 4(1), 35-47. 10.4236/ars.2015.41004

Affairs, Department of Economic and Social. The 17 Goals. https://sdgs.un.org/goals

Ahmadalipour, A., Moradkhani, H., & Kumar, M. (2019). Mortality risk from heat stress expected to hit poorest nations the hardest. Climatic Change, 152, 569-579. https://doi.org/10.1007/s10584-018-2348-2

Allam, M. N., & Allam, G. I. (2007). Water resources in Egypt: future challeges and opportunities. *Water International*, *32*(2), 205-218. https://doi.org/10.1080/02508060708692201

Andreou, E., & Axarli, K. (2012). Investigation of urban canyon microclimate in traditional and contemporary environment. Experimental investigation and parametric analysis. Renewable Energy, 43, 354-363. https://doi.org/10.1016/j.renene.2011.11.038

Andreou, E. (2013). Thermal comfort in outdoor spaces and urban canyon microclimate. Renewable energy, 55, 182-188. https://doi.org/10.1016/j.renene.2012.12.040

Armson, D., Rahman, M. A., & Ennos, A. R. (2013). A comparison of the shading effectiveness of five different street tree species in Manchester, UK. Arboriculture & Urban Forestry, 39(4), 157-164. https://www.cabidigitallibrary.org/doi/full/10.5555/20133290871

Ashoub, S. H., & ElKhateeb, M. W. (2021). Enclaving the City: New Models of Containing the Urban Populations-A Case Study of Cairo. Urban Planning, 6(2), 202-217. https://doi.org/10.17645/up.v6i2.3880

Balany, F., Ng, A. W., Muttil, N., Muthukumaran, S., & Wong, M. S. (2020). Green infrastructure as an urban heat island mitigation strategy—a review. Water, 12(12), 3577. https://doi.org/10.3390/w12123577

Ballinas, M., Morales-Santiago, S. I., Barradas, V. L., Lira, A., & Oliva-Salinas, G. (2022). Is PET an adequate index to determine human thermal comfort in Mexico City?. Sustainability, 14(19), 12539. https://doi.org/10.3390/su141912539

Bruse, M., & Skinner, C. J. (1999, November). Rooftop greening and local climate: A case study in Melbourne. In International Conference on Urban Climatology & International Congress of Biometeorology, Sydney. https://www.envi-met.net/documents/papers/Rooftop1999.pdf

Cao, S., Li, X., Yang, B., & Li, F. (2021). A review of research on dynamic thermal comfort. Building Services Engineering Research and Technology, 42(4), 435-448. https://doi.org/10.1177/01436244211003028

Chiesura, A. (2004). The Role of Urban Parks for the Sustainable City. Land-scape and Urban Planning, 68, 129-138.

Coutts, A. M., White, E. C., Tapper, N. J., Beringer, J., & Livesley, S. J. (2016). Temperature and human thermal comfort effects of street trees across three contrasting street canyon environments. Theoretical and applied climatology, 124, 55-68. https://doi.org/10.1007/s00704-015-1409-y

De Abreu-Harbich, L. V., Labaki, L. C., & Matzarakis, A. (2015). Effect of tree planting design and tree species on human thermal comfort in the tropics. Landscape and Urban Planning, 138, 99-109. https://doi.org/10.1016/j.landurbplan.2015.02.008

de Lieto Vollaro, A., De Simone, G., Romagnoli, R., Vallati, A., & Botillo, S. (2014). Numerical study of urban canyon microclimate related to geometrical parameters. Sustainability, 6(11), 7894-7905. https://doi.org/10.3390/su6117894

De, B., & Mukherjee, M. (2018). Optimisation of canyon orientation and aspect ratio in warm-humid climate: Case of Rajarhat Newtown, India. Urban climate, 24, 887-920. https://doi.org/10.1016/j.uclim.2017.11.003

De Dear, R. J., & Brager, G. S. (2002). Thermal comfort in naturally ventilated buildings: revisions to ASHRAE Standard 55. Energy and buildings, 34(6), 549-561. https://doi.org/10.1016/S0378-7788(02)00005-1

Déoux, S., & Déoux, P. (2004). Le guide de l'habitat sain: habitat qualité santé pour bâtir une santé durable. Medieco éditions. http://pascal-francis.inist.fr/vibad/index.php?action=getRecordDetail&idt=24013450

Dimitrova, B., Vuckovic, M., Kiesel, K., & Mahdavi, A. (2014). Trees and the microclimate of the urban canyon: A case study. http://dspace.epoka.edu.al/handle/1/953

Dimoudi, A., Kantzioura, A., Zoras, S., Pallas, C., & Kosmopoulos, P. (2013). Investigation of urban microclimate parameters in an urban center. Energy and Buildings, 64, 1-9. https://doi.org/10.1016/j.enbuild.2013.04.014

Doick, K., & Hutchings, T. (2013). Air temperature regulation by urban trees and green infrastructure (No. 012, pp. 10-pp). https://www.cabidigitallibrary.org/doi/full/10.5555/20133165696

Dukes, M. D. (2012). Water conservation potential of landscape irrigation smart controllers. Transactions of the ASABE, 55(2), 563-569. doi: 10.13031/2013.41391

Elbardisy, W. M., Salheen, M. A., & Fahmy, M. (2021). Solar irradiance reduction using optimized green infrastructure in arid hot regions: A case study in el-nozha district, Cairo, Egypt. Sustainability, 13(17), 9617. https://doi.org/10.3390/su13179617

Elmarakby, E., Khalifa, M., Elshater, A., & Afifi, S. (2020, November). Spatial morphology and urban heat island: comparative case studies. In Architecture and Urbanism: A Smart Outlook: Proceedings of the 3rd International Conference on Architecture and Urban Planning, Cairo, Egypt (pp. 441-454). Cham: Springer International Publishing. https://doi.org/10.1007/978-3-030-52584-2_31

Elmasry, L. (2014.). A Plant Guidebook for Al-Azhar Park and the City of Cairo. vol. II. Cairo: Shouruk international bookshop.

Elnabawi, M., Hamza, N., & Dudek, S. (2013). Outdoor thermal comfort in the old Fatimid city, Cairo, Egypt. In International Conference on "Changing Cities": Spatial, morphological, formal & socio-economic dimensions. Newcastle University. https://eprints.ncl.ac.uk/195989

El-Nashar, W. Y., & Elyamany, A. H. (2018). Managing risks of the Grand ethiopian renaissance dam on Egypt. Ain Shams Engineering Journal, 9(4), 2383-2388. https://doi.org/10.1016/j.asej.2017.06.004

El-Sadek, A. (2010). Water desalination: An imperative measure for water security in Egypt. Desalination, 250(3), 876-884. https://doi.org/10.1016/j.desal.2009.09.143

Emmanuel, R., Rosenlund, H., & Johansson, E. (2007). Urban shading—a design option for the tropics? A study in Colombo, Sri Lanka. International Journal of Climatology: A Journal of the Royal Meteorological Society, 27(14), 1995-2004. 10.1002/joc.1609

Envi-board. (n.d.). Envi-met support center. (Envi-met) Retrieved April 30, 2023, http://www.envi-hq.com/

Fahmy, M. (2010). Interactive urban form design of local climate scale in hot semi-arid zone. School of Architecture. Cross ref.

Fahmy, M., & Sharples, S. (2009). On the development of an urban passive thermal comfort system in Cairo, Egypt. Building and environment, 44(9), 1907-1916. https://doi.org/10.1016/j.buildenv.2009.01.010

Fang, Y., Chen, G., Bick, M., & Chen, J. (2021). Smart textiles for personalized thermoregulation. Chemical Society Reviews, 50(17), 9357-9374. https://doi.org/10.1039/D1CS00003A

Fathy, H. (1973). Architecture for the poor: an experiment in rural Egypt. University of Chicago press. Cross ref.

Fereres, E., & Soriano, M. A. (2007). Deficit irrigation for reducing agricultural water use. Journal of experimental botany, 58(2), 147-159. https://doi.org/10.1093/jxb/erl165

Flora and Funa Web. (n.d.). Retrieved 2022, https://www.nparks.gov.sg/florafaunaweb

Georgi, J. N., & Dimitriou, D. (2010). The contribution of urban green spaces to the improvement of environment in cities: Case study of Chania, Greece. Building and environment, 45(6), 1401-1414. https://doi.org/10.1016/j.buildenv.2009.12.003

Guterres, A. (2024, June). United Nations. Retrieved from un.org; accessed 2024 Cross ref.

Guo, W., Liu, X., & Yuan, X. (2015). A case study on optimization of building design based on CFD simulation technology of wind environment. Procedia Engineering, 121, 225-231. https://doi.org/10.1016/j.proeng.2015.08.1060

Group, World Bank. (2019). Sustainable Development Goals - Annual report. https://documents1.worldbank.org/curated/en/106391567056944729/pdf/World-Bank-Group-Partnership-Fund-for-the-Sustainable-Development-Goals-Annual-Report-2019.pdf

Hamdi, R., & Schayes, G. (2008). Sensitivity study of the urban heat island intensity to urban characteristics. International Journal of Climatology: A Journal of the Royal Meteorological Society, 28(7), 973-982. 10.1002/joc.1598

Hamdy, O. (2022). Using remote sensing techniques to assess the changes in the rate of urban green spaces in Egypt: a case study of greater Cairo. International Design Journal, 12(3), 53-64. 10.21608/idj.2022.128280.1039

Hassan, A. A. M. (2011). Dynamic expansion and urbanization of greater Cairo metropolis, Egypt. na. https://conference.corp.at/archive/CORP2011_163.pdf

Hassan, A., Tao, J., Li, G., Jiang, M., Aii, L., Zhihui, J., ... & Qibing, C. (2018). Effects of walking in bamboo forest and city environments on brainwave activity in young adults. Evidence-Based Complementary and Alternative Medicine, 2018(1), 9653857. https://doi.org/10.1155/2018/9653857

Haley, M. B., & Dukes, M. D. (2012). Validation of landscape irrigation reduction with soil moisture sensor irrigation controllers. Journal of Irrigation and Drainage Engineering, 138(2), 135-144. https://doi.org/10.1061/(ASCE)IR.1943-4774.0000391

Heaviside, C., Macintyre, H., & Vardoulakis, S. (2017). The urban heat island: implications for health in a changing environment. Current environmental health reports, 4, 296-305. https://doi.org/10.1007/s40572-017-0150-3

Heritage, S. N. (2008). Health impact assessment of greenspace a guide. http://www.ukmaburbanforum.co.uk/docunents/other/greenspace_HIA.pdf

Höppe, P. (2002). Different aspects of assessing indoor and outdoor thermal comfort. Energy and buildings, 34(6), 661-665. https://doi.org/10.1016/S0378-7788(02)00017-8

Huang, T., Niu, J., Xie, Y., Li, J., & Mak, C. M. (2020). Assessment of "lift-up" design's impact on thermal perceptions in the transition process from indoor to outdoor. Sustainable Cities and Society, 56, 102081. https://doi.org/10.1016/j.scs.2020.102081

Hwang, R. L., Weng, Y. T., & Huang, K. T. (2022). Considering transient UTCI and thermal discomfort footprint simultaneously to develop dynamic thermal comfort models for

pedestrians in a hot-and-humid climate. Building and Environment, 222, 109410. https://doi.org/10.1016/j.buildenv.2022.109410

Huynh, C., & Eckert, R. (2012). Reducing heat and improving thermal comfort through urban design-A case study in Ho Chi Minh city. International Journal of Environmental Science and Development, 3(5), 480. 10.7763/IJESD.2012.V3.271

Jamei, E., Ossen, D. R., Seyedmahmoudian, M., Sandanayake, M., Stojcevski, A., & Horan, B. (2020). Urban design parameters for heat mitigation in tropics. Renewable and sustainable energy reviews, 134, 110362. https://doi.org/10.1016/j.rser.2020.110362

Jia, X., Cao, B., & Zhu, Y. (2022). A climate chamber study on subjective and physiological responses of airport passengers from walking to a sedentary status in summer. Building and Environment, 207, 108547. https://doi.org/10.1016/j.buildenv.2021.108547

Karimimoshaver, M., Khalvandi, R., & Khalvandi, M. (2021). The effect of urban morphology on heat accumulation in urban street canyons and mitigation approach. Sustainable Cities and Society, 73, 103127. https://doi.org/10.1016/j.scs.2021.103127

Katavoutas, G., Flocas, H. A., & Matzarakis, A. (2015). Dynamic modeling of human thermal comfort after the transition from an indoor to an outdoor hot environment. International journal of biometeorology, 59, 205-216. https://doi.org/10.1007/s00484-014-0836-2

Ketterer, C., & Matzarakis, A. (2014). Human-biometeorological assessment of heat stress reduction by replanning measures in Stuttgart, Germany. Landscape and Urban Planning, 122, 78-88. https://doi.org/10.1016/j.landurbplan.2013.11.003

Ki-moon, B. (2024, October). United Nations. Retrieved from un.org; accessed 2024 Cross ref.

Kolokotsa, D., Lilli, K., Gobakis, K., Mavrigiannaki, A., Haddad, S., Garshasbi, S., ... & Santamouris, M. (2022). Analyzing the impact of urban planning and building typologies in urban heat island mitigation. Buildings, 12(5), 537. https://doi.org/10.3390/buildings12050537

Kotharkar, R., Bagade, A., & Ramesh, A. (2019). Assessing urban drivers of canopy layer urban heat island: A numerical modeling approach. Landscape and Urban Planning, 190, 103586. https://doi.org/10.1016/j.landurbplan.2019.05.017

Kottek, M., Grieser, J., Beck, C., Rudolf, B., & Rubel, F. (2006). World map of the Köppen-Geiger climate classification updated. DOI: 10.1127/0941-2948/2006/0130

Konarska, J., Uddling, J., Holmer, B., Lutz, M., Lindberg, F., Pleijel, H., & Thorsson, S. (2016). Transpiration of urban trees and its cooling effect in a high latitude city. International journal of biometeorology, 60, 159-172. https://doi.org/10.1007/s00484-015-1014-x

Kong, F., Yan, W., Zheng, G., Yin, H., Cavan, G., Zhan, W., ... & Cheng, L. (2016). Retrieval of three-dimensional tree canopy and shade using terrestrial laser scanning (TLS) data to analyze the cooling effect of vegetation. Agricultural and Forest Meteorology, 217, 22-34. https://doi.org/10.1016/j.agrformet.2015.11.005

Kong, L., Lau, K. K. L., Yuan, C., Chen, Y., Xu, Y., Ren, C., & Ng, E. (2017). Regulation of outdoor thermal comfort by trees in Hong Kong. Sustainable Cities and Society, 31, 12-25. https://doi.org/10.1016/j.scs.2017.01.018

Kosmopoulos, P., Kazadzis, S., & El-Askary, H. (2018). The solar atlas of Egypt. Geo-Cradle. Cross Ref.

Lan, H., Lau, K. K. L., Shi, Y., & Ren, C. (2021). Improved urban heat island mitigation using bioclimatic redevelopment along an urban waterfront at Victoria Dockside, Hong Kong. Sustainable Cities and Society, 74, 103172. https://doi.org/10.1016/j.scs.2021.103172

Lau, K. K. L., Shi, Y., & Ng, E. Y. Y. (2019). Dynamic response of pedestrian thermal comfort under outdoor transient conditions. International journal of biometeorology, 63, 979-989. https://doi.org/10.1007/s00484-019-01712-2

Li, J., Niu, J., Huang, T., & Mak, C. M. (2022). Dynamic effects of frequent step changes in outdoor microclimate environments on thermal sensation and dissatisfaction of pedestrian during summer. Sustainable Cities and Society, 79, 103670. https://doi.org/10.1016/j.scs.2022.103670

Lin, B. S., & Lin, Y. J. (2010). Cooling effect of shade trees with different characteristics in a subtropical urban park. HortScience, 45(1), 83-86. https://doi.org/10.21273/HORTSCI.45.1.83

Liu, B. Y., Mei, Y., & Kuang, W. (2016). Experimental research on correlation between microclimate element and human behavior and perception of residential landscape space in Shanghai. Landsc. Archit, 32, 5-9.

Liu, Y., Lai, Y., Jiang, L., Cheng, B., Tan, X., Zeng, F., ... & Shang, X. (2023). A study of the thermal comfort in urban mountain parks and its physical influencing factors. Journal of Thermal Biology, 118, 103726. https://doi.org/10.1016/j.jtherbio.2023.103726

Lobaccaro, G., & Acero, J. A. (2015). Comparative analysis of green actions to improve outdoor thermal comfort inside typical urban street canyons. Urban Climate, 14, 251-267. https://doi.org/10.1016/j.uclim.2015.10.002

Lobaccaro, G., Acero, J. A., Sanchez Martinez, G., Padro, A., Laburu, T., & Fernandez, G. (2019). Effects of orientations, aspect ratios, pavement materials and vegetation elements on thermal stress inside typical urban canyons. International journal of environmental research and public health, 16(19), 3574. https://doi.org/10.3390/ijerph16193574

Matzarakis, A., & Amelung, B. (2008). Physiological equivalent temperature as indicator for impacts of climate change on thermal comfort of humans. In Seasonal forecasts, climatic change and human health: health and climate (pp. 161-172). Dordrecht: Springer Netherlands. https://link.springer.com/content/pdf/10.1007/978-1-4020-6877-5_10?pdf=chapter%20toc

McCready, M. S., & Dukes, M. D. (2011). Landscape irrigation scheduling efficiency and adequacy by various control technologies. Agricultural Water Management, 98(4), 697-704. https://doi.org/10.1016/j.agwat.2010.11.007

Memon, R. A., Leung, D. Y., & Liu, C. H. (2010). Effects of building aspect ratio and wind speed on air temperatures in urban-like street canyons. Building and Environment, 45(1), 176-188. https://doi.org/10.1016/j.buildenv.2009.05.015

Middel, A., Chhetri, N., & Quay, R. (2015). Urban forestry and cool roofs: Assessment of heat mitigation strategies in Phoenix residential neighborhoods. Urban Forestry & Urban Greening, 14(1), 178-186. https://doi.org/10.1016/j.ufug.2014.09.010

Mohamed, E. (2012). Analysis of urban growth at Cairo, Egypt using remote sensing and GIS. Natural Science, 2012. DOI:10.4236/ns.2012.46049

Monteiro, M. V., Handley, P., Morison, J. I., & Doick, K. J. (2019). The role of urban trees and greenspaces in reducing urban air temperatures. https://www.cabidigitallibrary.org/doi/full/10.5555/20219922312

Morakinyo, T. E., & Lam, Y. F. (2016). Simulation study on the impact of tree-configuration, planting pattern and wind condition on street-canyon's micro-climate and thermal comfort. Building and environment, 103, 262-275. https://doi.org/10.1016/j.buildenv.2016.04.025

Morakinyo, T. E., Kong, L., Lau, K., CHAO, Y., & Ng, E. (2017). A study on the impact of shadow-cast and tree-species on in-canyon and neighborhood's thermal comfort Building and Environment. https://scholarbank.nus.edu.sg/handle/10635/193650

Mortimer, A., Ahmed, I., Johnson, T., Tang, L., & Alston, M. (2023). Localizing Sustainable Development goal 13 on Climate action to build local resilience to floods in the Hunter Valley: A literature review. Sustainability, 15(6), 5565. https://doi.org/10.3390/su15065565

Nada, A., Nasr, M., & Hazman, M. (2014). Irrigation expert system for trees. International Journal of Engineering and Innovative Technology (IJEIT), 3(8), 170-175. https://www.researchgate.net/profile/Ayman-Mohamed-24/publication/322977612_Irrigation_Expert_System_for_Trees/links/5a919f92aca2721405642a6f/Irrigation-Expert-System-for-Trees.pdf

Nakayoshi, M., Kanda, M., Shi, R., & de Dear, R. (2015). Outdoor thermal physiology along human pathways: a study using a wearable measurement system. International journal of biometeorology, 59, 503-515. https://doi.org/10.1007/s00484-014-0864-y

Ng, E., Chen, L., Wang, Y., & Yuan, C. (2012). A study on the cooling effects of greening in a high-density city: An experience from Hong Kong. Building and environment, 47, 256-271. https://doi.org/10.1016/j.buildenv.2011.07.014

Nunfam, V. F., Adusei-Asante, K., Van Etten, E. J., Oosthuizen, J., & Frimpong, K. (2018). Social impacts of occupational heat stress and adaptation strategies of workers: A narrative synthesis of the literature. Science of the total environment, 643, 1542-1552. https://doi.org/10.1016/j.scitotenv.2018.06.255

Ochiai, H., Ikei, H., Song, C., Kobayashi, M., Miura, T., Kagawa, T., ... & Miyazaki, Y. (2015). Physiological and psychological effects of a forest therapy program on middle-aged females. International journal of environmental research and public health, 12(12), 15222-15232. https://doi.org/10.3390/ijerph121214984

Osman, R., Ferrari, E., & McDonald, S. (2016). Water scarcity and irrigation efficiency in Egypt. Water Economics and Policy, 2(04), 1650009. https://doi.org/10.1142/S2382624X16500090

Panagiotis Kosmopoulos, H. E.-A. (2018). The solar atlas of Egypt. cairo: The EUMETSAT Network of Sataliete application facilities. http://www.nrea.gov.eg/Content/files/SOLAR%20ATLAS%202018%20digital1.pdf

Pearlmutter, D. (2000). Patterns of sustainability in desert architecture. Arid Lands Newslett, 47, 1-12. https://cales.arizona.edu/OALS/ALN/aln47/pearlmutter.html

Pioppi, B., Pigliautile, I., & Pisello, A. L. (2020). Human-centric microclimate analysis of Urban Heat Island: Wearable sensing and data-driven techniques for identifying mitigation strategies in New York City. Urban Climate, 34, 100716. https://doi.org/10.1016/j.uclim.2020.100716

Pittenger, D. (2014). Methodology for Estimating Landscape Irrigation Demand. https://bseacd.org/uploads/BSEACD_Irr_Demand_Meth_Rprt_2014_Final_140424.pdf

Qaid, A., & Ossen, D. R. (2015). Effect of asymmetrical street aspect ratios on microclimates in hot, humid regions. International journal of biometeorology, 59, 657-677 https://doi.org/10.1007/s00484-014-0878-5

Rahman, M. A., Armson, D., & Ennos, A. R. (2015). A comparison of the growth and cooling effectiveness of five commonly planted urban tree species. Urban Ecosystems, 18, 371-389. https://doi.org/10.1007/s11252-014-0407-7

Rahman, M. A., Moser, A., Rötzer, T., & Pauleit, S. (2017). Within canopy temperature differences and cooling ability of Tilia cordata trees grown in urban conditions. Building and Environment, 114, 118-128. https://doi.org/10.1016/j.buildenv.2016.12.013

Rahman, M. A., Moser, A., Gold, A., Rötzer, T., & Pauleit, S. (2018). Vertical air temperature gradients under the shade of two contrasting urban tree species during different types of summer days. Science of the Total Environment, 633, 100-111. https://doi.org/10.1016/j.scitotenv.2018.03.168

Rajabi, T. (2011). The study of vegetation effects on reduction of urban heat Island in Dubai (Master's thesis, The British University in Dubai). http://bspace.buid.ac.ae/handle/1234/638

Ramadan, M. F. A. (2010). Interactive urban form design of local climate scale in hot semi-arid zone (Doctoral dissertation, University of Sheffield). Cross Ref.

Ribeiro, K. F. A., Justi, A. C. A., Novais, J. W. Z., de Moura Santos, F. M., Nogueira, M. C. D. J. A., Miranda, S. A., & Marques, J. B. (2022). Calibration of the Physiological Equivalent Temperature (PET) index range for outside spaces in a tropical climate city. Urban Climate, 44, 101196. https://doi.org/10.1016/j.uclim.2022.101196

Rizwan, A. M., Dennis, L. Y., & Chunho, L. I. U. (2008). A review on the generation, determination and mitigation of Urban Heat Island. Journal of environmental sciences, 20(1), 120-128. https://doi.org/10.1016/S1001-0742(08)60019-4

Rodríguez-Algeciras, J., Tablada, A., Chaos-Yeras, M., De la Paz, G., & Matzarakis, A. (2018). Influence of aspect ratio and orientation on large courtyard thermal conditions in the historical centre of Camagüey-Cuba. Renewable energy, 125, 840-856. https://doi.org/10.1016/j.renene.2018.01.082

Rowntree, R. A., & Nowak, D. J. (1991). Quantifying the role of urban forests in removing atmospheric carbon dioxide. Arboriculture & Urban Forestry (AUF), 17(10), 269-275. https://doi.org/10.48044/jauf.1991.061

Sánchez-Azofeifa, G. A., & Castro-Esau, K. (2006). Canopy observations on the hyperspectral properties of a community of tropical dry forest lianas and their host trees. International Journal of Remote Sensing, 27(10), 2101-2109. https://doi.org/10.1080/01431160500444749

Sanusi, R., Johnstone, D., May, P., & Livesley, S. J. (2016). Street orientation and side of the street greatly influence the microclimatic benefits street trees can provide in summer. Journal of environmental quality, 45(1), 167-174. https://doi.org/10.2134/jeq2015.01.0039

Sauter, Daniel. (2008). Measuring Walking: towards internationally standardised monitoring methods of walking and public space. 8th International Conference on Survey Methods in Transport. Annecy,France,.https://download.measuringwalking.org/mw_sauter_wedderburn_annecy_conf_may_08.pdf

Shahidan, M. F., Shariff, M. K., Jones, P., Salleh, E., & Abdullah, A. M. (2010). A comparison of Mesua ferrea L. and Hura crepitans L. for shade creation and radiation modification in improving thermal comfort. Landscape and Urban Planning, 97(3), 168-181. https://doi.org/10.1016/j.landurbplan.2010.05.008

Shashua-Bar, L., Tsiros, I. X., & Hoffman, M. E. (2010). A modeling study for evaluating passive cooling scenarios in urban streets with trees. Case study: Athens, Greece. Building and Environment, 45(12), 2798-2807. https://doi.org/10.1016/j.buildenv.2010.06.008

Shishegar, N. (2013). Street design and urban microclimate: analyzing the effects of street geometryand orientation on airflow and solar access in urban canyons. Journal of clean energy technologies, 1(1), 52-56. DOI: 10.7763/JOCET.2013.V1.13

Smithers, R. J., Doick, K. J., Burton, A., Sibille, R., Steinbach, D., Harris, R., ... & Blicharska, M. (2018). Comparing the relative abilities of tree species to cool the urban environment. Urban Ecosystems, 21, 851-862. https://doi.org/10.1007/s11252-018-0761-y

Sodoudi, S., Shahmohamadi, P., Vollack, K., Cubasch, U., & Che-Ani, A. I. (2014). Mitigating the urban heat island effect in megacity Tehran. Advances in Meteorology, 2014(1), 547974. https://doi.org/10.1155/2014/547974

Song, C., Ikei, H., Igarashi, M., Miwa, M., Takagaki, M., & Miyazaki, Y. (2014). Physiological and psychological responses of young males during spring-time walks in urban parks. Journal of physiological anthropology, 33, 1-7. https://doi.org/10.1186/1880-6805-33-8

Souch, C. A., & Souch, C. J. J. A. (1993). The effect of trees on summertime below canopy urban climates: a case study Bloomington, Indiana. J. Arboric, 19(5), 303-312. Cross Ref.

Stewart, I. D. (2011). Redefining the urban heat island (Doctoral dissertation, University of British Columbia). http://hdl.handle.net/2429/38069

Taheri Shahraiyni, H., Sodoudi, S., El-Zafarany, A., Abou El Seoud, T., Ashraf, H., & Krone, K. (2016). A comprehensive statistical study on daytime surface urban heat island during summer in urban areas, case study: Cairo and its new towns. Remote Sensing, 8(8), 643. https://doi.org/10.3390/rs8080643

Takayama, N., Korpela, K., Lee, J., Morikawa, T., Tsunetsugu, Y., Park, B. J., ... & Kagawa, T. (2014). Emotional, restorative and vitalizing effects of forest and urban environments at four sites in Japan. International journal of environmental research and public health, 11(7), 7207-7230. https://doi.org/10.3390/ijerph110707207

Takebayashi, H., & Moriyama, M. (2012). Relationships between the properties of an urban street canyon and its radiant environment: Introduction of appropriate urban heat island mitigation technologies. Solar Energy, 86(9), 2255-2262. https://doi.org/10.1016/j.solener.2012.04.019

Taleghani, M., Kleerekoper, L., Tenpierik, M., & Van Den Dobbelsteen, A. (2015). Outdoor thermal comfort within five different urban forms in the Netherlands. Building and environment, 83, 65-78. https://doi.org/10.1016/j.buildenv.2014.03.014

Theeuwes, N. E., Steeneveld, G. J., Ronda, R. J., Heusinkveld, B. G., Van Hove, L. W. A., & Holtslag, A. A. M. (2014). Seasonal dependence of the urban heat island on the street canyon aspect ratio. Quarterly Journal of the Royal Meteorological Society, 140(684), 2197-2210. https://doi.org/10.1002/qj.2289

Upreti, R., Wang, Z. H., & Yang, J. (2017). Radiative shading effect of urban trees on cooling the regional built environment. Urban Forestry & Urban Greening, 26, 18-24. https://doi.org/10.1016/j.ufug.2017.05.008

Vasilikou, C., & Nikolopoulou, M. (2013, September). Thermal walks: identifying pedestrian thermal comfort variations in the urban continuum of historic city centres. In Proceeding of PLEA2013-29th Conference, Sustainable architecture for a renewable future, Munich, Germany (pp. 10-12).

Vasilikou, C., & Nikolopoulou, M. (2020). Outdoor thermal comfort for pedestrians in movement: thermal walks in complex urban morphology. International journal of biometeorology, 64, 277-291. https://doi.org/10.1007/s00484-019-01782-2

Wang, Y., Bakker, F., de Groot, R., Wortche, H., & Leemans, R. (2015). Effects of urban trees on local outdoor microclimate: synthesizing field measurements by numerical modelling. Urban Ecosystems, 18, 1305-1331. https://doi.org/10.1007/s11252-015-0447-7

Wang, Y., Berardi, U., & Akbari, H. (2016). Comparing the effects of urban heat island mitigation strategies for Toronto, Canada. Energy and buildings, 114, 2-19. https://doi.org/10.1016/j.enbuild.2015.06.046

Ward, F. A., & Pulido-Velazquez, M. (2008). Water conservation in irrigation can increase water use. Proceedings of the National Academy of Sciences, 105(47), 18215-18220. https://doi.org/10.1073/pnas.0805554105

Wei, D., & Liu, B. (2018). The analysis and evaluation of thermal comfort at Shanghai knowledge & innovation community square. Chinese Landscape Architecture, 34(2), 5-12.

Xiao, J., & Yuizono, T. (2022). Climate-adaptive landscape design: Microclimate and thermal comfort regulation of station square in the Hokuriku Region, Japan. Building and Environment, 212, 108813. https://doi.org/10.1016/j.buildenv.2022.108813

Yin, C., Yuan, M., Lu, Y., Huang, Y., & Liu, Y. (2018). Effects of urban form on the urban heat island effect based on spatial regression model. Science of the Total Environment, 634, 696-704. https://doi.org/10.1016/j.scitotenv.2018.03.350

Yola, L., Siong, H. C., & Djaja, K. (2020, September). Climatically responsive urban configuration in residential area: Research gaps. In AIP Conference Proceedings (Vol. 2255, No. 1). AIP Publishing. https://doi.org/10.1063/5.0013796

Zalesny Jr, R. S., Stanturf, J. A., Evett, S. R., Kandil, N. F., & Soriano, C. (2011). Opportunities for woody crop production using treated wastewater in Egypt. I. Afforestation strategies. International journal of phytoremediation, 13(sup1), 102-121. https://doi.org/10.1080/15226514.2011.568539

Zhai, H., Fan, D., & Li, Q. (2022). Dynamic radiation regulations for thermal comfort. Nano Energy, 100, 107435. https://doi.org/10.1016/j.nanoen.2022.107435

Zhang, J., Gou, Z., Cheng, B., & Khoshbakht, M. (2022). A study of physical factors influencing park cooling intensities and their effects in different time of the day. Journal of Thermal Biology, 109, 103336. https://doi.org/10.1016/j.jtherbio.2022.103336

Zhang, J., Gou, Z., Zhang, F., & Yu, R. (2023). The tree cooling pond effect and its influential factors: A pilot study in Gold Coast, Australia. Nature-Based Solutions, 3, 100058. https://doi.org/10.1016/j.nbsj.2023.100058

Zhang, J., Khoshbakht, M., Liu, J., Gou, Z., Xiong, J., & Jiang, M. (2022). A clustering review of vegetation-indicating parameters in urban thermal environment studies towards various factors. Journal of Thermal Biology, 110, 103340. https://doi.org/10.1016/j.jtherbio.2022.103340

Zhang, Y., Liu, J., Zheng, Z., Fang, Z., Zhang, X., Gao, Y., & Xie, Y. (2020). Analysis of thermal comfort during movement in a semi-open transition space. Energy and Buildings, 225, 110312. https://doi.org/10.1016/j.enbuild.2020.110312

Zied, E., & Vialard, A. (2017). Syntactic Stitching: Towards a Better Integration of Cairo's Urban Fabric. http://nrl.northumbria.ac.uk/id/eprint/31461

Part II

Publications

This Page Intentionally Left Blank.

Article 1: Key facts and author contributions

Refrence	Abdelmejeed, A.Y., Gruehn, D. Optimizing an efficient urban tree strategy to improve microclimate conditions while considering water scarcity: a case study of Cairo. Discov Sustain 5, 66 (2024). https://doi.org/10.1007/s43621-024-00247-w
Contributions	AY. A, 85%, and DG, 15% Words count: 12042
Review Model	Single blind peer review
History	Submitted: 19 November 2023 Accepted: 3 April 2024 Published: 15 April 2024

Signature:

Ahmed Yasser Abdelmejeed

Date: 15. July 2025

Discover Sustainability

Research

Optimizing an efficient urban tree strategy to improve microclimate conditions while considering water scarcity: a case study of Cairo

Ahmed Yasser Abdelmejeed[1,2] · **Dietwald Gruehn**[1]

Received: 19 November 2023 / Accepted: 3 April 2024
Published online: 15 April 2024

Abstract
This study aims to develop an efficient urban tree strategy (UTS) to enhance the microclimate conditions of cities that suffer from heat stress and strong solar radiation, such as the metropolitan area of Greater Cairo. Cairo recently lost its limited greenery to enhance traffic. The proposed UTS aims to achieve a balance between enhancing microclimate conditions and considering the city's water scarcity. It seeks to consider all strategic factors suitable for local conditions, including the selection of tree species (Step 1), the utilization of new technologies for irrigation (Step 2), and the optimization of the usage of an efficient number of trees (Step 3). When applying the strategy's recommendations to a study area within Cairo's downtown center and when testing different tree coverage percentages within urban canyons of various aspect ratios and orientations using ENVI-met, the microclimate conditions are significantly enhanced in certain streets during summertime compared to wintertime. Applying the UTS not only enhances thermal comfort but also helps to create a better comfort zone during certain hours. In one street, for example, there are average physiological equivalent temperature (PET) reductions of – 5.18° and – 6.36° at 16:00 and 17:00, respectively, which also changes the thermal comfort zone from extreme heat stress to very heat stress. The results show a strong positive correlation between thermal comfort enhancement and a reduction in the total mean radiant temperature (TMRT), verifying that shading plays a primary role in enhancing the microclimate conditions of urban canyons. Applying the UTS to the study area significantly enhances the microclimate conditions. Furthermore, through the implementation of irrigation technologies that are part of the UTS, water demand is reduced to only 15% when trees with larger canopies are used. Additionally, when the tree coverage percentage reaches 35 to 50% in some streets, it results in a significant enhancement in the PET.

Keywords Urban heat island (UHI) · Outdoor thermal comfort · Urban tree effect · Recommended tree species · Urban tree strategy (UTS) · Greenery effect · ENVI-met Greenery simulation · Urban cooling strategies

Abbreviations

UTS	Urban tree strategy
PET	Physiological equivalent temperature
TMRT	Total mean radiant temperature
WS	Wind speed
LAI	Leaf area index
WP	Water productivity

✉ Ahmed Yasser Abdelmejeed, ahmed.abdelmejeed@tu-dortmund.de, https://sciprofiles.com/profile/2172391; Dietwald Gruehn, dietwald.gruehn@tu-dortmund.de, https://sciprofiles.com/profile/1601806 | [1]Research Group Landscape Ecology and Landscape Planning, Department of Spatial Planning, TU Dortmund University, 44227 Dortmund, Germany. [2]Faculty of Urban and Regional Planning, Cairo University, Cairo 11562, Egypt.

SMS	Soil moisture sensor-based controller
DI	Deficit irrigation
UHI	Urban heat island
EPW	Energy plus weather format
TA	Air temperature
DP	Drip irrigation
H	Specific humidity
LAD	Leaf area density
ET	Evapotranspiration-based controller
RS	Rain sensor controller

1 Research background

1.1 The climate of Greater Cairo

The metropolitan area of Greater Cairo is located in a hot, arid area, which means that the air temperature is high, there is a large amount of solar radiation, and an urban heat island (UHI) appears. Cairo has a hot and dry climate with limited rainfall and frequently high humidity, influenced by the presence of the Nile River Valley. The mean air temperature in Cairo ranges from 9 to 24.8 °C during winter and 20.1 °C to 34.7 °C during summer, sometimes surpassing 40 °C during heat stress events in summer [1]. During the summer, between June and August, the climate is hot and dry, with a maximum average temperature of 28 °C [2]. The city is exposed to large amounts of solar radiation, which can be converted to energy at solar power stations [3]. The city of Cairo experiences a hot and arid climate, characterized by high levels of solar radiation. This significantly impacts the thermal comfort and health of its inhabitants, as well as the social impacts of occupational heat stress on workers' health, safety, productivity, and social well-being [4]. According to statistics from 2012, the metropolitan area of Cairo has a population of approximately 20.5 million [5]. By 2050, the city is estimated to grow substantially, with an expected increase in population of 11.2 million people [5]. Subsequently, this increase in population will have a direct effect on the demand for residential housing, making the city even denser. Both the air temperature and UHI effect will rise due to the increase in city size and population density, and this will, in turn, lead to a rise in anthropogenic heat [6–8].

1.2 UHI effects on greater Cairo

According to an urban study conducted in 2015, higher air temperatures were found in downtown Cairo, while lower air temperatures were found in suburban areas [2]. This illustrates the UHI phenomenon. The UHI phenomenon results in an above-average rise in the surface temperature of urban areas in Cairo, ranging from 0.5 to 3.5 °C. The maximum difference observed was 10 °C compared to the surrounding surfaces [2, 9]. The density of the UHI reached 7.8 °C during summer and 2.1 °C during winter [1]. Remote sensing and land surface temperature (LST) analyses assert that there is a strong presence of the UHI phenomenon in Cairo [1, 2, 9]. It is, therefore, evident that the UHI effect takes place in Cairo and leads to discomfort, particularly during nighttime.

1.3 Scarcity of water and greenery in Cairo

Cairo suffers from high levels of heat stress, which directly affects quality of life and human health. Urban cooling strategies, such as increasing the number of trees and the amount of vegetation, should, therefore, be implemented; however, the opposite is occurring: the city is losing its limited greenery and suffering from water scarcity.

Cairo has minimal green areas and open spaces. More than half of the city's population has less than 0.5 m^2 of green space per person, which is a staggering ratio that is considerably below the city's average of 1.7 m^2 [10]. During the last four years, Greater Cairo has lost many of its green areas, and many trees have been removed to widen road lanes in an attempt to improve traffic congestion. This has led to a significant reduction in the amount of greenery in the city, which was already quite low. Figure 1 illustrates an example in which trees and green spaces have been removed to widen roads during the renovation of Al-Hegaz Square in the district of Heliopolis [11].

Water resources in Egypt are limited to the Nile River, rainfall, flash floods, deep groundwater in deserts and the Sinai Peninsula, and the potential desalination of sea as well as brackish water [12, 13]. Egypt receives approximately 98% of its freshwater resources from outside its national borders. The main challenge for water policy and decision makers in the country is the fact that the Nile River supplies over 95% of the country's water needs [12, 14].

Egypt's per capita freshwater availability declined from 1893 m^3 in 1959 to 875–950 m^3 in 2000 and 670 m^3 in 2017. It is estimated to decline even further to 536 m3 by 2025 [12, 15]. The ever-increasing water demands are dictated by a rapidly growing population, increased urbanization, higher standards of living, and an agricultural policy that focuses on expanding production to feed the growing population. Domestic water use grew from 3.1 BCM in 1990 to 5.23 BCM in 2000 [16]. In addition, in 2011, the Ethiopian government announced the construction of a water dam on the main water source of the Nile River in Ethiopia [14].

1.4 Urban cooling strategies

There are two primary methods by which urban cooling strategies can enhance thermal comfort and mitigate the impact of urban heat islands (UHIs). The first approach involves modifying the urban layout of new communities by adjusting the orientation and aspect ratio of urban streets. The second approach entails incorporating an environmental layer into already established urban regions, which includes the addition of vegetation and cooling materials, such as trees, greenery, cool colors, roof gardens, vertical gardens, and bodies of water [6, 17–19]. This research is specifically centered around improving the microclimate conditions of existing areas, with a particular focus on vegetation.

Shady trees as well as other elements of vegetation, such as small trees, bushes, lawns, ground coverage, and climbing plants, help improve urban climate conditions by offering shade and evapotranspiration in urban areas and streets [6, 18, 19]. Vegetation also improves air quality by producing oxygen and removing carbon dioxide from the atmosphere. It also provides health benefits to the population by protecting them from shortwave radiation and reducing heat stress and energy demand for air conditioning [2, 20–22]. Previous study outcomes proved that mature trees with good foliage density absorb at least 60% of solar radiation [23]. The temperature within trees is 5 °C lower than the surrounding temperature, and the temperature above the agricultural land surface is 3 °C lower than the surrounding temperature [17]. Moreover, urban trees reduce the 2 m air temperature by up to 2 °C to 9 °C [24].

2 Literature review of cooling performance and irrigation efficiency of trees

Among all the vegetation elements that are used to improve microclimate conditions, planting trees yields the best results in reducing the surface temperature of urban areas. The results of many studies that have investigated the role of vegetation in urban areas, conducted in various cities, demonstrate that the role of urban trees is crucial.

In Port Fillip, a study revealed that the maximum reduction in air temperature occurred when green rooftops were combined with urban trees. The reduction reached 2.4 °C at the pedestrian level of the street [25]. A study conducted in Ho Chi Minh City revealed that the difference in the PET value reached 6 °C in shaded areas and 1 °C in unshaded areas

Fig. 1 Al-Hegaz Square before and after renovation. Both maps were exported from "Google Earth Pro". The image on the left was exported in October 2018 and the one on the right in May 2022. no editing applied, and the difference between the colors of both satellite images is due to the conditions of each photo in Google Earth

between the urban tree scenario and the base case scenario. Compared to other scenarios, the urban tree scenario had the best effect on improving the thermal comfort value [26]. In a study conducted in Dubai, the recommended scenario was to only apply trees, given that the results of the urban tree scenario were almost identical to the scenarios involving all other vegetation elements. This means that trees play a major and dominant role in improving the surface temperature of urban areas [27]. In Tehran, a study revealed that the maximum mitigation results occurred in the combined scenario and reached 1.5˚C on average, providing similar results to the urban tree scenario [28]. When five greenery planning scenarios were applied on three typical street canyons in Balbo, trees with green surfaces exhibited the best effect, reducing the PET by 2 °C. While the PET increased by 7 °C for low-rise compact urban areas, it increased by 5 °C for medium-rise compact urban areas and 4 °C for high-rise urban areas [29]. A study in the Phoenix Metropolitan area focused on the regional cooling effect of trees in arid environments. The simulation results demonstrated the capacity of urban trees to reduce urban surface and air temperatures by approximately 2 °C to 9 °C and 1 °C to 5 °C, respectively [30]. Another study conducted in the same city used several trees and greenery scenarios for small residential neighborhoods located within the city's downtown center. The study found that the ideal scenario occurred when using a tree shading percentage of 25% in urban canyons [31].

Based on previous case studies that were conducted worldwide, vegetation plays a significant role in urban climate adaptation, with trees being the most effective. A tree-only scenario is equivalent to a scenario that uses all vegetation elements (including trees).

2.1 Efficient morphological characteristics of trees

The performance of trees in urban areas includes providing shade and evapotranspiration [6, 18, 19]. Shade is more important than evapotranspiration for trees because it sets them apart from other types of vegetation that do not provide shade [25–29]. Numerous studies have shown that the physical characteristics of tree species, such as their shape, size, density, and leaf features, affect their shading and cooling effects [32–35]. Different tree species have inherent traits that determine their growth, form, physiology, and ability to cool their surroundings [36]. The cooling effects of trees depend on the size and density of their canopy, as well as the properties of their leaves. The tree canopy plays a significant role in creating a microclimatic environment, mainly due to its cooling effect [32, 37].

The characteristics of the vegetation canopy are important in predicting thermal mitigation in urban areas and in helping select the best species for urban greening [37]. The overall shape of the canopy and the arrangement and density of the leaves and branches of trees influence the amount of shade that they provide. Trees that have a wide canopy and a high density of leaves and branches produce more effective shading [36]. Among the parameters of different tree species, the leaf area index (LAI) is considered a central parameter affecting light penetration and below-canopy microclimate [38, 39]. In 2013, urban researchers reported that maximum air temperature reduction occurred under the canopies of trees with a high LAI [32]. The leaf area (based on crown diameter and LAI) is important in relation to all three cooling mechanisms considered (transpiration, reflection of solar radiation, and shading) [36–41]. Species with higher canopy density might be preferred over asphalt surfaces, but low-water-using species with lower canopy density might be chosen over grass surfaces [31]. It can be concluded that the cooling effect of urban trees is species-specific and depends mainly on the tree canopy, although the leaf characteristics, LAI, and local microclimate also play an important role [37].

2.2 Trees adapting to local conditions (low water demand and salt and drought tolerance)

The selection process of efficient trees should consider the tree species' ability to grow in the local climate conditions of the city to counteract the UHI effect. There is a need to plant large tree species that can tolerate drought and are able to grow in the arid and dry climate of Cairo. In examining the suitability of trees to adapt to the country's climatic conditions, the average and maximum temperatures of the warmest month should be considered, as well as the ease of tree propagation. Adaptations to drought, high pH, and saline soil are also important [42].

When selecting a tree, the type of tree (evergreen or deciduous) should also be considered, as the cooling effects of trees are twice as high on clear and hot days compared to cloudy and cold days. Additionally, evergreen trees slightly lower the air temperature in winter, and weather conditions do not significantly affect the trees' impact on the microclimate [43]. Evergreen trees will, therefore, not have a significant impact during winter but may cause negative effects by blocking the wind and the desirable warming by the sun. As water demand varies from one tree species to another [44, 45], trees that demand a low to moderate water supply are most suitable for this study. Implementing the strategy citywide will result in significant savings

in water supply due to the small amount of water saved by each tree. Therefore, when choosing the most appropriate tree species, it is crucial to consider water demand as an important factor.

2.3 Efficient irrigation technology

Irrigation is the single largest water consumption process in the world [46]. There is a widespread belief among environmental and water policy makers that if irrigators can use water more efficiently, more water could be saved for environmental and urban use [47]. Many emerging irrigation techniques and technologies can enhance irrigation efficiency and reduce water consumption. An example of such a technique is the use of deficit irrigation (DI). This is defined as the application of water below full crop-water requirements and is an important tool in reducing water use during irrigation [46]. A well-designed DI regime can optimize water productivity (WP) over an area when full irrigation is not possible. In many horticultural crops, regular DI has been shown to improve not only WP but also the operator's net income [48]. Another successful technique that has recently become popular is the drip irrigation system (DP), which can also be applied as a part of the DI and is widely believed to conserve water. The DP allows for the precise application of water into the root zones of plants with little loss to run-off or deep percolation. It produces higher evapotranspiration than flood irrigation while also producing higher crop yields. Raising the subsidy on DPs encourages the expansion of drip acreage and total acreage in production [42, 47].

An additional technique to enhance the performance of the DI and DP involves the use of software, which can be programmed and used to compute the exact amount of water, soil parameters, and weather conditions required. Having a day-to-day weather data system is often not available to those who operate irrigation systems and who, therefore, end up using historical data to analyze weather condition requirements. Linking an irrigation system to day-to-day weather forecast websites will ensure that it constantly updates with new weather data and can enhance the daily generation of irrigation [48]. Increasing the scheduling efficiency of an automated irrigation system allows for the conservation of water resources while maintaining landscape quality [49]. To increase water efficiency and savings, it is better to provide software with another source of daily data on weather and site conditions. This could be performed via the automation of landscape irrigation scheduling to improve convenience and minimize irrigation application while maintaining high landscape quality [50]. The different types of irrigation controllers that can help reduce the amount of irrigation include the following:

- Evapotranspiration-based controllers (ETs).
- Soil moisture sensor-based controllers (SMSs).
- Rain sensor controllers (RSs).

2.4 Research gaps, objectives, and questions

This research aims to provide a comprehensive green strategy that improves thermal comfort and mitigates the UHI effects in the urban areas of Cairo. It intends to do so by using the most suitable elements of urban greenery. According to the results of other studies, urban trees should serve as the most suitable element. This study seeks to provide an urban tree strategy for the whole metropolitan city of Cairo. The strategy should consider the limited water availability in Egypt, particularly because trees are one of the largest water consumers of greenery elements [44, 45], and large amounts of water will be required to irrigate the large number of trees proposed to be planted all over the city. This aided in generating the research question: ''What is the impact of implementing a comprehensive urban tree strategy that considers climate conditions and water scarcity on the city of Cairo?''. The strategy should have a significant positive impact that not only motivates its application but also raises awareness regarding the use and application of trees once applied, thereby helping to reduce the current removal of trees from Cairo's urban areas.

3 Research methodology

To improve microclimate conditions and consider the scarcity of water, a comprehensive examination should be conducted on all aspects of the strategy. Figure 2 illustrates the three steps involved in the strategy: (1) choosing appropriate tree species, (2) implementing effective irrigation methods, and (3) determining the optimal number of trees to be planted in urban areas.

3.1 UTS step 1: efficient tree species

The tree species(s) selected for the UTS should require the consumption of less water to achieve the target of the study, which is primarily because the city is suffering from water scarcity and lacking greenery. To provide and implement a strategy for the metropolitan city of Cairo, millions of trees need to be planted. The selection of tree species should, therefore, be carefully carried out, as the very small effect and consumption of one single tree will have an even larger impact when applied all over the city. All parameters of the tree should be considered when selecting suitable tree species. As in previous studies conducted in different cities, the daily average difference between street air temperatures with and without tree shading varies. While it was 0.1 °C in Indiana, United States, it increased to 0.9 °C in Melbourne, Australia; 1 °C in Munich, Germany; and up to 2.8 °C in southeastern Brazil [51–54]. Microclimatic shading and air-cooling methods vary among tree species [55–57] and depend on the morphological characteristics of the tree, including shape, canopy size, canopy density, and tree leaf features [32, 33, 58]. A comparative study should, therefore, be conducted on the main characteristics and parameters of trees when deciding which tree species should be selected. This study should compare the main elements that can provide better performances with regard to enhancing the microclimate conditions within the limited availability of resources.

3.1.1 Step 1 outcomes: recommended efficient urban tree species

Based on previous studies and recommendations, the ideal tree species should be selected based on the following criteria:

- The size of the tree canopy (bigger canopies are indispensable and should be classified as shading trees).
- Tree density (trees with a higher LAI are preferred).
- Tree type (deciduous trees are preferred).
- The adaptability of the tree to location conditions (trees with high water demand; salt and drought intolerance must be excluded).

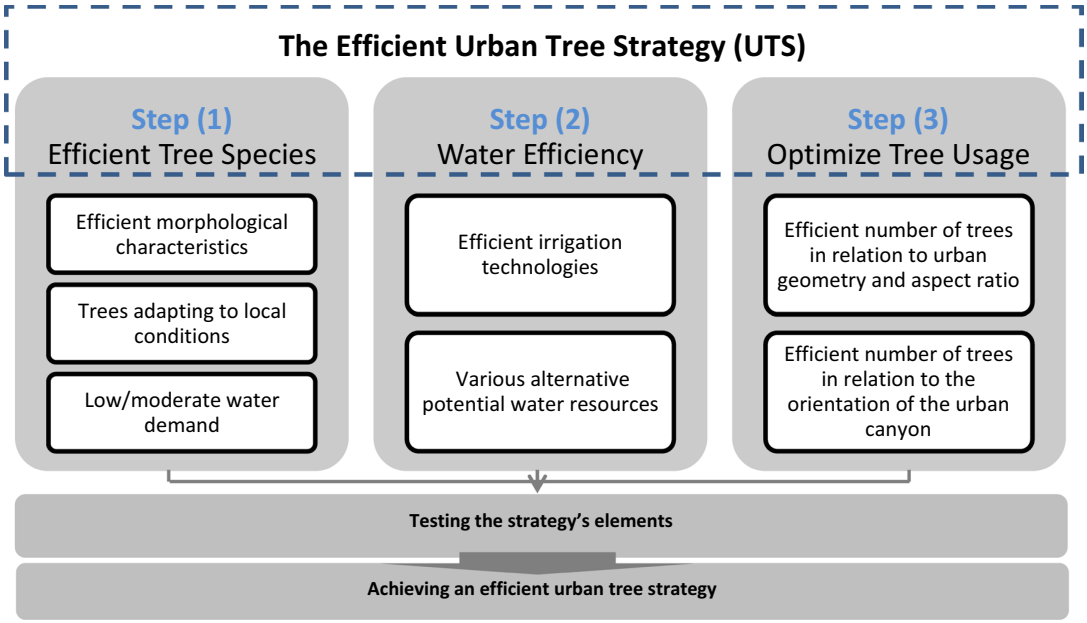

Fig. 2 Research methodology

The selection criteria were applied to 114 trees listed in the planting database for Cairo, titled "Plant Guidebook for Al-Azhar Park and the City of Cairo" [44]. Table 1 shows the 21 trees that were selected from the 114 trees based on the selection criteria of the research study.

As shown in Table 1, there were slight variations in crown size, water demand, LAI, and tolerance to drought and salinity among the chosen trees. While we could have chosen fewer trees, based solely on their characteristics, to include in the table for the intended strategy, we opted to include the aforementioned tree species for two reasons:

- The different tree sizes will be useful when dealing with different street widths, different types of streetscapes, and the available planting areas inside the urban canyons.
- With the 21 shortlisted tree species, a wide range of visual variety and biodiversity can be offered, which is very important for enhancing the city's image and streetscape.

To maximize the benefits from the selected trees, three main categories should be applied, as shown in Table 1. Category A is for trees with the best properties, category B is for those with good properties, and category C is for those possessing fewer good properties than category B. These three categories should be used as a guide when applying an efficient tree strategy to any urban area in Cairo. However, while category A must be used in all urban areas, categories B and C can sometimes be added to category A to provide more variety and biodiversity to urban areas.

3.2 UTS step 2: irrigation technologies

The study seeks to quantify the use of water during irrigation and compare the use of traditional time-based irrigation systems with new technologies such as SMS and RS. SMSs provide significant savings in the amounts of irrigation required, reducing the required amount by 65% compared to homes utilizing traditional irrigation systems [61].

3.2.1 Different water resources for irrigation

Reducing water consumption is very important, and finding different water resources is also a significant factor for irrigation. As it is not possible for Egypt to meet the increase in water demand by relying solely on the Nile, it has been developing non-conventional wastewater reuse strategies to meet future demands [42]. Based on the released data from the Holding Company for Water and Wastewater in 2013, Egypt produced approximately 9.6 mcm of treated wastewater per day, which is approximately 3.5 bcm of treated wastewater per year [62]. This amount equates to 6.5% of the total volume of the Nile's water. These different water resources will support the greening strategy of this study and make its application possible. Assessing the current availability of various water resources and minimizing water consumption make the greening strategy achievable.

3.2.2 Water demand for tree irrigation

One of the main objectives of this study is to consider water demand and water efficiency. Calculating water demand is the main factor needed in assessing the UTS. Equation 1 can be used to calculate irrigation water demand for isolated trees, which are widely spaced without other plant material under or around them. Water demand depends on three items: the plant factor, evapotranspiration, and the crown size of the tree, all of which vary among different tree species. The cooling criteria for all trees indicate that having large tree canopies is necessary to increase the percentage of tree coverage. This, in turn, directly leads to an increase in the amount of water needed. To reduce water demand, it is important to minimize both the percentage of tree coverage and the number of trees as much as possible. Therefore, there should be a balance between the required tree coverage percentage and the required water demand to avoid compromising either an improvement in thermal comfort or a decrease in water demand.

Equation 1 can be used to calculate water demand for isolated trees [63]:

$$\text{Gallons} = \text{ETo} \times \text{PF} \times (\text{R} \times \text{R} \times 3.14) \times 0.623 \quad (1)$$

- ETo represents inches of historical average, or real-time evapotranspiration, for the period of interest.
- PF represents the plant factor for the established landscape trees (0.5 for all trees).

Table 1 The selection of tree species based on the tree efficiency criteria

Category	Scientific name of tree	Common name	Canopy width (m)	Canopy height (m)	LAI [59]	Seasonality	Water demand	Salinity	Drought tolerance
A	*Vachellia nilotica*	Gum arabic tree	5–10	8–15	3	Evergreen	Low	Tolerant	H. tolerant
A	*Prosopis juliflora*	Mesquite	Up to 8	10–15		Evergreen	Low	Tolerant	H. tolerant
A	*Terminalia catappa*	Indian almond	5–10	10–15	3	Deciduous	Moderate	M. tolerant	H. tolerant
B	*Albizia lebbek*	Lebbek tree	4–8	6–12	3	Deciduous	Moderate	M. tolerant	Tolerant
B	*Azadirachta indica*	Neem tree	6–10	15–20	3	Deciduous	Moderate	M. tolerant	M. tolerant
B	*Bombax ceiba*	Cotton tree	6–8	Up to 25	3 [60]	Deciduous	Moderate	M. tolerant	M. tolerant
B	*Ceiba speciosa*	Silk floss tree	Up to 10	15–20	3	Deciduous	Moderate	M. tolerant	Tolerant
B	*Ficus benjamina*	Weeping Fig	Up to 15	6–30	3	Evergreen	Moderate	M. tolerant	Tolerant
B	*Ficus elastica*	India rubber fig	12	9–12	3	Evergreen	Moderate	M. tolerant	Tolerant
B	*Ficus infectoria*	White fig	8–10	10–12	3	Deciduous	Moderate	M. tolerant	Tolerant
B	*Ficus nitida*	Indian laurel fig	9	9–18	3	Evergreen	Moderate	M. tolerant	Tolerant
B	*Ficus religiosa*	Sacred fig	4–8	7–9	3	Semi- Deciduous	Moderate	M. tolerant	Tolerant
B	*Ficus sycomorus*	Sycamore fig	12–20	15–20	3	Evergreen	Moderate	M. tolerant	Tolerant
B	*Jacaranda mimosifolia*	Blue jacaranda	7–10	10–15	2.5	Deciduous	Moderate	M. tolerant	Tolerant
B	*Peltophorum africanum*	African wattle	8–10	10–15	3	Deciduous	Moderate	M. tolerant	Tolerant
B	*Tipuana tipu*	Yellow jacaranda	6–8	13–15	3	Semi- Deciduous	Moderate	Tolerant	Tolerant
C	*Cassia javanica*	Pink shower	6–8	10–15	2.5	Deciduous	Moderate	L. tolerant	Tolerant
C	*Senna spectabilis*	American cassia	10–12	10–15	2.5	Evergreen	Moderate	L. tolerant	Tolerant
C	*Delonix regia*	Royal poinciana	6–8	10–12	2.5	Deciduous	Moderate	Tolerant	Tolerant
C	*Entrolobium cyclocarpum*	Elephant's ear tree	Up to 9 m	10–12	2 [59]	Deciduous	Moderate	M. tolerant	Tolerant
C	*Leucaena leucocephala*	Lead tree	4–9	6–15		Evergreen	Moderate	Tolerant	Tolerant

- R denotes the radius of the tree canopy in ft., which can be calculated as follows: canopy diameter in ft. ÷ 2 (use widest crown spread as the diameter).
- R × R × 3.14 represents the area of the circle created by the tree's canopy projection over the soil.
- 0.623 is the factor used to convert inches of water into gallons.

3.3 UTS step 3: tree amounts and shading percentage

The effect of the tree coverage percentage varies and depends on the street canyon's aspect ratio and orientation [39]. In a study conducted in Athens, the analysis of air temperature patterns for different tree coverage scenarios indicates that the variability in results is mainly due to the effects of tree percentages and the level of aspect ratio [64]. A study carried out in Phoenix showed that an increase in the percentage of tree coverage from 0 to 25% reduces the air temperature by 4.4 °C [31]. A study conducted in Hong Kong, however, recommends 56% tree coverage to achieve the best enhancement of microclimate conditions [65]. Moreover, a study dealing with the effects of tree coverage on deep street canyons within Cairo's downtown center recommends coverage percentages of 22% for northern–western streets and 54% for northern–eastern streets [66]. However, another study conducted in Cairo suggests 50% tree coverage for highly dense urban areas [67]. From all relevant studies within and outside Cairo, it can be concluded that the tree coverage percentage should not be the same for different types of urban canyons with different aspect ratios and street orientations. A detailed study should be conducted to test the ideal tree coverage percentage for each canyon to avoid implementing a tree strategy that will not be efficient given a shortage, or excess, in tree coverage percentages.

3.4 Testing the strategy

After studying the three steps, selecting suitable tree species and irrigation technologies, and optimizing tree amounts, the strategy should be tested to examine its efficiency. The outputs of each step should be tested in a study area located in downtown Cairo. This test should validate the strategy's efficiency and measure the impact of applying the strategy to the study area as an example before generalizing the strategy's outputs/recommendations and applying them throughout the entire city of Cairo.

4 Method of testing the strategy

As shown in Figure 3, the efficient UTS will be tested using ENVI-met simulations to examine the strategy's impact on the microclimate conditions and ensure that, in alignment with the other studies conducted around the world, the performance of the strategy will also be useful in Cairo.

To test the strategy performance, a comparative study should be carried out between the results of the ENVI-met simulation on the current situation of the study area and the results after the application of the UTS criteria. The results should be statistically analyzed to measure the differences and relationships between the various factors.

4.1 The study area

The study area should be located in Cairo's downtown center to observe the effects of the UHI, as they appear most clearly in the central part of the city [2, 9]. The comparative study should be applied using the microclimate simulation tool ENVI-met, which is the most extensively evaluated microclimate model available, with capabilities to accurately simulate an outdoor microclimate for any given location [68]. Using simulation software will also be useful in assessing different scenarios and comparing their results to the results of the current situation.

4.1.1 Study area location and urban characteristics

The study area is situated in the heart of Cairo, specifically in the downtown district or Khedival Cairo. The total area of the site is 150,000 square meters. According to Fig. 4A, it is bordered by 26th of July Street to the north, Kasr AlNil Street to the south, Sherif Basha Street to the west, and Opera Square to the east.

The urban form of the study area follows a grid pattern, oriented in the north direction, as shown in Fig. 4B. The aspect ratios of the urban canyons and spaces vary. Table 2 shows the selected street canyons' aspect ratios and the elements

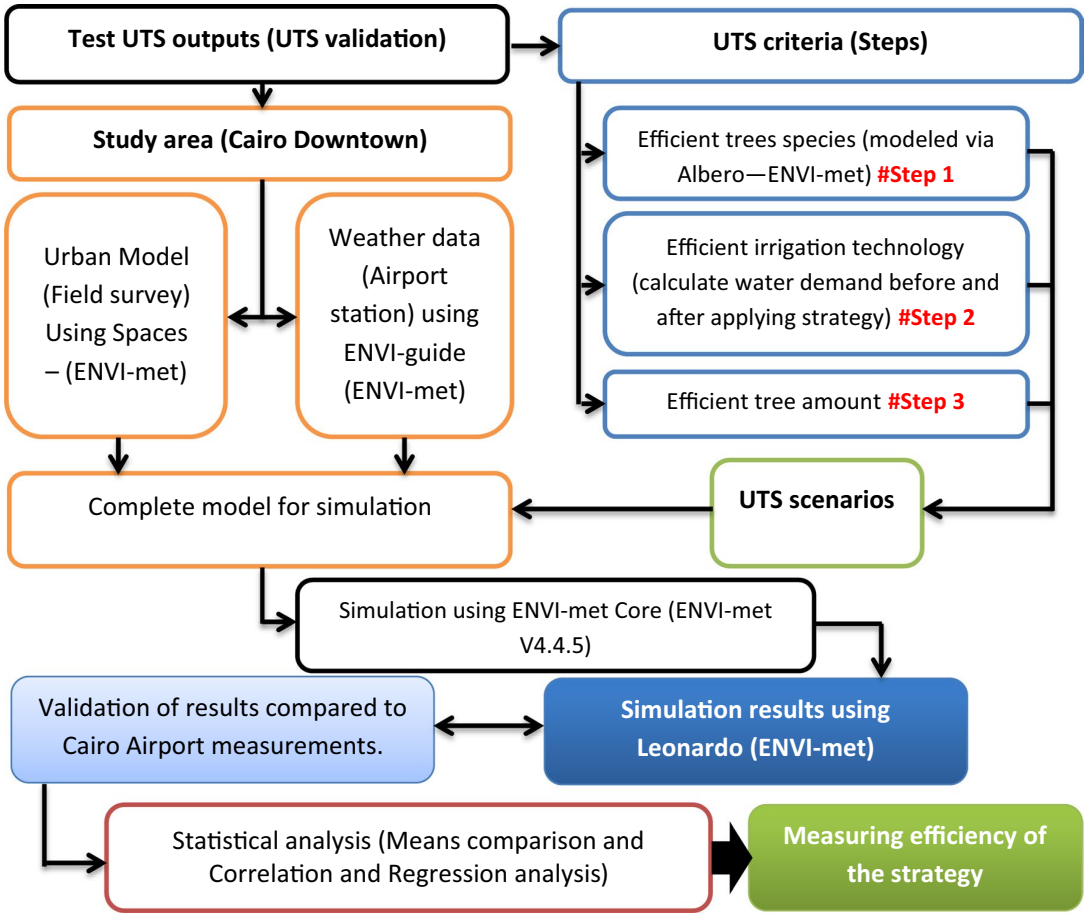

Fig. 3 Method of testing and validating the UTS criteria

of their built environment, such as the building heights, width of roads, tree coverage percentages, and the materials of the street canyon. All urban geometry information is based on the GIS database by the General Organization for Physical Planning (GOPP—Cairo), which was updated through a field survey conducted in September 2021.

4.1.2 Existing trees

As shown in Fig. 4D, some trees already existed within the study area. Fortunately, and as observed during the field survey, these existing trees represent the opposite of what the UTS proposes for selecting tree species; they have very small crown sizes (from 1 to 4 m), are randomly distributed, comprise only one tree species (*Ficus benjamina*—Evergreen), and require manual immersion irrigation. All these differences provide a good opportunity to compare the current situation with the proposed UTS scenarios and, in turn, measure the effectiveness of all criteria and steps of the UTS.

4.2 Different scenarios

Based on the outcomes of the UTS (Step 3), four different scenarios will be applied on selected inner streets of the study area, as illustrated in Fig. 5. Tree coverage percentages should be different for streets with different aspect ratios and orientations [69]. According to two external studies that were conducted and applied in Cairo's downtown center, tree coverage percentages should be between 20 and 50% [66, 67]. Each of the four scenarios will test a different tree coverage percentage. While scenario A will test 0% tree coverage, scenario B will test 20%, scenario C will test 35%, and scenario D will test 50%. All scenarios will be tested during the summer and winter (and, thus, there will be scenarios e, f, g, and h for winter scenarios). For winter scenarios and due to having deciduous trees that lose their leaves during winter, the tree

Fig. 4 **A** Study area location in Cairo's downtown district (indicated by the pink zone). **B** Selected inner streets for the study (S1, S2, and S3) and buildings heights (m). **C** and **D** Images of the study area's buildings and existing trees from a field survey

percentage in each scenario will not match the same percentage in summer, as clarified in Table 3. As demonstrated in Fig. 5, the results will be compared to the results of the base case scenario during both summer and winter. All information and percentages of the different scenarios are presented in Table 3. For the recommended tree species, three trees from the recommended list will be modeled and used for all scenarios, as shown in Table 3.

4.3 Model setup and data input

4.3.1 Model setup, geometry, soil, and materials

The model geometry and the selected soil and materials represent the current situation of the study area based on the available data and the field survey and do not change for any of the scenarios. To measure the effect of only applying trees, the study area model was built using the model geometry, soil, and materials outlined in Table 4.

4.3.2 Trees and vegetation

This study specifically focuses on the role of urban trees; thus, the modeling of vegetation only focuses on trees. To accurately represent and model different tree scenarios, such as crown size, height, shape, and seasonality, custom tree models need to be developed. These models should meet the criteria and recommendations outlined in Step 1 and

Table 2 Urban information and field survey outputs for selected streets in the study area

Street name	Abbr	Street orientation	Avg. height	Avg. width	Aspect ratio	Tree coverage %. No. of trees	Tree species	Buildings and Streetscape materials
Muhammad Farid	S1	North–South	24 m	20 m	1:1.2	7.3% 33 trees	*Ficus benjamina*	Buildings: Rendered concrete Sidewalks: Concrete pavers Streets: Asphalt
'Adly	S2	East–West	24 m	24 m	1:1	8.27% 90 trees	*Ficus benjamina*	
'Abd Al Khaliq Tharwat	S3	East–West	25 m	20 m	1:1.25	11.25% 72 trees	*Ficus benjamina*	

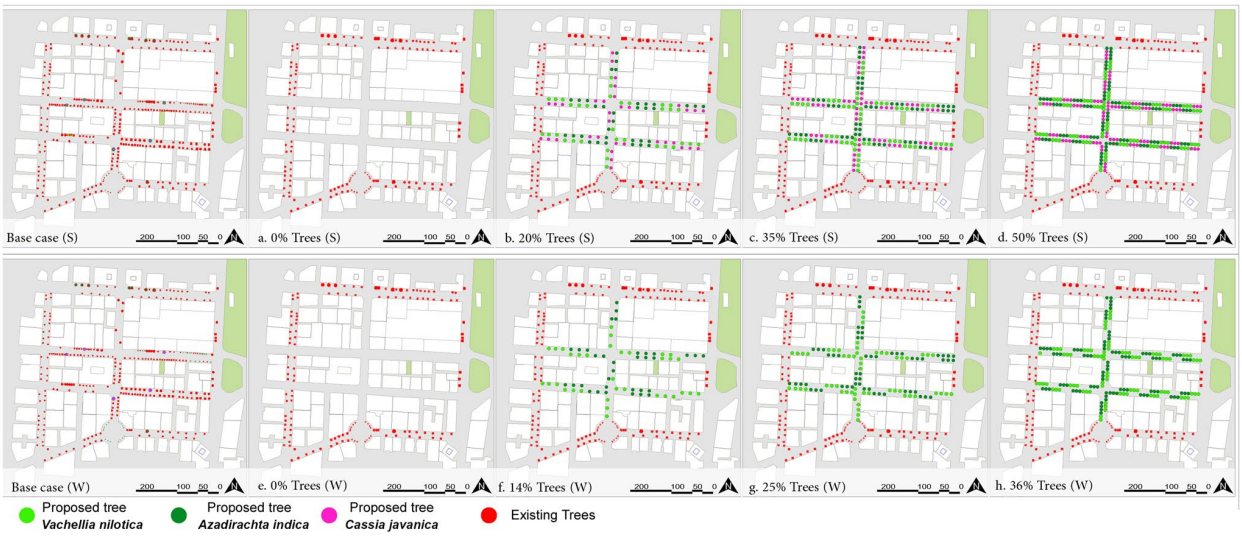

Fig. 5 All scenario plans for trees during summer and winter

allow for the measurement of the effects of different tree types in each scenario compared to existing trees in the base case. The ENVI-met application "Albero" is a useful tool for modeling these required tree models and designing their geometries and properties, including crown size, tree height, root size, tree seasonality by month, tree shape, and leaf area density (LAD) of each tree layer [68]. After the trees have been modeled, Albero is able to offer trees with varying crown sizes that can be applied to a specific situation. Albero can also assign an LAD value and determine appropriate heights for the trees. These factors are extremely valuable when integrating small trees into the current conditions of the study area. Additionally, the utilization of tree seasonality aids in elucidating the disparities in performance between deciduous trees during summer and winter. All of these factors will contribute to an efficient and detailed method of measuring tree performance. The distinctions between the different tree scenarios will be evaluated proficiently. While tree modeling and tree variety are based on the existing trees, the proposed trees are based on the efficient UTS, as shown in Table 3 above. Figure 6 shows the differently modeled trees (7 m, 5 m, and 3 m) for the proposed trees scenarios and the current base case scenario.

4.3.3 Meteorological data input

We utilized the recorded data from Cairo Airport on both July 1st, as a representation of summer, and January 1st, as a representation of winter in 2020, [70–72] and employed simple forcing instead of full forcing due to irregular results that did not align with the measured data from Cairo Airport.

4.3.4 Simulation configuration

The simulation setup took two days to prepare: one in the summer on July 1st and one in the winter on January 1st. The simulation started at 1:00 am and lasted for 24 h. We used simple forcing for the measured data from Cairo Airport. Data output was collected every hour and converted using the ENVI-met "Bio-met" program to calculate the PET values for each hour and scenario. The main factor of comparison was the different mean PET values. We compared them across all scenarios to evaluate the impact of each scenario and determine the ideal urban tree model that represents an efficient UTS. We calculated the mean PET values for all cells on each street and compared them to the mean values of the other streets. In addition, we also measured other parameters, such as air temperature (TA), wind speed (WS), humidity (H), and total mean radiant temperature (TMRT). As illustrated in Fig. 7, these parameters were measured at a given point located at the center of each street, away from the shade of tree canopies (R1, R2, and R3). Comparing such detailed results would greatly help in increasing our understanding of the effect of the UTS, after understanding its general effect, by comparing the mean PET values of each street.

Table 3 Tree data for each scenario

Scenario	Tree species	No. of trees	Avg. crown size	Overall tree coverage (%)
Base case—summer	*Ficus benjamina*	187	1—4 m	9
	Cassia javanica	5	6.5 m	
	Phoenix dactalfera	3	5 m	
	Total	195		
Base case—winter	*Ficus benjamina*	187	1—4 m	8.2
	Cassia javanica	5	0*	
	Phoenix dactalfera	3	5 m	
	Total	195		
0% trees—summer—winter	N/A	0	N/A	0
b. 20% trees—summer	*Vachellia nilotica*	34	7.5 m	20
	Azadirachta indica	34	8 m	
	Cassia javanica	34	7 m	
	Total	102		
f. 20% trees—winter	*Vachellia nilotica*	34	7.5 m	14
	Azadirachta indica	34	8 m	
	Cassia javanica	34	0*	
	Total	102		
c. 35% trees—summer	*Vachellia nilotica*	58	7.5 m	35
	Azadirachta indica	60	8 m	
	Cassia javanica	06	7 m	
	Total	178		
g. 35% trees—winter	*Vachellia nilotica*	58	7.5 m	25
	Azadirachta indica	60	8 m	
	Cassia javanica	06	0*	
	Total	178		
d. 50% trees—summer	*Vachellia nilotica*	86	7.5 m	50
	Azadirachta indica	85	8 m	
	Cassia javanica	85	7 m	
	Total	256		
h. 50% trees—winter	*Vachellia nilotica*	86	7.5 m	36
	Azadirachta indica	85	8 m	
	Cassia javanica	85	0*	
	Total	256		

*Deciduous trees have zero crowns during winter

4.4 Validation of results

The simulation was performed for all cases based on the model setup and the meteorological data of Cairo's Airport. Before reading and analyzing the outputs and results, it is important to examine the validation results by comparing the values of the results to the measured data. Additionally, the root-mean-square index (RMSE) and the index of agreement (d) are calculated for all results to ensure that the results obtained from the simulation are valid. Air temperature and relative humidity, measured on the 1st of July 2020, are compared to the output results of the simulation to assess whether the results are in line with the measured data, and for better validation, the ENVI-met results are not only compared to airport station measured data but also to data measured in Fatimid Cairo on the same day but in a previous study (1 km away from the study area) conducted in 2013 [73]. As shown in Fig. 8, by applying ENVI-met simple forcing using the measured data, the results for summer air temperature and relative humidity show significant matching, the RMSE for air temperature was 1.45 for the airport data and 2.11 for the site data, with an index of agreement d of 0.94 for the airport data and 0.87 for the site data, and the RH% RMSE was 7.15 for the

Table 4 Model setup, geometry, soil, and materials

Model information (base case, 0%, 20%, 35%, and 50%) for models in summer and winter	
Model location	30.02 latitude and 31.22 longitude
Area size (Grids)	X = 166, Y = 140, Z = 21
Grid resolution (m)	X = 3, Y = 3, Z = 3
Orientation (from North)	0
Split lower grid box into 5 sub cells	Yes
Telescoping applied	The telescoping factor is 20%, and telescoping should start after 42 m in height
Maximum model height*	88 m
Nesting grids**	Not applied
DEM	Not applied, as the site is flat
Soil	Asphalt for roads, concrete for sidewalks, green turf for green areas, and sand under buildings
Building materials	Default wall—moderate insulation

*The model's height is more than double the height of the tallest building, as recommended by the software [68]

**Nesting grids were not applied; however, 5 cells from the boundary sides of the model were kept empty, as recommended by the software developers [68]

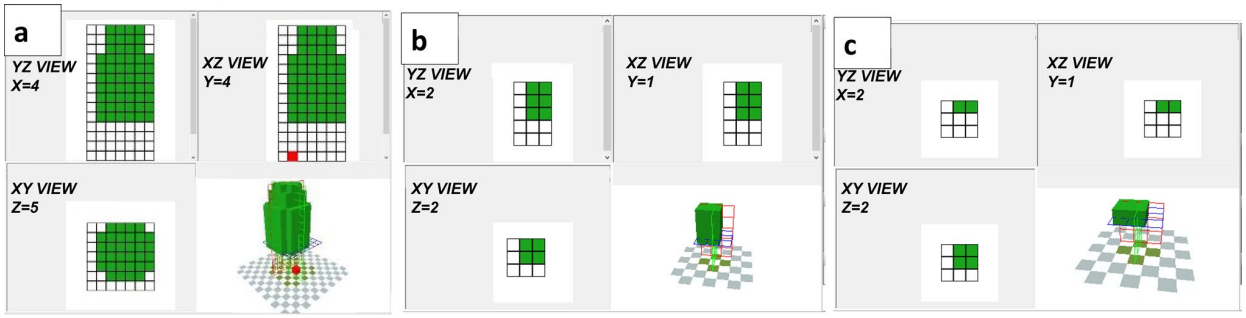

Fig. 6 Modeled trees using Albero, **a** the 7 m tree, **b** the 5 m tree, and **c** the 3 m tree

Fig. 7 The location, types, and coordinates of receptors

P.	X	Y
R1	70	100
R2	111	77
R3	110	45
R4	64	06

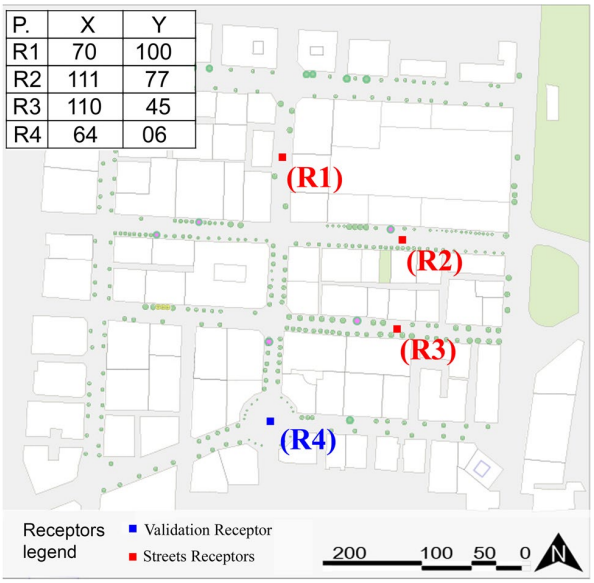

airport data and 6.91 for the site data, with a d of 0.89 for the airport data and d of 0.90 for the site data. Additionally, as depicted in Fig. 8, the ENVI-met results for the same point in the model closely align with the measured data. Similarly, when the validation process is performed during winter, the results closely match the measured data, with an air temperature RMSE of 1.27 and d of 0.93, and an RH% RMSE of 6.37 and d of 0.94. Additionally, these results demonstrate that employing a simpler forcing method yields more accurate outcomes compared to the full forcing method, which was applied at the beginning using EPW files of Cairo and showed mismatching results, as shown in Appendix (1). This indicates that all results accurately represent the current situation, with minor discrepancies arising from changes in the surrounding urban context, as the differences in the results are very similar or even better than some ENVI-met simulation studies applied in Cairo [67, 74, 75]. Hence, the simulation output can be utilized to evaluate the impact and influence of various tree scenarios during both summer and winter.

5 Results

5.1 Comparison of PET (mean values of each street)

To understand the different impacts of each tree scenario in relation to the base case scenario, a comparison of the mean PET values between each street (S1, S2, and S3) and each scenario was performed. The PET value is a good measure to use when comparing the impact of each scenario, as it represents the physiological equivalent temperature felt by people inside the urban canyon. All measured data are selected at a height of 1.5 m, which is the average height of street pedestrians. The PET values are classified under many ranges to represent outdoor thermal comfort. Temperatures of less than 4 °C are considered within a very cold range, between 4 and 18 °C are within a cold range, between 18 and 23° are within a thermal comfort range, between 23 and 41° are within a hot range, and above 41 °C are within a very hot range [76]. Table 5 presents a more detailed PET classification from another study for a subtropical climate (a similar climate zone to Cairo) [77].

5.1.1 Comparison of PET results during summer

By comparing the summer PET values of all the streets, it is clear that the addition of trees to urban canyons has a positive impact on enhancing PET values in general. This impact, however, varies from one street to another and from daytime to nighttime. To further understand this impact, a more detailed comparison is conducted per hour to measure this impact and generate recommendations regarding the application of trees to different urban canyons.

5.1.1.1 Comparison of mean PET values for S1 scenarios during summer Applying different percentages of urban trees to S1 slightly enhances its mean PET values. As shown in Fig. 9, the PET values indicate that the base case results during peak hours and during the day are in the hot range. The PET values of the base case scenario are extremely similar to those of the 0% tree coverage scenario. The maximum difference between both scenarios is – 0.37 °C, the average difference is – 0.04 °C, and most differences are less than – 0.1 °C. Therefore, the application of numerous trees with small crowns will not enhance the thermal comfort of this urban canyon, in any way, aligning with the theoretical recommendations of the efficient UTS [32, 78].

Applying 20% tree coverage to S1 slightly increases the PET values, which reach a maximum of – 0.83 °C and an average of – 0.10 °C during the daytime. Although this scenario yields better results than the one that does not apply any trees, it achieves only a slight enhancement in the PET values during the daytime.

When applying 35% tree coverage to S1, the enhancement in the PET values increases, reaching a maximum of – 0.69 °C and an average of – 0.41 °C during the daytime. While this scenario also yields better results than the one that does not apply any trees, it achieves only a slight enhancement in the PET values during the daytime as well. The values are higher during nighttime but still fall within the same range.

Applying 50% tree coverage to S1 increases the enhancement in the PET values, reaching a maximum of – 1.52 °C and an average of – 0.79 °C during daytime. This is very similar to the 35% tree coverage scenario and is still considered only a slight enhancement during the daytime. The PET values are higher during nighttime but fall within the same range.

The overall impact of applying different tree coverage percentages to S1 is not significant at all. Although it slightly enhances thermal comfort, this minor enhancement does not lead to any noticeable improvement, such as changing

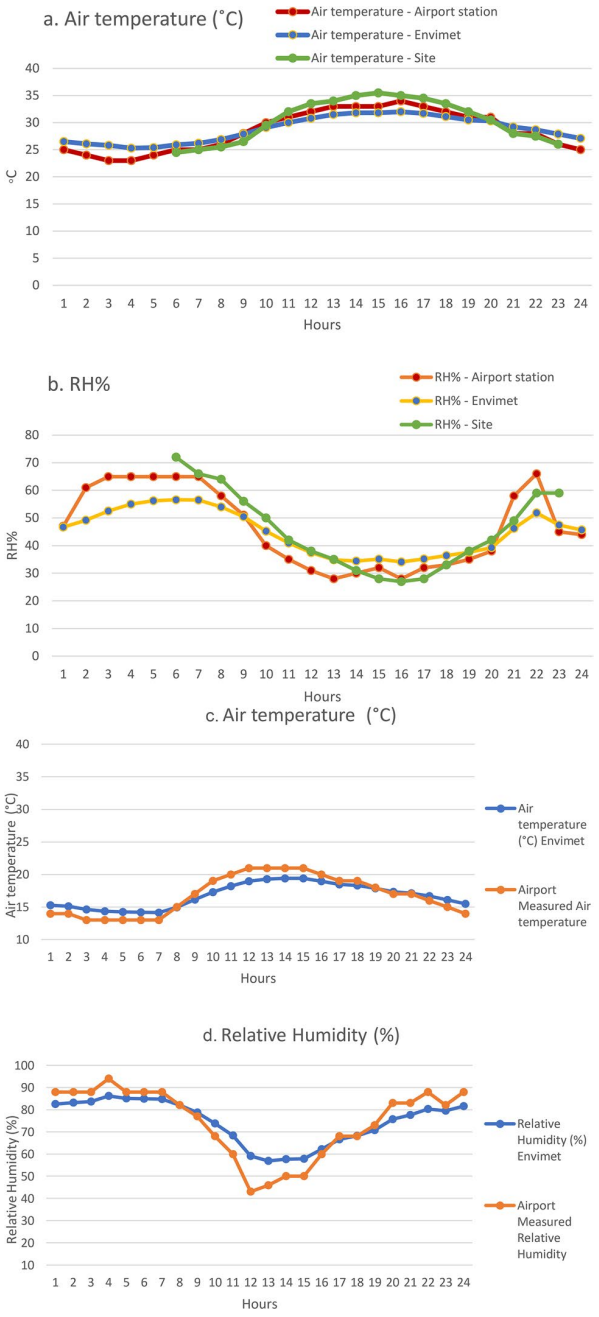

Fig. 8 Air temperature and RH% validation, summer (**a**, **b**) and winter (**c**, **d**) (simple forcing)

Table 5 PET detailed classification for a subtropical climate

Range*	13–18	18.1–23	23.1–29	29.1–35	35.1–41	41.1 ≤
Thermal perception	Slightly Cool	Comfortable	Slightly Warm	Warm	Hot	Very Hot
Grade of physiological stress	Slight cold stress	No thermal stress	Slight heat stress	Moderate heat stress	Strong heat stress	Extreme heat stress

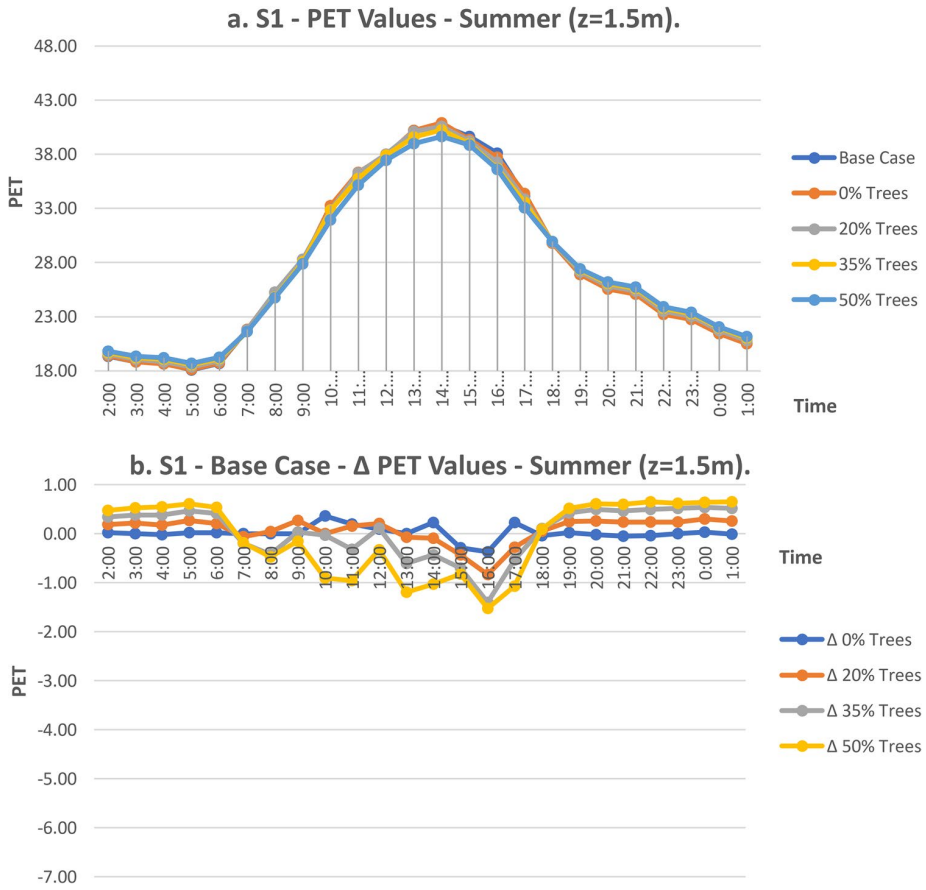

Fig. 9 **a** S1: mean PET values for S1 scenarios, **b** S1—base case ΔPET—summer (01-07-20)

the thermal range. The PET values were higher during nighttime across all scenarios (20%, 35%, and 50%); however, the increase was very minor and still fell within the same thermal range.

Applying different percentages of urban trees to S2 and S3 significantly enhances their mean PET values. As shown in Fig. 10, the PET values indicate that the base case results during peak hours and daytime are in the extreme heat stress zone. The PET values of the base case are extremely similar to those of the 0% tree coverage scenario. The maximum difference between both scenarios is 0.04 °C, the average difference is 0.02 °C, and most differences are less than 0.01 °C. This means that the application of many trees with very small crowns to both these urban streets (S2 and S3) will not enhance their thermal comfort, in any way, aligning with theoretical recommendations of the efficient UTS [32, 78].

When applying 20% tree coverage, the enhancement in the PET values noticeably increases, reaching a maximum of – 3 °C in S2 and – 3.16 °C in S3 during the daytime. The average increase during the daytime is – 1.55 °C in S2 and – 1.89 °C in S3, which is higher than the results of the scenario that uses 0% tree coverage, which is considered a good enhancement. The PET values are higher during the nighttime and lie within a smaller range, reaching a maximum of – 0.35 °C in both streets. When applying 35% tree coverage, the enhancement in the PET values increases and reaches a maximum of – 4.71 °C in S2 and – 4.51 °C in S3 during the daytime. The average increase during the daytime is – 2.69 °C in S2 and – 3.18 °C in S3, which is considered a very good enhancement. The PET values are slightly higher during the nighttime and reach a maximum of – 0.55 °C in both streets.

When applying 50% tree coverage, the enhancement in the PET value significantly increases and reaches a maximum of – 6.36 °C in S2 and 6.49 °C in S3 during the daytime. The average increase during the daytime is – 3.95 °C in S2 and – 4.66 °C in S3, which is considered a significant enhancement, as the average enhancement during peak hours is – 3.56 °C in S2 and – 4.41 °C in S3. The PET values are higher during the nighttime and reach a maximum of – 0.7 °C in both streets.

The overall impact of applying different tree coverage percentages is clearly significant and strongly enhances thermal comfort, helping change the thermal comfort zone in S2 at 11:00, 12:00, 16:00, and 17:00 and in S3 at 11:00, 12:00, and 17:00. PET reduction helps change the thermal comfort zone from extreme heat stress to strong heat stress. Figure 11 illustrate the effects of trees at 13:00 and 15:00.

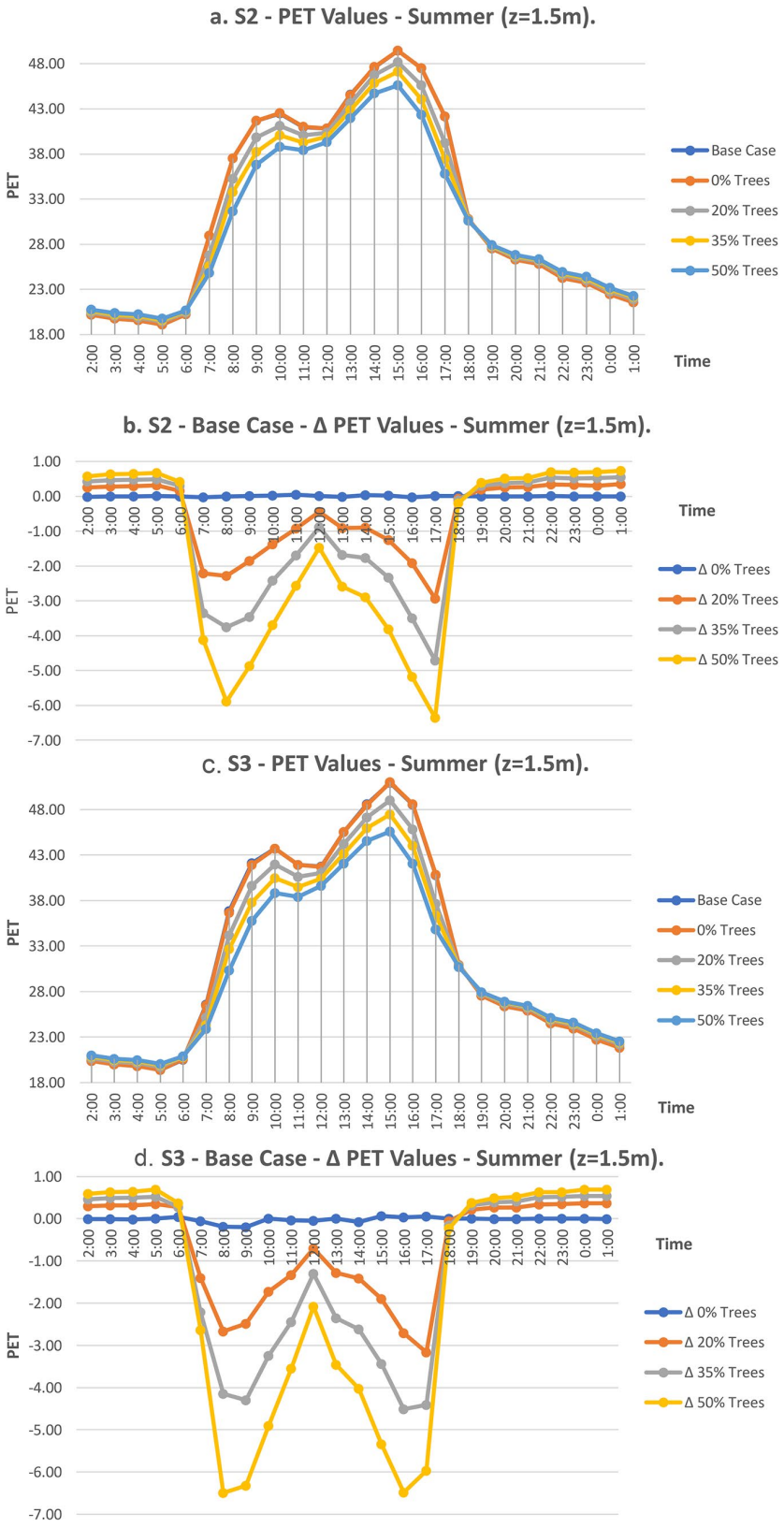

Fig. 10 **a** S2: mean PET values for S2 scenarios, **b** S2—base case ΔPET, **c** S3: mean PET values for S3 scenarios, **d** S3—base case ΔPET—summer (01-07-20)

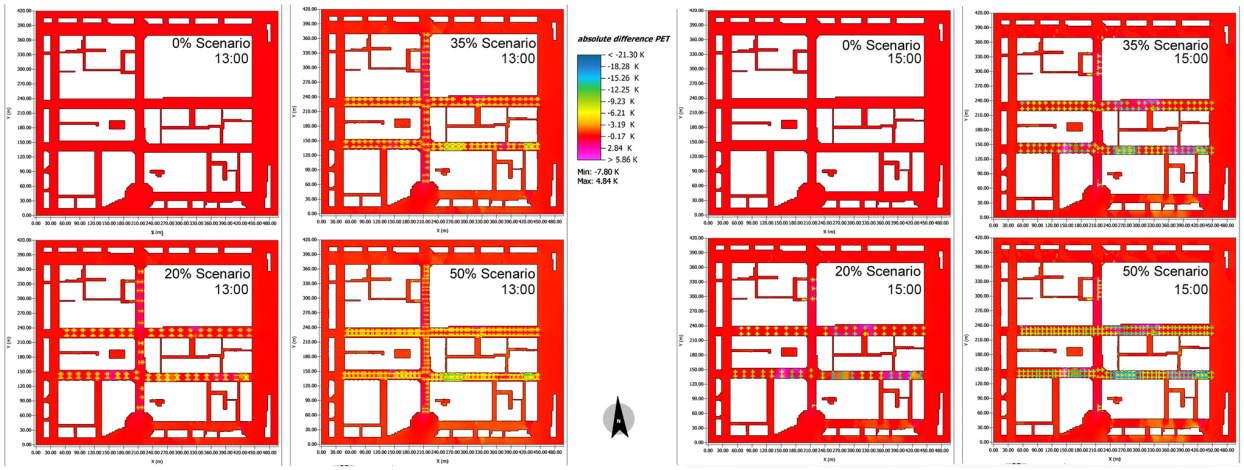

Fig. 11 PET reduction values for each scenario compared to the base case (on the right at 13:00, and on the left at 15:00 on 01-07-20) Z = 1.5 m

5.1.2 Comparison of PET values during winter

By comparing the PET values of all the streets during winter, it is clear that the addition of trees to the urban canyons does not have an impact on enhancing their PET reduction values. Such an impact is usually not recognized due to the cold microclimate conditions of winter, as all the simulation scenarios were carried out on the 1st of January, which is considered the middle of winter. In general, the absence of trees in urban canyons will not have a negative impact on human thermal comfort. The application of different tree species (whether evergreen or deciduous) will not change the microclimate conditions that occur during winter.

5.1.2.1 Comparison of PET values for S1 (winter scenarios) As shown in Fig. 12A, the maximum reduction in the PET reached 0.58 °C and 0.55 °C at 11 am and 12 pm only and in the 50% tree coverage scenario. This reduction equates to only 9% of the reduction value for the same tree scenario in the summer. During some hours, the addition of trees increases the PET. For example, the maximum reduction in the PET is 0.43 °C at 10 am in the 20% tree coverage scenario. The average reduction in the PET during peak hours is 0.02 °C in the 20% tree coverage scenario, 0.045 °C in the 35% scenario, and 0.07 °C in the 50% scenario.

5.1.2.2 Comparison of PET values for S2 and S3 (winter scenarios) As shown in Fig. 12B and C, the maximum reduction in the PET for S2 ranged between 0.32 and 0.42 °C between 10 am and 1 pm in the 50% tree coverage scenario. This reduction equates to only 6.8% of the reduction value for the same tree scenario for S2 in the summer. For S3, the maximum reductions in PET are 0.58 °C and 0.55 °C at 11 am and 2 pm, respectively, in the 50% tree coverage scenario.

This reduction equates to only 6.5% of the reduction value for the same tree scenario for S3 in the summer. The average reduction in the PET for S2 during peak hours is 0.07 °C in the 20% tree coverage scenario, 0.13 °C in the 35% scenario, and 0.19 °C in the 50% scenario. For S3, the average reduction in the PET value during peak hours is 0.10 °C for the 20% tree coverage scenario, 0.15 °C for the 35% scenario, and 0.21 °C for the 50% scenario.

5.2 Comparing PET parameter results for all receptors

To understand the main factors contributing to the enhancement in the microclimate conditions in S2 and S3, a detailed investigation should be conducted by studying all thermal comfort parameters of both streets. All parameters should be measured at the same point, located in the middle of each street (indicated as R2 and R3 in Fig. 7). Measuring and comparing all parameters, including air temperature (TA), wind speed (WS), TMRT, and specific humidity (H), will help to clarify which parameter is enhanced by the addition of trees, consequently leading to an enhancement in the PET. Figure 13 demonstrates that when comparing the results of each factor for both R2 and R3, significant changes are found to

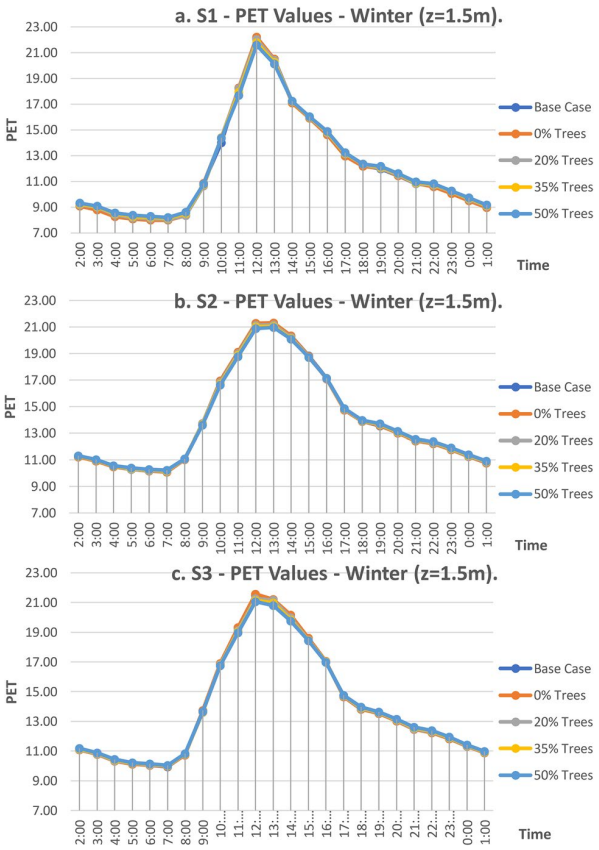

Fig. 12 Mean PET values—winter (01-01-21) Z = 1.5 m. (**A**: S1, **B**: S2, **C**: S3)

occur in WS and TMRT upon the addition of trees. Changes in these two specific factors explain why the shading provided by trees reduces the TMRT and their physical blocking of the wind reduces wind speed. No major changes take place, however, in the air temperature and humidity of both streets before and after the addition of trees.

5.2.1 The impact of adding trees on air temperature and humidity

The addition of trees leads to a very slight enhancement in air temperature, which reaches a maximum of – 0.124 °C at 17:00 in R3 and – 0.113 °C at 16:00 in R2. This slight enhancement is not considered to be the reason behind the observed significant enhancements in the PET values. Similarly, the results for specific humidity showed very minor enhancements when trees were added to both streets, in which humidity was reduced by a maximum of 0.09% at 10:00, 11:00, and 12:00 in R2 and reached a maximum reduction of 0.17% during the same hours in R3.

5.2.2 The impact of adding trees on wind speed

As shown in Fig. 13, the addition of trees to all streets leads to significant changes in wind speed. The wind speed is reduced due to the vertical blocking of the trees planted on both sides of the street. This impact, however, varies from one street to another, as the wind speed is different within each street due to the different orientations of the streets. While S1 is oriented toward the north, S2 and S3 are oriented toward the east. Figure 14.a illustrates a comparison between wind speed figures for the base case scenario at the receptor points of each street (R1, R2, and R3). As shown in the figure, the wind speed is significantly different and high in S1 given that its northern orientation matches Cairo's main wind direction. The wind speed in S1 ranges between a maximum of 3.25 m/s and a minimum of 2.86 m/s, which lies within the comfort limit of 1 m/s to 5 m/s [79]. In S2 and S3, which have an eastern orientation that goes against

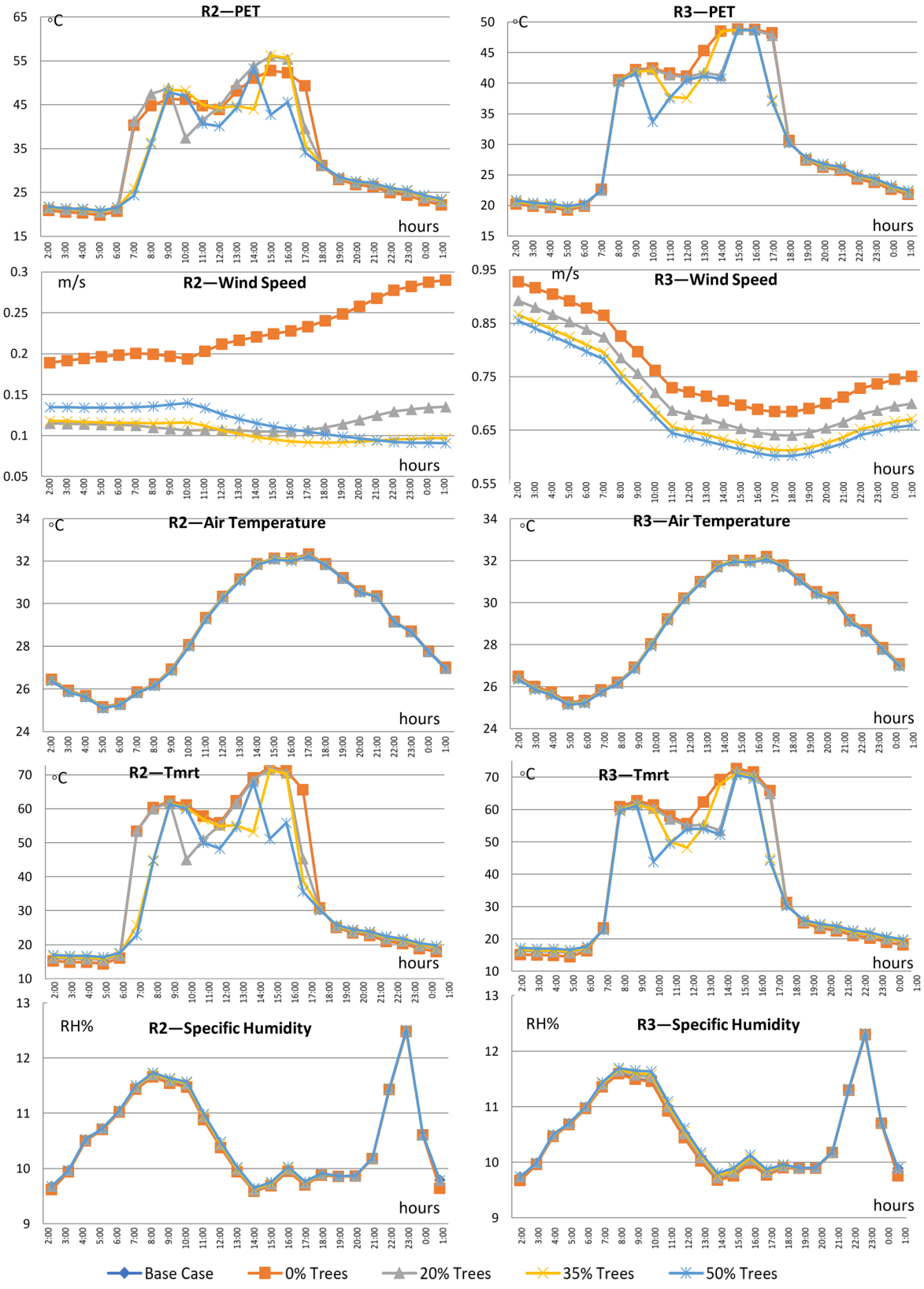

Fig. 13 Comparison between PET, WS, TA, TMRT, and H for R2 and R3

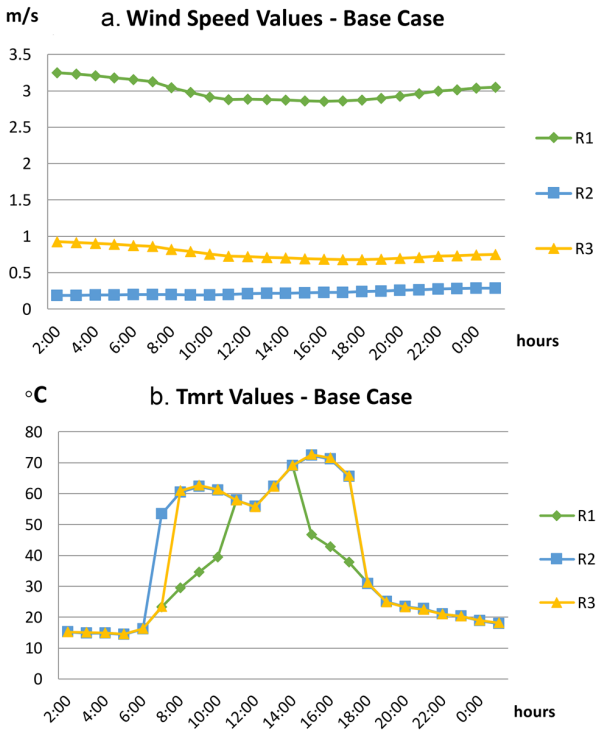

Fig. 14 **a** Wind speed values, **b** Tmrt values for the base case for R1, R2, and R3

Cairo's wind direction, wind speed values are between 0.29 m/s and 0.19 m/s in R2 and 0.74 m/s and 0.92 m/s in R3. These are considered very minor values in comparison to those of S1. Although the addition of trees reduces wind speed in all streets, the large difference in wind speed between S1 and the other two streets indicates that their impact varies from one street to the other. In S1, the addition of trees reduces the wind speed in R1 by – 1.7 m/s to – 1.8 m/s during the day, which is more than double the maximum wind speed figures of the other streets. In S2 and S3, the addition of trees reduces the wind speed by -0.05 m/s to – 0.2 m/s in R2 and – 0.07 m/s to -0.09 m/s in R3.

The impact of adding trees on the wind speed of both S2 and S3 cannot, therefore, be considered the main factor affecting their PET, as the wind speed of both streets is already extremely low. A reduction in wind speed will, thus, not impact their PET values. This is due to other factors that significantly enhance the PET values in both streets, as shown in Fig. 10. In contrast, the wind speed reduction in S1 is quite significant, being reduced to almost half of its original figure. According to Fig. 9, the enhancement in the PET in S1 is very limited. It can, therefore, be claimed that the addition of trees to S1 does not enhance the PET and significantly reduces wind speed.

5.2.3 The impact of adding trees on TMRT

Figure 13 shows how the addition of trees clearly changes the TMRT figures for R2 and R3. The changes in the TMRT charts are significant in comparison to the other measured parameters outlined in Fig. 13. This means that the addition of trees to urban areas, with the additional shading they provide, significantly reduces the total radiant temperature (including solar radiation) of the urban canyon at the pedestrian level. After the addition of trees to S2, the maximum reductions in TMRT at R2 reached – 21.3 °C, – 15.4 °C, and – 29.9 °C at 15:00, 16:00, and 17:00, respectively. After the addition of trees to S3, the maximum reductions in TMRT at R3 reached – 17.0 °C and – 21.6 °C at 17:00 and 14:00, respectively. As illustrated in Fig. 13, the PET and TMRT charts look very similar, and their reduction values are almost the same for both streets. This means that the significant enhancement in the PET is directly related to the major reduction in TMRT. In S1, the TMRT reduction is minor, and the PET enhancement is not significant, further demonstrating the relationship between PET and TMRT.

Figure 14b shows the TMRT values of all the streets for the base case scenario. As displayed, during the daytime (i.e., during solar radiation), the TMRT values are much lower in S1 than in S2 and S3 due to the different street orientations. The addition of trees helps protect the street canyon at the pedestrian level from such high levels of radiation. Accordingly,

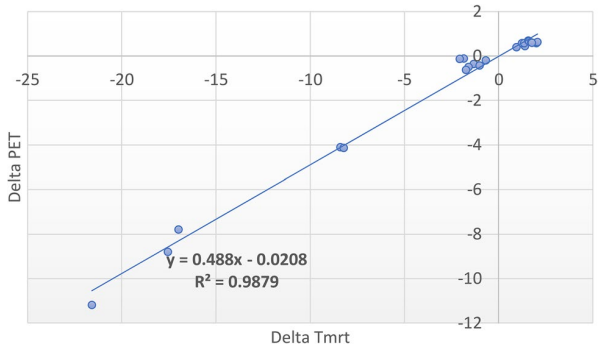

Fig. 15 Correlation between ΔPET and ΔTMRT

Table 6 Water demand increase/decrease in relation to the base case scenario

Scenario	Tree coverage %	Number of trees	Water demand increase (+)/decrease (–)	Water demand decreased based on irrigation and planting technologies criteria – 65%
Base case	9	195	0	0
0%	0	0	– 9%	– 9%
20%	20	102	+ 11%	+ 3.85%
35%	35	174	+ 26%	+ 9.1%
50%	50	256	+ 41%	+ 14.35%

and because the TMRT values in S2 and S3 are much higher, adding trees significantly reduces the TMRT, which leads to significant enhancements in the PET for both streets. In contrast, and because TMRT values are lower in S1 (given its northern orientation), the added trees are not able to further enhance the TMRT as the urban canyon is already protected from solar radiation and shaded by buildings; thus, the enhancements in the PET values are minor.

5.3 Correlation between PET and TMRT

It is clear that there is a strong relationship between TMRT reduction and PET enhancement within urban canyons and at the pedestrian level. To demonstrate this relationship, an SPSS statistical analysis is conducted the examine the correlation between the reduction in TMRT and the enhancement in PET. The correlation study is applied to the results of the 50% tree coverage scenario in R3. Before calculating the correlation between both mentioned variables, the Kolmogorov–Smirnov (K–S) test is applied to all input data to check if the data are normally distributed. This (K–S) is because the test results guide the selection of the method for calculating the correlation. After applying Spearman correlation, since the data were not normally distributed in the K–S test, and as shown in Fig. 15, the results of this correlation study reveal a strong positive correlation, and the degree of association (correlation coefficient) is $r = 0.898$, indicating a strong relationship between ΔTMRT and ΔPET. When testing the regression, the R2 value is 0.9879, and the significant F value is < 0.001, indicating that the results of the study are reliable and statistically significant, and the co-efficiency value is $Y = 0.488x - 0.0208$. This statistically demonstrates the strong relationship between ΔTMRT and ΔPET and proves the direct relationship between shading and PET enhancement. It is also a clear indication to focus on increasing overall shading (through various elements, including buildings, trees, and shading structures) to further enhance the PET.

5.4 Comparison of water demand

As shown in Table 3, different scenarios require different numbers of trees and tree coverage percentages. Although the 20% and 35% tree coverage scenarios require a smaller number of trees in comparison to the existing trees in the base case, both scenarios require larger amounts of water for irrigation, as they have high coverage percentages, as calculated in Eq. 1. The only advantage in these scenarios is that the required amount of maintenance is less given the fewer number of trees. Table 6 illustrates the percentages of irrigation required for each scenario in comparison to the base case scenario. The green-highlighted column in Table 6 shows the increased or decreased percentage of water demand for each scenario compared to the base case (the current situation). This percentage is calculated based on the increase

Table 7 UTS recommendation for each step. Tree species, coverage percentages, and the calculated water demand for each street in comparison to the base case

Street	(Step 1) recommendations	(Step 3) recommendations		(Step 2) recommendations	
	Proposed Trees species	Recommended tree coverage percentage (%)	Number of trees	Increase (+)/decrease (–) in water demand (%)	65% Water demand decreasing (%)
S1	- *Vachellia nilotica* or similar from Category (A)	0	0 added (33 small trees removed)	− 7.3	− 7.3
S2	- *Azadirachta indica* or similar from Category (B)	35	60 added (90 small trees removed)	+ 26.73	+ 9.36
S3	- *Cassia javanica* or similar from Category (C)	50	86 added (72 small trees removed)	+ 38.75	+ 13.56
Total			146 added (195 small trees removed)	+ 58.18	+ 15.62

and decrease in the canopy percentage, which is the primary factor controlling the water demand. The recommended urban tree model should consider using the lowest percentage of tree coverage possible to avoid an increase in water demand without compromising enhancements in thermal comfort. In addition, the irrigation and planting technologies recommended in Step (2) should be applied to reduce the water demand.

6 Discussion

The results of this study indicate that the application of trees has a positive impact on various types of street canyons in the study area. Enhancements from the addition of trees are greater when the street orientation, aspect ratio of the street, and season change. The results also show that it is not just about adding trees to the urban canyon; tree species and their properties should also be carefully considered, as such factors can lead to significant variations in performance.

The application of trees to S1 (northern/southern orientation and an aspect ratio of 1:1.2) shows slight improvements in the microclimate conditions during the summer and winter. Although the addition of trees to S2 and S3 (east/west orientation, aspect ratios of 1:1 and 1:1.25) leads to significant enhancements in microclimate conditions, such enhancements only occur during the summertime. During the wintertime, the application of different tree coverage percentages exhibits no impact, and the maximum enhancement in their microclimate conditions then only equates to 9% of their mean enhancement values during the summertime. The type of tree that is applied, whether evergreen or deciduous, would not change the impact during winter. The enhancements that occur during the summer in S1 are very minor, and increasing the tree coverage percentage of this street would not lead to any significant enhancements. It would also result in the loss of various resources (water, trees, and maintenance). In addition, it significantly reduces the wind speed and slightly increases the relative humidity due to evapotranspiration. For S2 and S3, using trees and increasing tree percentages significantly enhances the microclimate conditions. During some hours, they not only help to enhance the PET values but also change the thermal comfort zone. During winter for S2 and S3, the results show no enhancements across all scenarios, which is in line with recommendations from reference [43] regarding the use of trees during winter.

The overall results of this study align with the results of other studies. The maximum PET reduction of 6.5˚C is quite similar to the PET reduction values between 1 and 6 ℃ for case studies conducted in Ho Chi Minh and Spain [26, 29]. The slight enhancements in air temperature are also similar to case studies conducted in Dubai, Tehran, and Phoenix [27, 28, 31]. Additionally, the overall results and improvements in the PET values are similar to those of the two prior case studies conducted in downtown Cairo (although this study presents more promising microclimate enhancements during some hours) [66, 67]. The minor differences between the enhancement values of the different case studies are due to the different street orientations

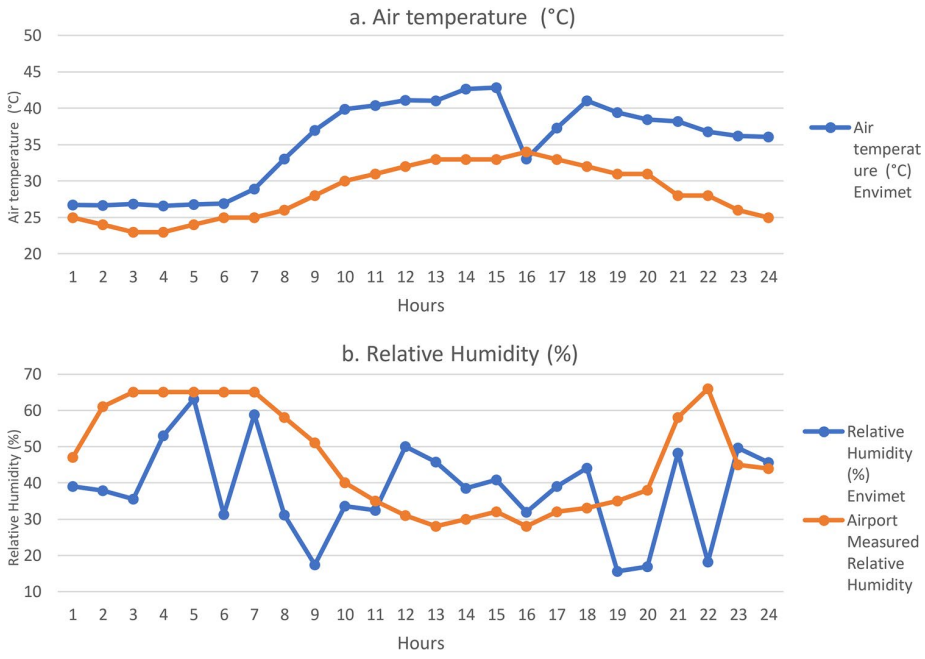

Fig. 16 Result validation (using full forcing)

and aspect ratios within each study. Moreover, the results demonstrate the strong relationship between shading and microclimate enhancement, as shown by the strong correlation between TMRT reduction values and PET enhancement values.

7 Conclusion

According to the results of all scenarios, the recommended tree coverage percentage to be applied should not be the same for all streets; it should vary. Additionally, the tree model should be independently designed for each street such that matches its geometry, orientation, and other conditions, which aligns with findings of previous studies [66, 67, 69]. The recommended tree model should consider tree seasonality and tree variety for biodiversity, as well as contribute to a visually appealing image for the city. Nothing, however, would be required to enhance the microclimate condition, as all winter results show that applying different tree coverage percentages to different street canyons would not have a significant impact on thermal comfort. For water demand, it is recommended that the use of trees be reduced. The ideal way to reduce water demand is to minimize the use of trees without compromising enhancements in the microclimate conditions, in addition to applying irrigation technologies.

7.1 Recommended tree percentages and tree species for each street

The recommended tree coverage percentages for all three streets that enhance microclimate conditions while also considering water demand are 0% for S1, 35% for S2, and 50% for S3. As trees did not provide any significant enhancement in S1, the enhancement by the 35% tree coverage was very similar to the enhancement by the 50% tree coverage in S2. In S3, the enhancement by the 50% tree coverage was higher than the enhancement by the 35% tree coverage, which is due to the wider aspect ratio in S3. The recommended ratio of deciduous trees relies on the suggested motivation of the design itself and not on the requirements of thermal comfort and UHI. Based on the abovementioned tree coverage percentages, Table 6 demonstrates the total number of trees and the total tree coverage percentages recommended for each street. The table also states the selected seasonal tree species ratio for each street and calculates water demand, comparing it to the current condition of the case study.

According to the recommended model, and as shown in Table 7, although the total number of trees is lower than the existing number of trees (146 large trees are added instead of the 195 small existing trees that are removed), the total water demand increases by 58.18% in comparison to the current situation. This is because water demand depends on the crown size of the trees and not their numbers, as shown in Eq. 1. Based on the recommendations of the efficient UTS, irrigation methods and technologies should help absorb this increase in water demand. Applying such methods and technologies to the current situation should reduce at least 65% of the total water consumption [61]. Their application would also help reduce water demand for irrigation, reducing the increase in water demand from + 65.48% in both S2 and S3 to + 22.92%, in addition to saving 7.3% in S1, while increasing the tree coverage percentage and reaching significant PET enhancements with very limited water demand increase.

Although the results of this study can be applied and generalized to the city of Cairo, the recommended tree coverage percentage cannot be generalized, as different urban canyons, with varied aspect ratios and/or orientations, lead to completely different results. The methodology used to determine the tree percentages in this research can be generalized and applied in the same way (with the same inputs, scenarios, and analyses) in any location in Cairo. A limitation of this study is that it was only applied to one existing area in downtown Cairo, which was adequate to measure the efficiency of the study; however, application in diverse situations would provide more comprehensive results and a stronger assessment of the strategy's effectiveness. Additionally, the lack of current information regarding the required level of irrigation for trees prevented a full comparison and assessment of irrigation consumption, as the trees were irrigated manually. In addition, the field survey was somewhat challenging due to security restrictions.

Urban shading is a critical factor that should be prioritized, as it consistently influences the effects of urban trees and impacts the application of the strategy. Therefore, the UTS should be carefully considered in relation to urban shading when implementing the strategy in various locations throughout the city.

Author contributions Ahmed Yasser Abdelmejeed: conceptualization, methodology, writing—original draft, visualization Dietwald Gruehn: writing—review and editing, supervision.

Funding Open Access funding enabled and organized by Projekt DEAL.

Data availability The data that support the findings of this study (all ENVI-met files) are available upon request.

Declarations

Competing interests The authors declare that they have no known competing financial interests or personal relationships that could have appeared to influence the work reported in this paper.

Appendix 1

Validating the results of the model using the full forcing ENVI-met method, the resulting values in R4 (using the full forcing method) do not match the measured values. As shown in Fig. 16, air temperature was always higher with ENVI-met in comparison to the measured air temperature. The difference in temperatures was obvious and significant, reaching 8 ℃ in 5 h and more than 10 ℃ in 10 h. The results for air temperatures with ENVI-met were, therefore, completely different than the air temperatures that were measured in reality. Regarding the relative humidity figures, the simulation results demonstrate completely different figures than the measured results, showing a difference of – 40% in five hours less than the measured results. During some hours, the difference was approximately + 10% in 3 h. This means that the results of relative humidity do not represent the relative humidity of the study area. The differences in these two sets of figures show that the simulation results are not only valid but also that the irregularity of the results itself indicates the same. By conducting a results analysis on the air temperature charts, one finds that a great decrease in air temperature occurs from 43 °C at 15:00 to 33 °C at 16:00, which then increases again to 41 °C at 18:00. These significant increases and decreases are inexplicable and do not reflect real-world conditions. Upon analyzing the relative humidity charts, it becomes evident that the figures lack any discernible pattern, fluctuating consistently every hour. For example, at 5:00am, it is 60%, which decreases to 30% at 6:00am, and then increases to 55% at 7:00 am. This does not reflect real-world conditions. These results are, therefore, not valid and do not represent the real-world meteorological conditions of the study area. A step back should, thus, be taken to revise the simulation setup, with which new validation results can be achieved.

References

1. Abou El-Magd I, Ismail A, Zanaty N. Spatial variability of urban heat islands in Cairo City, Egypt using time series of Landsat Satellite images. Int J Adv Remote Sens GIS. 2016;5(3):1618–38.
2. Abutaleb K, Ngie A, Darwish A, Ahmed M, Arafat S, Ahmed F. Assessment of urban heat island using remotely sensed imagery over Greater Cairo, Egypt. Adv Remote Sens. 2015;4(1):35–47.
3. Kosmopoulos P, Kazadzis S, El-Askary H. The solar atlas of Egypt. Geo-Cradle; 2018.
4. Nunfam VF, Adusei-Asante K, Van Etten EJ, Oosthuizen J, Frimpong K. Social impacts of occupational heat stress and adaptation strategies of workers: a narrative synthesis of the literature. Sci Total Environ. 2018;643:1542–52.
5. Newgeography.com. 2012. https://www.newgeography.com/content/002901-the-evolving-urban-form-cairo. Accessed 2024.
6. Pearlmutter D. Patterns of sustainability in desert architecture. Arid Lands Newslett. 2000;47:1–12.
7. Rizwan AM, Dennis LY, Chunho LIU. A review on the generation, determination and mitigation of Urban Heat Island. J Environ Sci. 2008;20(1):120–8.
8. Fahmy M, Sharples S. On the development of an urban passive thermal comfort system in Cairo, Egypt. Build Environ. 2009;44(9):1907–16.
9. Taheri Shahraiyni H, Sodoudi S, El-Zafarany A, Abou El Seoud T, Ashraf H, Krone K. A comprehensive statistical study on daytime surface urban heat island during summer in urban areas, case study: Cairo and its new towns. Remote Sens. 2016;8(8):643.

10. Hamdy O. Using remote sensing techniques to assess the changes in the rate of urban green spaces in Egypt: a case study of greater Cairo. Int Design J. 2022;12(3):53–64.
11. Ashoub SH, ElKhateeb MW. Enclaving the city: new models of containing the urban populations—a case study of Cairo. Urban Plan. 2021;6(2):202–17.
12. Abdin AE, Gaafar I. Rational water use in Egypt. Technological perspectives for rational use of water resources in the Mediterranean region. 2009.
13. Allam MN, Allam GI. Water resources in Egypt: future challeges and opportunities. Water Int. 2007;32(2):205–18.
14. El-Nashar WY, Elyamany AH. Managing risks of the Grand Ethiopian renaissance dam on Egypt. Ain Shams Eng J. 2018;9(4):2383–8.
15. El-Sadek A. Water desalination: an imperative measure for water security in Egypt. Desalination. 2010;250(3):876–84.
16. Abdelhaleem FS, Helal EY. Impacts of Grand Ethiopian Renaissance Dam on different water usages in upper Egypt. Br J Appl Sci Technol. 2015;8(5):461–83.
17. Doick K, Hutchings T. Air temperature regulation by urban trees and green infrastructure (No. 012). Forestry Commission. 2013.
18. Stewart ID. Redefining the urban heat island (Doctoral dissertation, University of British Columbia). 2011.
19. Fahmy M. Interactive urban form design of local climate scale in hot semi-arid zone. School of Architecture. 2010.
20. Sundseth K, Raeymaekers G. Biodiversity and Natura 20000 in urban areas–Nature in cities across Europe: a review of key issues and experiences. Brussels: IBGE/BIM; 2006.
21. Chiesura A. The role of urban parks for the sustainable city. Land-sc Urban Plan. 2004;68:129–38.
22. Heritage SN. Health impact assessment of greenspace a guide. 2008.
23. Rowntree RA, Nowak DJ. Quantifying the role of urban forests in removing atmospheric carbon dioxide. Arboricult Urban For. 1991;17(10):269–75.
24. Déoux S, Déoux P. Le guide de l'habitat sain: habitat qualité santé pour bâtir une santé durable. Medieco éditions. 2004
25. Bruse M, Skinner CJ. Rooftop greening and local climate: a case study in Melbourne. In: International Conference on Urban Climatology & International Congress of Biometeorology, Sydney. 1999.
26. Huynh C, Eckert R. Reducing heat and improving thermal comfort through urban design—a case study in Ho Chi Minh city. Int J Environ Sci Dev. 2012;3(5):480.
27. Rajabi T. The study of vegetation effects on reduction of urban heat Island in Dubai. Doctoral dissertation, The British University in Dubai. 2011.
28. Sodoudi S, Shahmohamadi P, Vollack K, Cubasch U, Che-Ani AI. Mitigating the urban heat island effect in megacity Tehran. Adv Meteorol. 2014;2014:1–19.
29. Lobaccaro G, Acero JA. Comparative analysis of green actions to improve outdoor thermal comfort inside typical urban street canyons. Urban Clim. 2015;14:251–67.
30. Upreti R, Wang ZH, Yang J. Radiative shading effect of urban trees on cooling the regional built environment. Urban For Urban Green. 2017;26:18–24.
31. Middel A, Chhetri N, Quay R. Urban forestry and cool roofs: assessment of heat mitigation strategies in Phoenix residential neighborhoods. Urban For Urban Green. 2015;14(1):178–86.
32. Rahman MA, Moser A, Gold A, Rötzer T, Pauleit S. Vertical air temperature gradients under the shade of two contrasting urban tree species during different types of summer days. Sci Total Environ. 2018;633:100–11.
33. Shahidan MF, Shariff MK, Jones P, Salleh E, Abdullah AM. A comparison of *Mesua ferrea* L. and *Hura crepitans* L. for shade creation and radiation modification in improving thermal comfort. Landsc Urban Plan. 2010;97(3):168–81.
34. Zhang J, Khoshbakht M, Liu J, Gou Z, Xiong J, Jiang M. A clustering review of vegetation-indicating parameters in urban thermal environment studies towards various factors. J Therm Biol. 2022;110:103340.
35. Zhang J, Gou Z, Zhang F, Yu R. The tree cooling pond effect and its influential factors: a pilot study in Gold Coast, Australia. Nat-Based Solut. 2023;3:100058.
36. Monteiro MV, Handley P, Morison JI, Doick KJ. The role of urban trees and greenspaces in reducing urban air temperatures. Res Note-For Comm. 2019;37:12.
37. Kong F, Yan W, Zheng G, Yin H, Cavan G, Zhan W, Cheng L. Retrieval of three-dimensional tree canopy and shade using terrestrial laser scanning (TLS) data to analyze the cooling effect of vegetation. Agric For Meteorol. 2016;217:22–34.
38. Kong L, Lau KKL, Yuan C, Chen Y, Xu Y, Ren C, Ng E. Regulation of outdoor thermal comfort by trees in Hong Kong. Sustain Cities Soc. 2017;31:12–25.
39. Lin BS, Lin YJ. Cooling effect of shade trees with different characteristics in a subtropical urban park. HortScience. 2010;45(1):83–6.
40. Zhang J, Gou Z, Cheng B, Khoshbakht M. A study of physical factors influencing park cooling intensities and their effects in different time of the day. J Therm Biol. 2022;109:103336.
41. Liu Y, Lai Y, Jiang L, Cheng B, Tan X, Zeng F, Shang X. A study of the thermal comfort in urban mountain parks and its physical influencing factors. J Therm Biol. 2023;118:103726.
42. Zalesny RS Jr, Stanturf JA, Evett SR, Kandil NF, Soriano C. Opportunities for woody crop production using treated wastewater in Egypt. I. Afforestation strategies. Int J Phytoremed. 2011;13(sup1):102–21.
43. Wang Y, Bakker F, de Groot R, Wortche H, Leemans R. Effects of urban trees on local outdoor microclimate: synthesizing field measurements by numerical modelling. Urban Ecosyst. 2015;18:1305–31.
44. Elmasry L. A plant guidebook for Al-Azhar Park and the City of Cairo, vol. II. Cairo: Shouruk International Bookshop; 2014.
45. AUB. AUB Landscape database. AUB, https://landscapeplants.aub.edu.lb/. Accessed 2024.
46. Fereres E, Soriano MA. Deficit irrigation for reducing agricultural water use. J Exp Bot. 2007;58(2):147–59.
47. Ward FA, Pulido-Velazquez M. Water conservation in irrigation can increase water use. Proc Natl Acad Sci. 2008;105(47):18215–20.
48. Nada A, Nasr M, Hazman M. Irrigation expert system for trees. Int J Eng Innov Technol. 2014;3(8):170–5.
49. McCready MS, Dukes MD. Landscape irrigation scheduling efficiency and adequacy by various control technologies. Agric Water Manag. 2011;98(4):697–704.
50. Dukes MD. Water conservation potential of landscape irrigation smart controllers. Trans ASABE. 2012;55(2):563–9.

51. Souch CA, Souch C. The effect of trees on summertime below canopy urban climates: a case study Bloomington, Indiana. J Arboric. 1993;19(5):303–12.
52. Coutts AM, White EC, Tapper NJ, Beringer J, Livesley SJ. Temperature and human thermal comfort effects of street trees across three contrasting street canyon environments. Theoret Appl Climatol. 2016;124:55–68.
53. Rahman MA, Moser A, Rötzer T, Pauleit S. Within canopy temperature differences and cooling ability of *Tilia cordata* trees grown in urban conditions. Build Environ. 2017;114:118–28.
54. De Abreu-Harbich LV, Labaki LC, Matzarakis A. Effect of tree planting design and tree species on human thermal comfort in the tropics. Landsc Urban Plan. 2015;138:99–109.
55. Armson D, Rahman MA, Ennos AR. A comparison of the shading effectiveness of five different street tree species in Manchester, UK. Arboricult Urban For. 2013;39(4):157–64.
56. Konarska J, Uddling J, Holmer B, Lutz M, Lindberg F, Pleijel H, Thorsson S. Transpiration of urban trees and its cooling effect in a high latitude city. Int J Biometeorol. 2016;60:159–72.
57. Rahman MA, Armson D, Ennos AR. A comparison of the growth and cooling effectiveness of five commonly planted urban tree species. Urban Ecosyst. 2015;18:371–89.
58. Georgi JN, Dimitriou D. The contribution of urban green spaces to the improvement of environment in cities: case study of Chania, Greece. Build Environ. 2010;45(6):1401–14.
59. Flora and Funa Web. https://www.nparks.gov.sg/florafaunaweb. Accessed 2022.
60. Sánchez-Azofeifa GA, Castro-Esau K. Canopy observations on the hyperspectral properties of a community of tropical dry forest lianas and their host trees. Int J Remote Sens. 2006;27(10):2101–9.
61. Haley MB, Dukes MD. Validation of landscape irrigation reduction with soil moisture sensor irrigation controllers. J Irrig Drain Eng. 2012;138(2):135–44.
62. Abdel Wahaab R, Omar M. Wastewater reuse in Egypt: opportunities and challenges. Arab World. Arab Water Council Report. 2011.
63. Pittenger D. Methodology for estimating landscape irrigation demand. 2014.
64. Shashua-Bar L, Tsiros IX, Hoffman ME. A modeling study for evaluating passive cooling scenarios in urban streets with trees: case study: Athens, Greece. Build Environ. 2010;45(12):2798–807.
65. Ng E, Chen L, Wang Y, Yuan C. A study on the cooling effects of greening in a high-density city: an experience from Hong Kong. Build Environ. 2012;47:256–71.
66. Ahmed Y. Numerical optimization of tree coverage and distribution to improve pedestrian thermal comfort and mitigate the UHI phenomenon: a microclimatic study in Cairo, Egypt. Un-published, Cairo: master thesis. Cairo University, 2017.
67. Aboelata A, Sodoudi S. Evaluating urban vegetation scenarios to mitigate urban heat island and reduce buildings' energy in dense built-up areas in Cairo. Build Environ. 2019;166:106407.
68. Envi-met. https://www.ENVI-met.com/. Accessed 2024.
69. Morakinyo TE, Kong L, Lau KKL, Yuan C, Ng E. A study on the impact of shadow-cast and tree species on in-canyon and neighborhood's thermal comfort. Build Environ. 2017;115:1–17.
70. Weather Atlas. https://www.weather-atlas.com/en/egypt/cairo-weather-july. Accessed 2024.
71. Weather and climate. https://weather-and-climate.com/Cairo-July-averages. Accessed 2024.
72. Time and date. https://www.timeanddate.com/weather/egypt/cairo/historic?month=7&year=2020. Accessed 2024.
73. Elnabawi MH, Hamza N, Dudek S. Outdoor thermal comfort in the old Fatimid city, Cairo, Egypt. In: 13th Conference of International Building Performance Simulation Association. Chambéry, France, August. 2013. pp. 26–8.
74. Abdelmejeed AY, Gruehn D. Optimization of microclimate conditions considering urban morphology and trees using ENVI-met: a case study of Cairo City. Land. 2023;12(12):2145.
75. Elbardisy WM, Salheen MA, Fahmy M. Solar irradiance reduction using optimized green infrastructure in arid hot regions: a case study in el-nozha district, Cairo, Egypt. Sustainability. 2021;13(17):9617.
76. Ribeiro KFA, Justi ACA, Novais JWZ, de Moura Santos FM, Nogueira MCDJA, Miranda SA, Marques JB. Calibration of the physiological equivalent temperature (PET) index range for outside spaces in a tropical climate city. Urban Clim. 2022;44:101196.
77. Ballinas M, Morales-Santiago SI, Barradas VL, Lira A, Oliva-Salinas G. Is PET an adequate index to determine human thermal comfort in Mexico City? Sustainability. 2022;14(19):12539.
78. Smithers RJ, Doick KJ, Burton A, Sibille R, Steinbach D, Harris R, Blicharska M. Comparing the relative abilities of tree species to cool the urban environment. Urban Ecosyst. 2018;21:851–62.
79. Guo W, Liu X, Yuan X. A case study on optimization of building design based on CFD simulation technology of wind environment. Proc Eng. 2015;121:225–31.

This Page Intentionally Left Blank.

Article 2: Key facts and author contributions

Refrence	Abdelmejeed AY, Gruehn D. Optimization of Microclimate Conditions Considering Urban Morphology and Trees Using ENVI-Met: A Case Study of Cairo City. *Land*. 2023; 12(12):2145. https://doi.org/10.3390/land12122145
Contributions	AY. A, 85%, and DG, 15% Words count: 11967
Review Model	Single blind peer review
History	Submitted: 3 November 2023 Accepted: 6 December 2023 Published: 9 December 2023

Signature:

Ahmed Yasser Abdelmejeed

Date: 15. July 2025

land

MDPI

Article

Optimization of Microclimate Conditions Considering Urban Morphology and Trees Using ENVI-Met: A Case Study of Cairo City

Ahmed Yasser Abdelmejeed [1,2,*] and Dietwald Gruehn [1]

[1] Research Group—Landscape Ecology and Landscape Planning (LLP), Department of Spatial Planning, TU Dortmund University, 44227 Dortmund, Germany; dietwald.gruehn@tu-dortmund.de
[2] Faculty of Urban and Regional Planning, Cairo University, Cairo 11562, Egypt
* Correspondence: ahmed.abdelmejeed@tu-dortmund.de

Abstract: This research aims to optimize the use of trees to enhance microclimate conditions, which has become necessary because of climate change and its impacts, especially for cities suffering from extreme heat stress, such as Cairo. It considers elements of urban morphology, such as the aspect ratio and orientation of canyons, which play an important role in changing microclimate conditions. It also considers both sides of each canyon because the urban shading is based on the orientation and the aspect ratio, which can provide good shade on one side of the canyon but leave the other side exposed to direct and indirect radiation, to ensure a complete assessment of how the use of trees can be optimized. As Cairo city is very large and has a variety of urban morphologies, a total of 144 theoretical cases have been tested for Cairo city using ENVI-met to cover the majority of the urban cases within the city (Stage 1). Then, the same tree scenarios used in the theoretical study are applied to an existing urban area in downtown Cairo with many urban morphology varieties to validate the results of the theoretical study (Stage 2). After testing all cases in both stages, it became very clear that the addition of trees cannot be the same for the different aspect ratios, orientations, and sides of the different canyons. For example, eastern roads should have more trees than other orientations for all aspect ratios, but the required number of trees is greater for the northern side than the southern side, as the southern side is partially shaded for a few hours of the day by buildings in moderate and deep canyons. Northern streets require a very limited number of trees, even in shallow canyons, on both sides. The correlation between the number of trees on each side for the different orientations and aspect ratios shows a strong negative relationship, but the correlation values change between the different sides and orientations. The results of applying trees to an existing urban area show almost the same results as the theoretical study's results, with very slight differences occurring because of the irregularity of the existing study area. This proves that when adding trees, not only the aspect ratio and orientation but also the side of each canyon should be considered to ensure that pedestrians, in all cases, have better microclimate conditions and that the use of trees is optimized.

Keywords: urban heat island (UHI); outdoor thermal comfort; urban trees; urban shading; street canyon aspect ratio and orientation; greenery effect; ENVI-met greenery simulation; urban cooling strategies

Citation: Abdelmejeed, A.Y.; Gruehn, D. Optimization of Microclimate Conditions Considering Urban Morphology and Trees Using ENVI-Met: A Case Study of Cairo City. *Land* **2023**, *12*, 2145. https://doi.org/10.3390/land12122145

Academic Editors: Apostolos Lagarias, Poulicos Prastacos, Despina Dimelli and Alexandra Delgado-Jiménez

Received: 3 November 2023
Revised: 2 December 2023
Accepted: 6 December 2023
Published: 9 December 2023

1. Introduction

1.1. Heat Stress and UHI Appearance and Causes

Cities grow over many decades with different urban fabrics and morphologies, and they continue to evolve in various shapes to meet their populations' growing needs. Because of rapid expansion and increases in population density, cities absorb more heat and suffer from heat stress and the effects of urban heat islands (UHIs), which disturb human health [1]. Cities' centers have been observed to be hotter than their suburbs. This is due to urban

areas absorbing and trapping longwave radiation, which supports UHIs [2]. In one study, the air and surface temperatures in city centers were higher than those in suburban areas by 5.0 to 5.5 C° [3]. In another study conducted in downtown Cairo, an increase of 0.5 to 3.5 C° in the surface temperature was observed and reached 10 C° as the maximum difference in comparison to the suburbs [4,5]. The urban climate is an important issue pertaining to local and global climates, and it is influenced by several urban design factors, such as urban morphology and density, properties of urban surfaces, and different types of vegetation cover [6]. The process of trapping longwave radiation mainly controls UHIs. When buildings are taller and streets are narrower, urban canyons absorb less longwave radiation; however, they trap the absorbed heat [2]. Distance from the city center, surface albedo, aspect ratio, and vegetation density are major predictors of the UHI response. In one study, it was found that every 500 m increase in the distance from the city center reduced the interurban heat island by 0.13 C°. Increasing the surface albedo by 0.01 decreased the UHI by 0.18 C°, whereas increasing the vegetation density ratio by 0.10 yielded a 0.17 C° reduction in the UHI. A 10% increase in the aspect ratio increased the UHI by 0.17 C° [7].

1.2. Urban Morphology Relating to Urban Shading and PET Parameters

Urban morphology, sky view factor (SVF), and shading are the major factors that have a significant role in enhancing microclimate conditions and reducing UHI effects [2,8]. The shadow-cast effect produced by buildings helps reduce pedestrian radiant load and, consequently, improves thermal comfort, especially in high-density cities, although ventilation is reduced [9,10]. Shallow canyons are susceptible to worse thermal conditions than their deeper counterparts with similar aspect ratio values [9]. Asymmetrical streets are better than low, symmetrical streets at enhancing wind flow and blocking solar radiation [11]. Increasing the SVF in the selection of an urban configuration reduces UHI intensity [12]. Deep urban canyons can reduce the amount of direct solar radiation during the daytime. Therefore, the level of thermal comfort in an open space (i.e., high SVF) is lower than that in a shaded space (i.e., low SVF) [13]. The results of the analysis prove that thermal comfort is mainly affected by exposure to solar radiation [14]. In conclusion, shading from direct radiation is more important than the increase in absorbed radiation due to urban reflectance.

The physiological equivalent temperature (PET) meteorological parameters (air temperature, wind speed, radiant temperature, and humidity) [15] can be controlled and enhanced using urban morphology. The mean radiant temperature (TMRT) is a key meteorological parameter governing human energy balance and is used to evaluate the thermal comfort of humans [16]. The target is to keep the TMRT below 45 C° [8]. Air temperature and specific humidity have emerged as the least effective, suggesting that urban configurations can alter their values only to a limited extent [10,17]. The outdoor thermal comfort level significantly depends on the speed and direction of the urban wind flow [18]. Wind speed has been widely reported to have an influence on urban heating, and there is a strong negative correlation between wind speed and air temperature [19]. All of these PET meteorological parameters, along with urban shading and SVF, can be optimized using urban morphology and urban geometry elements, such as by adjusting the street canyon aspect ratio and orientation, in addition to using different densities of vegetation [10,16,20,21].

1.2.1. Aspect Ratio Effect

The aspect ratio (AR), or a canyon's height-to-width ratio (H/W), is an important parameter that is usually used to investigate the influence of urban geometry on an outdoor environment, especially temperature and building energy demand [17,22]. The aspect ratio is the dominant factor for daily net solar radiation gains on road and wall surfaces. The effects of shadows on surrounding buildings are also important factors for the radiation environment in urban street canyons [23], as the enhancement of shade due to increased H/W ratios is capable of producing significant reductions in the PET [16,24]. There is a strong relationship between UHIs and the aspect ratio during the night, as the effect of the

street canyon on UHI intensity is significant. According to one study conducted in the city of Basel, Switzerland, the intensity of the maximum nighttime UHI has a linear relationship with the SVF, which is controlled by the aspect ratio [25]. In addition, the lowest daytime mean radiant temperatures result from the high aspect ratios of streets. Air temperatures decrease slightly with an increase in aspect ratios, but the radiation fluxes expressed by the mean radiant temperature are, by far, more decisive [26].

In Osaka, the daily net solar radiation gains are large for roads in which the aspect ratio is greater than approximately 1.5 (H/W). Roads in which the aspect ratio is between 1.0 and 1.5 (H/W) are also in the target range for effective urban heat island mitigation measures, and particular attention is needed for the north sides of east–west roads and the centers of north–south roads [23]. In Malaysia, for the six asymmetrical aspect ratios of Putrajaya Boulevard, an aspect ratio of 2–0.8, which reduces the temperature of surfaces by 10 to 14 C° and the air by 4.7 C°, is recommended for enhancing the boulevard's microclimates and mitigating tropical heat islands. In the northeast to southwest direction, aspect ratios of 0.8–2 reduce the morning microclimate and night heat islands, yet the negative effects during the day are greater than the positive effects during the nighttime [11]. Along Wall Street, New York City, the outcomes of winter and summer analyses show high values of daytime air temperatures along the widest street canyon (aspect ratio = 0.33) [27]. In the center of Camagüey, Cuba, aspect ratios higher than one are advisable, as they contribute to improving the thermal conditions of courtyards in the summer. When the aspect ratio of a courtyard is H/W = 0.5, no variations in the TMRT are obtained when using different orientations because most of the courtyards have surfaces that are exposed to direct solar radiation during the critical period of the day (11:00 h and 14:00 h), and particular subzones of the courtyard that are adjacent to the surrounding facades are more comfortable than the central subzone, increasing the aspect ratio from 0.5 to 3 and reducing the TMRT by 15.7 C° [8]. An increase of 0.5 in the aspect ratio's values can decrease the maximum mean radiant temperature by 2.90 C° on average in the early morning and late afternoon and, consequently, decrease the PET [17]. Regarding the impact of the AR on UHIs, streets featuring a lower aspect ratio have a high frequency of heat stress in the daytime but low PET in the nighttime [10]. Comparing both east–west- and north–south-oriented streets against surface temperature measurements in Tokyo, it was found that the shading effect of a tall building in north–south street canyons had less of an impact on solar gains than that in east–west streets. Tall buildings and narrow canyons reduce the SVF and increase the amount of shaded area on the surface, resulting in lower temperatures in canyons during the daytime but higher temperatures at night [24].

1.2.2. Street Orientation Effect

Street orientation is considered to play an influential role in altering the microclimate in urban areas, and it influences the exposure of canyon surfaces to direct solar radiation. A north–south (N–S) street orientation will be fully exposed to solar radiation at midday but mostly shaded in the early morning and late afternoon. This is contrary to an east–west (E–W) street orientation, which is fully exposed in the early morning and late afternoon [17,22,28,29]. North–south-oriented streets are cooler than those with an east–west orientation, and the comfort level in these areas increases along with their H/W ratio [20], because east–west-oriented canyons are exposed to sunlight throughout the day regardless of their H/W ratio, whereas north–south-oriented canyons are only exposed to sunlight during certain times of the day [20]. One study conducted on urban heat island mitigation measures found that the top priorities are the north side of east–west roads and the center of north–south roads [23]. The NW–SE orientation shows a slightly lower PET level than N–S and E–W orientations [30]. It has been found that an orientation angle between 30° and 60° with wind direction and a canyon aspect ratio of 2.5 can reduce the PET value by 5 to 9 C° throughout most of the study area during midafternoon on a summer day [18].

In a study conducted in Sydney [17], it was concluded that streets situated on the north–south axis offer a superior level of thermal comfort than east–west-oriented streets. The PET values presented a comfortable range of 12.33% during the daytime; streets on the NE–SW axis provided the highest level of thermal comfort, on average at 24.95%, and the worst option was evaluated as the NW–SE orientation. As the duration of solar exposure and the average mean radiant temperature (TMRT) increase, mainly because the wind velocity decreases, outdoor users face a lack of thermal satisfaction.

1.2.3. Combined Effect of Aspect Ratio and Street Orientation

The orientation and canyon aspect ratio have a profound influence on the urban microclimate that directly impacts street-level thermal comfort, as PETs at the street level strongly depend on the aspect ratio and street orientation [14,18,28–30]. Street geometry and orientation influence the amount of solar radiation received by street surfaces, as well as the airflow in urban canyons [6]. For E–W orientations, streets with an H/W greater than two should be fully shadowed only during the hottest and coolest months of the year [20]. Streets on the E–W axis present the worst conditions for all H/W ratios (up to 3.0). An increase in the H/W ratio on an E–W street does not improve PET levels [14]. It is difficult to mitigate the heat stress along an E–W-oriented street. The walls provide only a limited amount of shading, even for proportions with an H/W ratio of 4:1. In comparison, an N–S orientation combined with a high aspect ratio, equal to or greater than an H/W ratio of 2:1, provides a much better thermal environment with lower PET maxima and shorter periods of high stress [14,20]. Thermal stress can be reduced in a street canyon with a northwest–southeast orientation combined with an aspect ratio of at least 1.5, and these street configurations can reduce heat stress, increase the frequency of comfortable thermal conditions, and enable solar access throughout the year in the midlatitudes [10]. An orientation angle of 30–60° in the wind direction and a canyon aspect ratio of 2.5 can reduce PETs by 5–9 C° during the midafternoon on a summer day [20].

1.2.4. Urban Trees

The effectiveness of trees in enhancing daytime thermal comfort decreases as urban density increases and vice versa at night [9,22]. Urban trees can reduce the effects of the surrounding building mass and help create a low-SVF environment that is cooler during both daytime and nighttime [13]. It has been demonstrated that urban morphology and urban vegetation shading affect solar radiation storage during the day in the summer, and urban shading significantly contributes to UHI mitigation [13]. Significant temperature differences between vegetated and non-vegetated areas have been observed, which can be explained by both the shading and evapotranspiration effects of trees [31]. As a rule, on summer days, outdoor activities in unshaded areas are not recommended between 10:00 h and 15:00 h. Therefore, the provision of shade, using canopies and vegetation, is necessary if outdoor activities are to occur during this time of day [8]. In open-set high-rise urban areas, the presence of trees could produce a relevant reduction in thermal stress at the pedestrian level [30]. Trees can be considered as a solution to improve the thermal condition of streets, especially in streets designed along nonoptimal orientations with low-rise buildings [17]. In a previous study, an area that was at an angle of 30° from the north with an aspect ratio of 1.0 was found to not require any plantings, as a continuous shaded zone was created by the buildings along both streets in the parallax and perpendicular directions. However, decreasing the aspect ratio creates a need for shade-providing trees for the streets in the perpendicular direction, as the distance between the buildings increases [18]. A study [14] demonstrated that trees have a much more considerable effect on E–W streets. The reduction in PET values is very significant, especially for the side of the street facing south. Increasing 10% of the urban vegetation can reduce Ta and MRT throughout the entire day and nighttime by up to 0.8 C° [16]. PET has been found to be approximately 10 C° lower under trees than in green areas (38 C°) and at least 25 C° lower than in enclosed areas (48 C°) [10]. Increasing the density of vegetation in shallow urban canyons (H/W = 0.5)

increased PET enhancement by more than 4% compared with low-density vegetation in the same urban canyon [17].

1.3. Cairo City: The Case Study

1.3.1. Cairo City's Climate

Cairo is in a subtropical climatic region with a dry climate. During summer (June to August), it is hot and dry with a maximum mean temperature of 28 C° [5]. Cairo city receives an enormous amount of solar radiation, which causes the city to experience massive heat stress.

1.3.2. City Urban Morphology

The Greater Cairo Metropolitan Area boasts the largest urban area in Africa and ranks as the 11th largest city in the world [4]. A study found that Cairo's land cover was 233.78 km^2 in 1973, growing to 557.87 km^2 in 2006, which means that it has more than doubled in size, and the rate of urbanization is 9.8 km^2 per year [32]. Figure 1 shows its rapid urban growth over 22 years on both agricultural and desert land [33]. A total area of 187.32 km^2 of agricultural lands has been lost because of this urban expansion [32]. The New Urban Community Authority considers 25% of Cairo to be informal, but some research considers 50% or 66.6% of Cairo to be informal [34]. This formal and informal rapid growth has increased the city's density and size, in addition to creating different urban morphologies and fabrics (i.e., different aspect ratios, from very shallow to shallow, moderate, deep, and very deep) as shown in Figure 2, which react in different ways to the meteorological parameters, creating different microclimate conditions inside the different urban canyons.

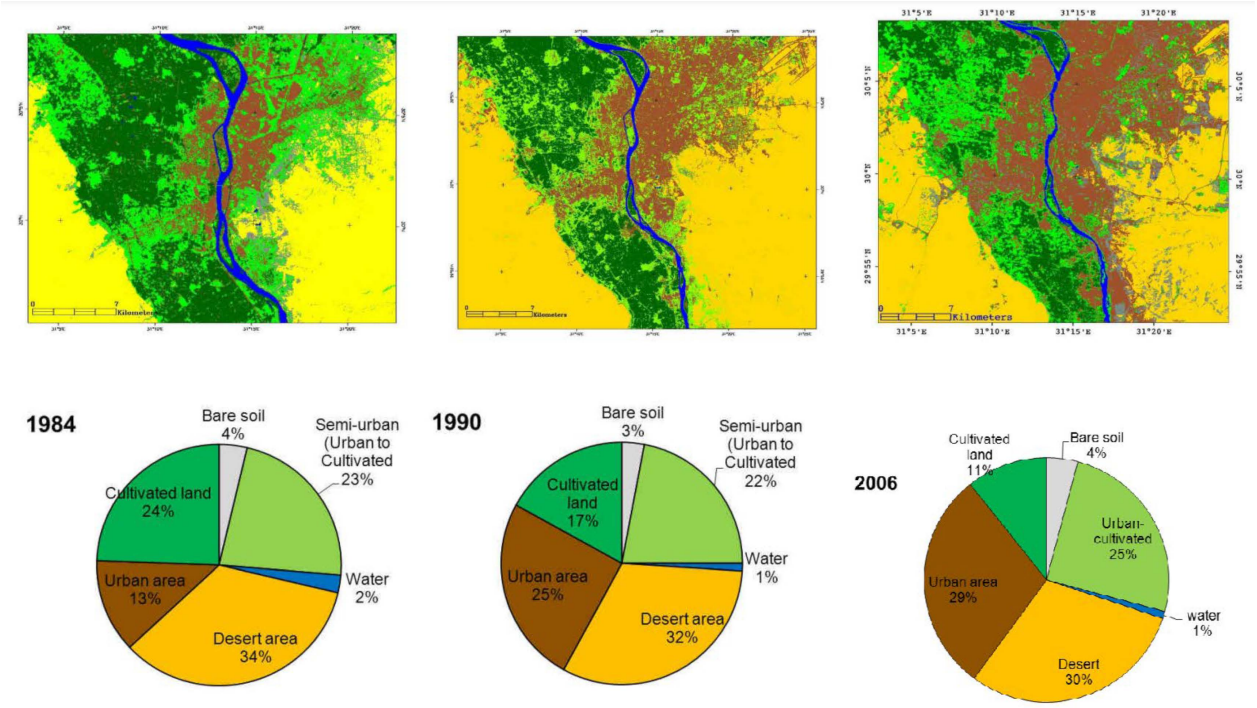

Figure 1. Greater Cairo's urban growth between 1984 and 2006 [33].

Figure 2. Examples of different urban canyon aspect ratios in Cairo city.

1.4. Research Gap and Target

This research aimed to optimize the integration of many different urban morphologies (with varying aspect ratios and orientations) and urban trees (low and high densities) to understand the correlation between them and maximize the enhancement of the microclimate conditions for the case study (i.e., Cairo city). The objectives of this research were not only to fill the gaps in the understanding of different urban canyons and how they respond to harsh microclimate conditions but also how to integrate various urban canyons with different densities of urban trees, as well as how these trees would perform inside different urban canyons. In addition, as previous studies mostly focused on the enhancement of the whole canyon, in this study, the main focus is on the sides of different canyons, as they are quite important because canyon sides are the places where people walk, sit, and stand, while the rest of the canyon is mainly for vehicles. The findings of this research should help urban designers and landscape architects choose an aspect ratio, street orientation, and tree density from an urban climate point of view while developing urban projects in Greater Cairo.

2. Materials and Methods

To achieve the research target, a study analyzing and testing the urban morphology's characteristics with and without different tree densities was conducted. The method of testing and analyzing the relationship was performed in two stages, as shown in Figure 3. Stage one was the creation of a theoretical model representing the different common urban canyons in Cairo city along different orientations. This model was tested first without trees and then with different tree densities. Stage two involved testing the theoretical model's outcomes when applied to an existing case study in downtown Cairo with similar aspect ratios and orientations. For a better understanding of the relationship and to go further in depth regarding the details of the urban canyons, this study conducted both stages on both sides of the urban canyon; this will help to understand how both sides of an urban canyon (i.e., where people are walking) react to climate conditions and how changing the aspect ratio and orientation, as well as adding different tree densities, will impact the thermal comfort and the UHI effects at the pedestrian level on each side. Studying both sides of a street provides more accurate and detailed results because in some canyons, one side is shaded by buildings but the other is totally exposed to direct sun radiation [35], which affects the control and optimization of the number of added trees; this is in line with water efficiency approaches, which is quite important in Egypt's case, as it suffers from water scarcity [36].

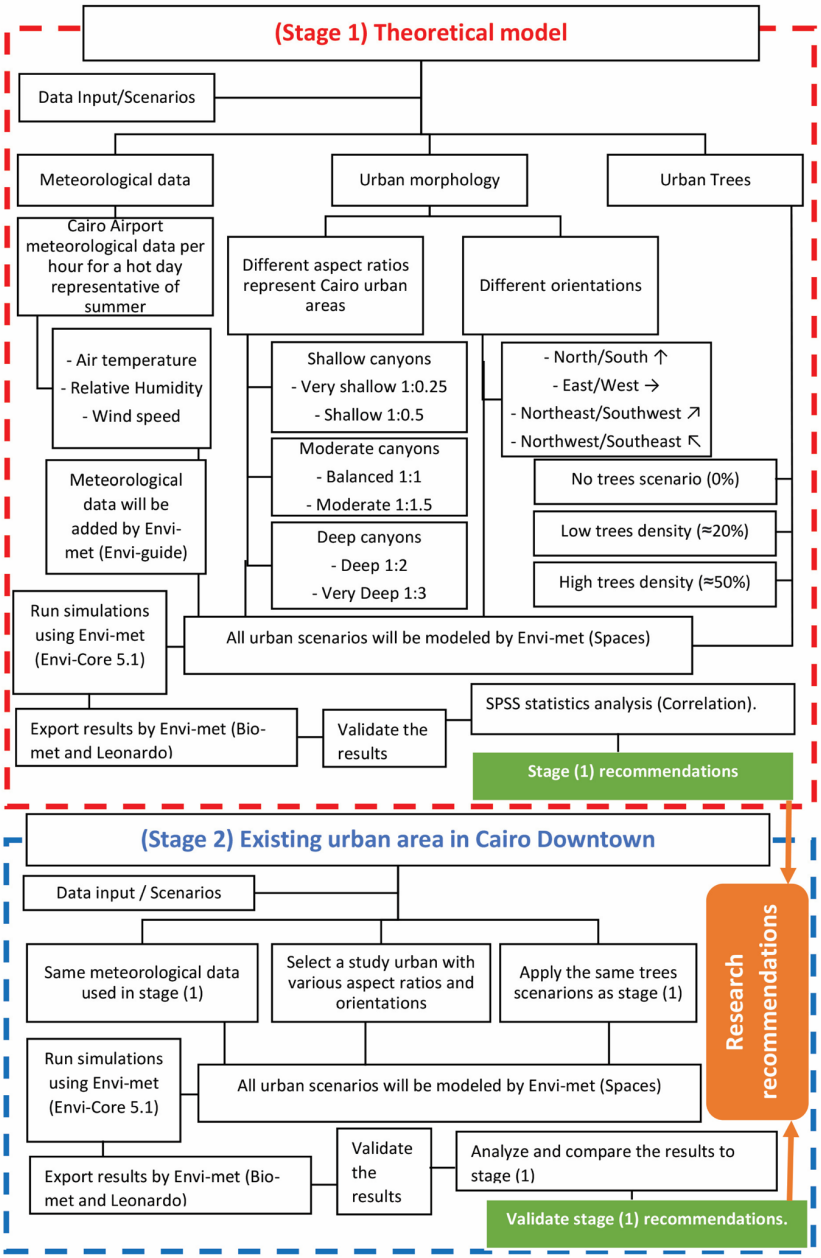

Figure 3. Research methodology.

2.1. Stage (1): Theoretical Model

In Stage One, a theoretical model was developed representing the different aspect ratios and orientations that are very common in Cairo city (Step a). Then, tree scenarios were applied to the base case (Step b) to understand the effects of the trees after comparing the results of both steps.

2.1.1. Stage (1): Step (a) Theoretical Model (Base Case)

The range of aspect ratios that were evaluated varied between very shallow and very deep, and six aspect ratios were developed and evaluated (3:1, 2:1, 1:1.5, 1:1, 0.5:1, and 0.25:1), which covers the majority of the various urban canyons in Cairo city. The six aspect ratios developed were oriented to four different orientations every 45 degrees, and the different orientations represented the main orientations (i.e., north–south, east–west,

northeast–southwest, and northwest–southeast); that is, the total number of cases in the theoretical model base case was 24. Figure 4 shows the base case of the theoretical model, and Figure 5 shows the shading analysis for the different aspect ratios and orientations. As the aim was to understand how each urban canyon reacts and performs, each side of an urban canyon was analyzed and compared to fully comprehend each urban canyon using receptors (i.e., measuring points), as shown in Figure 4A; hence, the total number of cases in the base case was 48.

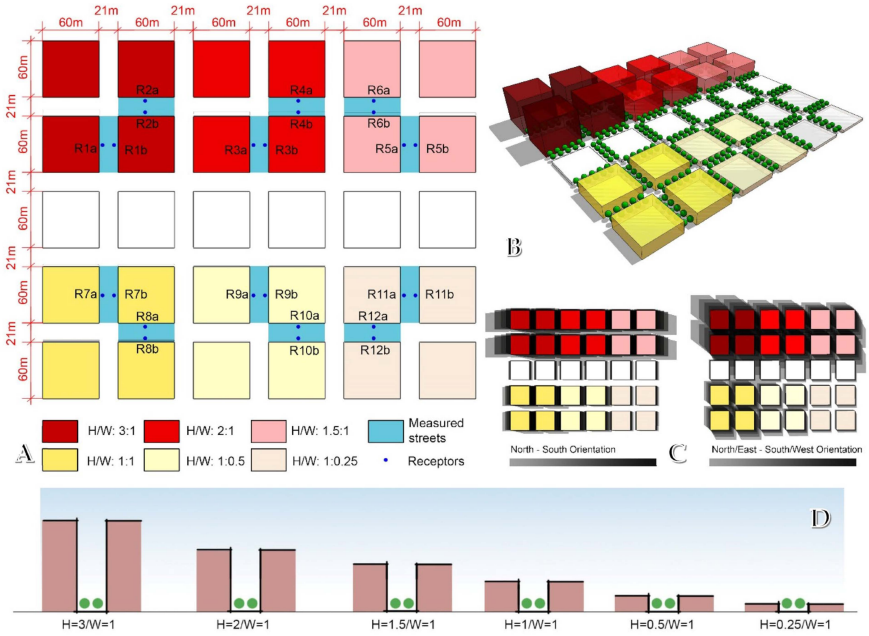

Figure 4. The theoretical model's urban geometry: (**A**) theoretical model's plan showing the measured canyons and receptors' locations; (**B**) 3D view of the theoretical model with trees; (**C**) full day shading analysis for both orientations; (**D**) AR cross-sections.

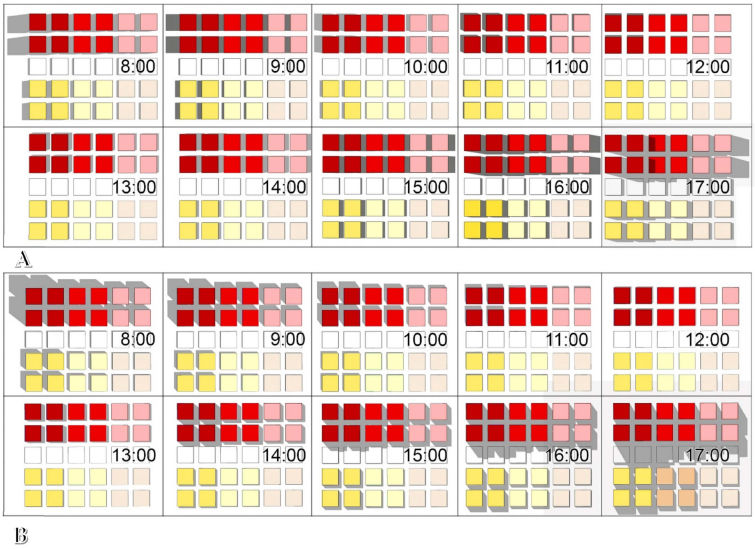

Figure 5. Shading distribution for each AR per hour from morning to sunset: (**A**) north orientation; (**B**) northeast orientation. Created using SketchUp after aligning the model to the original location of Cairo city.

2.1.2. Stage (1): Step (b) Tree Scenarios

The tree scenarios were developed and added to the base case to compare the tree results to the base case results without trees to understand the effect of the trees on every street on each side. Two tree scenarios were developed that represented two tree densities (low tree density ≈ 20%; high tree density ≈ 50%), as shown in Figure 6. The total number of cases after adding the tree scenarios, in addition to the base case scenarios, was 144 (base cases = 48; tree scenario cases = 96), as shown in Table 1, which is sufficient for comparing various urban cases with different aspect ratios and orientations, as well as for the integration of different tree scenarios. The tree scenarios were applied to all urban canyons with different aspect ratios and orientations, and both street canyon sides were measured for all the tree scenarios.

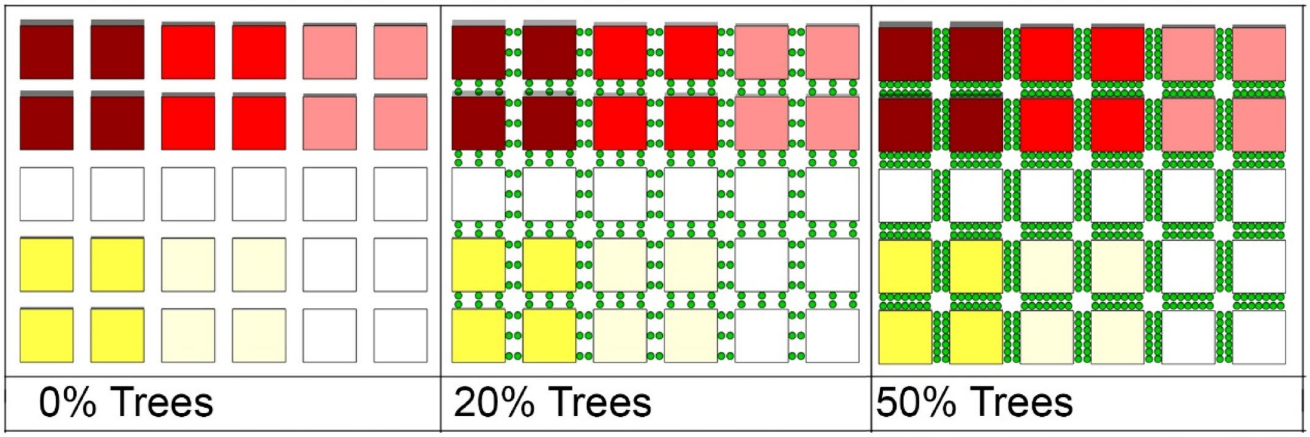

Figure 6. Tree density scenarios: 0%; low density (20%); high density (50%).

Table 1. All scenarios for the theoretical model.

Urban Canyon	Canyon Side (a or b)	Aspect Ratio	Orientation 1	Orientation 2	Tree Scenario 1	Tree Scenario 2	Tree Scenario 3	Total Number of Cases
R1	R1a	3 to 1	North–South	NE–SW	0%	20%	50%	6
	R1b	3 to 1	North–South	NE–SW	0%	20%	50%	6
R2	R2a	3 to 1	East–West	NW–SE	0%	20%	50%	6
	R2b	3 to 1	East–West	NW–SE	0%	20%	50%	6
R3	R3a	1 to 2	North–South	NE–SW	0%	20%	50%	6
	R3b	1 to 2	North–South	NE–SW	0%	20%	50%	6
R4	R4a	1 to 2	East–West	NW–SE	0%	20%	50%	6
	R4b	1 to 2	East–West	NW–SE	0%	20%	50%	6
R5	R5a	1.5 to 1	North–South	NE–SW	0%	20%	50%	6
	R5b	1.5 to 1	North–South	NE–SW	0%	20%	50%	6
R6	R6a	1.5 to 1	East–West	NW–SE	0%	20%	50%	6
	R6b	1.5 to 1	East–West	NW–SE	0%	20%	50%	6
R7	R7a	1 to 1	North–South	NE–SW	0%	20%	50%	6
	R7b	1 to 1	North–South	NE–SW	0%	20%	50%	6
R8	R8a	1 to 1	East–West	NW–SE	0%	20%	50%	6
	R8b	1 to 1	East–West	NW–SE	0%	20%	50%	6
R9	R9a	0.5 to 1	North–South	NE–SW	0%	20%	50%	6
	R9b	0.5 to 1	North–South	NE–SW	0%	20%	50%	6
R10	R10a	0.5 to 1	East–West	NW–SE	0%	20%	50%	6
	R10b	0.5 to 1	East–West	NW–SE	0%	20%	50%	6
R11	R11a	0.25 to 1	North–South	NE–SW	0%	20%	50%	6
	R11b	0.25 to 1	North–South	NE–SW	0%	20%	50%	6
R12	R12a	0.25 to 1	East–West	NW–SE	0%	20%	50%	6
	R12b	0.25 to 1	East–West	NW–SE	0%	20%	50%	6
Total number of cases								**144**

2.1.3. Result Measurement

The results for both sides of a canyon in each scenario were compared to better comprehend the performance and the relationship between different urban canyons and trees. This comparison provides extensive information to aid urban planners and landscape architects

in making decisions during the development of urban areas in Cairo city, particularly after implementing the findings in an existing urban area (Stage 2) in downtown Cairo.

2.2. Stage (2): Existing Case Study

The purpose of this section is to assess an existing urban area and compare its findings with those of the theoretical model. This will help validate the results of the theoretical model, which is highly symmetrical and uniform; however, in reality, urban areas, especially in old city zones, are not that uniform. Thus, comparing the results of both theoretical and existing case studies will provide insight into the tolerance and accuracy of the findings. This evidence can then be used to apply the research recommendations.

2.2.1. Study Area Location and Urban Characteristics

The selected study area should be located in the center of Cairo city so that it will be under the influence of the UHI and represent the urban density of the city downtown [4,5]. The selected study area, located in Khedival Cairo, in the city's downtown area, has varying street widths due to its hierarchical road systems, resulting in different aspect ratios and orientations. These urban varieties make the case study suitable for studying and representing the majority of urban cases in the theoretical study. Figure 7 illustrates the selected study area's location and urban characteristics.

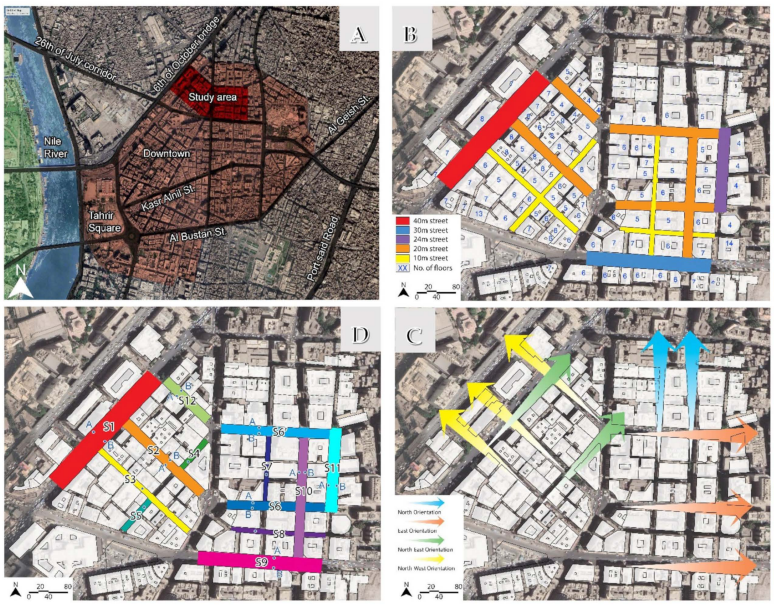

Figure 7. Existing urban case study: (**A**) location of the study area; (**B**) different street widths and building heights; (**C**) different street orientations; (**D**) streets selected for this study and location of the receptors for each street on both canyon sides.

As depicted in Figure 7B and Table 2, the study area contains numerous urban varieties that offer many different cases for comparison with the theoretical model. This study encompassed streets with different widths from 10 m for local pedestrian streets to 40 m for major roads within the study area (Rameses St., S1), with different building heights per street, leading to many aspect ratios ranging from 0.5:1 to 2:1, as shown in Table 2. In addition, the study area's streets have four urban orientations, as shown in Figure 7C and Table 2, providing urban canyons with various orientations (N–S, E–W, NE–SW, and NW–SE), covering all orientations in the theoretical model. This large variety within the study area aided in representing and validating the theoretical cases. Table 3 displays the number of theoretical study cases that were covered in the study area, with 12 cases from the theoretical model being covered, representing approximately 75% of the total

number of cases after excluding those with very deep and very shallow aspect ratios, which are uncommon in Cairo city. This demonstrates that the study area represented the urban varieties found in the theoretical model well. Furthermore, it was well suited to this research and significantly contributed to the achievement of this study's objectives. Figure 7D and Table 2 provide information on the streets selected for this study.

Table 2. Selected urban canyons in the study area and their aspect ratios and orientations.

Abbreviation in Figure 7D	Street Name	Avg. Width (m)	Avg. Height (m)	Aspect Ratio (H/W)	Orientation	No. of Cases
S1	Rameses St.	40	20	0.5 to 1	NE ↗	6
S2	Sayed Anbar St.	20	21	1.05 to 1	NW ↖	6
S3	Souq Al-Tawfikiya St.	12	17	1.42 to 1	NW ↖	3
S4	Al-Boursa Al-Kadyima St.	12	24	2 to 1	NE ↗	3
S5	Al-Boursa Al-Kadyima St.	12	18	1.5 to 1	NE ↗	3
S6	Mohamed Bek Al-Alfy St.	19	18	0.95 to 1	E →	6
S6′	Waked St.	20	19	0.95 to 1	E →	6
S7	Zakriya Ahmed St.	9	16	1.8 to 1	N ↑	3
S8	Saraya Al-Azbakiya St.	10	19	1.9 to 1	E →	3
S9	26 July St.	29	18	0.6 to 1	E →	6
S10	Emad Al-Din St.	19	17	0.9 to 1	N ↑	6
S11	Bostan Al-Dekkah St.	24	14	0.6 to 1	N ↑	6
S12	Suliman Al-Halabi St.	20	14	0.7 to 1	NW ↖	6
	Total number of cases					**63**

Table 3. Cases of the theoretical model covered in the study area (highlighted in green).

N	Street	NE	Street	E	Street	NW	Street
1 to 3		1 to 3		1 to 3		1 to 3	
1 to 2	**S7**	1 to 2	**S4**	1 to 2	**S8**	1 to 2	
1 to 1.5		1 to 1.5	**S5**	1 to 1.5		1 to 1.5	**S3**
1 to 1	**S10**	1 to 1		1 to 1	**S6 and S6′**	1 to 1	**S2**
1 to 0.5	**S11**	1 to 0.5	**S1**	1 to 0.5	**S9**	1 to 0.5	**S12**
1 to 0.25		1 to 0.25		1 to 0.25		1 to 0.25	

2.2.2. Study Area Tree Scenarios

The tree scenarios that were applied to the study area were the same as those in the theoretical model. In total, three different tree scenarios were applied: no trees at 0%, a low density of trees at 20%, and a high density of trees at 50%, as shown in Figure 8. Applying the same tree scenarios as in the theoretical model allowed for a comparison of the impact of the trees in different canyons between the theoretical model and the case study. Because of the presence of both wide and narrow streets in the study area, certain streets (S3, S4, S5, S7, and S8) only had a single row of trees located in the middle of the street. This is because the width of these streets is 10 m, making it impossible to accommodate two rows of trees. Conversely, in streets that are exceptionally wide, such as S1, three rows of trees were planted to achieve 50% tree coverage.

Figure 8. Tree scenarios for this study: (**A**) 0%; (**B**) 20%; (**C**) 50%.

2.3. Data Input, Model Setup, and Measuring Points

The software used to run the simulations for the different cases in the theoretical model and the study area was ENVI-met V5.1, 2022. All required information for the model was provided, representing existing urban configurations (material, soil) of common materials in Cairo, as well as meteorological data.

2.3.1. Model Setup and Geometry

The model's location was 30.02 latitude and 31.22 longitude. These coordinates were obtained from the ENVI-met V5.1 2022 database by selecting the location of Greater Cairo from the ENVI-met application "Spaces". As shown in Table 4, for both the theoretical and case study models, the study area's model was created using the following model geometry: materials, soil, and trees.

Table 4. Model setup and geometry for both the theoretical model and the case study.

Modeling Information	Theoretical Model	Case Study Model
Area size	X = 165, Y = 140, Z = 30	X = 212, Y = 151, Z = 22
Grid resolution	X = 3, Y = 3, Z = 3	X = 3, Y = 3, Z = 3
Orientation	Model (1) = 0, Model (2) = −45	0
Split lower grid box into 5 sub cells	Yes	Yes
Telescoping applied	Telescoping factor of 20%, starting at a 63 m height	Not applied, as the maximum building height is not very tall
Maximum model height *	198 m	66 m
Nesting grids **	5 Grids, sandy soil	5 Grids, sandy soil
DEM	Not applied, as the site is flat	Not applied, as the site is flat
Soil	Asphalt for roads, concrete for sidewalks, and sand under buildings	Asphalt for roads, concrete for sidewalks, and sand under buildings
Buildings materials	Default wall—moderate insulation	Default wall—moderate insulation
Tree model and size	*Latin name: Acer Platanoides* *** Height = 15 m; crown width = 7 m	*Latin name: Acer Platanoides* *** Height = 15 m; crown width = 7 m

* The model's height is more than double the height of the tallest building, as recommended by the software [37]. ** Nesting grids were added, in addition to 5 cells from the boundary sides of the model being kept empty, as recommended by the software developers [37]. *** *Acer Platanoides* was selected from the ENVI-met database, as it met the required criteria of having a large canopy, high LAD, and good canopy height, matching the recommendations in [38,39].

2.3.2. Simulation Configuration

The simulation configuration was conducted for a representative summer day (i.e., hottest day of July: 28 July 2022). The air temperature, relative humidity, and wind speed were added to ENVI-met for each hour of the simulated day, and climate data were imported from the Cairo Airport weather station [40,41]. The starting time of the simulation was 1:00 a.m., and the total duration of the simulation was 24 h. ENVI-met simple forcing was used for the metrological data. Output data were extracted every hour and converted using the ENVI-met ''Bio-met" to calculate the PET values at each receptor for each hour in all scenarios. The different PET values were the main factors in the comparison. They were compared among all scenarios to assess the effect of each scenario. In addition, other main parameters were measured, such as wind speed (WS) and total mean radiant temperature (TMRT). As Figure 9 illustrates, the PET and its parameters were measured at one given point located at the center of each street's side and centralized between trees to avoid the direct shade of the tree canopies. The receptors were located on both sides of each selected street, exactly in the middle, and for the tree scenarios, they were shifted to be exactly in the middle between trees, helping to ensure that the results would not be affected by the direct shade of the trees and that the results that are compared represent the indirect impact of the tree scenarios.

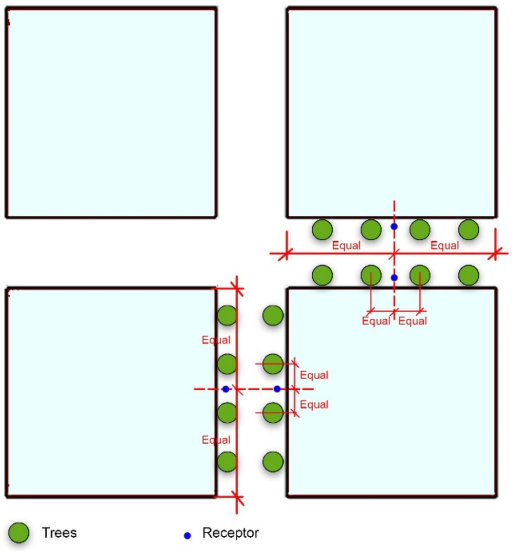

Figure 9. Locations of the receptors (i.e., measuring points) in the middle of each canyon and centralized between trees.

2.4. Validation of the Results

After comparing the meteorological data measured in Cairo city on the 28th of July [40,41] with the ENVI-met outputs for the potential air temperature and relative humidity for both the theoretical models and the case study model at an empty point located in the center of each model, it was found that there was a good match between the measured data and the output data, as shown in Figure 10a,c. Also, the root mean square error (RMSE) and the index of agreement (d) were calculated for the measured and simulated air temperature and relative humidity, and as shown in Figure 10b,d, the RMSE ranged between 1.04 and 0.662 for the air temperature and between 9.06 and 5.5 for the relative humidity. The index of agreement ranged between 0.977 and 0.993 for air temperature and between 0.903 and 0.974 for relative humidity. This means that all models accurately represented the weather conditions in Cairo city, and the results for the different scenarios and different urban cases are reliable and represent how these canyons would perform in real-life situations.

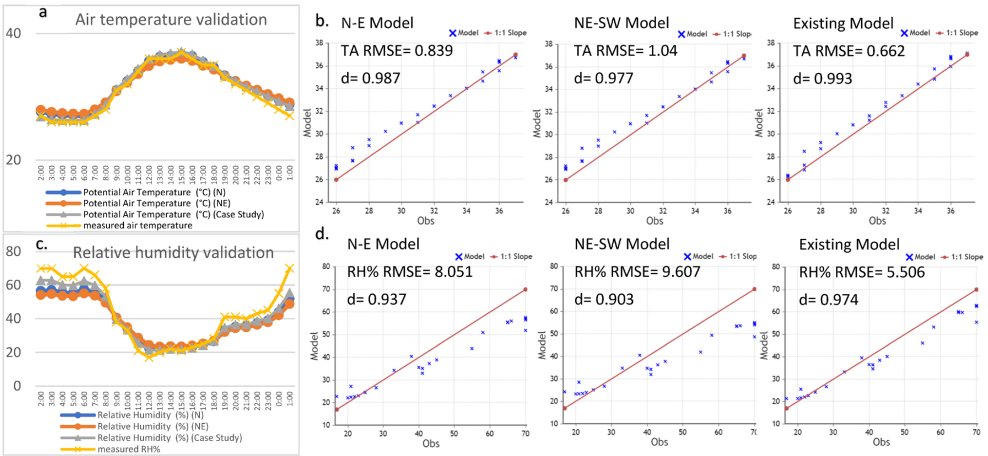

Figure 10. Results of the validation: (**a**,**c**) comparison between the measured and simulated air temperature and relative humidity; (**b**) TA RMSE and index of agreement for each model; (**d**) RH% RMSE and index of agreement for each model.

3. Results

The results are divided into three parts. The first part concerns the theoretical model's results (Stage 1), which present the results of the different aspect ratios with different orientations with and without applying the tree scenarios. The second part presents the results of the existing study area (Stage 2) and how the different canyons perform with and without trees. The final part is a comparison between both parts to gain a better understanding of the results and validate the results of the theoretical model. The ΔPET, ΔTMRT, and ΔWind speed were the major parameters in the comparison, as recommended in many studies, because they have the greatest impact on thermal comfort and they change significantly between different types of canyons, both with and without trees [16–18].

3.1. Theoretical Model Results

The results are presented in two stages, with the first stage explaining how the different canyons performed by comparing the PET values of each side of the different street canyons with various aspect ratios and orientations, and the second stage comparing the trees' impact on each side of the street canyons. The purpose of the first stage is to understand how changing the aspect ratio, orientation, and side of the canyon affect thermal comfort and changing PET values before adding trees, as well as to understand which canyons do not need trees and which require the addition of trees.

3.1.1. Stage One: Results for the 0% Tree Scenario

By comparing the PET values for each side of all the urban canyons, as shown in Figure 11 for the northern and eastern canyons and Figure 12 for the northwestern and northeastern canyons, it was found that the PET values varied between the different aspect ratios, orientations, and canyon sides. The worst PET values were measured on the (a) sides of the eastern streets, as shown in Figure 11c,d, where the PET values reached more than 50 C° for all aspect ratios over many hours during the daytime, in addition to reaching the highest PET value of 58 C° (R2a) at 15:00. On the (b) sides of the eastern canyons, the PET values were slightly lower than those on the (a) sides; however, with different aspect ratios, both sides were under extreme heat stress, and the effect of the different aspect ratios in reducing the PET values was very limited, by around 2–3 C°, and only in moderate to deep urban canyons on the (b) side (i.e., R4b, R6b, and R8b). For other orientations, the aspect ratio played an important role in reducing PET values by providing good urban shading, which is increased in moderate and deep canyons. As shown in Figure 11a,b, in the northern canyons, on the (a) street sides, an increase in the aspect ratio reduced the PET by approximately 5 C° in R1a for 4 h, in R3a and R5a for 7 h, in R7a for 6 h, and in R9a for 3 h compared with R11a, which is the shallowest urban canyon. On the (b) side, the impact of the aspect ratio was less than that on the (a) side, as the decrease in PET was lower, both in terms of the value and reduction in the number of hours. As shown in Figure 12a–d, the performance of the different aspect ratios on both sides of the canyon is very good, and the urban shading is very effective, especially for the northwest orientation's (a and b) sides, as the PET in all cases did not exceed 50 C° and decreased by 5 C° or more with an increase in the aspect ratio. Moreover, the number of hours with a reduced PET increased in R9a,b for 4 h, in R7a,b for 6 h, in R5a,b for 7 h, in R3a,b for 8 h, and in R1a,b for 3 h compared with R11a,b, which is the shallowest canyon. Similar PET enhancements occurred along the northeast orientation on both canyon sides with an increase in the aspect ratio, especially during the afternoon hours, when PET values decreased on average by 5 C° in R2a,b for 8 h, in R4a,b for 9 h, in R6a,b for 7 h, in R8a,b for 7 h, and in R10a,b for 4 h and 2 h compared with the shallowest canyon (R12a,b). In conclusion, the effect of the urban aspect ratio appears clearly in the northern, northeast, and northwest orientations, especially on side (a) for the northern streets and side (b) for the northeast and northwest street canyons.

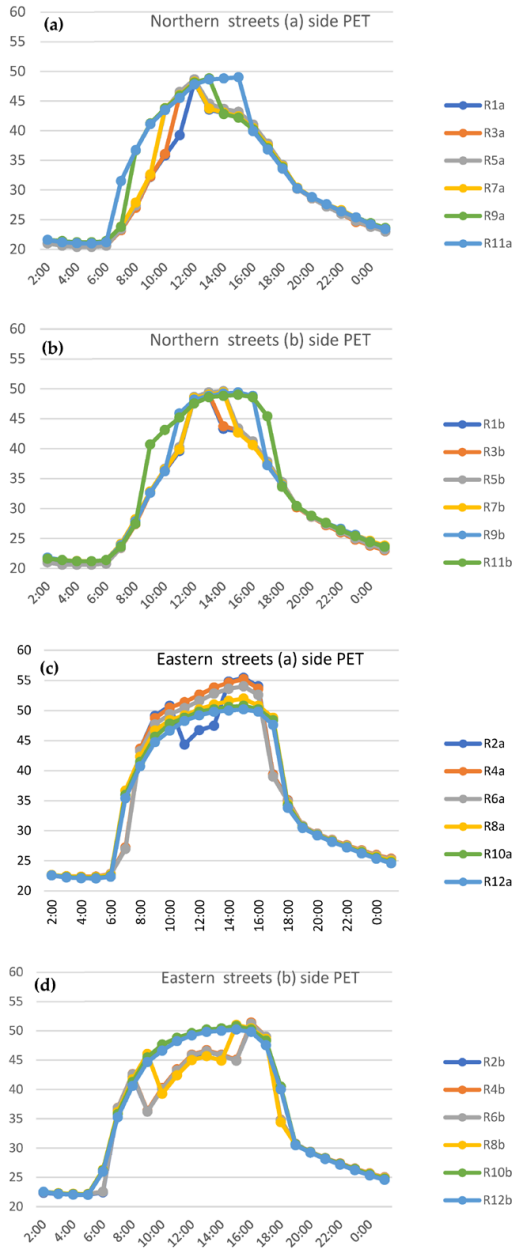

Figure 11. PET values for all aspect ratios of the northern and eastern canyons on both sides at Z = 1.5 m.

To better understand the differences in the PETs on each canyon side for the different orientations and aspect ratios, a detailed study of the main PET parameters (total mean radiant temperature (TMRT) and wind speed) [17] was applied to each side of the different street canyons.

As shown in Figure 13, the TMRT values and the charts' shapes are quite similar to those of the PET charts, which signifies that the PET reduction was mainly driven by the decrease in the TMRT [10]. The highest TMRT values with a limited TMRT reduction via a change in the aspect ratio were measured for the eastern canyons. The reduction on the (a) sides was limited in R2 to 10 C° for 3 h only, and it was slightly better on side (b) for R4, R6, and R8, with the same reduction range of 7 h as in R4 and R6, and for 5 h in R8.

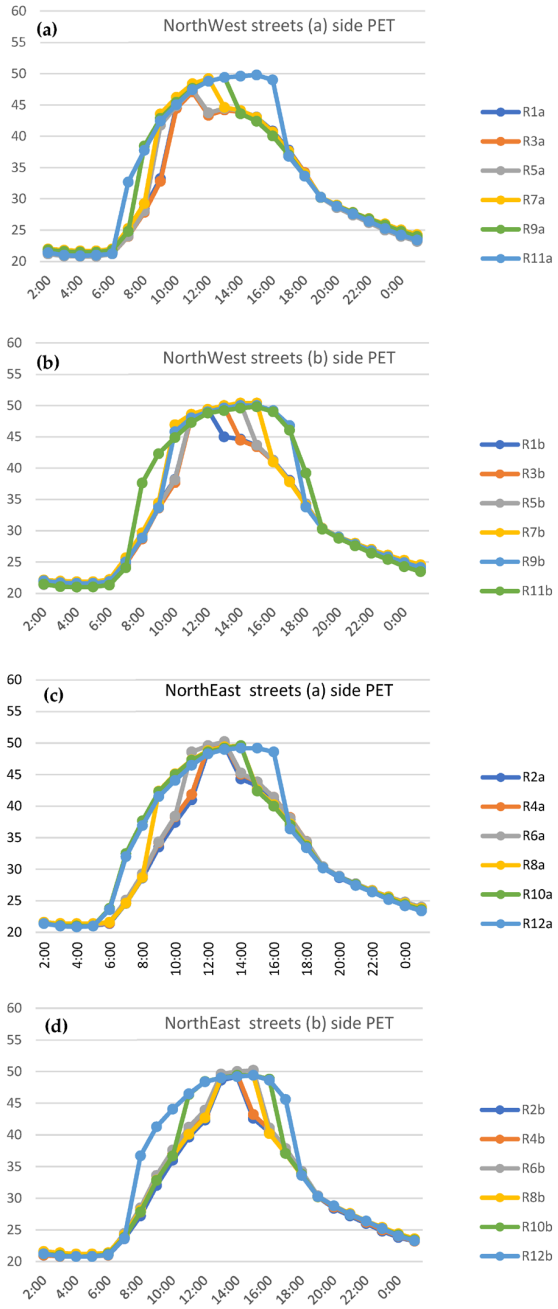

Figure 12. PET values for all aspect ratios of the northwest and northeast canyons on both sides at Z = 1.5 m.

The reduction in the TMRT values was significant in the northern canyons on side (b), northwest canyons on side (b), and northeast canyons on side (b) during the afternoon hours. The reduction exceeded 10 C° for many hours (more than 5 h) in the moderate and deep canyons, and the TMRT reduction decreased gradually as the canyons became shallower. In the northern canyons on side (a), northwest canyons on side (a), and northeast canyons on side (a), the main TMRT reduction took place during the morning to noon hours. The TMRT values decreased by more than 10 C° for many hours, up to 5 h for deep canyons, and the reduction and number of reduction hours gradually decreased with a decrease in the aspect ratio from deep to shallow.

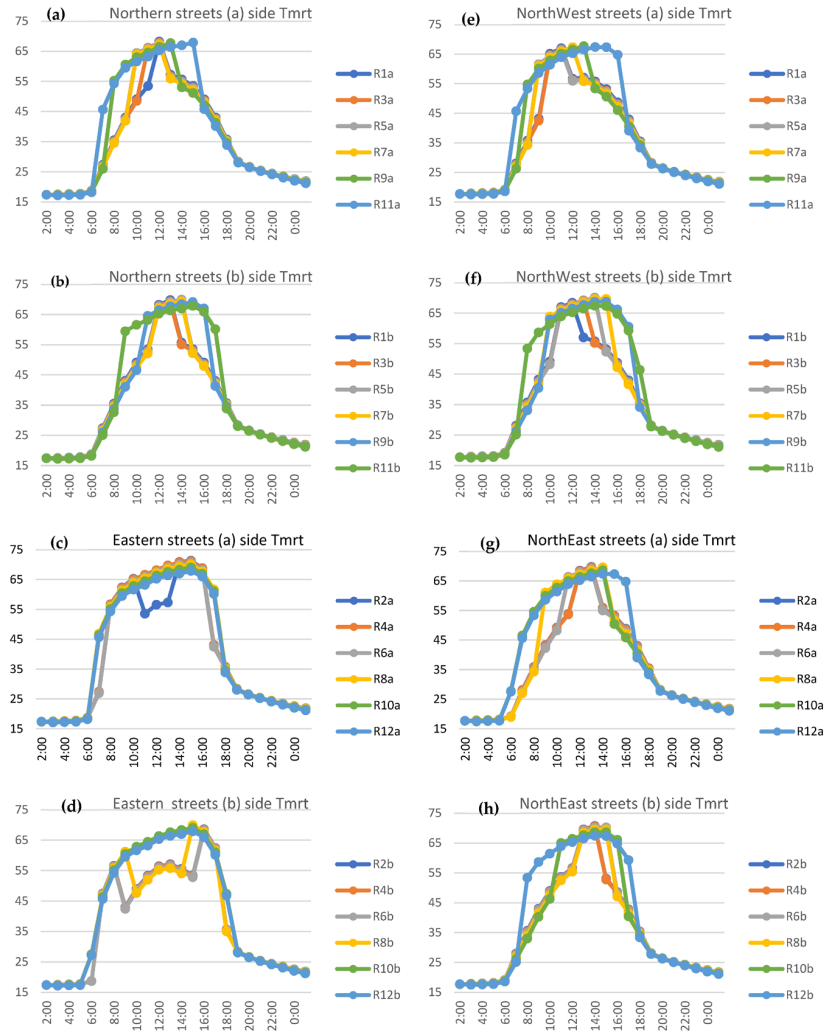

Figure 13. TMRT values for all aspect ratios of the northern, eastern, northeast, and northwest canyons on both sides at Z = 1.5 m.

Studying the wind speed values is crucial for gaining a better understanding of the performance of each canyon orientation, as it helps in the investigation and comprehension of the reasons behind the varying PET values and aids in further research on different orientations, aspect ratios, and canyon sides. As shown in Figure 14, the wind speed changed significantly among the different orientations and changed slightly between the different aspect ratios and canyon sides of the same orientation. A significant change in the wind speed primarily occurred between the northern and eastern streets; as shown in Figure 14a,b, the drop in the wind speed was significant, as the values decreased from a range of 3.5 to 2 m/s in the northern streets to a range of 0.6 to 0.2 m/s in the eastern streets for the different aspect ratios and street sides. This large drop clarifies an additional reason for the high PET values in the eastern roads in general. In the northwest and northeast roads, on side (a), the wind speed for all aspect ratios were within the range of 1–2 m/s, which implies that the wind speed for this orientation is within a middle range, which did not significantly differ with a change in any of their orientations (NW or NE). However, on the (b) side of the northeast and northwest orientations, the difference in the range of wind speed increased from 1 to 2.8 m/s, and the highest value was measured for the northeast orientations.

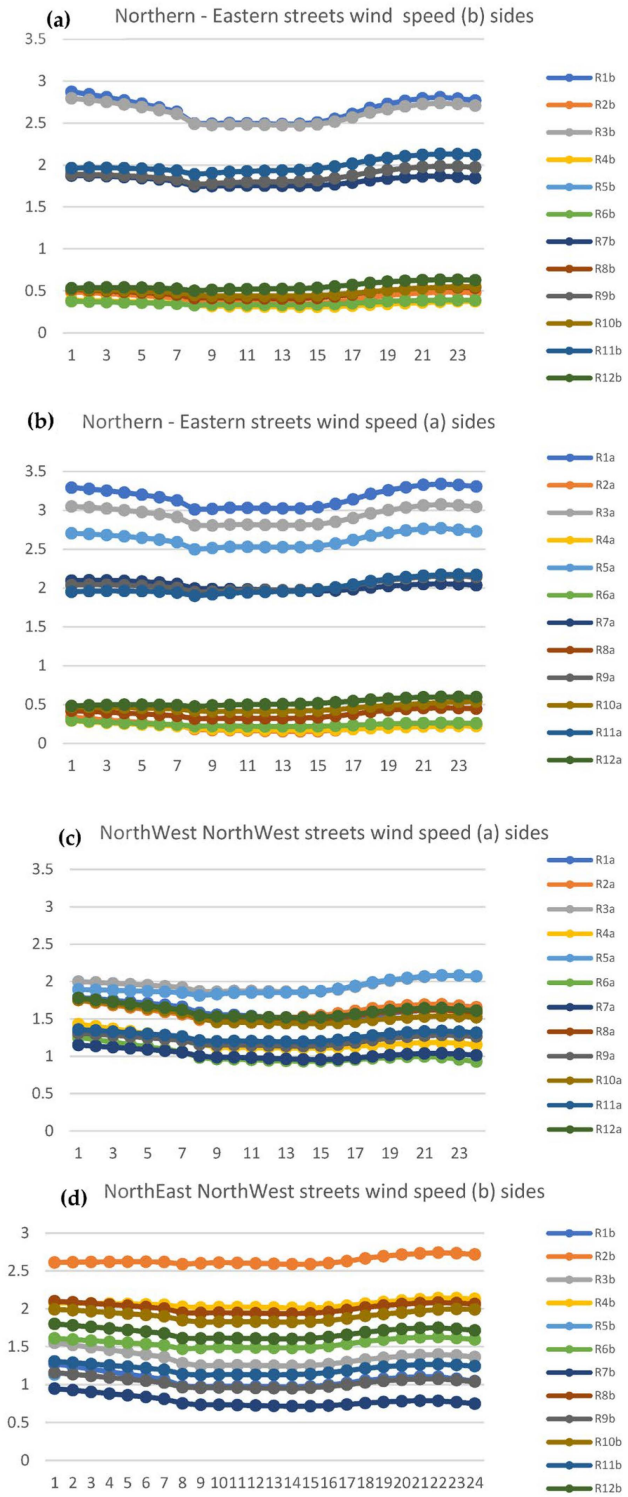

Figure 14. Wind speed values for all aspect ratios of all orientations on both sides at Z = 1.5 m.

By measuring the TMRT and wind speed for the different aspect ratios and orientations on both canyon sides, the reason behind the difference in the PET values is elaborated: the urban shading based on the sun's path and angle in relation to the aspect ratio is not significant along the eastern roads on both sides; however, it is very significant in the

northern, northwest, and northeast on side (b) during the afternoon hours. It has a good impact on the northern, northeast, and northwest canyons on side (a) during the morning to noon hours. Also, the wind speed is very low or almost non-noticeable on the eastern roads. However, it is strong on northern roads and moderate in the northeast and northwest canyons.

Figure 15 shows the ΔPET between each side of each street canyon with different aspect ratios and orientations, and it clarifies the significant change that occurred for the eastern roads between side (a) and side (b), as the maximum PET difference reached 14 C° in the deep and moderate canyons. This significant difference within the same canyon is because of the effect of the aspect ratio and orientation, which reduces the PET on the (b) side much more than that of the (a) side for most of the daytime. The differences in the northern, northeast, and northwest canyons vary between the morning and afternoon hours; thus, the aspect ratio plays an important role that varies during the day because of the sun's path, which changes its angle during the daytime. The main enhancement in the morning hours was measured in the northeast roads, and the main enhancement in the afternoon hours was measured in the northern canyons. The northwest canyons showed a balanced enhancement between the morning and afternoon hours. Shallow canyons, such as R11 and R12, in all orientations showed a very minor change between sides. This signifies that the effect of the aspect ratio was not considered in the shallow canyons; however, in the moderate and deep canyons, the difference between the canyon sides was significant in the N, NE, and NW and varied based on the orientations.

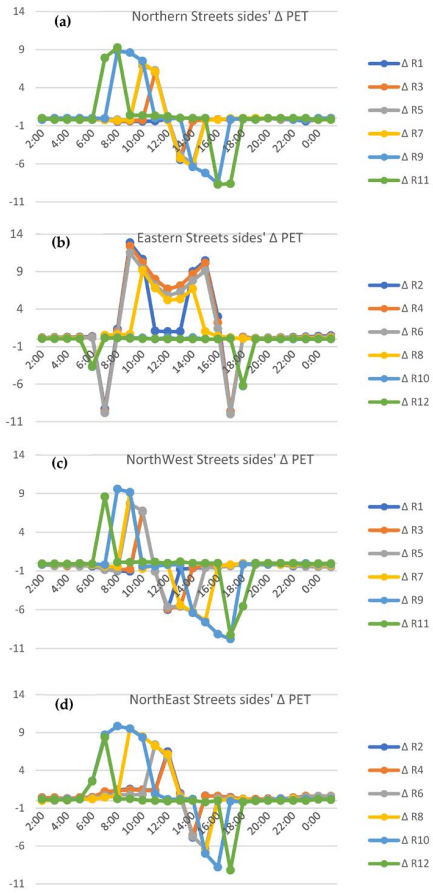

Figure 15. ΔPET for both sides of each canyon (a side–b side) for the different aspect ratios and orientations at Z = 1.5 m.

This concludes how the different sides of the aspect ratios and orientations perform without adding trees. This provides a clear understanding and some insight into the expected performance of trees when they are added to different sides with various aspect ratios and orientations.

3.1.2. Stage Two: Results of the Tree Scenarios

In this stage, the effect of adding different tree percentages was measured by comparing the PET values in each tree scenario for each side of the road for different aspect ratios and orientations. As clarified, the two tree densities (20% and 50%) were tested on different sides of various street canyons to understand the relationship between trees and different sides of various street canyons.

As shown in Figure 16, tree performance varied based on aspect ratio, orientation, and street side. Trees reduced PET values significantly in two cases. The first case involved all aspect ratios of the eastern canyons, and the second case involved shallow urban canyons in all other orientations. In Figure 16, there are two shapes of charts: M-like shape and A-like shape. The M-like shape represents a significant performance of the trees in charts (b, d, f, h, i, j, k, and l). These charts depict the PET reduction reaching a maximum, which remained for most of the daytime, except during the noon hours. This led to an M-like shape for PET reduction, which occurred for most of the time. In these canyons, the ΔPET reached up to 17 C° as the maximum and an average of 12–15 C°, and this average reduction lasted, on average, for 8–10 h, which is almost the entire daytime period and a significant PET reduction. However, in the northern orientation in the moderate and deep canyons, all of the charts showed an A-like shape, which represents a limited enhancement of the PET compared to other cases because the ΔPET reached 13 C° as the maximum for only 3 h in very few cases, and the average ΔPET reached between 4 and 7 C° for most of the daytime. The results in Figure 16 also show that increasing the tree percentage from 20% to 50% in shallow canyons is very promising for both sides of shallow canyons and on side (a) in moderate and deep eastern canyons. However, increasing the tree density in deep and moderate northern canyons did not lead to any significant enhancements.

In Figure 17, the northwest and northeast canyons showed equal tree performance, with a significant enhancement in the shallow canyons for both orientations on both sides, as shown in canyons R9, R10, R11, and R12. For the moderate and deep aspect ratios, the tree performance of the canyons in both orientations was almost the same and very similar to the performance of the trees in the moderate and deep canyons of the northern orientation. In addition, the maximum ΔPET reduction reached an average of 12–14 C°, and the average reduction reached 4–7 C°. The performance of the trees on both sides of the canyons was almost the same, with a slight enhancement on side (b). Increasing the density of the trees from 20% to 50% played an important role in reducing the PET values in both orientations in the shallow canyons, as the ΔPET between the 20% and 50% tree scenarios reached 10 C° in some hours in the shallow canyons. In the moderate and deep canyons, increasing the tree percentage led to minor PET reductions, with an average of 2–3 C° only between the 20% and 50% tree scenarios.

Figure 18 shows the ΔPET for the 20% and 50% tree scenarios compared to the 0% tree scenario for all aspect ratios and orientations at 12:00 and 15:00. At noon (12:00), the 20% tree performance in all orientations was almost the same; also, the 50% tree performance in all orientations was almost the same. This is due to the sun's location at this hour, which is almost perpendicular to the urban canyons, and the role of the aspect ratio almost vanishes. The 50% tree enhancement of the PET values is significant compared with the enhancement produced by the 20% tree scenario at that hour due to the provision of more shading to the urban canyons, and the only difference was in the deepest canyon (H:W = 3:1) because a slight appearance of urban shading occurred for all orientations, reducing the significance of the high-density tree scenario's enhancement slightly.

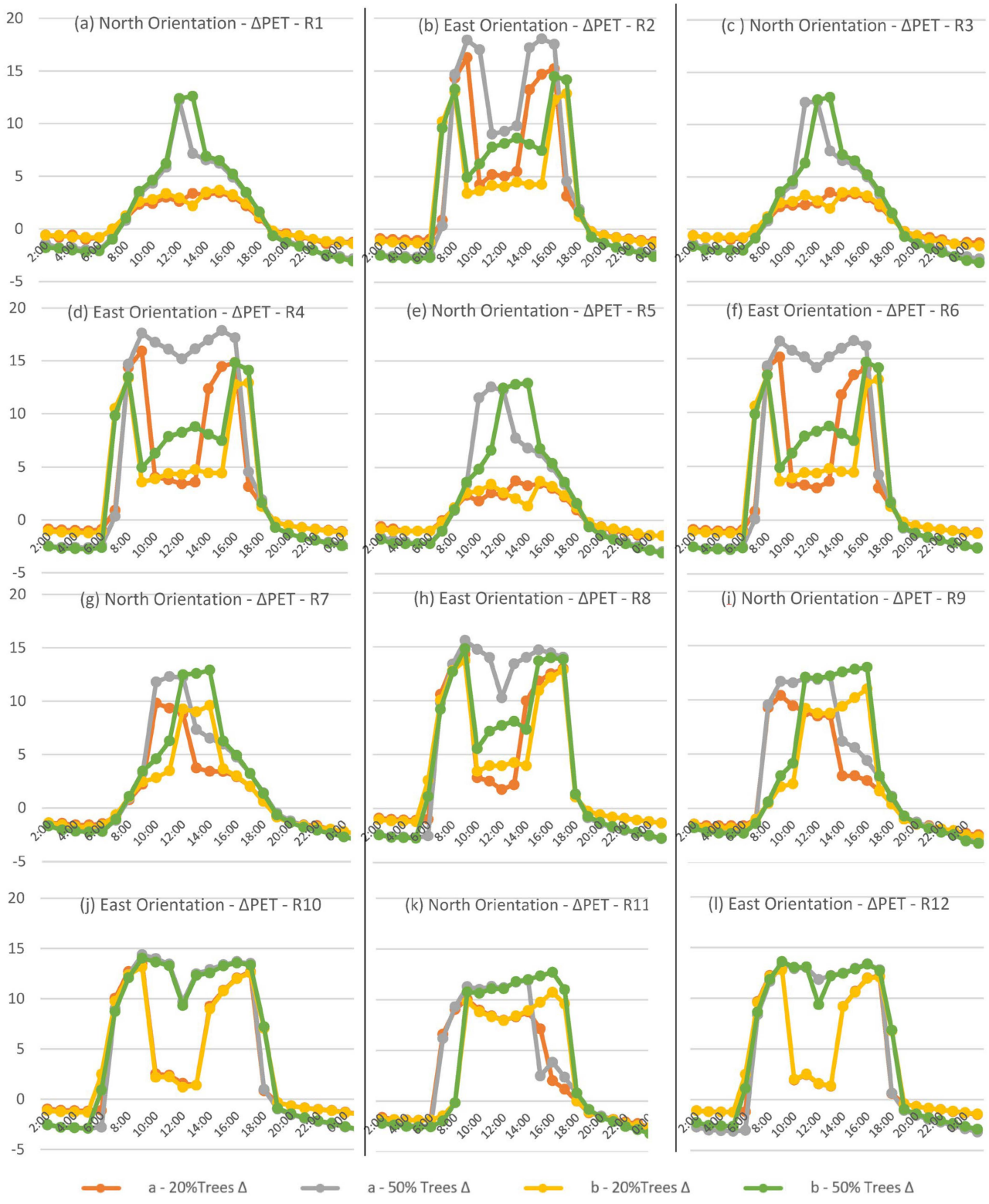

Figure 16. ΔPET with the 20% and 50% tree scenarios in comparison with the 0% tree scenario for northern and eastern canyons on both sides (a and b) at Z = 1.5 m.

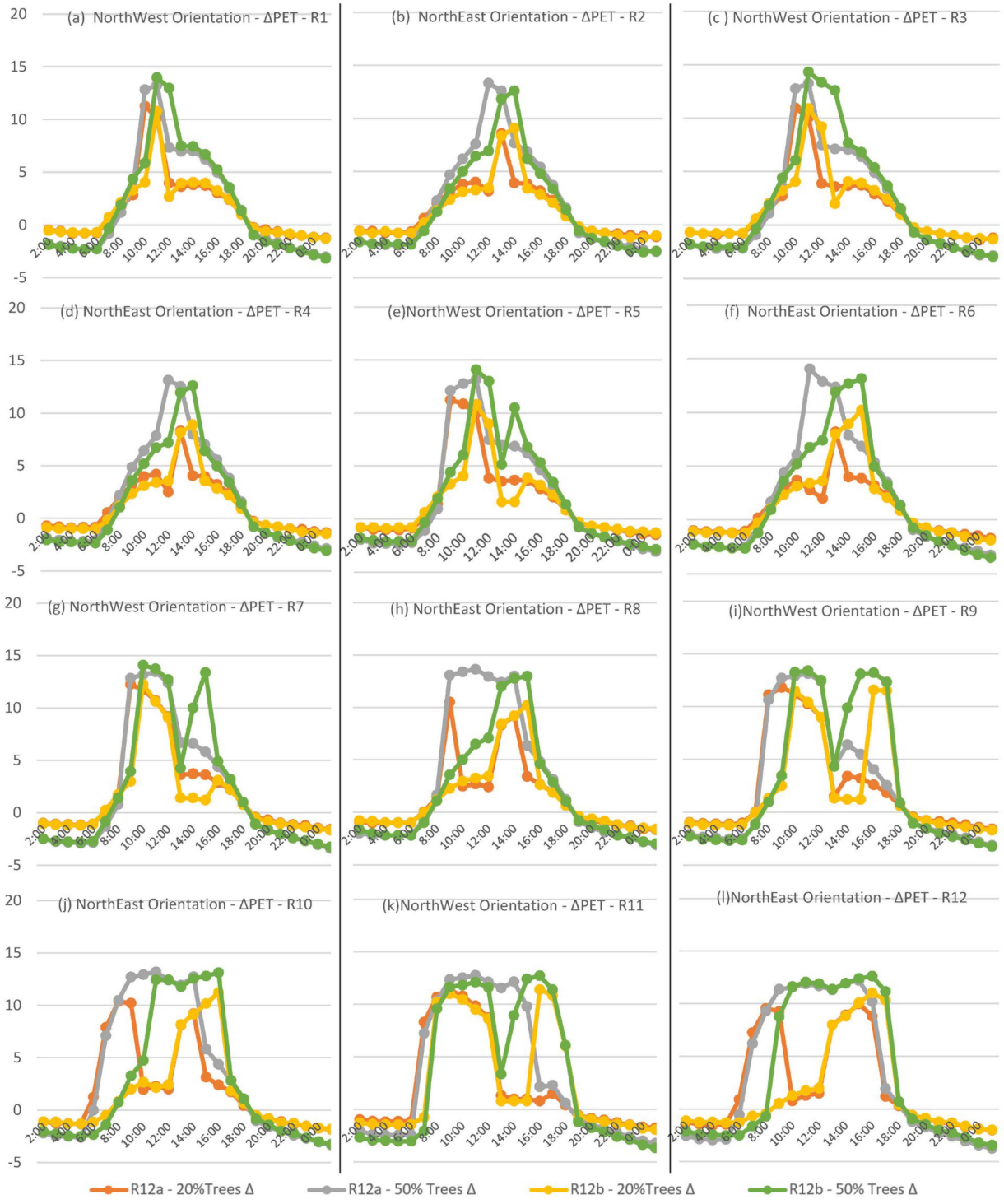

Figure 17. ΔPET with the 20% and 50% tree scenarios in comparison with the 0% tree scenario for the northeast and northwest canyons on both sides (a and b) at Z = 1.5 m.

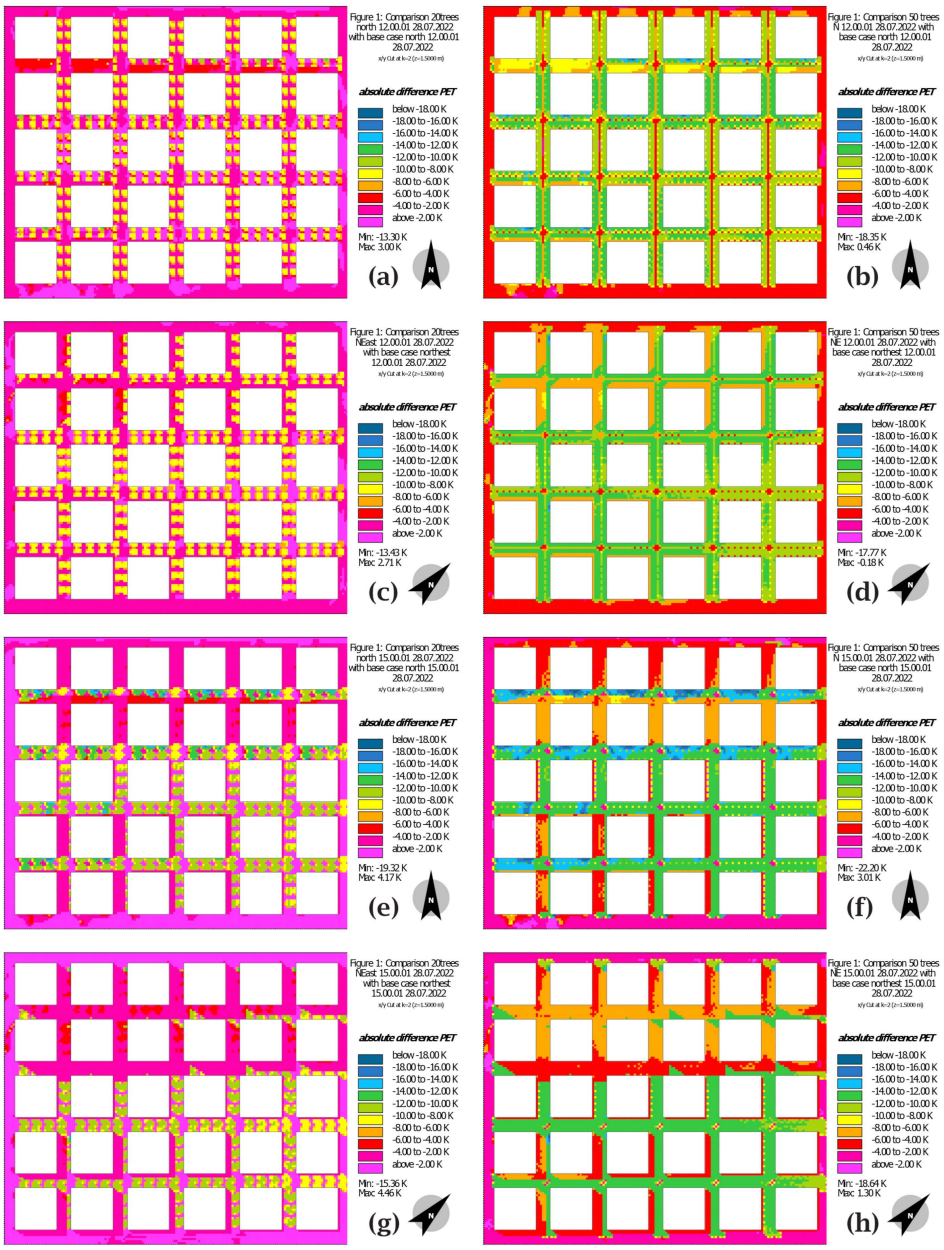

Figure 18. ΔPET at Z = 1.5 m for the 20% and 50% tree scenarios compared to the 0% tree scenario for all aspect ratios and orientations at 12:00 (**a**,**c**,**e**,**g**) and 15:00 (**b**,**d**,**f**,**h**).

In the same figure, in the afternoon (15:00), when tree shading is mixed with urban canyon shading, the actual importance of the trees appears in some canyons and disappears in other canyons. In the shallow canyons, the dark green category, which represents a reduction of 12 to 14 C°, appears clearly in most of the shallow canyons for the 50% tree scenario, and this changed gradually from dark green to orange, which represents a reduction of 6 to 8 C°, in the moderate canyons. Then, it gradually changed to a red color, which represents a reduction of 2 to 4 C°, in the deep canyons, especially in the north, northeast, and northwest orientations, with the eastern orientation showing a greater reduction. It was better than the other orientations, even in the deep canyons. Also, the 20% tree scenario showed the same gradual enhancements with lower values, as it ranged between light green (10 to 12 C°) and red (2 to 4 C°), and the effect is presented on the

map in a dotted form, covering an area that is not fully continuous, as shown for the 50% scenario.

Figures 19 and 20 show a detailed comparison of both sides of the various street canyons with different orientations and aspect ratios that were applied in two ways. The first method compared the average ΔPET during the peak hours in the daytime (from 11:00 to 16:00), as presented in Figure 19. The second method compared how many hours the PET was reduced by 8 C° or more. This reduction helps change the level of thermal comfort by almost two thermal zones and should be considered a significant enhancement [30]. Both comparisons (Figures 19 and 20) show the significant impact of applying high tree densities on shallow streets and in eastern canyons on both sides. In addition to explaining the gradual performance of the trees with various aspect ratios (moderate to deep), in the other orientations, the trees' performance decreased with an increase in the aspect ratio (H/W). It also demonstrates that for deep and moderate canyons with northern, northeast, and northwest orientations, increasing the tree density from 20% to 50% does not lead to significant PET reductions and remains almost the same in some cases.

Figure 19. Comparing the average ΔPET during the peak daytime period (from 11:00 to 16:00) on both sides for all aspect ratios and orientations at Z = 1.5 m.

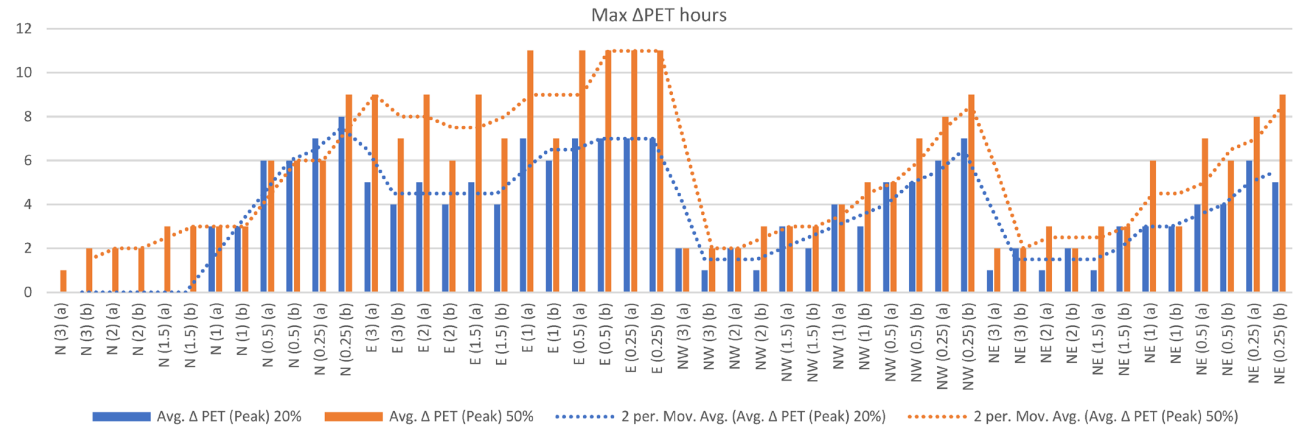

Figure 20. Comparing the number of hours that the PET was reduced by 8 C° or more on both sides for all aspect ratios and orientations at Z = 1.5 m.

For a better understanding of the relationship between the aspect ratio and tree scenario performance for different orientations on both canyon sides, an additional statistical analysis was performed. Different aspect ratios were analyzed against the reduced hours

with different tree densities for each street orientation on each side using SPSS analysis to calculate the correlation, mean, standard deviation, and regression. Before calculating the correlation between both mentioned variables, as shown in Table 5, all input data for the aspect ratio and avg. ΔPET (peak hours) for all orientations on both sides were normally distributed based on the Kolmogorov–Smirnov (KS) test, except the ΔPET values for the 50% tree scenario for a north orientation on the ''b" side and the 50% tree scenario for an east orientation on the ''b" side therefore Pearson correlation was applied for all cases, except for the mentioned cases in which Spearman correlation was applied. Table 5 proves that there was a very strong negative correlation between an increase in the aspect ratio and the ΔPET for peak hours with different tree percentages for all orientations on both sides. However, the correlation value was not the same for all orientations and sides. For example, the correlation for eastern roads was lower than that for the other orientations at −0.849, −0.849, −0.878, and −0.802, which reached −0.971 to −0.900 in most cases. Also, the NE on side (b) and NW on side (a) showed a less significant correlation, and this result is very similar to that of the eastern orientation, which is in line with the measured PET reduction. This means that the trees' performance was less dependent on the urban canyon shading because the urban shading is very minor in this orientation, and the other elements, such as the wind speed, do not help; therefore, the trees' presence is very important in these canyons. In addition, the mean values presented in Table 5 represent the huge difference between the eastern cases and the rest of the orientations; this is also in line with the PET reduction and correlation results. The correlation results could show more significant changes if the results of the shallow aspect ratios (0.5 and 0.25) were excluded because the results of both ratios are the same for the eastern orientation, whereby the impact of the aspect ratio disappears. Figure 21 shows linear scatter plots and regressions of the aspect ratio and ΔPET of the number of 8 C° or greater reduction hours for both tree scenarios (20% and 50%). This clearly shows that there was a negative linear relationship between the aspect ratio and the ΔPET for both tree densities; however, this varied based on the street's aspect ratio, orientation, and canyon side, in addition to the percentage of trees changing the overall values in some cases. The 50% tree scenario showed a stronger relationship than the 20% tree scenario in all orientations. The northern, northwest, and northwest showed higher R^2 values between the ΔPET and aspect ratio, with values $R^2 \geq 0.8$ for the 50% tree scenario; however, in the eastern canyons, on both sides, the values were much lower, reaching $R^2 \leq 0.72$ for side (a) and $R^2 \leq 0.77$ for side (b).

Table 5. Statistical analysis of the correlation between the aspect ratio and the 20% and 50% tree scenarios' avg. ΔPET (peak hours) for all orientations on both sides.

SPSS Statistics Analysis	N(a) Avg. ΔPET (Peak) 20% Trees	N(a) Avg. ΔPET (Peak) 50% Trees	N(b) Avg. ΔPET (Peak) 20% Trees	N(b) Avg. ΔPET (Peak) 50% Trees	E(a) Avg. ΔPET (Peak) 20% Trees	E(a) Avg. ΔPET (Peak) 50% Trees	E(b) Avg. ΔPET (Peak) 20% Trees	E(b) Avg. ΔPET (Peak) 50% Trees	NW(a) Avg. ΔPET (Peak) 20% Trees	NW(a) Avg. ΔPET (Peak) 50% Trees	NW(b) Avg. ΔPET (Peak) 20% Trees	NW(b) Avg. ΔPET (Peak) 50% Trees	NE(a) Avg. ΔPET (Peak) 20% Trees	NE(a) Avg. ΔPET (Peak) 50% Trees	NE(b) Avg. ΔPET (Peak) 20% Trees	NE(b) Avg. ΔPET (Peak) 50% Trees
Mean	2.667	3.500	2.833	4.167	6.000	10.000	5.333	8.167	3.667	4.000	3.167	4.833	2.667	4.833	3.167	4.000
Std. Deviation	3.204	2.074	3.488	2.787	1.095	1.095	1.506	2.229	1.633	2.280	2.401	2.714	2.066	2.483	1.169	2.898
(K-S) Test, c	0.105	0.200 e	0.121	0.041	0.056	0.056	0.069	0.012	0.200 e	0.200 e	0.200 e	0.200 e	0.125	0.197	0.200 e	0.094
Correlation AR	−0.871 *	−0.932 **	−0.863 *	−0.971 **	−0.849 *	−0.849 *	−0.878 *	−0.802	−0.929 **	−0.858 *	−0.887 *	−0.911 *	−0.853 *	−0.936 **	−0.900 *	−0.794
Sig. (2-tailed)	0.024	0.007	0.027	0.001	0.033	0.033	0.022	0.055	0.007	0.029	0.019	0.012	0.031	0.006	0.014	0.059

* Correlation is significant at the 0.05 level (2-tailed).
** Correlation is significant at the 0.01 level (2-tailed).
Kolmogorov–Smirnov test: data are not normally distributed.
Spearman correlation.
Pearson correlation.
c Lilliefors significance correction.
e This is the lower bound of the true significance.

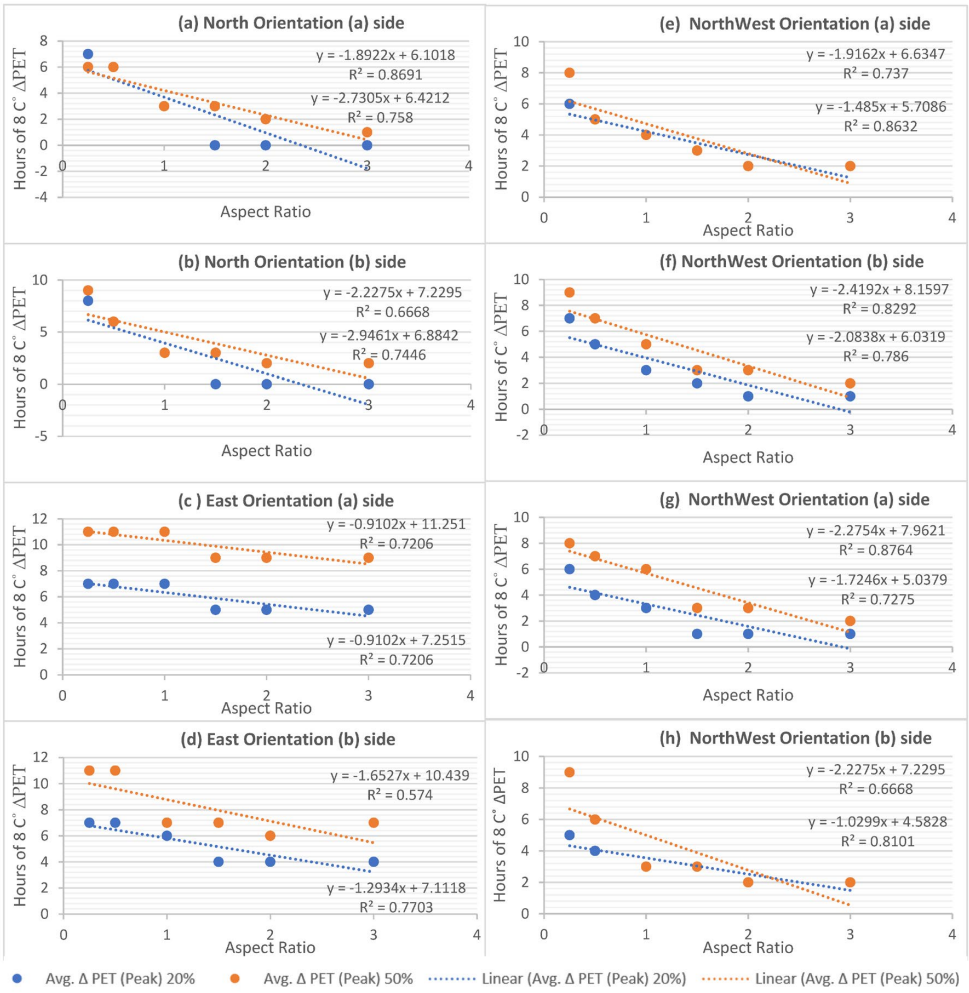

Figure 21. The correlation between the aspect ratio and ΔPET of each orientation for both sides (a and b) at Z = 1.5 m.

3.1.3. Conclusion of the Trees' Performance in the Theoretical Model

On the basis of the analysis of all the results, it has been proven that the performance of the trees varied depending on the aspect ratio, orientation, and side of the urban canyon. The eastern roads are the most in need of a high density of trees. This is because the canyon experiences heat stress throughout the day, and the urban shading on both sides is insufficient to improve the microclimate conditions for the varying aspect ratios. Additionally, the wind speed is extremely low, exacerbating the already poor thermal comfort along this orientation. Northern streets are more shaded by buildings; therefore, increasing the aspect ratio for these orientations is very efficient. Adding trees to moderate to deep canyons will not help enhance the thermal comfort significantly. In addition, the good wind speed helps to enhance thermal comfort when combined with the shade provided by buildings. The northeast and northwest orientations are very similar to the northern canyon, with good canyon shading and moderate wind speed, and the role of trees is not as significant as in the eastern orientation.

3.2. Case Study Results

In order to validate the results of the theoretical study, all the findings were compared to the outcomes by implementing the same tree scenarios in the case study area located in downtown Cairo. As shown in Figure 22, after applying different tree densities to different

canyon aspect ratios and orientations on both sides, the results are quite similar to the theoretical model's results for the same tree scenarios. The trees' impact is very significant in shallow canyons and eastern canyons, as charts (f and i) in Figure 22 for the eastern canyons show significant PET reductions on both sides, in which the PET is reduced by approximately 18 C° as a maximum and reaching an average of a 13 to 14 C° reduction for most of the daytime hours. Significant results were mainly found for the 50% tree scenario with an average of 4 to 5 C° more than in the 20% tree scenario. PET reduction was limited in the other orientations (northern, northeast, and northwest) and hardly exceeded 10 C° PET reductions in very few hours in some canyons. The average PET reduction reached from 4 to 7 C°, which is very similar to the theoretical model's results. A slight change was measured in S1 (northeast) and S12 (northwest) because the PET reduction was slightly better than the theoretical model's results but still much less than the enhancement of the eastern canyons.

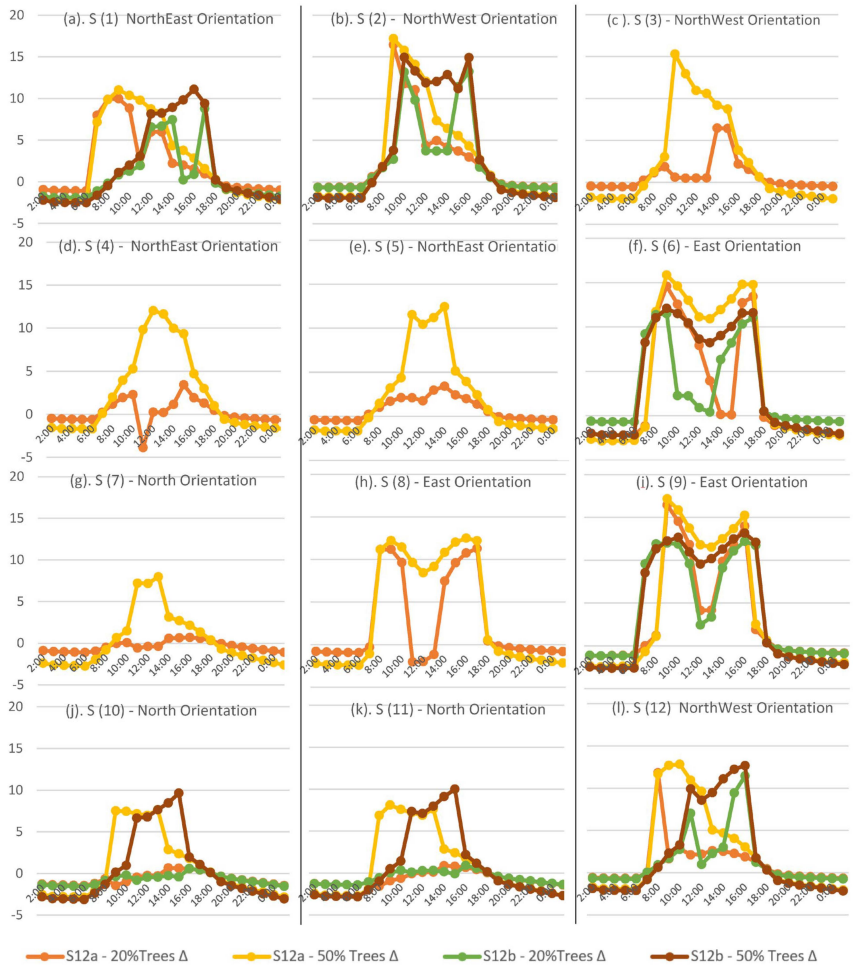

Figure 22. ΔPET with the 20% and 50% tree scenarios compared with the 0% tree scenario for all canyons on both sides (a and b) at Z = 1.5 m.

Figure 23 demonstrates the ΔPET for the same canyon orientation and aspect ratio (S6 and S6′) on both sides (a and b), as shown in Table 2. Although the street widths and buildings heights are irregular, both canyons with the same aspect ratio showed almost the same results, with slight differences occurring most probably because of the irregular building heights in each canyon. The ΔPET difference between both canyons reached 1 to 3 C° in only a very few hours in both canyons on both sides, and this clarifies that as long as the aspect ratio is the same between different canyons, the performance will be

very similar regardless of any slight change in the height of the buildings and width of the street, as long as the canyon aspect ratio is still the same.

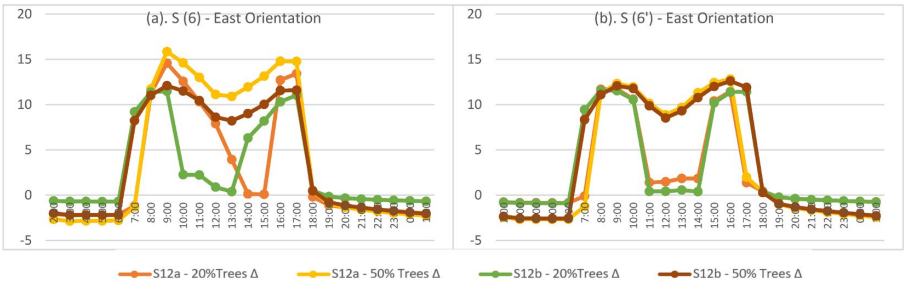

Figure 23. ΔPET for the 20% and 50% tree scenarios in comparison with the 0% tree scenario for S6, and S6′ on both sides (a and b) at Z = 1.5 m.

Figure 24 illustrates the impact of the trees on the entire study area for the 20% and 50% tree scenarios at 12:00 and 15:00. This shows that increasing the tree density is crucial for the eastern canyons, and the blue color (12 to 14 C° ΔPET) represents the four eastern canyons (S6, S6′, S8, and S9). The blue color in Figure 24d for the 50% tree scenario at 15:00in S1 on the (b) side, shows that the trees' impact was significant because this canyon is very shallow. The performance of the 20% and 50% tree scenarios varied with the different aspect ratios and orientations at 15:00, when the tree performance mixed with the various effects of urban shading based on the aspect ratio and orientation. The maps also show the equal impact of the trees at 12:00 for both tree scenarios when the sun is almost perpendicular, and the effect of the different aspect ratios and orientations disappeared. These maps/results are quite similar to the theoretical study's maps/results, and slight differences in a very few cases occurred due to irregular aspect ratios, as the buildings' heights in the existing study area are not exactly the same as those in the theoretical model, which is 100% regular in terms of the building heights and street widths.

Figure 24. ΔPET at Z = 1.5 m for the 20% and 50% tree scenarios compared to the 0% tree scenario for all aspect ratios and orientations at 12:00 (**a**,**b**) and at 15:00 (**c**,**d**).

By reviewing Figures 25 and 26, which show a comparison of the average ΔPET for the peak time (from 11:00 to 16:00) on both sides for the various aspect ratios and orientations in Figure 25 and a detailed comparison between the total hours of PET reduction of 7 h or more on both sides for the various aspect ratios and orientations in Figure 25, both studies prove that the impact of the trees varied significantly for all shallow canyons in addition to the eastern canyons on both sides. The overall linear shape of each chart in Figures 25 and 26 is very similar to the same charts of the theoretical model analysis, as shown in Figures 19 and 20. This validates the results and findings of the theoretical model; however, in the case study, there are slight differences compared to the theoretical model. This is a normal occurrence that happens because of the irregularity of the existing study area in terms of the aspect ratios and various heights of buildings inside each urban canyon; the existing study area cannot have the same regularity as the theoretical model. Despite this, the overall results match the theoretical model and the existing study area.

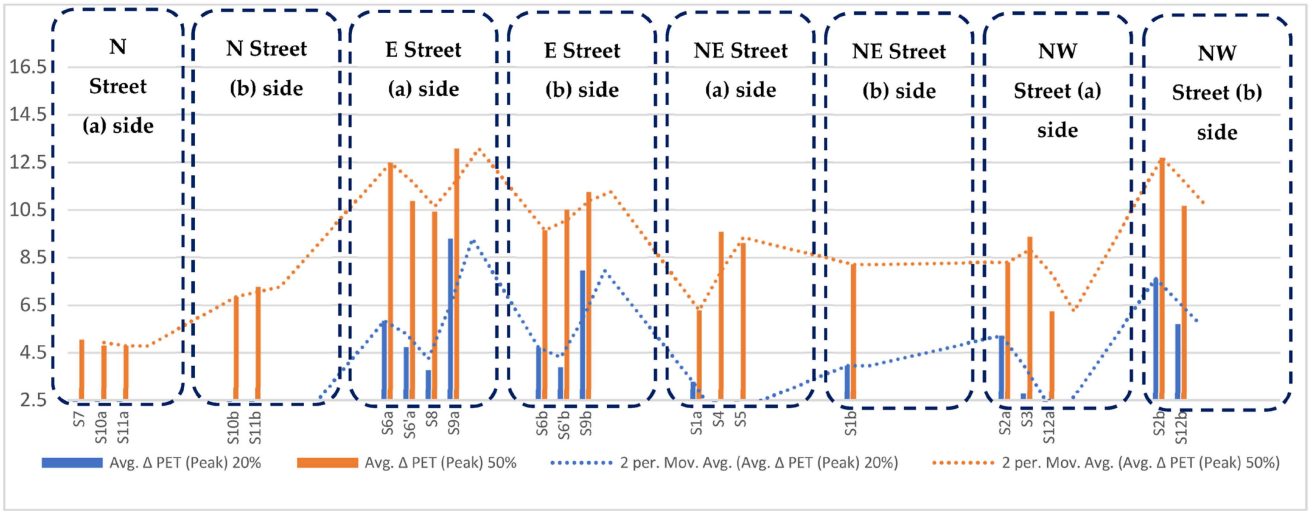

Figure 25. Comparing the average ΔPET for the peak daytime hours (from 11:00 to 16:00) on both sides for all aspect ratios and orientations at Z = 1.5 m.

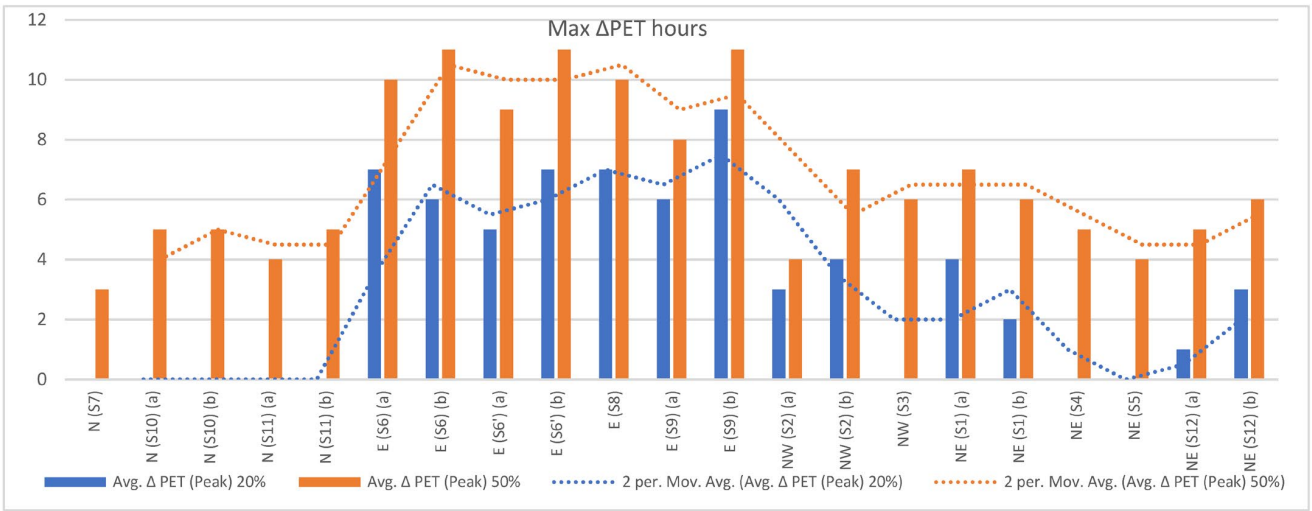

Figure 26. Comparing the number of hours that the PET was reduced by 7 C° or more on both sides for all aspect ratios and orientations at Z = 1.5 m.

4. Discussion

After reviewing the theoretical and case study results, it is obvious that trees are important and add value to different urban canyons. This importance varies depending on the orientation, aspect ratio, and side of the canyon.

The eastern canyon requires a high density of trees, and this is applicable to both sides, particularly the northern side. Moreover, this finding is consistent with those of previous studies [8,14,20]. The northern, northeast, and northwest canyons showed better performance than the eastern canyons. The addition of trees to the Northern canyons improved it slightly, but it was not as significant as the effect of adding trees to the eastern canyons. This aligns with previous findings from other studies [20,30]. For some canyons in the northern, northeastern, and northwestern areas, having tall buildings (moderate to deep canyons) helps keep the area cooler. This is because the buildings block the hot sun from shining directly on the streets. These canyons also have strong winds, which help make them feel cooler. Adding trees to these canyons (moderate and deep canyons in these orientations) might not make much of a difference in how comfortable it feels, and it might even block some of the wind. However, it can be helpful to add trees to one side of the canyons, which is side (b). The trees on side (b) provide shade in the afternoon and make the canyons feel cooler without blocking the wind. Shallow canyons in all orientations and all aspect ratios on both sides of the canyons do not provide enough shading at all. In addition, placing high densities of trees in these canyons is mandatory to enhance thermal comfort conditions, as the canyon effect completely disappears, especially on the northern side of the eastern canyon (side a). Applying a low density of trees on one side of the road (side b) could be useful in deep canyons with northern, northwestern, and northeastern orientations. On the other hand, high density is necessary on both sides of the eastern and shallow canyons. When comparing the results of the theoretical study and the existing case study, it becomes apparent that the unity and regularity of urban canyons will yield slightly different outcomes compared to the irregular canyons found in existing urban areas. However, the main results are similar but not exactly the same due to changes in the urban conditions at the measurement point. Any alteration to the aspect ratio, orientation, or other urban elements will have an impact, albeit not a significant one. It is not feasible to obtain exact numbers from a uniform and regular theoretical model. Slight variations in the results were observed when altering the street widths and building heights while maintaining the same aspect ratio and orientation, which aligns with [42].

5. Conclusions

This study applied an ENVI-met simulation to explore the effect of aspect ratios, orientations, and trees on the microclimate of different sides of urban canyons in Cairo city. Firstly, a total of 144 theoretical cases were simulated to reveal the microclimate's relationship with urban morphologies and tree densities. Then, a real neighborhood in Cairo was simulated to verify the results obtained from the theoretical cases. The results showed a significant tree performance; this performance became more significant based on the aspect ratio (PET reduction reached 12 C° using a high density of trees in shallow canyons), the canyon orientation (PET reduction reached 14 C° in the eastern orientation compared to the northern orientation of the same deep canyon), and the side of the canyon (PET reduction at the northern side of the eastern canyon reached 6 to 7 C° more than the other side of the same canyon by adding a high density of trees). On the basis of the results of this study, the addition of trees to urban canyons should be based on urban morphology characteristics, such as aspect ratio and orientation. Additionally, careful consideration should be given to the side on which trees are planted, as any alteration to these three elements of urban geometry necessitates a wholly different approach. This guidance is of paramount importance, particularly for cities grappling with significant challenges like heat stress and water scarcity, as is the case in Cairo. The findings of this study are broad and cover the majority of urban cases in Cairo city. They should be considered by stakeholders and decision makers in Cairo's authorities and municipalities, as this study could be part of

design guidelines and city management while developing new communities or upgrading existing areas because the study provides a detailed approach on how applying trees can be optimized to enhance microclimate conditions for pedestrians. The research methodology and approach could be also applied to different urban cases in Cairo city which are not covered in this research, especially cases in which the urban canyon is not fully defined, to reach the same target of optimizing the use of trees.

Author Contributions: Conceptualization, A.Y.A.; Methodology, A.Y.A.; Writing—original draft, A.Y.A.; Writing—review & editing, D.G.; Visualization, A.Y.A.; Supervision, D.G. All authors have read and agreed to the published version of the manuscript.

Funding: The research is not receiving any fund only the APC is funded by the TU Dortmund University.

Data Availability Statement: The data that support the findings of this study (All Envi-met files) are available upon request.

Conflicts of Interest: The authors declare no conflict of interest.

Abbreviations

UHI	Urban Heat Island
PET	Physiological Equivalent Temperature
TMRT	Total Mean Radiant Temperature
WS	Wind Speed
RH%	Relative Humidity
AR	Aspect Ratio
RMSE	Root Mean Square Error
d	Index of Agreement

References

1. Yin, C.; Yuan, M.; Lu, Y.; Huang, Y.; Liu, Y. Effects of urban form on the urban heat island effect based on spatial regression model. *Sci. Total Environ.* **2018**, *634*, 696–704. [CrossRef]
2. Theeuwes, N.E.; Steeneveld, G.J.; Ronda, R.J.; Heusinkveld, B.G.; van Hove, L.W.A.; Holtslag, A.A.M. Seasonal dependence of the urban heat island on the street canyon aspect ratio. *Q. J. R. Meteorol. Soc.* **2014**, *140*, 2197–2210. [CrossRef]
3. Dimoudi, A.; Kantzioura, A.; Zoras, S.; Pallas, C.; Kosmopoulos, P. Investigation of urban microclimate parameters in an urban center. *Energy Build.* **2013**, *64*, 1–9. [CrossRef]
4. Taheri Shahraiyni, H.; Sodoudi, S.; El-Zafarany, A.; Abou El Seoud, T.; Ashraf, H.; Krone, K. A Comprehensive Statistical Study on Daytime Surface Urban Heat Island during Summer in Urban Areas, Case Study: Cairo and Its New Towns. *Remote Sens.* **2016**, *8*, 643. [CrossRef]
5. Abutaleb, K.; Ngie, A.; Darwish, A.; Ahmed, M.; Arafat, S.; Ahmed, F. Assessment of urban heat island using remotely sensed imagery over Greater Cairo, Egypt. *Adv. Remote Sens.* **2015**, *04*, 35–47. [CrossRef]
6. Shishegar, N. Street Design and Urban Microclimate: Analyzing the Effects of Street Geometry and Orientation on Airflow and Solar Access in Urban Canyons. *J. Clean Energy Technol.* **2013**, *1*, 52–56. [CrossRef]
7. Kotharkar, R.; Bagade, A.; Ramesh, A. Assessing urban drivers of canopy layer urban heat island: A numerical modeling approach. *Landsc. Urban Plan.* **2019**, *190*, 103586. [CrossRef]
8. Rodríguez-Algeciras, J.; Tablada, A.; Chaos-Yeras, M.; De la Paz, G.; Matzarakis, A. Influence of aspect ratio and orientation on large courtyard thermal conditions in the historical centre of Camagüey-Cuba. *Renew. Energy* **2018**, *125*, 840–856. [CrossRef]
9. Morakinyo, T.E.; Kong, L.; Lau, K.K.-L.; Yuan, C.; Ng, E. A study on the impact of shadow-cast and tree species on in-canyon and neighborhood's thermal comfort. *Build. Environ.* **2017**, *115*, 1–17. [CrossRef]
10. Ketterer, C.; Matzarakis, A. Human-biometeorological assessment of heat stress reduction by replanning measures in Stuttgart, Germany. *Landsc. Urban Plan.* **2014**, *122*, 78–88. [CrossRef]
11. Qaid, A.; Ossen, D.R. Effect of asymmetrical street aspect ratios on microclimates in hot, humid regions. *Int. J. Biometeorol.* **2015**, *59*, 657–677. [CrossRef]
12. Yola, L.; Siong, H.C.; Djaja, K. Climatically responsive urban configuration in residential area: Research gaps. In *The 4th International Tropical Renewable Energy Conference (i-TREC 2019)*; AIP Publishing LLC: Bali, Indonesia, 2020.
13. Wang, Y.; Berardi, U.; Akbari, H. Comparing the effects of urban heat island mitigation strategies for Toronto, Canada. *Energy Build.* **2016**, *114*, 2–19. [CrossRef]
14. Andreou, E. Thermal comfort in outdoor spaces and urban canyon microclimate. *Renew. Energy* **2013**, *55*, 182–188. [CrossRef]

15. Matzarakis, A.; Amelung, B. Physiological equivalent temperature as indicator for impacts of climate change on thermal comfort of humans. In *Seasonal Forecasts, Climatic Change and Human Health: Health and Climate*; Springer: Dordrecht, The Netherlands, 2008; pp. 161–172.
16. Morakinyo, T.E.; Lam, Y.F. Simulation study on the impact of tree-configuration, planting pattern and wind condition on street-canyon's micro-climate and thermal comfort. *Build. Environ.* **2016**, *103*, 262–275. [CrossRef]
17. Abdollahzadeh, N.; Biloria, N. Outdoor thermal comfort: Analyzing the impact of urban configurations on the thermal performance of street canyons in the humid subtropical climate of Sydney. *Front. Archit. Res.* **2021**, *10*, 394–409. [CrossRef]
18. De, B.; Mukherjee, M. Optimisation of canyon orientation and aspect ratio in warm-humid climate: Case of Rajarhat Newtown, India. *Urban Clim.* **2018**, *24*, 887–920. [CrossRef]
19. Memon, R.A.; Leung, D.Y.C.; Liu, C.-H. Effects of building aspect ratio and wind speed on air temperatures in urban-like street canyons. *Build. Environ.* **2010**, *45*, 176–188. [CrossRef]
20. Jamei, E.; Ossen, D.R.; Seyedmahmoudian, M.; Sandanayake, M.; Stojcevski, A.; Horan, B. Urban design parameters for heat mitigation in tropics. *Renew. Sustain. Energy Rev.* **2020**, *134*, 110362. [CrossRef]
21. Kolokotsa, D.; Lilli, K.; Gobakis, K.; Mavrigiannaki, A.; Haddad, S.; Garshasbi, S.; Mohajer, H.R.H.; Paolini, R.; Vasilakopoulou, K.; Bartesaghi, C.; et al. Analyzing the Impact of Urban Planning and Building Typologies in Urban Heat Island Mitigation. *Buildings* **2022**, *12*, 537. [CrossRef]
22. Balany, F.; Ng, A.W.; Muttil, N.; Muthukumaran, S.; Wong, M.S. Green Infrastructure as an Urban Heat Island Mitigation Strategy—A Review. *Water* **2020**, *12*, 3577. [CrossRef]
23. Takebayashi, H.; Moriyama, M. Relationships between the properties of an urban street canyon and its radiant environment: Introduction of appropriate urban heat island mitigation technologies. *Sol. Energy* **2012**, *86*, 2255–2262. [CrossRef]
24. Lan, H.; Lau, K.K.-L.; Shi, Y.; Ren, C. Improved urban heat island mitigation using bioclimatic redevelopment along an urban waterfront at Victoria Dockside, Hong Kong. *Sustain. Cities Soc.* **2021**, *74*, 103172. [CrossRef]
25. Hamdi, R.; Schayes, G. Sensitivity study of the urban heat island intensity to urban characteristics. *Int. J. Climatol. A J. R. Meteorol. Soc.* **2008**, *28*, 973–982. [CrossRef]
26. De Lieto Vollaro, A.; De Simone, G.; Romagnoli, R.; Vallati, A.; Botillo, S. Numerical Study of Urban Canyon Microclimate Related to Geometrical Parameters. *Sustainability* **2014**, *6*, 7894–7905. [CrossRef]
27. Pioppi, B.; Pigliautile, I.; Pisello, A.L. Human-centric microclimate analysis of Urban Heat Island: Wearable sensing and data-driven techniques for identifying mitigation strategies in New York City. *Urban Clim.* **2020**, *34*, 100716. [CrossRef]
28. Andreou, E.; Axarli, K. Investigation of urban canyon microclimate in traditional and contemporary environment. Experimental investigation and parametric analysis. *Renew. Energy* **2012**, *43*, 354–363. [CrossRef]
29. Aboelata, A. Vegetation in different street orientations of aspect ratio (H/W 1: 1) to mitigate UHI and reduce buildings' energy in arid climate. *Build. Environ.* **2020**, *172*, 106712. [CrossRef]
30. Lobaccaro, G.; Acero, J.A.; Sanchez Martinez, G.; Padro, A.; Laburu, T.; Fernandez, G. Effects of Orientations, Aspect Ratios, Pavement Materials and Vegetation Elements on Thermal Stress inside Typical Urban Canyons. *Int. J. Environ. Res. Public Health* **2019**, *16*, 3574. [CrossRef]
31. Vuckovic, M.; Kiesel, K.; Mahdavi, A. Trees and the microclimate of the urban canyon: A case study. In Proceedings of the 2nd ICAUD International Conference in Architecture and Urban Design, Tirana, Albania, 8–10 May 2014.
32. Mohamed, E. Analysis of urban growth at Cairo, Egypt using remote sensing and GIS. *Nat. Sci.* **2012**, *4*, 355–361.
33. Hassan, A.A.M. Dynamic expansion and urbanization of greater Cairo metropolis, Egypt. In Proceedings of the 6th International Conference on Urban Planning—Essen and Regional Development in the Information Society, Essen, Germany, 18–20 May 2011.
34. Zied, E.; Vialard, A. Syntactic Stitching: Towards a Better Integration of Cairo's Urban Fabric. In Proceedings of the 11th International Space Syntax Symposium, Instituto Superior Técnico—Universidade de Lisboa, Lisbon, Portugal, 3–7 July 2017.
35. Elbardisy, W.M.; Salheen, M.A.; Fahmy, M. Solar Irradiance Reduction Using Optimized Green Infrastructure in Arid Hot Regions: A Case Study in El-Nozha District, Cairo, Egypt. *Sustainability* **2021**, *13*, 9617. [CrossRef]
36. Osman, R.; Ferrari, E.; McDonald, S. Water scarcity and irrigation efficiency in Egypt. *Water Econ. Policy* **2016**, *2*, 1650009. [CrossRef]
37. Envi-Board. Envi-Met Support Center. Envi-Met. Available online: http://www.envi-hq.com/ (accessed on 30 April 2023).
38. Middel, A.; Chhetri, N.; Quay, R. Urban forestry and cool roofs: Assessment of heat mitigation strategies in Phoenix residential neighborhoods. *Urban For. Urban Green.* **2015**, *14*, 178–186. [CrossRef]
39. Shahidan, M.F.; Shariff, M.K.M.; Jones, P.; Salleh, E.; Abdullah, A.M. A comparison of *Mesua ferrea* L. and *Hura crepitans* L. for shade creation and radiation modification in improving thermal comfort. *Landsc. Urban Plan.* **2010**, *97*, 168–181. [CrossRef]
40. Weather and Climate. Available online: https://weather-and-climate.com/Cairo-July-averages (accessed on 10 October 2022).
41. Time and Date. Available online: https://www.timeanddate.com/weather/egypt/cairo/historic?month=7&year=2022 (accessed on 10 October 2022).
42. Karimimoshaver, M.; Khalvandi, R.; Khalvandi, M. The effect of urban morphology on heat accumulation in urban street canyons and mitigation approach. *Sustain. Cities Soc.* **2021**, *73*, 103127. [CrossRef]

This Page Intentionally Left Blank.

Article 3: Key facts and author contributions

Refrence	Abdelmejeed AY, Gruehn D. Pedestrian Dynamic Thermal Comfort Analysis to Optimize Using Trees in Various Urban Morphologies: A Case Study of Cairo City. *Land*. 2024; 13(9):1489. https://doi.org/10.3390/land13091489
Contributions	AY. A, 85%, and DG, 15% Words count: 11868
Review Model	Single blind peer review
History	Submitted: 7 August 2024 Accepted: 12 September 2024 Published: 14 September 2024

Signature:

Ahmed Yasser Abdelmejeed

Date: 15. July 2025

land

MDPI

Article

Pedestrian Dynamic Thermal Comfort Analysis to Optimize Using Trees in Various Urban Morphologies: A Case Study of Cairo City

Ahmed Yasser Abdelmejeed [1,2,*] and Dietwald Gruehn [1]

[1] Research Group Landscape Ecology and Landscape Planning (LLP), Department of Spatial Planning, TU Dortmund University, 44227 Dortmund, Germany; dietwald.gruehn@tu-dortmund.de
[2] Faculty of Urban and Regional Planning, Cairo University, Cairo 11562, Egypt
* Correspondence: ahmed.abdelmejeed@tu-dortmund.de

Abstract: Considering the impacts of climate change on the goal of obtaining sustainable and healthier cities, this research aimed to analyze and assess the impact of different urban forms with different trees densities on the dynamic physiological equivalent temperature (DPET) for pedestrians while walking further than the average walking distance (750 m) using ENVI-met. This study included five different areas within Greater Cairo, which is suffering from extreme heat stress. The selected study areas had lots of urban variety in terms of the canyons' aspect ratios, orientations, urban form, green areas, mixed uses, and tree densities. Two tree scenarios were analyzed: the current tree density situation and a scenario where the tree density of each study area was increased to its capacity. The results proved that the DPET had different values than the steady physiological equivalent temperature (SPET) at each point within the walking routes. However, the DPET was closely related to changes in the SPET. Keeping the SPET lower or higher for a long time reduced or increased the DPET, and frequent changes (up and down) in the SPET kept the DPET stable. Changes between DPET values were driven more by the microclimate conditions of a space or canyon than the conditions of the overall area, and controlling the microclimate conditions of a whole urban canyon controlled the DPET. Changes in the DPET could reach as high as 10 °C between different walking routes, and increasing the tree density could help lower the DPET by as much as 6 °C in some cases.

Keywords: urban heat island (UHI); outdoor thermal comfort; urban trees; urban shading; dynamic thermal comfort; static/steady thermal comfort; ENVI-met greenery simulation; urban cooling strategies

Citation: Abdelmejeed, A.Y.; Gruehn, D. Pedestrian Dynamic Thermal Comfort Analysis to Optimize Using Trees in Various Urban Morphologies: A Case Study of Cairo City. *Land* **2024**, *13*, 1489. https://doi.org/10.3390/land13091489

Academic Editors: Yongze Song and Zihao Zheng

Received: 7 August 2024
Revised: 11 September 2024
Accepted: 12 September 2024
Published: 14 September 2024

1. Introduction

Developing healthy cities and communities is necessary, especially in light of the impacts of climate change. A healthy and sustainable urban environment consists of a series of pedestrian walkways for commuting, exercising, and leisure use [1]. Walking is considered the most widespread mode of transport [2] as it is a crucial link between the other modes, and pedestrian activity helps to fulfill recreational requirements [3]. People moving between interconnected spaces perform non-sedentary activities, enhancing sustainability and well-being. However, adverse weather conditions may create uncomfortable thermal sensations that change or ruin the experiences of people walking outdoors [4]. The thermal conditions of linear walking paths, which affect a person's thermal comfort, will inherently influence people's usage probability [1]. Therefore, enhancing pedestrian thermal comfort and microclimate conditions is crucial.

1.1. Thermal Comfort

Thermal comfort is defined in ASHRAE 55 [5] as a condition of the mind where satisfaction with the thermal environment is expressed. Maintaining a body temperature

at approximately 36–37 °C is essential for regulating the body's metabolic rate and organ function [6]. Hyperthermia and hypothermia both take a toll on physical and psychological health [7].

The PET (physiological equivalent temperature) was designed to measure environmental and personal parameters, including air temperature, air humidity, air velocity, the mean radiant temperature (Tmrt), clothing insulation, and the level of activity, to predict thermal comfort [8]. Thermal comfort can be studied and analyzed in two main ways. The first, which has been used in many studies, is to analyze thermal comfort at a fixed point, which is assumed to be close to steady, based on individuals' instantaneous subjective thermal sensation or comfort while sitting or standing [1]. In this research, this is named the steady PET (SPET). The other way to measure the PET is more dynamic as it focuses on the thermal comfort of pedestrians while walking. In this way, the outdoor thermal environment and the human physiological response are both important determinants of thermal comfort during the dynamic process of walking [1]. In this research, this is named the dynamic PET (DPET).

1.2. Difference between DPET and SPET

Pedestrians receive various continuous changes in microclimate conditions while walking outdoors. Their actual sensations vary over the entire length of a route, sometimes showing significant changes in thermal perception. Subtle environmental changes can affect skin temperature receptors. Physiological responses and thermal experience history are important factors for pedestrian thermal sensation. The steady thermal comfort model is only applicable to people who stay in outdoor environments for 10 to 30 min [1,9,10].

Thermal comfort indices and findings from early studies, which were obtained in thermally homogenous and stable environments, are insufficient to explain constructively the transient thermal perceptions of pedestrians, who are exposed to constantly changing environmental conditions due to urban geometry [11,12]. Traditional environments with steady thermal comfort sometimes cannot meet people's requirements, and dynamic thermal comfort is considered better. In an outdoor summer study, participants walked along a specific route that passed through diverse urban textures, exposing them to a variety of thermal environments that routine fixed-point observations could not capture [13]. In another study, simulation experiments were conducted in a climate chamber. Airport passengers experienced three different durations of walking (5 min, 10 min, and 15 min) at 26 °C and subsequently transitioned to sedentary conditions at three different operative temperatures (23 °C, 26 °C, and 29 °C). By analyzing the variations in subjective perception and physiological parameters, it was concluded that the thermal equilibrium requires 17–21 min to recover to steady-state sedentary levels after walking [14]. Also, a study determined that the SPET has a big impact on the DPET. For example, the steady thermal conditions at the start of a walk significantly impacted the DPET. For a person coming out of a shaded area of a sidewalk and entering a 200 m long sunny segment, after 180 s, his actual skin temperature was approaching the value simulated by a steady-state thermal comfort model, and his core temperature was lower than the simulated value. It was further suggested that around 30 min were required for a person to reach a steady state after leaving a room with thermal comfort to enter hot conditions [15].

1.3. DPET Parameters

Dynamic thermal comfort is affected by the same thermal comfort parameters. Efforts to achieve comfort during walking need to consider both temporal and spatial variations, as well as opportunities for adaptation [4]. Pedestrians are usually alternately exposed to cool-biased and warm-biased environments during outdoor activities, such as when being exposed to indoor and outdoor places or moving through areas with sunlight and shade on the street [9]. Step changes in microclimate environments occur during the above alternate exposures to cool-biased and warm-biased environments, which are mainly characterized by mixed changes in radiation, wind speed, and air temperature. Additionally, these

step changes happen at various frequencies due to the movement speed, the needs of activities, and environmental designs. Essentially, people are in highly dynamic and complex environments when conducting outdoor activities and are speculated to produce thermal responses different from those in relatively steady environments [9]. A previous study found that wind and solar radiation were the main factors attributed to variations in outdoor thermal comfort in any given period [4]. During walking, disturbances due to wind velocity had a significant effect on thermal sensation, which was reflected in an enhancement of convective heat transfer on the skin surface [16]. Another study was carried out from May to July at a university campus in Hong Kong with subtropical weather conditions. The results showed that subjective thermal perceptions varied with alternating exposure to sunlight and shade at different frequencies. With a higher alternating frequency, there was reduced thermal dissatisfaction with hot summer days and a lower comfort requirement for shade [9]. Also, a very important factor that impacted the DPET was the metabolic rate. Full consideration should be given to variations in this variable. Typically, it takes 3–5 min to reach a new metabolic level when walking indoors, whereas it takes 9–11 min in a transition space. In the meantime, the metabolic rate returns to a normal sedentary level 3–5 min after walking ceases in both indoor and transition spaces [16].

1.4. Urban Geometry Effect

Improving urban geometric design is necessary to mitigate thermal discomfort and create better pedestrian environments, especially in high-density cities [12]. Urban morphology, the sky view factor (SVF), and shading are the major factors that have significant roles in enhancing microclimate conditions [17,18]. The shadows cast by buildings help reduce the pedestrian radiant load and, consequently, improve thermal comfort [19–21]. Openness is a predominant factor that influences pedestrians' thermal comfort, and pedestrians have also been shown to feel more comfortable when moving from sunlit places to shaded places [12]. A study showed that greater cooling of road microclimates occurs on roads with low SVFs [22]. The street canyon orientation and aspect ratio have significant influences on urban microclimates and directly impact street-level thermal comfort [23,24], as the aspect ratio controls the amount of shadow and the orientation affects the wind speed based on the wind direction. Optimizing shadows and wind speeds using the aspect ratio and orientation will lead to significant enhancements for both the SPET [21,25–27] and DPET [4,9].

1.5. Urban Trees

Urban greenery and biotopes represent discernible cool spots along walking paths [13]. They can reduce the effects of the surrounding building mass and help to create a low-SVF environment that is cooler during both daytime and nighttime [28]. Studies have demonstrated that walking in forest environments diminishes blood pressure, skin conductivity, muscle tension, pulse rate, cortisol levels, and sympathetic nerve activity and enhances parasympathetic activity (the components of heart rate variability) [29,30]. Also, a roadside landscape may have a proportionally greater impact on urban dwellers due to the limited availability of green spaces in cities. Urban roadside trees can improve urban dwellers' feelings and can make a city cooler [22]. According to this study, we can infer that a short walk along an urban road surrounded by trees is a simple, attainable, and effective method of improving the quality of life and well-being of urban dwellers [22]. As a combined impact, it has been demonstrated that urban morphology and vegetation shading affect solar radiation storage during the day in summer, especially for low-rise buildings [21,28,31]. Also, trees' thermal performance is significant for different orientations of canyons, especially the eastern–western orientation [21,32,33].

1.6. Research Gap and Target

This research aimed to study the impacts of different urban forms and different densities of urban trees on pedestrian thermal comfort while walking from a dynamic

thermal comfort perspective under the same climate conditions (same climate data input), as pedestrian dynamic thermal comfort for people who are moving at a certain speed and not stopping at any one place for a long period is not well studied [1]. This study sought to understand the impacts of different urban forms (different aspect ratios, orientations, and tree densities) on pedestrian dynamic thermal comfort while walking between different destinations within different urban areas.

This knowledge helped clarify how different urban forms perform thermally and how many trees are needed to enhance the thermal performance of each urban form to improve the microclimate conditions and the dynamic thermal comfort of pedestrians while walking.

2. Materials and Methods

To assess dynamic thermal comfort for different urban forms and tree densities, this study was conducted on various walking routes in different urban areas with different tree densities. It tested different urban forms (with different aspect ratios and orientations) and different tree canopy covering densities by measuring the DPET on each route in each study area under different tree scenarios using the microclimate simulation software ENVI-met V5.6.1 and its dynamic thermal comfort analysis capability, which was released in June 2023 [34]. This study was carried out through two main steps, as shown in Figure 1.

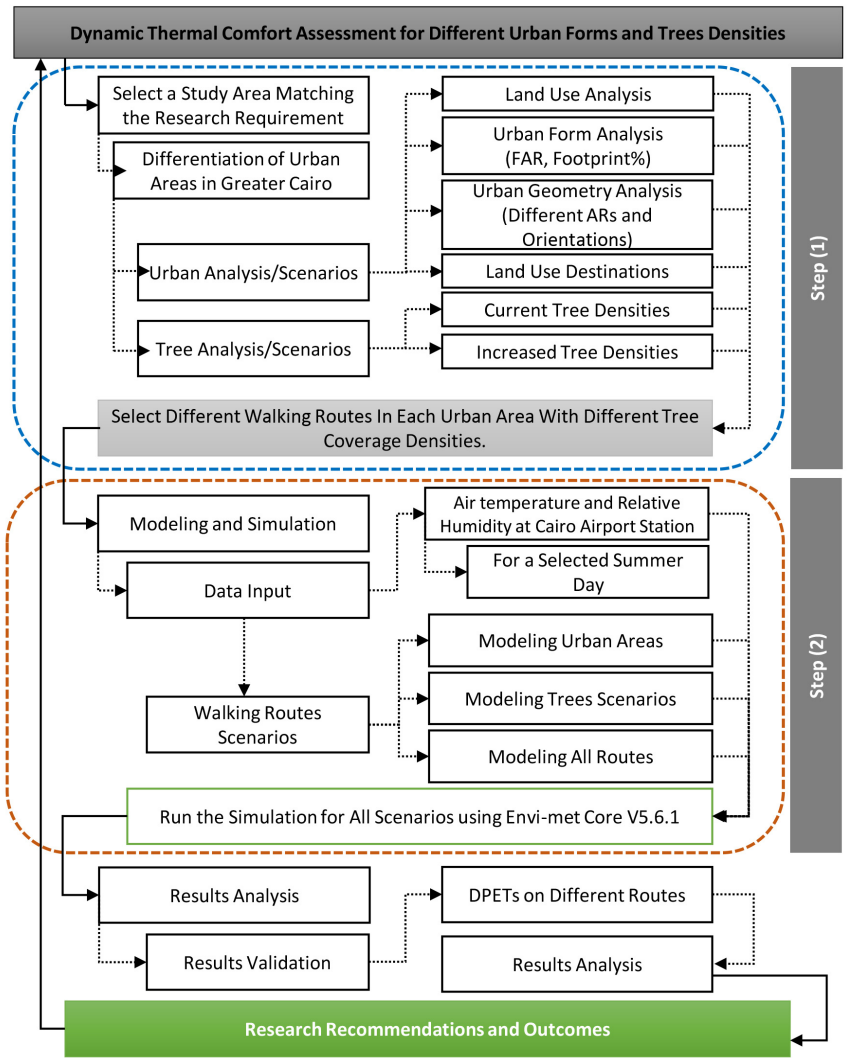

Figure 1. Research methodology.

In step (1), a city that suffers from very high levels of heat stress and high solar radiation with variety between different areas was selected to obtain better results for different urban cases before and after applying trees scenarios. Also, the study areas included land use destinations that people would be moving between and access to public transportation modes. In the same step, a complete urban geometry and tree analysis was applied to understand how the existing urban geometries and proposed tree variations impacted the results. In step (2), scenarios were simulated after completing all meteorological inputs for the city and modeling different scenarios and routes. Then, the simulation results were validated and analyzed to understand the differences in each urban area with different tree coverage densities.

2.1. Step (1): Study Area Selection and Analysis

The city selected as the study area was the metropolitan area of Cairo, which suffers from heat stress as the city is located in a dry desert in a subtropical climatic region and has a warm summer climate based on the Köppen–Geiger climate classification [35]. During summer (June to August), it is hot and dry with an average temperature of around 28 °C [36,37] and a maximum average temperature of around 35 °C. The urban heat island effect (UHI) appears clearly in the city of Cairo. In previous studies, it was found that the UHI ranges from 0.5 to 3.5 °C [38]. The maximum observed difference was 10 °C compared to the surrounding rural or desert areas [36,39,40]. Cairo City is very large and has lots of urban variety as the city has grown over many decades and is still evolving and growing rapidly [41,42]. The selection of Cairo City allowed different urban areas with different urban forms, morphologies, and tree scenarios to be studied, which suited the purpose of this study. The selection of the study areas within Cairo was carried out carefully to ensure that there were appropriate differences between them in terms of urban forms and morphologies as this helped clarify the different intensities of the impacts on pedestrians while walking, especially the impacts of trees in the respective situations and when the tree densities were increased.

2.1.1. Urban Analysis of Study Areas

As shown in Figure 2, five study areas were selected (Bulaq Ad Daqrur (known as Bulaq), Khedival Cairo (known as Downtown), Mohandisen, New Cairo, and Mivida). They were characterized by different urban morphologies, and the tree density varied between them. Additionally, the locations of the selected study areas were different, as three of them (Bulaq, Downtown, and Mohandisen) were very close to the center of Cairo (within a 4 to 5 Km range) and two areas (New Cairo and Mivida) were suburban areas (around 17–29 Km away from the city center). Table 1 shows the local climate zones and the main urban characteristics of each study area. As shown in Figure 3, the selected study areas had similar sizes, as they varied between 18 and 22.9 hectares, and changes in the solid-to-void ratio (footprint of buildings divided by the site area) were obvious. It varied from 75% solid in Bulaq to 61% and 59% in Mohandisen and Downtown to a low solid percentage of 29% in New Cairo and a very low solid percentage of 13% in Mivida. Also, the green areas were different, as they were 0% in Bulaq and Khedival Cairo, with a very limited green area of 3% in Mohandisen and good amounts of greenery of 12% in New Cairo and 23% in Mivida.

The floor area ratio (FAR, the total built-up area divided by the site area) changed between the different areas as a reflection of the footprint percentage and building heights. It ranged from a high of 5.2 in Bulaq to moderate values of 4.58 and 4.31 in Downtown and Mohandisen to a low value of 1.15 in New Cairo and a very low value of 0.39 in Mivida. Figure 4 shows the variation in building heights and the urban destinations (including public transportation) in each area. The maximum building height was in Mohandisen, where most of the buildings were in the range of 28 m to 40 m (9 to 13 floors). Medium building heights in the range of 22 m to 27 m (7 to 9 floors) were observed in Bulaq and Downtown. The lowest buildings, in the range of 9 m to 12 m (3 to 4 floors), were in New

Cairo and Mivida. A greater number of public transportation facilities were located in Downtown, which had a metro station and a bus stop. Two bus stops were located in Bulaq and Mohandisen, and one bus stop was located in New Cairo. No public transportation facilities were located in Mivida, as it is a gated community that is more car-centric, and the walking circulation depends on internal movements between the community amenities. The different urban analyses showed that there were too many differences between the study areas and that the selected study areas had significant variety. This was reflected in the results, helped to cover more cases, and provided a better understanding of the impact of each change.

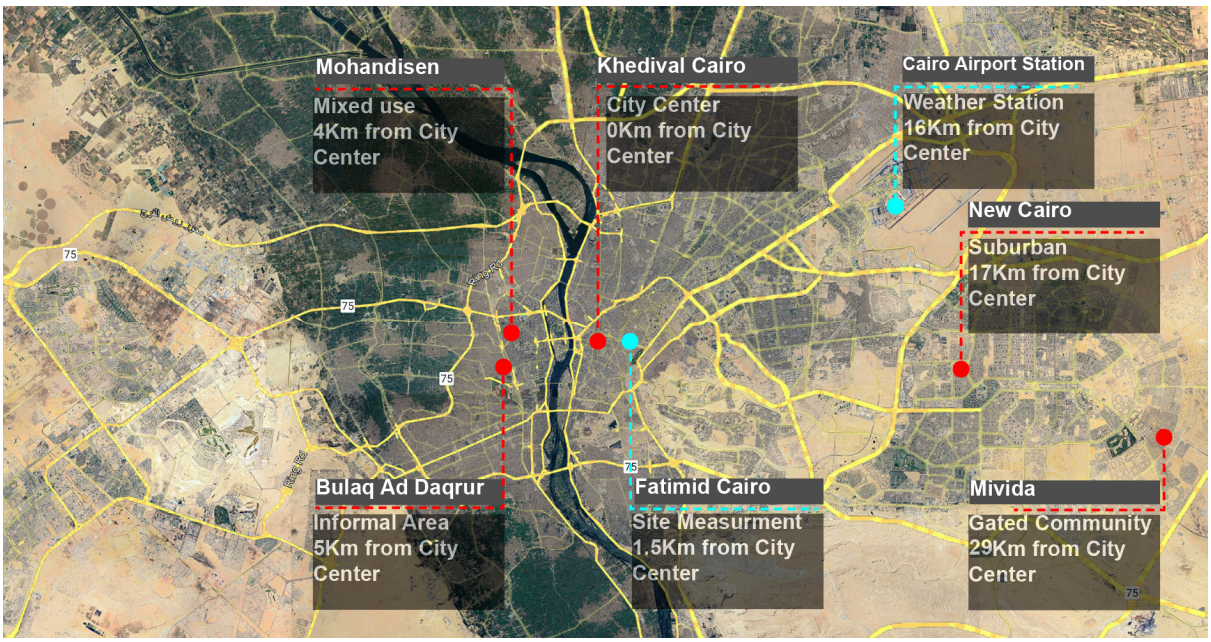

Figure 2. Selected study areas, Cairo weather station, and site measurement location.

Table 1. The climate zones and characteristics of the urban areas.

Study Area	Bulaq Ad Daqrur (Bulaq)	Khedival Cairo (Downtown)	Mohandisen	New Cairo	Mivida
Local Climate Zone (LCZ) *	LCZ2 Compacted midrise	LCZ2 Compacted midrise	LCZ1 Compacted high rise.	LCZ5 Open midrise	LCZ6 Open low rise
Urban Classification	Informal area	City center	Business center	Suburban community	Gated community
Aspect ratio	Deep	Moderate	Moderate	Open canyons	Shallow canyons
Mixed uses and car/transit orientation	Low mixed uses, transit-oriented	High mixed uses, transit-oriented	High mixed uses, transit- and car-oriented	Low mixed uses, car-oriented	No mixed uses, car-oriented
Density	Very high	Moderate	Moderate	Low	Very low

* Local climate zones (LCZs) were classified as explained in [43,44].

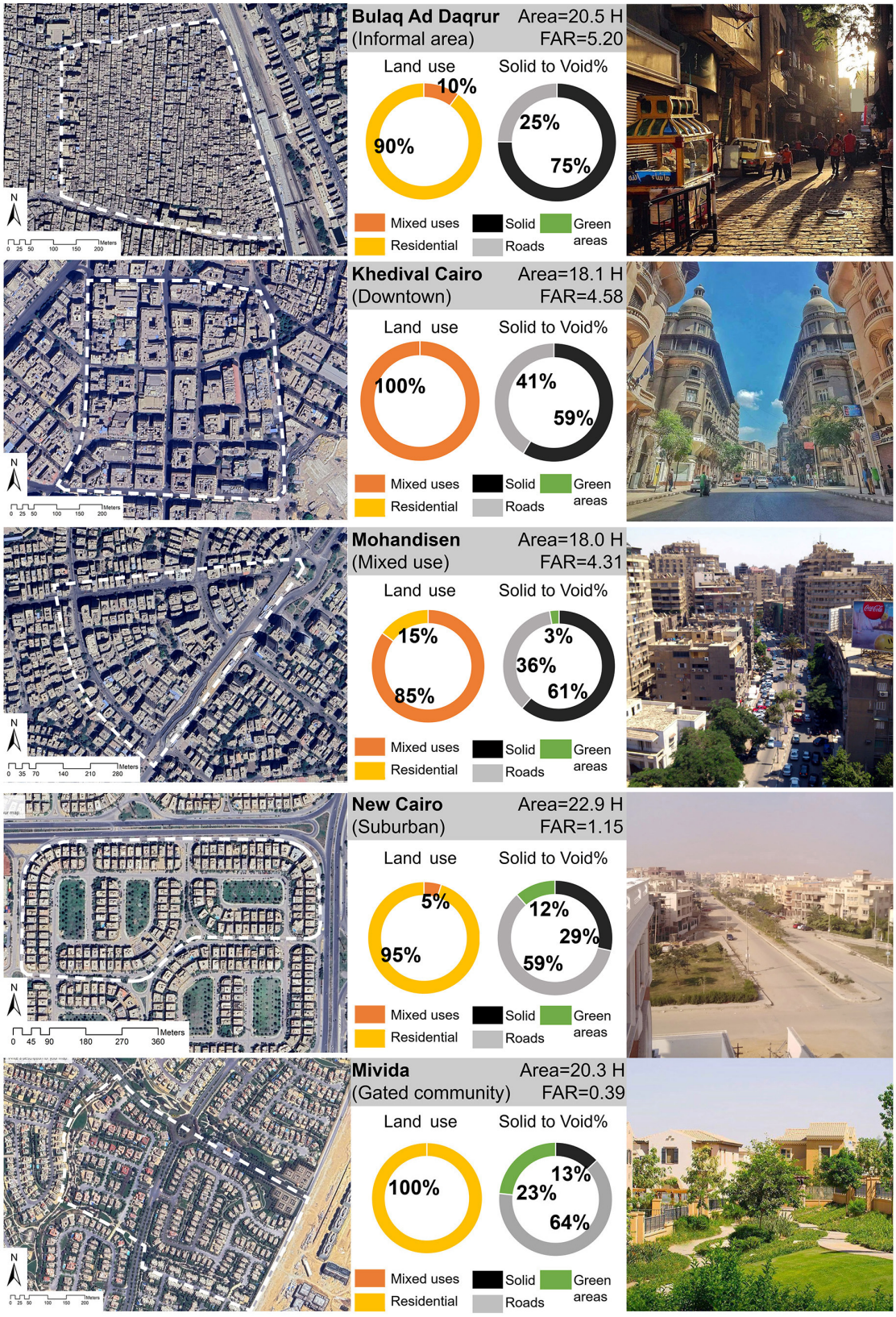

Figure 3. Urban analysis of study areas.

Figure 4. Study areas (building heights, street names, and main urban features).

2.1.2. Tree Scenarios

The study areas not only had various urban morphologies and changes; they also had good variety with respect to tree density. As shown in Figure 5, the existing tree coverage percentages varied significantly between the study areas. They were very low (2.1%) in Bulaq and reached 6.2% in Downtown and 7.8% in Mohandisen. These percentages were very low, indicating that there were only a few open spaces in these three study areas. On the contrary, the percentages of tree coverage for open spaces were moderate in New Cairo (9.4%) and high in Mivida (13%), indicating that open spaces occurred more frequently in these study areas.

Figure 5. Current and proposed tree densities for each study area.

To investigate the impacts of trees in each area, this study not only tested the current tree situations but also scenarios with increasing tree densities. The proposed increases in tree densities are indicated on the right side of Figure 5. They were tested to understand the impacts of increases in trees in each urban morphology to better understand how this would impact the DPET of people walking in each study area. Tree density was increased to achieve a good distribution of trees and good tree spacing on roads and in parks. Adding trees led to different tree coverage percentages in each study area, as shown in Figure 5. In Bulaq, increasing the number of trees helped to increase the tree coverage percentage of the open spaces from 2.1% to 26.6%, which was significant because of the limited open space areas. In Downtown, it was increased from 6.2% to 26%, which was also a significant increase, as the open space areas were bigger than in Bulaq. A similar increase from 7.8% to 25% occurred in Mohandisen, as the open space areas were similar to those in Downtown. In New Cairo and Mivida, the tree coverage percentages were similar, with limited increases from 9.4% to 19% in New Cairo and from 13% to 21% in Mivida. However, many more trees were added than in the other areas. Because of the bigger open spaces, the density increased at lower rates compared to the other areas.

Testing these tree scenarios and the impacts of low and high densities of trees in each study area provided a comprehensive understanding of how trees perform in each urban morphology/local climate zone and helped clarify which tree density is required for each urban morphology. This will lead to optimization of the use of trees in each urban area, as shown in previous studies [21,45].

2.1.3. Walking Routes

As this study focused on the dynamic thermal comfort of pedestrians, the selection of the walking routes in each of the different scenarios was very important. As the study results focused on the DPETs of the routes and locations, the design of each route (in relation to different aspect ratios, orientations, and trees densities) was the focus of this study. Therefore, in each study area, two routes were provided to ensure that the majority of the area was covered by walking routes. The walking routes did not overlap, and each route connected the main urban features in each study area, such as the transportation stations, retail areas, amenities, parks, etc. [1]. Figure 6 shows the proposed routes in each study area. They were designed to pass the different elements in each area. In Bulaq, the routes passed different aspect ratios and orientations. Route (A) started at the bus stop, moved through the wide eastern canyon (H:W 1:0.75), then moved through the narrow northern canyon (H:W 3:1) to reach a residential destination. Route (B) started at the second bus stop, moved through the narrow eastern canyon (H:W 3:1), then moved to a second residential destination through the narrow northern canyon (H:W 1:2.5). Similarly, in Downtown, route (A) started at the metro station, moved through a wide eastern canyon (H:W 1:1.25), through a moderate northern canyon (H:W 1:1), then through a moderate eastern canyon (H:W 1:1.25) to reach a retail destination. Route (B) started at the urban park next to the bus stop, moved through a moderate eastern canyon (H:W 1:1), a moderate northern canyon (H:W 1:1.3), then a moderate eastern canyon (H:W 1:1.5) to reach the coffee shop area.

In Mohandisen, route (A) started at the bus stop, moved through a moderate eastern canyon (H:W 1:1) and a northern canyon, passing by an urban park with dense vegetation, and moved through an eastern canyon (H:W 1:1) to reach a residential destination. Route (B) started at the same point at the bus station, moved through a shallow northeastern canyon (H:W 1:3.5) for most of the trip, then through a moderate northwestern canyon (H:W 1:1). In New Cairo and Mivida, the routes passed different urban contexts, including very shallow roads (H:W 1:3) and urban parks, as shown in Figure 6.

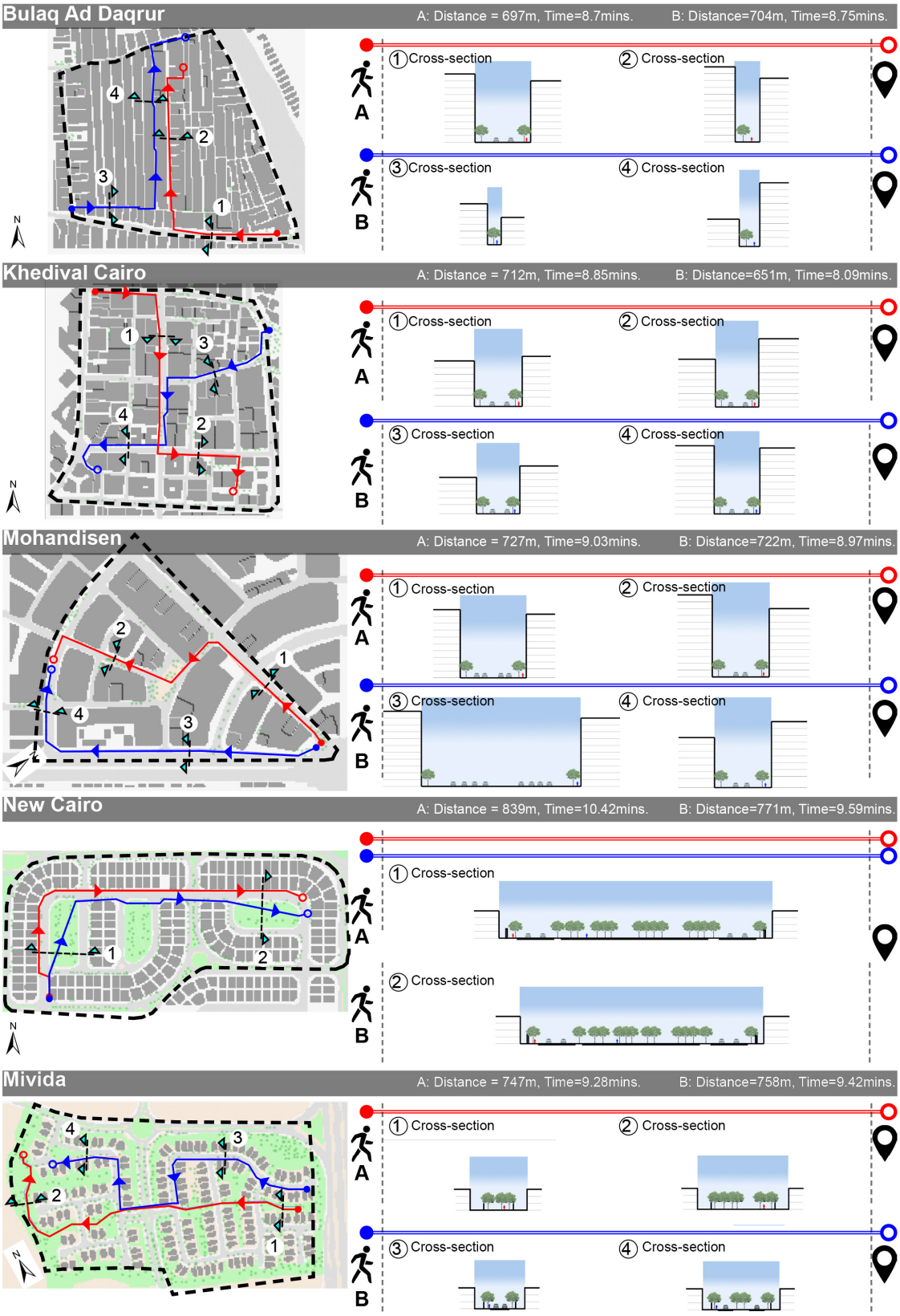

Figure 6. Alignment of pedestrian routes and cross-sections of different segments in each study area.

The routes were designed to be as long as possible as this study was more focused on long-distance pedestrian routes, which represent the main research gap [1]. Therefore, all designed routes were longer than the walking distance range, which is 500 m [4]. The route lengths in Bulaq, Downtown, Mohandisen, New Cairo, and Mivida were A = 697 m and B = 704 m, A = 712 m and B = 651 m, A = 727 m and B = 722 m, A = 839 m and B = 771 m, and A = 747 m and B = 758 m.

The different routes in each study area were tested under the two tree scenarios (the current tree coverage and the proposed tree coverage). This study was applied to 20 different routes with different morphologies and urban tree densities. This variation in the tested routes provided more detailed and variable results, which enriched the research findings.

2.2. Step (2): Data Input, Model Set-Up, and Measuring Points

The software used to run the simulations for the different cases in each study area under different tree scenarios was ENVI-met V5.6.1, Winter 2023. All of the information required for the model was provided, representing existing urban configurations (material and soil) of common materials in Cairo, as well as meteorological data.

2.2.1. Model Set-Up and Geometry

The model's location was 30.02 latitude and 31.22 longitude. This was obtained from the ENVI-met V5.6.1, Winter 2023 database by selecting the location of Greater Cairo in the ENVI-met application "Spaces". As shown in Table 2, all models were created using the following model geometry: materials, soil, and trees.

Table 2. Model set-up and geometry for each study area.

Model Information	Bulaq	Downtown	Mohandisen	New Cairo	Mivida
Area size (grids)	X = 205, Y = 186, Z = 30	X = 167, Y = 170, Z = 30	X = 233, Y = 192, Z = 27	X = 259, Y = 121, Z = 12	X = 239, Y = 128, Z = 8
Grid resolution (m)	X = 3, Y = 3, Z = 3	X = 3, Y = 3, Z = 3	X = 3, Y = 3, Z = 3	X = 3, Y = 3, Z = 3	X = 3, Y = 3, Z = 3
Orientation	0	0	−50	0	32
Split lower grid box into 5 sub-cells	Yes				
Telescoping applied	Not applied, as the maximum building height was not very high				
Maximum model height *	90 m	90 m	81 m	36 m	24 m
Nesting grids **	5 grids, sandy soil				
DEM	Not applied, as the site was flat				
Soil	Asphalt for roads, concrete for sidewalks and under buildings, loamy soil for green areas.				
Building materials	Default wall—moderate insulation				
Tree model and size	Latin name: *Acer platanoides* *** Height = 15 m; crown width = 7 m				

* The model's height was more than double the height of the tallest building, as recommended by the software [34]. ** Nesting grids were added, in addition to five cells from the boundary sides of the model being kept empty, as recommended by the software developers [34]. *** *Acer platanoides* was selected from the ENVI-met database as it met the required criteria of having a large canopy, a high LAD, and a good canopy height, matching the recommendations in [46–49]. Different trees would have different impacts and performances [50]. This study used one recommended tree characteristic to measure the impacts of other elements such as the aspect ratio, orientation, canyon side, and tree density.

2.2.2. Simulation Configuration

The simulation was configured for a representative summer day (i.e., the hottest day of July: 2 July 2023) as the hottest days in summer occur between June and July based on an analysis of 30 years of data from the Cairo Airport station [51]. The same air temperature,

relative humidity, and wind speed were added to ENVI-met for each hour of the simulated day, and climate data were imported from the Cairo Airport weather station for all study areas as the main focus is the analyze the impact of the urban form and trees densities under the same climate conditions. Its location is shown in Figure 2 [52,53]. The starting time of the simulation was 1:00 a.m., and the total duration was 24 h. ENVI-met simple forcing was used for the metrological data.

2.2.3. Simulation Outputs

Output data were extracted using the ENVI-met ''Bio-met" to calculate the DPET and SPET values of each route in each study area under the different tree scenarios. The results were exported for five different hours during daytime from sunrise until sunset. The chosen hours were selected to cover the different times when people perform activities and move between different destinations in each urban area. Table 3 shows the selected hours and the trips expected at each hour. The dynamic thermal comfort (DPET), steady thermal comfort (SPET), dynamic skin temperature (T Skin), and average core temperature were exported for each route in each study area for both tree scenarios for the five selected hours (9:00, 11:00, 13:00, 15:00, and 17:00). These hours not only covered the whole daytime but also covered the majority of the pedestrian trips during daytime.

Table 3. Selected hours and trips expected at each hour.

Hour	9:00 a.m.	11:00 a.m.	13:00 p.m.	15:00 p.m.	17:00 p.m.
Activity (1)	Trip to work	Trip to park	Work break	Leaving work	Leaving work late
Activity (2)	Trip from school		Nursery school closing	Leaving school	Trip to park
Activity (3)	Trip to park			Late break	Shopping trip

Table 4 below shows the pedestrian data and the thermal conditions of the starting point of each route as applied in ENVI-met (Biomet). These conditions were applied to all routes for each hour considering the start of a walk with static thermal conditions, as explained in Table 4. These static thermal conditions were exported from the Downtown study area and unified for all other study areas to maintain the same static thermal comfort conditions at the starting points.

Table 4. Pedestrian data and the initial climate conditions at each hour.

Pedestrian Data (for All Hours) *				**Initial Climate Conditions at 9:00 ****			
Gender	Age	Clothing	Speed	Air temperature (°C)	Wind speed (m/s)	MRT	Spec. Humidity
Male	35	0.9 clo ***	1.34 m/s	28.7	0.46	49.04	11.11
Initial climate conditions at 11:00 **				Initial climate conditions at 13:00 **			
Air temperature (°C)	Wind speed (m/s)	MRT	Spec. Humidity	Air temperature (°C)	Wind speed (m/s)	MRT	Spec. Humidity
31.6	0.45	56.37	10.84	33.5	0.44	59.35	10.71
Initial climate conditions at 15:00 **				Initial climate conditions at 17:00 **			
Air temperature (°C)	Wind speed (m/s)	MRT	Spec. Humidity	Air temperature (°C)	Wind speed (m/s)	MRT	Spec. Humidity
34.1	0.44	57.63	10.22	33.3	0.43	47.46	10.38

* Default personal data in ENVI-met (category named Michael average). ** The current average Downtown microclimate was used for all. *** The selected value (0.9 clo) represents the default value for clothes insulation, not the summer low value because of the study conditions, as this study mainly focused on daytime trips, which are mainly related to work or school, as explained in Table 3, and need more formal clothes. Also, due to cultural aspects of the people in the study area (people usually wear long sleeves and long trousers), using the default value of 0.9 clo was more suitable for this study.

2.3. Results Validation

The results (air temperature and relative humidity, as they were more stable than the mean radiant temperature and wind speed [31,54]) of each study area model were compared with the airport station data and data measured on the same day from another study at the center of Cairo. These site measurements were performed using a mobile weather station at a height of 1.1 m from the ground in an outdoor space on Al Muizz Street on the same day (the 2nd of July) in 2012 [51]. The locations of both the site measurements and the weather station are shown in Figure 2. These data are a limitation of this research. Due to a limited research team, limited funds, and security restrictions, which also affected previous studies in Cairo [21,27], the weather station at Cairo Airport provided input data for all cases and the simulation results were validated via comparison with the weather station data and the site measurements on the same day (2nd of July). It was clear that the results were aligned with the data from the Cairo Airport station and the site measurements. As shown in Figure 7, the air temperature and relative humidity had the same values in all models in relation to the station and site measurements. The changes were very minor, and the charts had the same linear shapes. To ensure that all results had good agreement with the measurements, the root-mean-square error (RMSE) and the degree of agreement (d) were calculated for all model results and both measurements. Tables 5 and 6 show the RMSE and d for air temperature and relative humidity. The RMSE values ranged between 1.3 °C and 1.9 °C for the station-measured air temperature and between 1.0 °C and 1.7 °C for the site measurements. The d values ranged between 0.93 and 0.95 for the station-measured air temperature and between 0.92 and 0.98 for the site measurements. For the relative humidity, the RMSE ranged between 4.4% and 9.8% for the station measurements and between 7.1% and 10.3% for the site measurements. Based on these results and comparisons with similar studies conducted in Cairo City [21,27,45], the simulation results are valid, and the output values represent the current situation in Cairo.

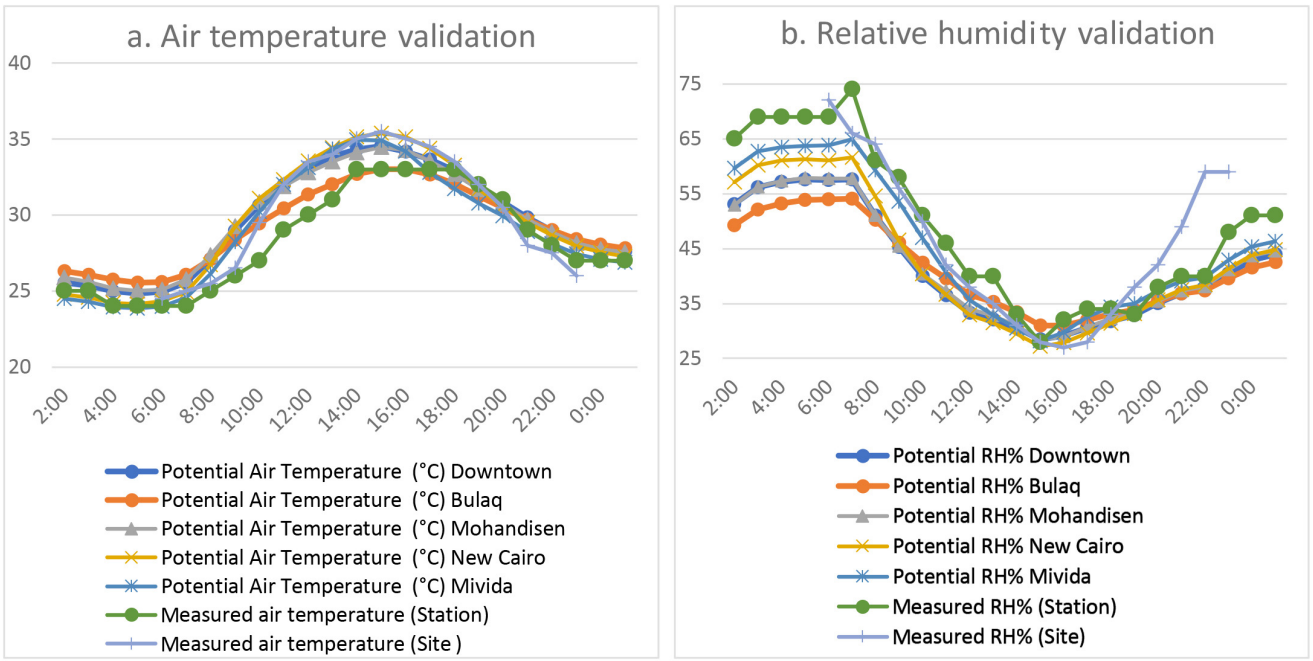

Figure 7. Results validation. (**a**) Air temperature. (**b**) Relative humidity.

Table 5. RMSE and d for air temperature values.

	Potential Ta (°C) in Downtown	Potential Ta (°C) in Bulaq	Potential Ta (°C) in Mohandisen	Potential Ta (°C) in New Cairo	Potential Ta (°C) in Mivida
RMSE (station)	1.686	1.337	1.708	1.886	1.59
RMSE (site)	1.168	1.699	1.248	1.041	0.969
d (station)	0.937	0.949	0.932	0.931	0.948
d (site)	0.97	0.921	0.964	0.979	0.981

Table 6. RMSE and d for relative humidity values.

	Potential RH% in Downtown	Potential RH% in Bulaq	Potential RH% in Mohandisen	Potential RH% in New Cairo	Potential RH% in Mivida
RMSE (station)	8.634	9.83	8.364	7.014	4.418
RMSE (site)	9.892	10.342	9.597	8.867	7.09
d (station)	0.884	0.823	0.89	0.932	0.973
d (site)	0.824	0.775	0.833	0.873	0.92

3. Results

The results are presented in two stages. In the first stage, the DPET, SPET, T Skin, and avg. TCore are presented for each route in each study area before and after increasing the tree density to understand the impacts of urban morphology, urban trees, and other elements such as the SPET and T Skin on the DPET. In the second stage, the DPET values of each route are compared. In the first case, the DPET of each route is compared to that of the same route after adding trees to understand the trees' impact. The trees' impact is also assessed by analyzing the thermal classification percentages of the walks in both tree scenarios. In the second case, both routes in each study area are compared before and after increasing trees, and in the third case, each route is compared with the other routes in the other study areas. These detailed and varied comparisons provide a complete understanding of how different factors impact dynamic thermal comfort.

3.1. SPET at the Starting Point

To obtain a complete understanding of the static thermal comfort at the starting point of each route in each study area with different tree densities, Figure 8 shows the exact SPET at the starting point of each route. These changes in the SPET values were considered while analyzing the DPET of each route. As shown in Figure 8, the SPET at the starting point of Bulaq route (B) was higher for the hours 11:00, 13:00, and 15:00, and in Mohandisen, the starting point for both routes (A and B) was lower. This was considered in the analysis of the results, as the most important part was how the DPET increased or decreased during the walk. Therefore, if the starting point was too high, the DPET would decrease, and if the starting point was too low, the DPET would increase during the walk. The main impact of the different urban morphologies and tree densities was how the DPET increased or decreased during the walk.

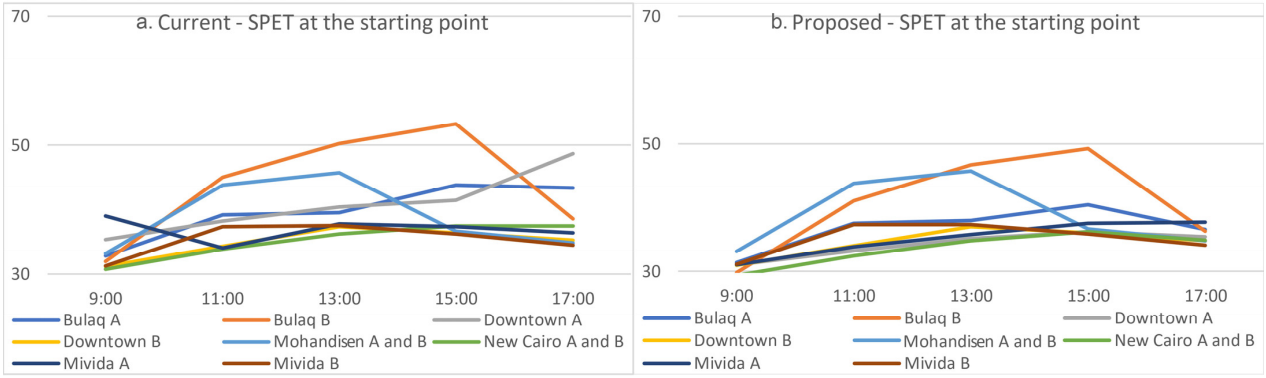

Figure 8. The SPET value at the starting point of each walking trip: (**a**) the current tree scenario; (**b**) the proposed tree scenario.

3.2. DPET Results

In Bulaq (Bulaq Ad Daqrur), as shown in Figure 9, at 9:00 both routes (A and B) had almost the same starting DPET value. The difference between them was 1.5 °C. Then, after reaching the end of the eastern route, the difference in the DPET reached 3.5 °C. Once moving on the northern road, both routes' DPET values started to decrease. On route A, the DPET decreased from 36.5 °C to 33 °C, and on route B, the DPET decreased from 34 °C to 31.2 °C at the end. Adding trees helped to reduce the DPET increase during movement on route A to a maximum increase of 1 °C, and route B had almost the same DPET value until the end.

At 11:00, the tight canyons on route B helped, with a total reduction of 5 °C. The opposite result was observed on route A, which had an increase of 4.5 °C on the eastern road over a very short distance. Then, on the northern road, the DPET started to decrease again and almost reached the same value as the starting point. This clearly showed the impact of the wide eastern canyon. Adding more trees led to the same performance for route B but decreased the impact of the eastern canyon on route A, as the increase was 1.5 °C instead of 5 °C.

At 13:00, when the shade from the buildings had almost vanished, the DPET on route A increased by 5 °C on the eastern route, then decreased slightly by 3 °C by the end of the northern road. Route B showed an irregular reduction within 1 °C from the beginning until the end. Increasing the tree density led to significant decreases in the DPET. On routes A and B, the trees helped to reduce the DPET by 3.5 °C and 7 °C.

At 15:00, the tight canyons on route B led to a significant DPET reduction of 6 °C at the end of the walk. On route A, the wide eastern canyon led to an increase of 5 °C. Then, the tight northern canyon helped to reduce this increase to reach the same value as the starting point (40 °C). Adding trees to both canyons helped to avoid this increase in the eastern canyon on route A, as it limited the increase to only 1 °C. On route B, the same regular reduction occurred but with DPET values that were reduced by 8 °C. At both hours (13:00 and 15:00), small fluctuations in the skin temperature occurred on route A due to the impact of the wide eastern road, which had strong heat stress. Then, once on the tight northern route, due to the good urban shading, the skin temperature dropped gradually until the end of the walk.

At 17:00, both roads showed good DPET values, with a slight increase on route B that reached 2 °C, and the values ranged between 36 °C and 40 °C. Adding trees to both routes helped keep the DPET values stable for the whole trips, with DPET values around 35 °C on both routes.

The results for Downtown (Khedival Cairo) are shown in Figure 10. At 9:00, both routes (A and B) showed the same regular increase in DPET, which increased by 5 °C. This increase only took place within the wide eastern canyon. Adding trees helped to reduce the DPET increase by 50%, as it ranged between 2.0 °C and 2.5 °C on both routes. Reducing the DPET values of the whole route to within 30 °C to 33 °C kept them under the skin temperature.

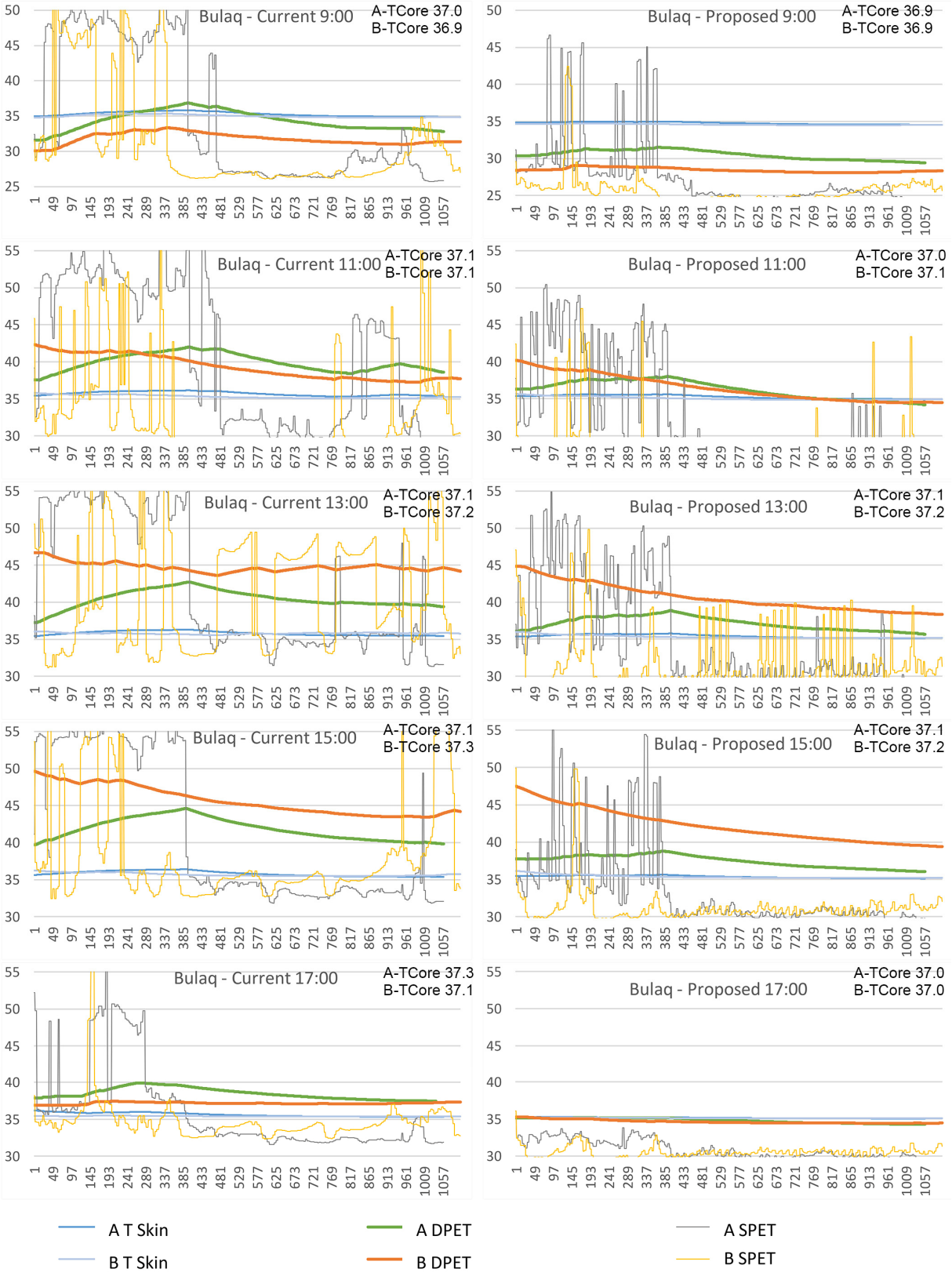

Figure 9. DPET, SPET, skin temperature (T Skin), and average core temperature (TCore) results for Bulaq routes (A and B) in both tree scenarios (current and proposed) at Z = 1.5 m. Y axis = °C and X axis = seconds while walking each route.

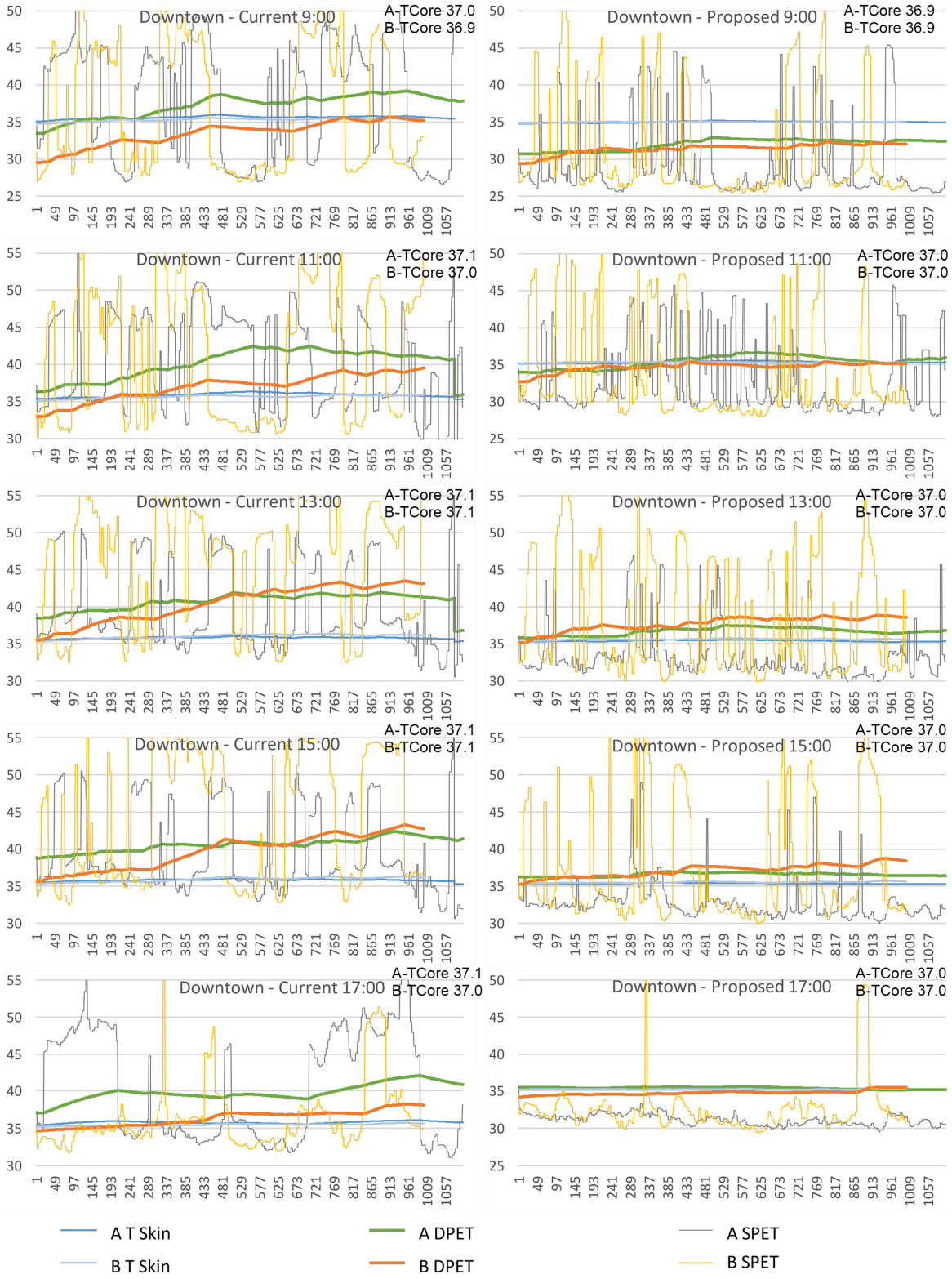

Figure 10. DPET, SPET, skin temperature (T Skin), and average core temperature (TCore) results for Downtown routes (A and B) in both tree scenarios (current and proposed) at Z = 1.5 m. Y axis = °C and X axis = seconds while walking each route.

At 11:00, the same regular increase in DPET occurred. It was lower on route A, which started at DPET = 36 °C, reached 42.5 °C, and ended at DPET = 41 °C for an increase of 5 °C. Route B showed a regular increase, especially on the eastern roads, with an increase of 6.5 °C. Increasing the tree density helped to keep the DPET almost stable during the whole walk within the range of 34 °C to 36 °C and in the range of the skin temperature

At 13:00, route A showed a good performance with a 2.5 °C increase. However, on route B, which started at a lower DPET value, the eastern canyons led to a significant increase of 7.5 °C, and the DPET reached 43 °C at the end of the walk. Increasing the tree density helped reduce the values at the starting points for both routes. Route A stayed within the same range until the end of the walk, and the increase on route B was significantly reduced. It only reached 3 °C, which was 60% lower.

At 15:00, a similar performance was observed. A slight increase in the DPET on route A reached 3 °C, which reflected the good cooling performance of the northern road. On route B, the same increase of 7 °C occurred by the end of the walk, with regular increases on the eastern roads and steady DPET values on the northern road. However, route B started with a DPET value that was 3.5 °C lower than that of route A's starting point, and route B ended 1 °C higher than route A. This was because of the impact of the canyon orientation. Increasing the tree density led to similar performances, and both routes maintained good DPET values. The values on route a were between 36 °C and 37.5 °C, and the slight increase on route B reached 1.5 °C.

At 17:00, due to the sun's direction, a noticeable increase in DPET on route A reached 5 °C at the end of the walk. Route B was in the shade for most of the walk, and that helped to maintain a slight increase in the DPET, which reached 3.0 °C. On both routes, adding trees helped to keep the DPET values steady from beginning to end.

The results for Mohandisen are shown in Figure 11. At 9:00, route A showed a regular slight DPET increase until reaching 37.5 °C at the end of the walk, which was an increase of 4 °C. Route B increased significantly to reach 45 °C, an increase of 10.5 °C, at the end of the northeastern shallow canyon, then started to decrease while moving within the moderate northwestern canyon to reach 42.0 °C at the end. Adding trees to both routes helped route A maintain almost steady DPET values of 33 °C to 34 °C and helped route B reduce the massive increase in the DPET by 2.5 °C, as it started at DPET = 33.0 °C, reached a maximum value of 42.0 °C, and decreased to 38.0 °C at the end.

At 11:00, both routes started with very high DPET values. Route A decreased by 2.5 °C then increased again to end the walk with the same value. Route B increased to reach 52.5 °C at the end of the shallow northeastern canyon then decreased in the moderate northwestern canyon to reach 48.5 °C at the end. Increasing the tree density somewhat controlled the massive increase and the extreme heat stress values on both routes. On route A, the trees helped to reduce the high starting value by 3.0 °C to end the walk with DPET = 42.5 °C. On route B, the trees helped to avoid any increase in the DPET above 50.0 °C, as the maximum DPET value recorded at the end of the shallow northeastern canyon was 49.0 °C, which was 3.5 °C lower than in the scenario with lower tree density. Route B started at DPET = 46.0 °C, and the walk ended with a lower DPET value = 45.0 °C. T Skin fluctuation occurred at both 9:00 and 11:00 due to the massive heat stress and a lack of shading, which led to an increase of 1.5 °C in the skin temperature.

At 13:00, a very similar DPET performance was observed. The only difference was that both routes had higher DPET values at 13:00. Route A fluctuated slightly (within 2 °C) because of the impact of the moderate canyons and the urban park in the middle until reaching the same value as the starting point at the end. Route B had a very high DPET value at the beginning of the walk (50.5 °C) then increased to reach 54.0 °C at the end of the shallow northeastern canyon and decreased to reach the same value as the starting point at the end of the route. Increasing the tree density was crucial at this hour when the building's shade had almost vanished. On route A, it provided a good DPET reduction of 3 °C at the end of the route. On route B, it helped to keep the DPET under 50.0 °C for the whole route with a reduction of 1.5 °C at the end.

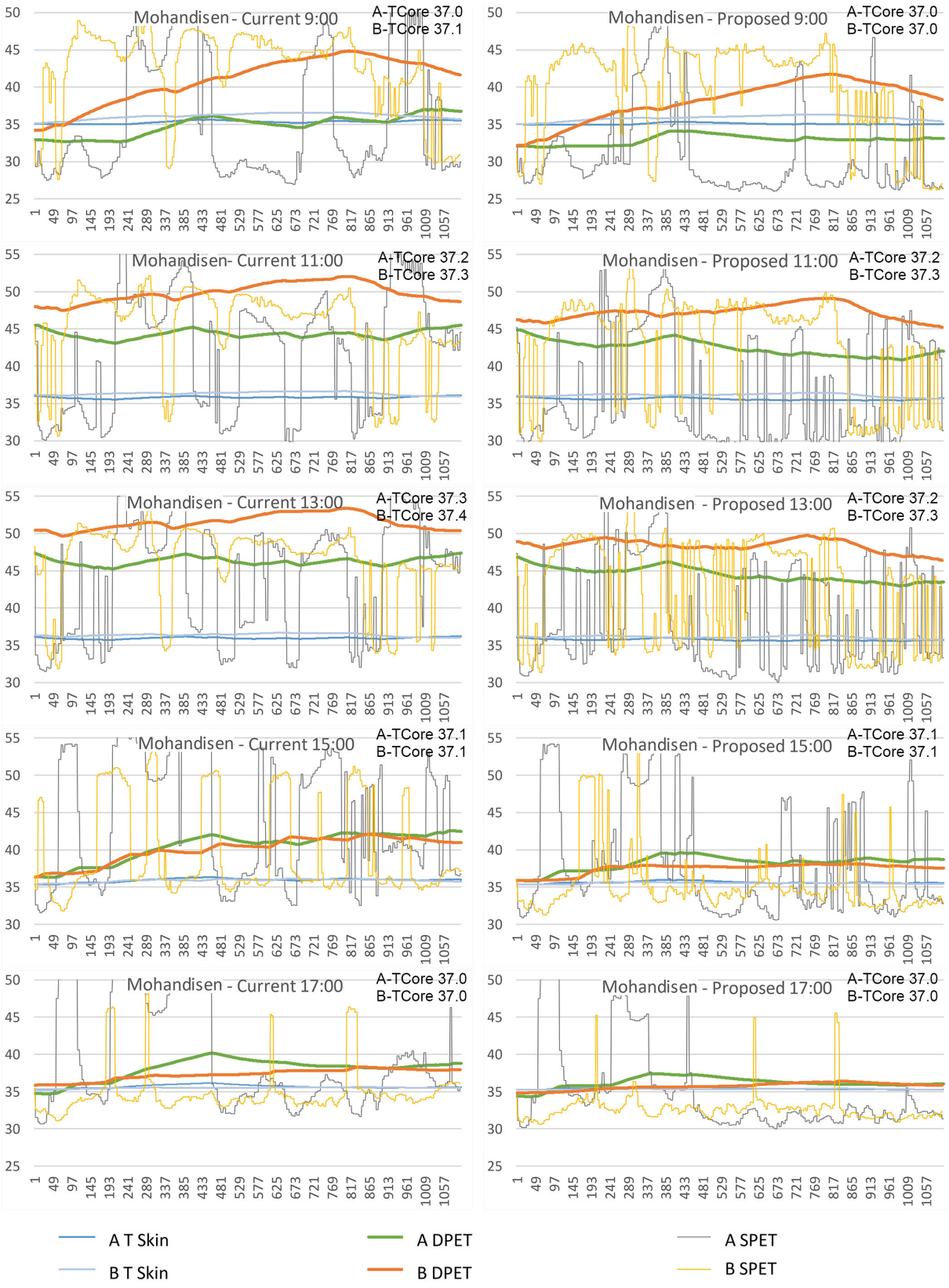

Figure 11. DPET, SPET, skin temperature (T Skin), and average core temperature (TCore) results for Mohandisen routes (A and B) in both tree scenarios (current and proposed) at Z = 1.5 m. Y axis = °C and X axis = seconds while walking each route.

At 15:00, when urban shading took place, the DPET values decreased significantly on both routes. Routes A and B both had slight regular increases in DPET of 7 °C at the end. Adding trees enhanced the performance more when tree shading was mixed with building shading, which limited the DPET increase to 3.0 °C to 4.0 °C on both routes. Here, the importance of urban shading when mixed with tree shading appeared for these moderate canyons at one of the peak hours (15:00).

At 17:00, the importance of urban shading appeared again, and it helped to keep the DPET values on both routes under 40.0 °C. On route A, the DPET was 35.0 °C at the starting point. It reached 40.0 °C before the urban park then decreased to 38.0 °C at the end. On route B, the DPET showed a regular slight increase of 1.5 °C at the end. Increasing the tree density on both routes helped to keep the DPET stable for the whole walk and within the range of the skin temperature.

In New Cairo, as shown in Figure 12, the good amounts of green open spaces (12%) and trees (9.4%) in the current situation helped to keep the DPET values lower. However, urban shading was very limited due to the lower heights of the buildings and the applied plot setbacks, and the impact of trees was essential to enhancing the thermal comfort of pedestrians. At 9:00, both routes had regular gradual increases that reached 8 °C at the end. Higher tree density helped to reduce these big increases. Route A showed a quick DPET increase of 4.5 °C while walking on the sidewalk then stayed steady until the end. Route B had a regular gradual increase of 4.5 °C.

At 11:00, both roads showed regular DPET increases that reached 9.0 °C at the end. Higher tree density helped to reduce the increases on both routes to only 4.5 °C, which was under the skin temperature. At 13:00, the same thermal performances took place with DPET values of 35.0 °C on both routes. Then, regular increases took place until reaching 43.0 °C at the ends of both routes for increases of 8.0 °C. In the scenario with increased tree density, the trees helped to reduce the increases to only 3.5 °C at the ends of both routes.

At 15:00, similar thermal conditions were observed with regular gradual increases of 9.0 °C on routes A and B. Then, the increase in tree density reduced the DPET increases significantly to only reach 2.5 °C at the ends of both routes. At 17:00, routes A and B had the same DPET value (34.0 °C) at the starting points. Then, the same increase happened, but it was lower than at the other hours, as it reached 5 °C, and both routes had values of 39.0 °C at the end. Increasing the tree density led to both routes maintaining very stable DPET values ranging between 34.0 °C and 35.0 °C from beginning to end.

The results in New Cairo showed the importance of trees in both scenarios (low tree density and high tree density). When the urban form is very open and urban shading has almost vanished, tree shading is a proper solution that can be used to enhance microclimate conditions. This case also showed that the surface material has a limited impact, as walking inside the park or on the sidewalk resulted in a slight performance change as long it occurred under the same tree's coverage.

In Mivida, as shown in Figure 13, similar DPET performances took place as the DPET mainly depended on the tree cover percentage due to the absence of building shading because the buildings were short (villas with G + 2) and because of the setbacks inside each plot, which set all buildings away from both the sidewalk and the walking trails inside the parks. At 9:00, route A had a higher DPET value. The good density of the trees inside the urban park helped to reduce the DPET, and both routes reached the same DPET value (34.0 °C) at the road crossings. Then, route A increased slightly by 1.5 °C at the end, and route B stayed almost the same until the end. Increasing the tree density, which occurred more inside the parks than on the streets, helped to keep route A cooler than route B by 2 °C, and increasing the number of trees led to both routes maintaining steady DPET performances, ranging between 29.0 °C and 32.5 °C.

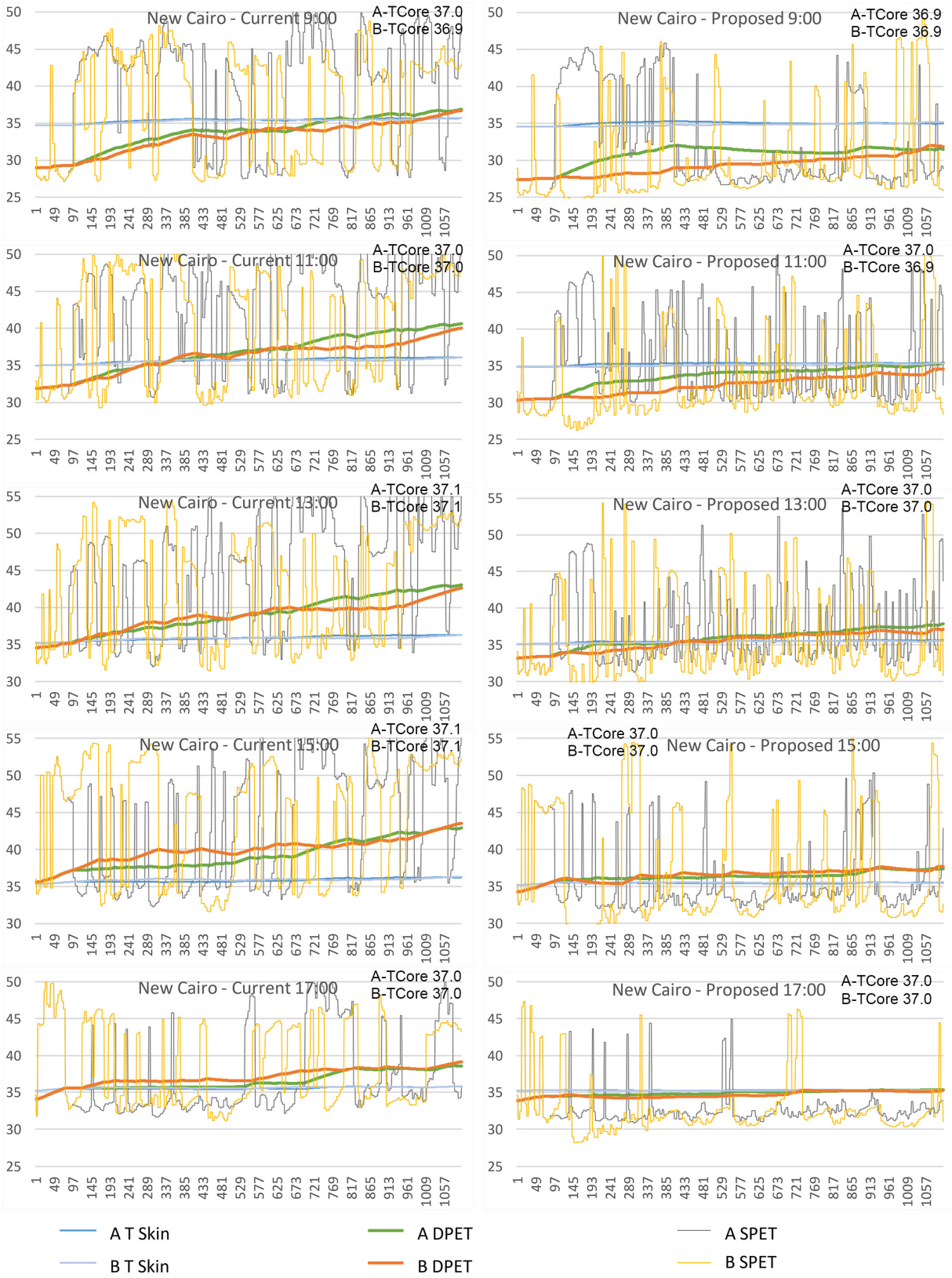

Figure 12. DPET, SPET, skin temperature (T Skin), and average core temperature (TCore) results for New Cairo routes (A and B) in both tree scenarios (current and proposed) at Z = 1.5 m. Y axis = °C and X axis = seconds while walking each route.

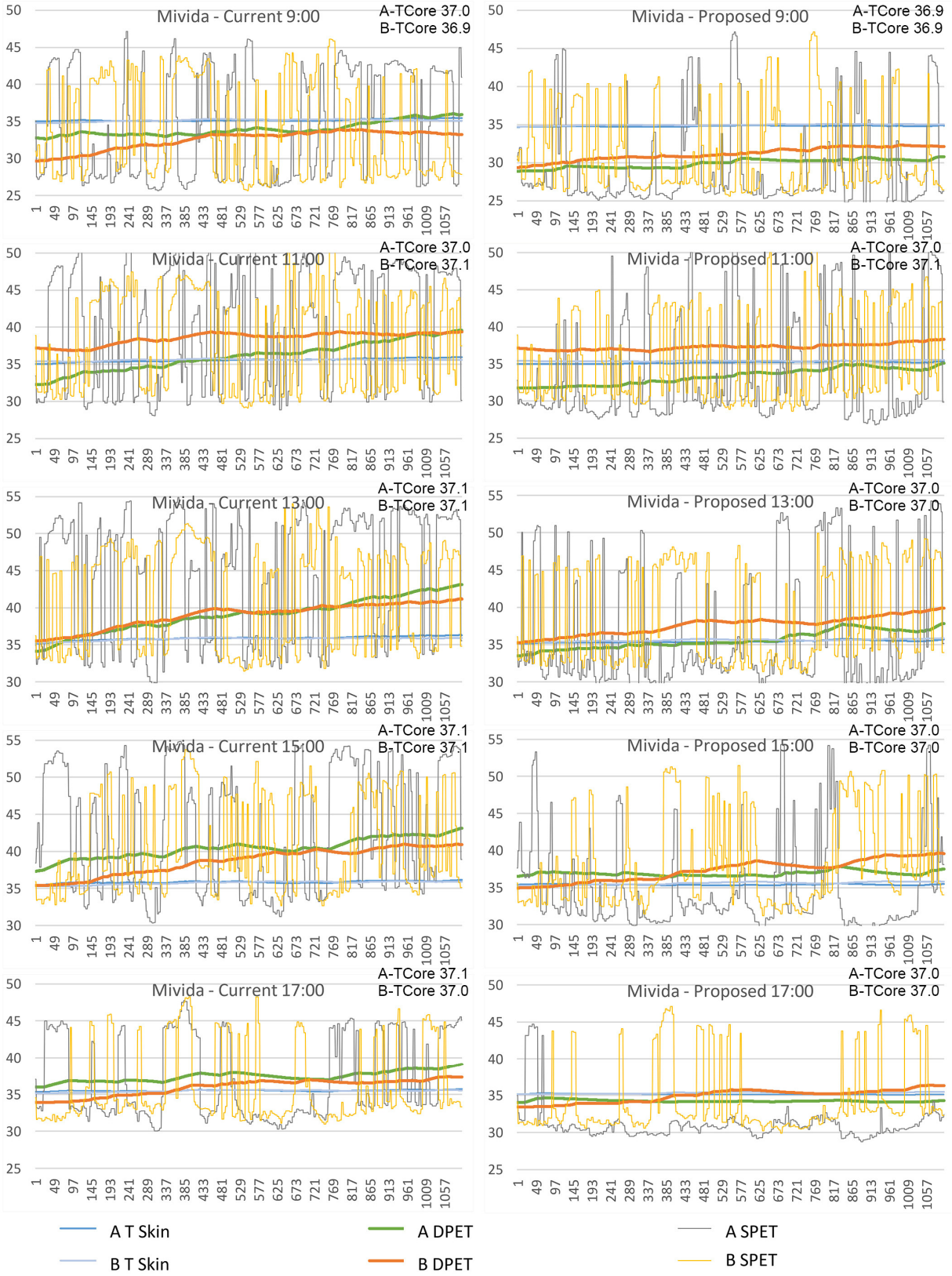

Figure 13. DPET, SPET, skin temperature (T Skin), and average core temperature (TCore) results for Mivida routes (A and B) in both tree scenarios (current and proposed) at Z = 1.5 m. Y axis = °C and X axis = seconds while walking each route.

At 11:00, route A had a good DPET value at the starting point (32.5 °C), which was lower than that of route B (37.5 °C). Then, route A had a larger DPET increase, and both routes reached the same value at the end of the walk (39.5 °C). This lower DPET increase on route B was due to the higher density of trees on the road in the current situation on this part of the route.

Increasing the tree density on both routes (the density was higher in parks) helped both routes to maintain lower DPET values, especially route A, which started and ended within the same range as the skin temperature. On route B, a slight increase in the tree density helped to keep the DPET value more stable within the range of 37.0 °C to 38.0 °C.

At 13:00, the DPET increased by 8.5 °C by the end of route A and by 6.5 °C by the end of route B. Increasing the tree density, especially in the parks, helped to keep route A cooler than route B by 2.0 °C to 3.0 °C and kept the whole walks on both routes under 40.0 °C.

At 15:00, route B was cooler than route A due to the impact of mixed shading from trees and buildings. Route A started with DPET = 37.0 °C then increased to reach 39.0 °C at the end of the route. Route B started with DPET = 34.0 °C then increased to reach 41.0 °C at the end of the route. Increasing the tree density totally changed the results. Route A was 2.0 °C cooler than route B at the end of the route. However, this route had a higher DPET value at the beginning (1 °C higher than route B).

At 17:00, additional building shading combined with tree shading helped to keep route B 1.5 °C to 2.0 °C cooler than route A for the whole walk. On the contrary, increasing the tree density in the parks helped to keep route A slightly cooler (1.0 °C). Increasing the tree density led to stable DPET values ranging between 34.0 °C and 34.5 °C on route A and in the range of 33.5 °C to 36.0 °C on route B.

In the Mohandisen study, the maximum core temperature and skin temperature were recorded, with an average core temperature of 37.4 °C on route B in the current Mohandisen scenario, which reflected how the climate conditions were harsh on this route at this hour (13:00). Similarly, the second highest average core temperature was recorded on route A in the current scenario at the same hour.

To conclude, the DPET changed between the different routes under the different tree scenarios. Table 7 shows the DPET values in the classified categories at the critical hours (13:00 and 15:00) every 50 s from the beginning until the end of each route. As shown in the table, routes A and B in Mohandisen and route B in Bulaq were the main critical routes that almost fell under the worst condition for the whole walks (red color range). However, in the tree scenarios, the DPET categories changed significantly, especially in the Bulaq cases. Other routes were in better conditions (the blue range) more often in the scenarios with increased trees.

3.3. Impact of SPET on DPET

Based on the DPET results, it was clear that each point of thermal comfort (SPET) had an impact on the DPET. In some cases, when the SPET values were in a lower range than the DPET, the DPET curve decreased. On the contrary, when the SPET values were higher than the DPET, the DPET curve increased. DPET values that fluctuated in a very small range were not the same as the SPET. Therefore, controlling the SPET at each point will lead to control of the DPET, and for better DPET values, the SPET should be controlled for a larger part of the route. Thus, trees should be optimized to be integrated with building shading. As shown in the results, trees had different performances based on the urban form (aspect ratio and orientation) and based on the time of day and the location of the sun. Figure 14 shows SPET comparisons for each study area and both tree scenarios (proposed and current) for the two peak hours of daytime (13:00 and 15:00). It is very obvious that trees are quite important at noon, when building shading disappears, and trees are also important at 15:00 in cases when buildings do not provide enough shading to the urban canyon. This applies in New Cairo and Mivida, where SPET reductions around 16.0 °C were identified due to the absence of building shading. On the contrary, in a compacted urban form such as Bulaq, the majority of open spaces are green, as shown in the maps,

which proves that increasing tree density in such a compacted form will help to enhance the SPET values. However, this enhancement is not as significant as in open urban forms with higher sky view factors (SVFs) and more open spaces. These maps provide evidence that for moderate urban forms such as those in Downtown and Mohandisen, higher tree density is better, especially for wider canyons such as those in Mohandisen, which need more trees. As shown in the map, many urban canyons were still in the green category even after increasing the tree cover percentage. When increasing the tree density, the amount of building shading should be considered, as overlapping shading from buildings and trees will not enhance the SPET, as shown in the Downtown maps, especially at 15:00. This would be a waste of resources, especially for a country like Egypt that suffers from water scarcity [55].

Table 7. Main DPET value classifications (every 50 s) on all routes in all scenarios at the critical hours (13:00 and 15:00).

Time	13:00												15:00							
	A					B					A					B				
	Downtown	Bulaq	Mohandisen	New Cairo	Mivida	Downtown	Bulaq	Mohandisen	New Cairo	Mivida	Downtown	Bulaq	Mohandisen	New Cairo	Mivida	Downtown	Bulaq	Mohandisen	New Cairo	Mivida
Current																				
0	38	37	47	35	34	36	47	50	35	36	39	40	36	36	37	36	50	36	36	35
50	39	39	46	35	36	37	45	50	35	36	39	41	37	37	39	36	48	37	37	36
100	40	41	45	37	37	38	45	51	37	37	40	43	38	38	39	37	48	38	39	37
150	41	42	46	37	38	38	45	52	38	38	40	44	40	38	39	37	47	40	40	37
200	41	43	47	38	39	40	44	51	39	39	41	45	41	38	41	39	46	40	40	38
250	42	41	46	38	39	42	44	52	38	40	41	43	42	38	41	41	45	41	39	39
300	41	41	46	39	39	42	44	53	40	39	41	42	41	39	40	41	45	40	40	40
350	42	40	46	40	40	43	45	53	40	40	41	41	41	40	40	41	44	42	41	40
400	41	40	47	41	40	43	45	53	40	40	41	41	42	41	41	42	44	41	41	40
450	42	40	46	42	41	43	45	52	40	40	42	40	42	42	42	43	44	42	41	41
500	41	40	47	42	42	43	44	51	41	41	42	40	42	42	42	43	43	41	42	41
Proposed																				
0	36	36	47	33	34	35	45	49	33	35	36	38	36	34	37	35	47	36	34	35
50	36	37	45	34	34	36	43	48	34	36	36	38	37	36	37	36	46	36	36	35
100	36	38	45	35	35	37	43	49	34	36	36	38	37	36	37	36	45	37	36	36
150	37	38	45	35	35	37	42	49	35	37	37	38	38	36	37	36	44	38	36	36
200	37	39	46	35	35	37	41	48	35	37	37	39	39	36	36	37	43	38	36	37
250	37	38	45	36	35	38	40	48	35	38	37	38	39	36	37	38	42	38	37	37
300	37	37	44	36	36	39	40	48	36	38	37	37	39	36	37	37	41	38	37	38
350	37	37	44	37	36	38	40	49	36	38	37	37	38	36	37	38	41	38	37	38
400	37	36	44	37	37	39	39	49	37	38	37	37	38	36	37	38	40	38	37	38
450	37	36	43	37	37	39	39	48	37	39	37	36	39	37	37	38	40	38	37	39
500	37	36	43	37	37	39	39	47	37	39	36	36	38	37	37	38	40	38	37	39
Scale	Better conditions																Worse conditions			

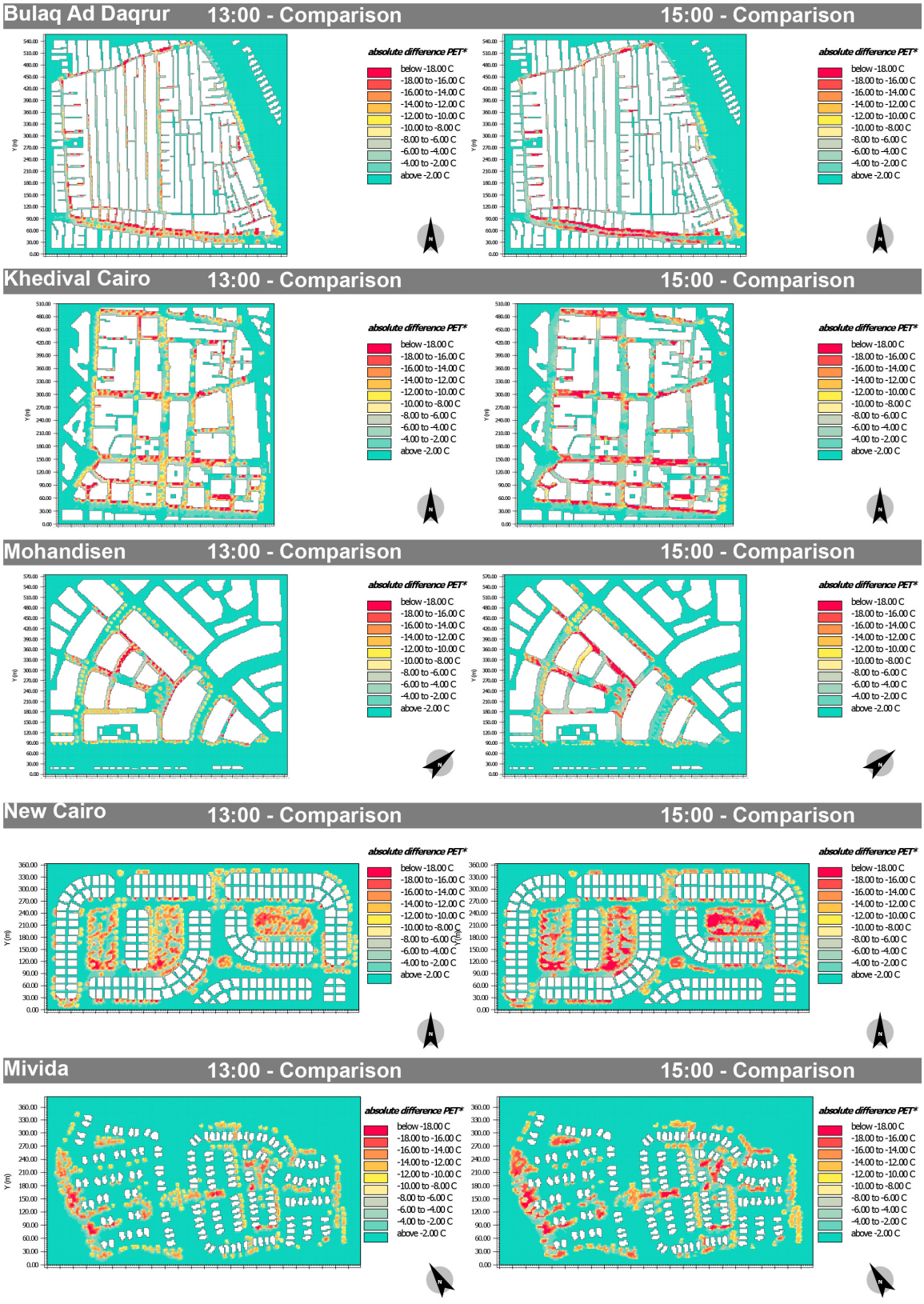

Figure 14. PET comparison (proposed vs. current) for all study areas at 13:00 and 15:00 at Z = 1.5 m.

3.4. Impact of Trees

The impact of trees can be observed based on the varying results (significant in some areas and minor in others). Increasing the tree density plays an important role when canyons are wide, especially when they are oriented to the east. This is in line with [21,26,31,50]. Full comparisons were applied to all routes before and after increasing the tree density to understand how the impact of the trees changed between different routes in different areas. This analysis helped to decide which cases need more trees to optimize thermal comfort. A classification analysis was applied to each route by the second to show how trees helped to change the thermal comfort zone for pedestrians while walking. This analysis clarified how long each walk was in each thermal comfort category. The thermal comfort zones considered the following grades of physiological stress (PET): 23 to 29 °C, slight heat stress (slightly warm); 29 to 35 °C, moderate heat stress (warm); 35 to 41 °C, strong heat stress (hot); more than 41 °C, extreme heat stress (very hot) [56]. The value used for internal heat production was 80 W, and heat transfer from clothing was 0.9 clo [57]. As shown in Figure 15, routes in some study areas were under extreme heat stress. Especially during the peak hours (11:00, 13:00, and 15:00) in Mohandisen, most of the walks (90% or more) were under extreme heat stress on both routes, while better performances took place in both Downtown and Bulaq, as each route had a balance between strong and moderate heat stress zones during the peak hours. In New Cairo and Mivida, better performances were observed, as all routes were mostly located within the moderate heat stress zone with a very limited percentage under extreme heat stress. In all tree scenarios, significant changes took place and new classifications appeared (such as slightly warm). Most of the classifications were within the warm zone, with very limited presence of extreme heat stress, which only occurred on route B in Mohandisen due to a large shallow canyon. Increasing the tree density was more significant on both routes in New Cairo and Mivida, as most of the routes fell within the warm to hot categories. Almost the same results were observed in Downtown and Bulaq, with some slight changes in Bulaq due to the wide canyon at the start of the walk.

The findings of this study matched those of many other scholars. For example, the performance of the trees was closely related to the urban form. In Bulaq, when pedestrians were walking inside the deep northern canyon, the DPET was enhanced even without trees [21,58], while trees' significance was clear when the canyons were shallow and lacked shading [59–61]. Also, it was clear that increasing the tree density in areas that already had adequate tree percentages (such as in New Cairo and Mivida) helped to provide better dynamic thermal comfort [62]. Therefore, it is obvious that adding trees is important, but the urban form and urban characteristics should be considered to optimize the use of trees [21,50].

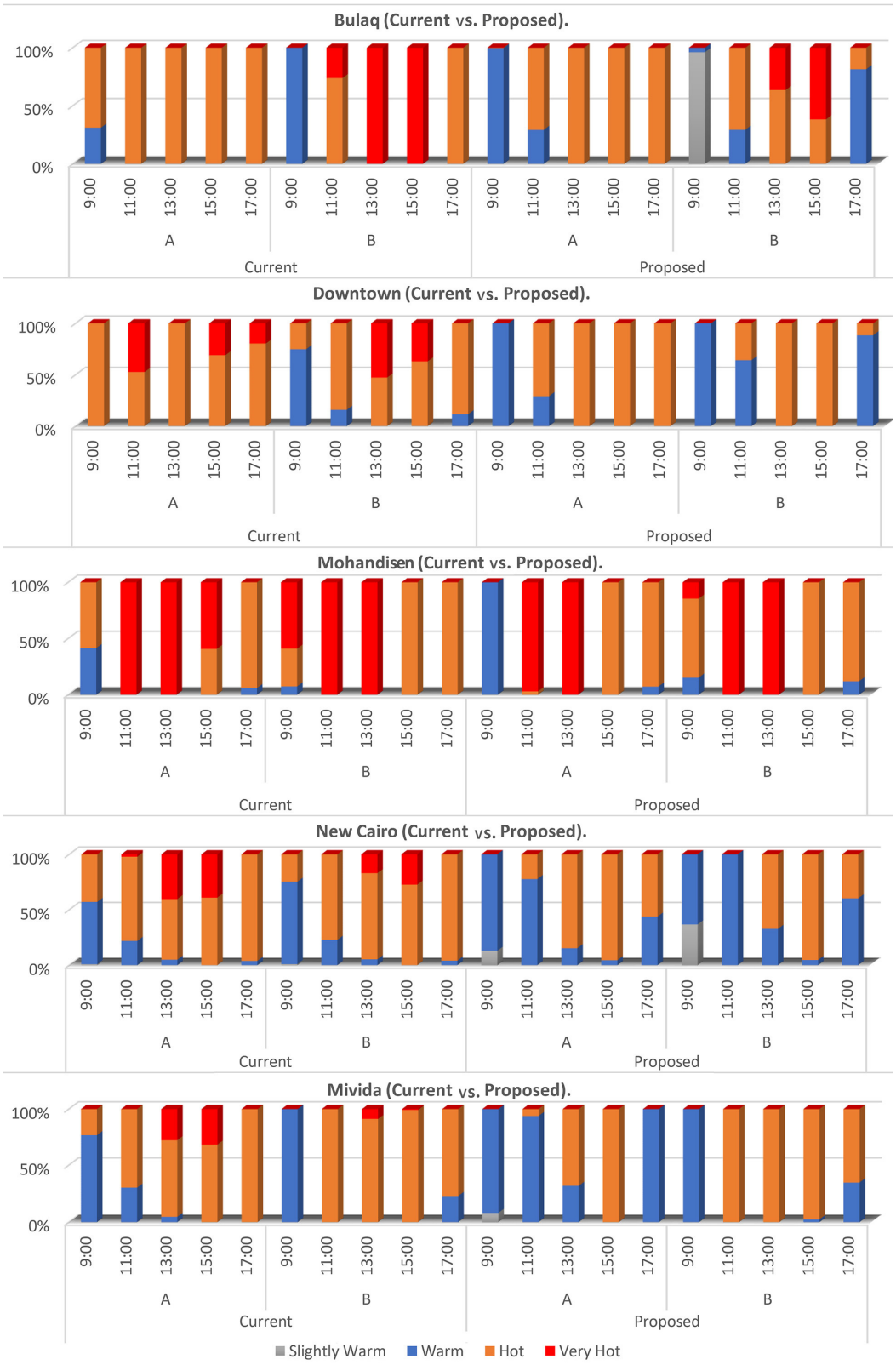

Figure 15. The dynamic thermal comfort classifications for each route (A and B) in both tree scenarios (current and proposed). The DPET values were exported at Z = 1.5. The X axis represents the hours, and the Y axis represents the percentages.

3.5. DPET Changes between Routes

A more detailed analysis was conducted, and the DPET results of each route (A and B) in both tree scenarios were compared to understand how the impact of the urban form and urban trees could change the DPET significantly even within the same area. As shown in Figure 16, starting with Bulaq's current scenario, route B started with very high values at 13:00 and 15:00, with DPET values reaching 10 °C. Due to the better canyon aspect ratio, this difference decreased significantly to only 1.5 °C. Then, both routes had the same performance on the northern road until the end. For the other hours, route B showed better performances than route A, with DPET values that were 3 °C lower on average. In the proposed tree scenario in Bulaq, the same performances happened at the same hours. The only difference was a slightly better DPET value. In Downtown, route A had higher DPET values at the starting point, with an average of 3.5 °C for all hours. However, the better canyon orientation helped to reduce this higher starting point, especially during the peak hours (13:00 and 15:00) and made route A better than route B by an average of 1 °C during the last part of the walk in the current scenario. In the proposed scenario, the trees controlled the DPET increase, especially at the starting point, and limited the changes to only 1 °C higher values at the beginning of route A and 1 °C lower values at the end of route A at almost all hours. In Mohandisen, however, routes A and B had the same DPET at the starting point. Due to the harsh climate conditions on route B, the difference in the DPET increased enormously and reached an average of 8 to 9 °C at three times (9:00, 11:00, and 13:00). A limited increase in trees did not help much, as the same performance, with an average DPET value of 2 °C, took place, which was an indicator that trees should be increased more in this study area. In New Cairo, routes A and B had slight DPET differences ranging between 1 °C and −1 °C. Route A was higher at the beginning. Then, route B became higher at most of the hours in the current scenario. In the proposed tree scenario, due to the increase in trees in the urban parks, route B became cooler for the whole walk and route A reached a DPET up to 2.5 °C higher during the first half of the walk before decreasing to 1 °C higher at the end of the walk. In Mivida, very similar performances took place. Route A (passing by the green parks) was higher due to the limited trees in the current scenario and reached an average of 2 °C higher after the various starting DPET values, except for at 11:00, when the DPET decreased from 5 °C higher to reach 0 and the end. In the trees scenario, the performances were reversed. Route A became cooler for the whole walk due to the greater increase in trees inside the parks than along the roads and reached an average of 2 °C cooler at most of the times. This proved that thermal comfort was mainly driven by the local microclimate conditions of a canyon or a space, and the overall study area did not control the thermal comfort of pedestrians.

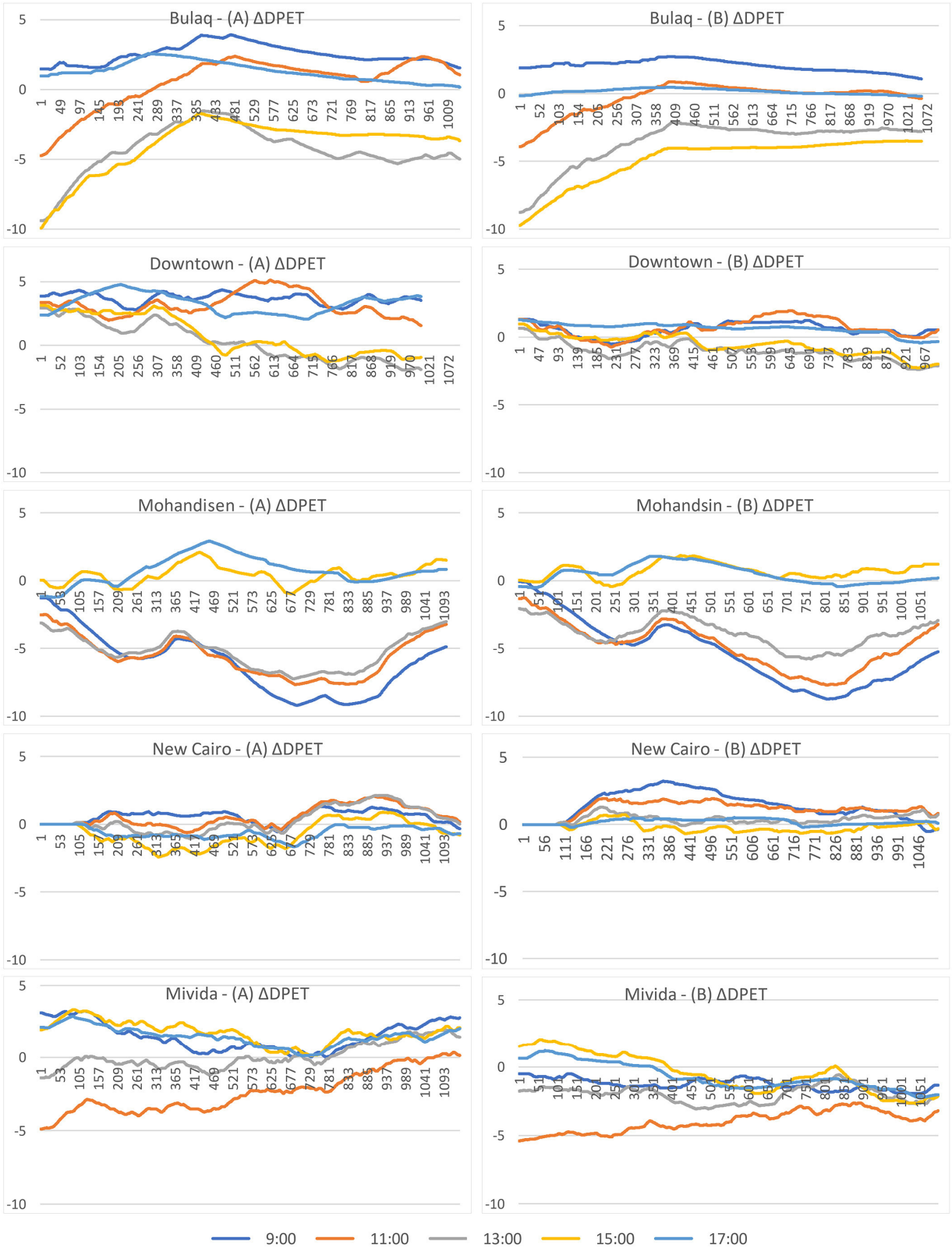

Figure 16. The Δ DPET in each study area. A represents (A–B) in the current situation, and B represents (A–B) in the proposed situation at Z = 1.5 m. The Y axis represents the ΔDPET (°C), and the X axis represents the time of the walk (seconds).

4. Discussion

The various results were driven by changes in the urban forms (aspect ratios and orientations) and tree densities, which was in line with [12,21,24,27,50]. More analyses were applied to have a full understanding of the effect of each factor. This included a detailed study of the changes between the different study areas.

DPET Changes between Different Study Areas

The changes between the hotter routes in each study area were analyzed to understand the range of differences not only in each area but also between them. The DPET values of route (A) in Bulaq, route (B) in Mohandisen, route (A) in New Cairo, and route (B) in Mivida were compared to route (B) in Downtown, as shown in Figure 17. At 9:00, all study areas except Mohandisen had a similar DPET range of 33 °C to 37 °C for the majority of the walks. Higher values were mainly observed in Bulaq, but route B in Mohandisen showed a significant DPET increase that reached 10 °C. Adding trees helped to keep the DPET range between 29 °C and 32 °C at the ends of the walks for all routes except route B in Mohandisen, where the higher range was reduced by 2 °C on average. At 11:00, the same performances took place, and all routes had similar DPET values of around 39.5 °C. However, most of them had different DPET values at the starting points. The only difference was for route B in Mohandisen, which still showed significantly higher DPET values with an average of 50 °C in the current situation. This was 10 °C higher than on route B in Downtown. Adding trees led to better DPET values around 36 °C at the ends of the walks for all routes, except for route B in Mohandisen, where the DPET value improved slightly to around 47 °C. At 13:00, the same performances took place. The difference in DPET on route B in Mohandisen was a range of 10 °C, and route A in Bulaq had slight DPET changes of around 3.0 °C. Increasing the tree density reduced this range to 1 °C and improved the condition on route B in Mohandisen by 1 °C. At 15:00 and 17:00, due to good shading by buildings, the increase on route B in Mohandisen decreased significantly, and the DPET values were within the same ranges for all routes (below 38 °C in the current scenario and 35 °C in the proposed tree scenario). This is also proof that the DPET was driven by the microclimate conditions of the canyons more than the overall urban context, and changes between different urban canyons could sometimes reach 10 °C.

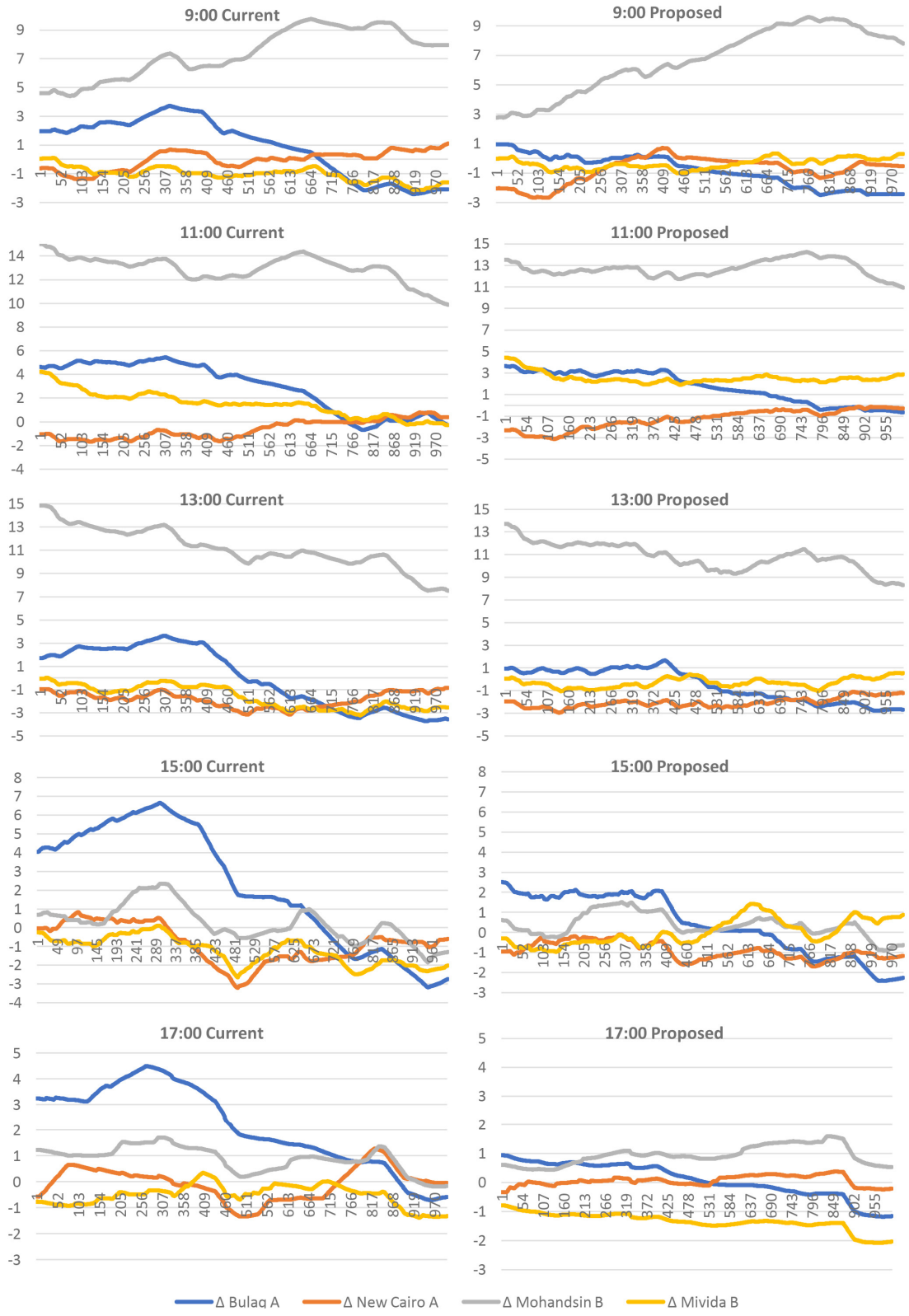

Figure 17. The ΔDPET values on the hot routes in each study area compared to route B in Downtown for the current and proposed scenarios at each hour at Z = 1.5 m. The Y axis represents the DPET (°C), and the X axis represents the time of the walk (seconds).

5. Conclusions

The parameters currently used to measure thermal comfort, such as the steady/static thermal comfort (SPET), are not sufficient to represent real pedestrian thermal comfort while walking because they do not consider changes and dynamic variations in the thermal environment [1]. This study aimed to enhance the dynamic thermal comfort (DPET) of pedestrians while walking under different urban forms with different aspect ratios, orientations, building density, and trees density under the same climate data for all cases. After assessing five different study areas in Cairo City under two tree scenarios (the current tree density and a proposed increase in tree density), the results proved that the DPET had different values than the SPET at each point along the routes. However, the DPET was closely related to changes in the SPET. The main study findings can be summarized as follows:

- As the DPET was impacted by the SPET, keeping the SPET lower or higher for a long time reduced or increased the DPET.
- Frequent equivalent changes (ups and downs) in the SPET kept the DPET stable.
- Changes between DPET values were driven more by the microclimate conditions of a space or canyon than the conditions of the overall area, and controlling the microclimate conditions of a whole urban canyon controlled the DPET.
- Changes in the DPET could reach 10 °C between different canyons, and increasing the tree density could lower the DPET by up to 6 °C in some cases.

The DPET is affected more by urban shading (by buildings or trees) and wind than by changing paving materials or adding grass surfaces.

This study covered many urban forms and tree varieties and tested them using the simulation software ENVI-met V5.6.1, Winter 2023. It could also be linked to a real experiment by investigating how people walking on these routes are feeling. In addition, more urban routes could be studied, including different urban cases such as waterfront promenades, large-scale park walkways, or walkways inside large parking areas. The study outcomes should support design decisions like positioning bus stops in relation to the surrounding land use and walking conditions as well as the allocation of retail and commercial uses on routes and the allocation of urban parks and their frequency, which would not only be defined by the urban situation but also by studying thermal comfort.

Author Contributions: Conceptualization, A.Y.A.; Methodology, A.Y.A.; Software, A.Y.A.; Formal analysis, A.Y.A.; Writing—original draft, A.Y.A.; Writing—review & editing, D.G.; Visualization, A.Y.A.; Supervision, D.G. All authors have read and agreed to the published version of the manuscript.

Funding: This research did not receive any funding. APC was funded by TU Dortmund University.

Data Availability Statement: The data that support the findings of this study (all ENVI-met files) are available upon request.

Conflicts of Interest: The authors declare no conflicts of interest.

Abbreviations

UHI	urban heat island
SPET	(steady/static) physiological equivalent temperature
DPET	(dynamic) physiological equivalent temperature
TMRT	the mean radiant temperature
RH%	relative humidity
T Skin	skin temperature
T Core	core temperature
RMSE	root-mean-square error
d	index of agreement
SVF	sky view factor

References

1. Hwang, R.-L.; Weng, Y.-T.; Huang, K.-T. Considering transient UTCI and thermal discomfort footprint simultaneously to develop dynamic thermal comfort models for pedestrians in a hot-and-humid climate. *Build. Environ.* **2022**, *222*, 109410. [CrossRef]
2. Sauter, D. Measuring Walking: Towards internationally standardised monitoring methods of walking and public space. In Proceedings of the 8th International Conference on Survey Methods in Transport, Annecy, France, 25–31 May 2008.
3. Carolina, V.; Nikolopoulou, M. Thermal walks: Identifying pedestrian thermal comfort variations in the urban continuum of historic city centres. In Proceeding of PLEA2013-29th Conference, Sustainable architecture for a renewable futu. In Proceedings of the PLEA2013-29th Conference, Sustainable Architecture for a Renewable Future, Munich, Germany, 10–12 September 2013.
4. Carolina, V.; Nikolopoulou, M. Outdoor thermal comfort for pedestrians in movement: Thermal walks in complex urban morphology. *Int. J. Biometeorol.* **2020**, *64*, 277–291.
5. Richard, J.D.D.; Brager, G.S. Thermal comfort in naturally ventilated buildings: Revisions to ASHRAE Standard 55. *Energy Build.* **2002**, *34*, 549–561.
6. Fang, Y.; Chen, G.; Bicka, M.; Chen, J. Smart textiles for personalized thermoregulation. *Chem. Soc. Rev.* **2021**, *50*, 9357–9374. [CrossRef] [PubMed]
7. Zhai, H.; Fan, D.; Li, Q. Dynamic radiation regulations for thermal comfort. *Nano Energy* **2022**, *100*, 107435. [CrossRef]
8. Taleghani, M.; Kleerekoper, L.; Tenpierik, M.; van den Dobbelsteen Taleghani, A. Outdoor thermal comfort within five different urban forms in the Netherlands. *Build. Environ.* **2015**, *83*, 65–78. [CrossRef]
9. Li, J.; Niu, J.; Huang, T.; Mak, C.M. Dynamic effects of frequent step changes in outdoor microclimate environments on thermal sensation and dissatisfaction of pedestrian during summer. *Sustain. Cities Soc.* **2022**, *79*, 103670. [CrossRef]
10. Huang, T.; Niu, J.; Xie, Y.; Li, J.; Mak, C.M. Assessment of "lift-up" design's impact on thermal perceptions in the transition process from indoor to outdoor. *Sustain. Cities Soc.* **2020**, *56*, 102081. [CrossRef]
11. Katavoutas, G.; Flocas, H.A.; Matzarakis, A. Dynamic modeling of human thermal comfort after the transition from an indoor to an outdoor hot environment. *Int. J. Biometeorol.* **2015**, *59*, 205–216. [CrossRef]
12. Lau, K.K.-L.; Shi, Y.; Ng, E.Y.-Y. Dynamic response of pedestrian thermal comfort under outdoor transient conditions. *Int. J. Biometeorol.* **2019**, *63*, 979–989. [CrossRef]
13. Nakayoshi, M.; Kanda, M.; Shi, R.; de Dear, R. Outdoor thermal physiology along human pathways: A study using a wearable measurement system. *Int. J. Biometeorol.* **2015**, *59*, 503–515. [CrossRef] [PubMed]
14. Jia, X.; Cao, B.; Zhu, Y. A climate chamber study on subjective and physiological responses of airport passengers from walking to a sedentary status in summer. *Build. Environ.* **2022**, *207*, 108547. [CrossRef]
15. Höppe, P. Different aspects of assessing indoor and outdoor thermal comfort. *Energy Build.* **2002**, *34*, 661–665. [CrossRef]
16. Zhang, Y.; Liu, J.; Zheng, Z.; Fang, Z.; Zhang, X.; Gao, Y.; Xie, Y. Analysis of thermal comfort during movement in a semi-open transition space. *Energy Build.* **2020**, *225*, 110312. [CrossRef]
17. Theeuwes, N.E.; Steeneveld, G.J.; Ronda, R.J.; Heusinkveld, B.G.; van Hove, L.W.A.; Holtslag, A.A.M. Seasonal dependence of the urban heat island on the street canyon aspect ratio. *Q. J. R. Meteorol. Soc.* **2014**, *140*, 2197–2210. [CrossRef]
18. Theeuwes, N.E.; Steeneveld, G.J.; Ronda, R.J.; Heusinkveld, B.G.; van Hove, L.W.A.; Holtslag, A.A.M. Influence of aspect ratio and orientation on large courtyard thermal conditions in the historical centre of Camagüey-Cuba. *Renew. Energy* **2018**, *125*, 840–856.
19. Morakinyo, T.E.; Kong, L.; Lau, K.K.-L.; Yuan, C.; Ng, E. A study on the impact of shadow-cast and tree species on in-canyon and neighborhood's thermal comfort. *Build. Environ.* **2017**, *115*, 1–17. [CrossRef]
20. Ketterer, C.; Matzarakis, A. Human-biometeorological assessment of heat stress reduction by replanning measures in Stuttgart, Germany. *Landsc. Urban Plan.* **2014**, *122*, 78–88. [CrossRef]
21. Abdelmejeed, A.Y.; Gruehn, D. Optimization of Microclimate Conditions Considering Urban Morphology and Trees Using ENVI-Met: A Case Study of Cairo City. *Land* **2023**, *12*, 2145. [CrossRef]
22. Elsadek, M.; Liu, B.; Lian, Z.; Xie, J. The influence of urban roadside trees and their physical environment on stress relief measures: A field experiment in Shanghai. *Urban For. Urban Green.* **2019**, *42*, 51–60. [CrossRef]
23. Emmanuel, R.; Rosenlund, H.; Johansson, E. Urban shading—A design option for the tropics? A study in Colombo, Sri Lanka. *Int. J. Climatol. J. R. Meteorol. Soc.* **2007**, *27*, 1995–2004. [CrossRef]
24. Lobaccaro, G.; Acero, J.A.; Martinez, G.S.; Padro, A.; Laburu, T.; Fernandez, G. Effects of orientations, aspect ratios, pavement materials and vegetation elements on thermal stress inside typical urban canyons. *Int. J. Environ. Res. Public Health* **2019**, *16*, 3574. [CrossRef] [PubMed]
25. Shishegar, N. Street Design and Urban Microclimate: Analyzing the Effects of Street Geometry and Orientation on Airflow and Solar Access in Urban Canyons. *J. Clean Energy Technol.* **2013**, *1*, 52. [CrossRef]
26. De, B.; Mukherjee, M. Optimisation of canyon orientation and aspect ratio in warm-humid climate: Case of Rajarhat Newtown, India. *Urban Clim.* **2018**, *24*, 887–920. [CrossRef]
27. Aboelata, A. Vegetation in different street orientations of aspect ratio (H/W 1: 1) to mitigate UHI and reduce buildings' energy in arid climate. *Build. Environ.* **2020**, *172*, 106712. [CrossRef]
28. Wang, Y.; Berardi, U.; Akbari, H. Comparing the effects of urban heat island mitigation strategies for Toronto, Canada. *Energy Build.* **2016**, *114*, 2–19. [CrossRef]

29. Song, C.; Ikei, H.; Igarashi, M.; Miwa, M.; Takagaki, M.; Miyazaki, Y. Physiological and psychological responses of young males during spring-time walks in urban parks. *J. Physiol. Anthropol.* **2014**, *33*, 1–7. [CrossRef]
30. Takayama, N.; Korpela, K.; Lee, J.; Morikawa, T.; Tsunetsugu, Y.; Park, B.-J.; Li, Q.; Tyrväinen, L.; Miyazaki, Y.; Kagawa, T. Emotional, restorative and vitalizing effects of forest and urban environments at four sites in Japan. *Int. J. Environ. Res. Public Health* **2014**, *11*, 7207–7230. [CrossRef]
31. Abdollahzadeh, N.; Biloria, N. Outdoor thermal comfort: Analyzing the impact of urban configurations on the thermal performance of street canyons in the humid subtropical climate of Sydney. *Front. Archit. Res.* **2021**, *10*, 394–409. [CrossRef]
32. Andreou, E. Thermal comfort in outdoor spaces and urban canyon microclimate. *Renew. Energy* **2013**, *55*, 182–188. [CrossRef]
33. Jamei, E.; Ossen, D.R.; Seyedmahmoudian, M.; Sandanayake, M.; Stojcevski, A.; Horan, B. Urban design parameters for heat mitigation in tropics. *Renew. Sustain. Energy Rev.* **2020**, *134*, 110362. [CrossRef]
34. Envi-Board, Envi-Met Support Center. Envi-Met. Available online: http://www.envi-hq.com/ (accessed on 30 April 2023).
35. Kottek, M.; Grieser, J.; Beck, C.; Rudolf, B.; Rubel, F. World map of the Köppen-Geiger climate classification updated. *Meteorol. Z.* **2006**, *15*, 259–263. [CrossRef] [PubMed]
36. Abutaleb, K.; Ngie, A.; Darwish, A.; Ahmed, M.; Arafat, S.; Ahmed, F. Assessment of urban heat island using remotely sensed imagery over Greater Cairo, Egypt. *Adv. Remote Sens.* **2015**, *35*, 4. [CrossRef]
37. Panagiotis Kosmopoulos, H.E.-A.S.K. *The Solar Atlas of Egypt, Cairo: The EUMETSAT Network of Sataliete Application Facilities*; EUMETSAT: Darmstadt, Germany, 2018.
38. Climate Top. Available online: https://www.climate.top/egypt/cairo/temperatures/ (accessed on 1 June 2024).
39. Shahraiyni, H.T.; Sodoudi, S.; El-Zafarany, A.; El Seoud, T.A.; Ashraf, H.; Krone, K. A comprehensive statistical study on daytime surface urban heat island during summer in urban areas, case study: Cairo and its new towns. *Remote Sens.* **2016**, *8*, 643. [CrossRef]
40. Islam, A.E.-M.; Ismail, A.; Zanaty, N. Spatial variability of urban heat islands in Cairo City, Egypt using time series of Landsat Satellite images. *Int. J. Adv. Remote Sens. GIS* **2016**, *5*, 1618–1638.
41. Mohamed, E. Analysis of urban growth at Cairo, Egypt using remote sensing and GIS. *Nat. Sci.* **2012**, *4*, 355–361.
42. Eman, Z.; Vialard, A. Syntactic Stitching: Towards a Better Integration of Cairo's Urban Fabric. In *Proceedings of the 11th International Space Syntax Symposium*; Instituto Superior Técnico: Lisbon, Portugal, 2017.
43. Abougendia, S.M. Investigating surface UHI using local climate zones (LCZs), the case study of Cairo's River Islands. *Alex. Eng. J.* **2023**, *77*, 293–307. [CrossRef]
44. Elmarakby, E.; Khalifa, M.; Elshater, A.; Afifi, S. Spatial morphology and urban heat island: Comparative case studies. In *Architecture and Urbanism: A Smart Outlook: Proceedings of the 3rd International Conference on Architecture and Urban Planning, Cairo, Egypt*; Springer International Publishing: Cham, Switzerland, 2020; pp. 441–454.
45. Elbardisy, W.M.; Salheen, M.A.; Fahmy, M. Solar irradiance reduction using optimized green infrastructure in arid hot regions: A case study in el-nozha district, Cairo, Egypt. *Sustainability* **2021**, *13*, 9617. [CrossRef]
46. Zhang, J.; Gou, Z.; Zhang, F.; Yu, R. The tree cooling pond effect and its influential factors: A pilot study in Gold Coast, Australia. *Nat.-Based Solut.* **2023**, *3*, 100058. [CrossRef]
47. Liu, Y.; Lai, Y.; Jiang, L.; Cheng, B.; Tan, X.; Zeng, F.; Liang, S.; Xiao, A.; Shang, X. A study of the thermal comfort in urban mountain parks and its physical influencing factors. *J. Therm. Biol.* **2023**, *118*, 103726. [CrossRef]
48. Middel, A.; Chhetri, N.; Quay, R. Urban forestry and cool roofs: Assessment of heat mitigation strategies in Phoenix residential neighborhoods. *Urban For. Urban Green.* **2015**, *14*, 178–186. [CrossRef]
49. Shahidan, M.F.; Shariff, M.K.M.; Jones, P.; Salleh, E.; Abdullah, A.M. A comparison of Mesua ferrea L. and Hura crepitans L. for shade creation and radiation modification in improving thermal comfort. *Landsc. Urban Plan.* **2010**, *97*, 168–181. [CrossRef]
50. Abdelmejeed, A.G.D. Optimizing an efficient urban tree strategy to improve microclimate conditions while considering water scarcity: A case study of Cairo. *Discov. Sustain.* **2024**, *5*, 66. [CrossRef]
51. Elnabawi, M.; Hamza, N.; Dudek, S. Outdoor thermal comfort in the old Fatimid city, Cairo, Egypt. In *International Conference on "Changing Cities": Spatial, Morphological, Formal & Socio-Economic Dimensions*; Newcastle University: Newcastle, UK, 2013.
52. Weather and Climate. Available online: https://weather-and-climate.com/Cairo-July-averages (accessed on 31 October 2023).
53. Time and Date. Available online: https://www.timeanddate.com/weather/egypt/cairo/historic?month=7&year=2022 (accessed on 30 October 2023).
54. Xiao, J.; Yuizono, T. Climate-adaptive landscape design: Microclimate and thermal comfort regulation of station square in the Hokuriku Region, Japan. *Build. Environ.* **2022**, *212*, 108813. [CrossRef]
55. Osman, R.; Ferrari, E.; McDonald, S. Water scarcity and irrigation efficiency in Egypt. *Water Econ. Policy* **2016**, *2*, 1650009. [CrossRef]
56. Ballinas, M.; Morales-Santiago, S.I.; Barradas, V.L.; Lira, A.; Oliva-Salinas, G. Is PET an adequate index to determine human thermal comfort in Mexico City? *Sustainability* **2022**, *14*, 12539. [CrossRef]
57. Heaviside, C.; Macintyre, H.; Vardoulakis, S. The urban heat island: Implications for health in a changing environment. *Curr. Environ. Health Rep.* **2017**, *4*, 296–305. [CrossRef]
58. Sanusi, R.; Johnstone, D.; May, P.; Livesley, S.J. Street orientation and side of the street greatly influence the microclimatic benefits street trees can provide in summer. *J. Environ. Qual.* **2016**, *45*, 167–174. [CrossRef]

59. Hassan, A.; Tao, J.; Li, G.; Jiang, M.; Aii, L.; Zhihui, J.; Zongfang, L.; Qibing, C. Effects of walking in bamboo forest and city environments on brainwave activity in young adults. *Evid. Based Complement. Altern. Med.* **2018**, *2018*, 9653857. [CrossRef]
60. Wei, D.; Liu, B. The analysis and evaluation of thermal comfort at Shanghai knowledge & innovation community square. *Chin. Landsc. Archit.* **2018**, *34*, 5–12.
61. Liu, B.Y.; Mei, Y.; Kuang, W. Experimental research on correlation between microclimate element and human behavior and perception of residential landscape space in Shanghai. *Landsc. Arch.* **2016**, *32*, 5–9.
62. Ochiai, H.; Ikei, H.; Song, C.; Kobayashi, M.; Miura, T.; Kagawa, T.; Li, Q.; Kumeda, S.; Imai, M.; Miyazaki, Y. Physiological and psychological effects of a forest therapy program on middle-aged females. *Int. J. Environ. Res. Public Health* **2015**, *12*, 15222–15232. [CrossRef]

This Page Intentionally Left Blank.